“N remobilisation during barley grain filling and the influence of sink-strength alteration in developing wheat grains”

Kumulative Dissertation

zur Erlangung des
Doktorgrades der Naturwissenschaften
(Dr. rer. nat.)

vorgelegt der
Naturwissenschaftlichen Fakultät I - Biowissenschaften
der Martin-Luther-Universität Halle-Wittenberg

von

Herrn Stefan Kohl
geboren am 04.06.1975 in Augsburg

Gutachter

1. Prof. Dr. T. Altmann

2. Prof. Dr. K. Humbeck

3. Prof. Dr. R. Kunze

Ort und Datum der Verteidigung: Halle (Saale), den 19.10.2015

Table of contents

Table of contents (continued)

1. Introduction

1.1. Grain development in barley

The term cereals summarises various members from the poaceae family of monocotyledonous flowering plants that are cultivated as crop plants. Their mature grains are the most important staple food for large parts of the world's population and grains, as well as other plant parts can serve a large variety of additional purposes, such as live stock food or precursors for industrial products. The nutritional value of cereals results from the accumulation of storage compounds in the main storage tissue (endosperm), which consists mainly of starch (70-80 wt%) and proteins (7-12 wt%). Cereals were subjected to conventional breeding for several millennia and, accompanied by technological advances and increasing fertilisation, yield per area (kg/ha) was drastically increased. However, in recent years it has become obvious that there is a natural limitation to this development, as neither new breeding varieties, nor increasing fertiliser input has managed to further substantially increase yield. In the face of the predicted and drastic increase in world population over the next decades, it seems inevitable that agricultural output must improve in order to secure the nourishment of people in the future. In order to adress these challenges and develop new strategies for improving yield and/or nutritional quality of cereals, detailed knowledge of the different aspects of grain development is necessary.

Barley (*Hordeum vulgare*) is widely used as a model organism for cereals and various approaches have elucidated the sequential events happening throughout grain development.

The ripe fruit of barley, as in all other poaceae species, is called caryopsis, which is characterised by the fusion of the maternal pericarp and the filial seed coat. Furthermore, the developing caryopsis is enclosed by differentiated bracts, namely the glumes, the lemma and the palea (summarised as glumes in the following chapters).

Detailed histological analyses of the embryo and the endosperm revealed cell differentiation fates from fertilisation to maturation (Engell, 1989; Olsen, 2001). Further developmental changes in respect to morphology, physiology, and transcriptional activity within the whole grain are reviewed in Wobus *et al.* (2005), and allow to separate development after fertilisation into three phases (Figures 1 and 2). In the first 8 days after fertilisation (DAF, cellularisation/pre-storage phase), cellular organisation within the grains is established and longitudial growth reaches its maximum. The maternal pericarp differentiates into two tissue types, the inner chloroplast containing chlorenchyma, and the outer cell layers, that harbour the vascular tissues. Endosperm development starts as a coenocytic tissue, before cell wall formation and further cell divisions result in the cellularized endsoperm and the surrounding aleurone layer (Wobus *et al.*, 2005). The pericarp is separated from the endosperm cells by a

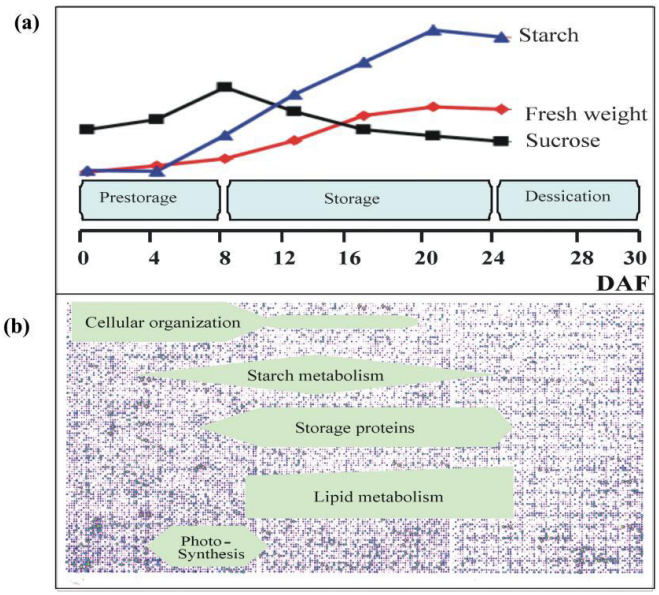

Figure 1 A general scheme of barley seed development.
(A) Developmental and biochemical parameters led to the widely accepted definition of three main stages (pre-storage, storage and desiccation phase) of (barley) seed development. DAF, Days after flowering. (B) Gene expression patterns underlying distinct developmental phases during barley grain development. A hybridised array with about 12,000 cDNA fragments of unique genes expressed in the developing barley grain is over-layed with expression pattern schemes of functional groups of genes. The expression pattern schemes result from a combination of expression analysis results and data mining of more than 40,752 ESTs out of four tissue and seed development-specific cDNA libraries (Sreenivasulu *et al.*, unpubl.). The figure is taken from (Wobus, *et al.*, 2005) with the publishers' permission.

cuticule layer, which allows nutrient exchange between maternal and filial grain parts only by specialised structures (Patrick and Offler, 2001). Cells of the maternal tissue adjacent to the central vein facing the endosperm differentiate into the nucellar projection (NP), while the opposing cells of the endosperm form the endosperm transfer cells (ETC, Cochrane and Duffus, 1980). Transcript data suggests a tightly controlled developmental gradient within the NP and distinct areas simultaneously undergo mitosis, cell elongation, and disintegration, which finally leads to the release of nutrients into the endosperm cavern (Thiel *et al.*, 2008; Melkus *et al.*, 2011). Furthermore, metabolite and transcript analyses revealed specific strategies in the NP of young barley grains for mobilisation and metabolism of transient N and S reserves and transfer into the endosperm (Thiel *et al.*, 2009). Transfer cells in general are characterised by secondary wall ingrowths that increase the plasma membrane surface and play a central role in nutrient distribution by facilitating high rates of transport at bottlenecks for apo-/symplasmic solute exchange (reviewed in Offler et al., 2003). Likewise, barley ETCs, in combination with the NP, exhibit an essential role during endosperm development, as they confer the whole nutrient exchange between maternal and filial tissue.

When all of these structures are established and functional (6 to 10 DAF), bulk storage product accumulation starts within the endosperm. Deposition of starch begins at around 6 DAF within the outer cell layers, and progresses to the central cells during development (Radchuk *et al.*, 2009). Although storage proteins, mainly globulins, can be found in the embryo and aluerone layer of cereals, prolamins represent the largest fractions of storage proteins in barley and are deposited after 10 DAF in protein bodies within the starchy endosperm (Xiang and Bao, 1997; Shewry and Halford, 2002). The main storage phase in barley lasts until ~20 DAF and is characterised by linear increases in starch content and fresh weight, acommpanied with decreasing hexose levels and growth in girth (Figures 1 and

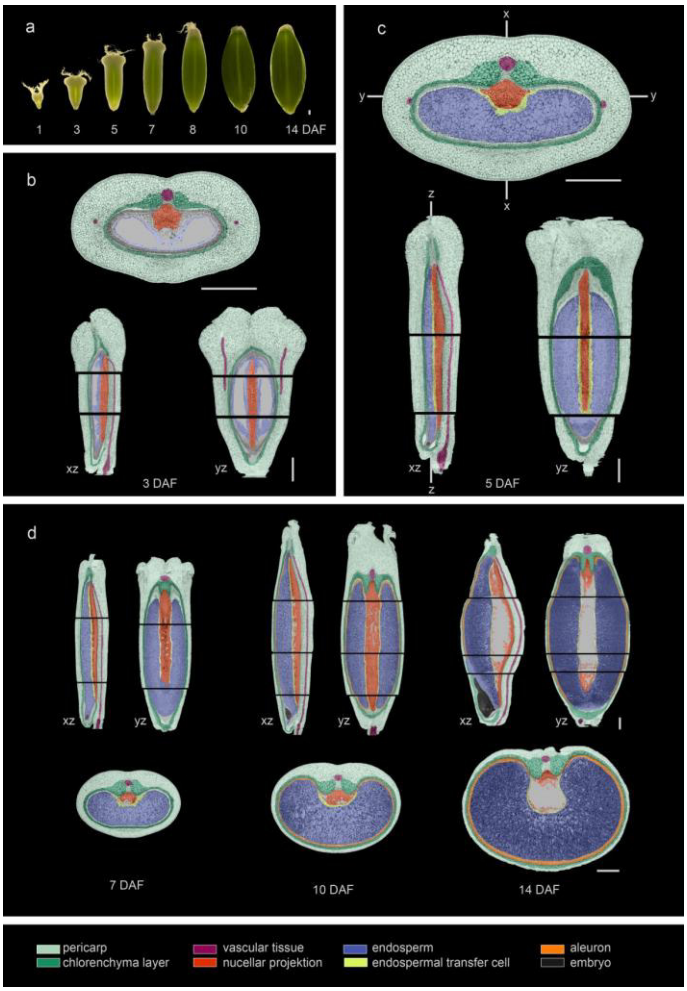

Figure 2 The developing barley grain. (A) Barley grains at different developmental stages. Glumes and awn were removed before taking photographs. (B) – (D) Median transverse, longitudinal (xz), and sagittal (yz) sections of barley grains at different developmental stages. The x, y, and z position of the sections is given in (C). Longitudinal and sagittal sections are created from simulated artificial grains generated by a combination of thin transverse sections from plastic-embedded material. Black bars dividing the longitudinal and sagittal sections into pieces result from cutting of the native caryopses necessary for optimal fixation and embedding. Colours representing individual tissues are shown at the bottom panel of the figure. The white patches within the nucellar projection in (D) indicate degeneration of tissue resulting into the endosperm cavity. Bars = 500 mm; DAF, days after flowering. The figure is taken from (Sreenivasulu *et al*., 2010) with the publishers' permission.

2). After 24 DAF the grain enters the desiccation phase, where water content is reduced to ~10 wt%, metabolic activity nearly ceases and dormancy is acquired (Leprince *et al*., 1993).

In addition to the three well established developmental phases, transcriptome data of developing barley grains elucidated a transition phase between 6 and 8 DAF, that separates cellularisation from accumulation processes and is characterised by large scale reprogramming of the transcriptome (Sreenivasulu *et al*., 2004). During their whole development cereal grains are heterotrophic organs, and therefore nutrients for growth and storage metabolism must be imported from vegetative tissues. Carbon is continuously provided by photosynthetic activity of vegetative tissues and ear photosynthesis highly contributes to carbon accumulation in grains (Grundbacher, 1963; Araus *et al*., 1993; Sanchez-Bragado *et al*., 2014). On the other hand, nitrogen supply relies on remobilisation processes, as the nitrogen demand of developing grains is higher than post anthesis nitrogen uptake from the soil and most nitrogen entering developing grains derives from pools stored in vegetative tissues during vegetative growth (Waters *et al*., 1980; Simpson *et al*., 1983; Hirel *et al*., 2007).

Increasing yield is often accompanied by decreases in the nutritional value of the grains. One reason is the well-established negative correlation between grain protein content (GPC) and yield and (Simmonds, 1995). Furthermore, the evaluation of several studies, which reported yield increases under elevated CO_2 conditions, indicates that not only GPC, but also the

contents of other nutrients, such as zinc and iron, are negatively correlated with yield increases (Myers *et al.*, 2014). Thus, when trying to increase yield, it is also important to consider the N nutrition of developing grains, in order to maintain constant nutritional quality. Recent studies have shown that a transcription factor from the NAC family in wheat enhances nutrient remobilisation from vegetative tissues, leading to increases in grain protein, zinc, and iron contents without significantly reducing thousand grain weight (Uauy *et al.*, 2006; Waters *et al.*, 2009). Comparably, the barley homologue is also positively correlated with GPC (Jamar *et al.*, 2010), which indicates the potential to use these transcription factors as tools to increase nutritional quality without decreasing yield.

1.2. Nitrogen uptake and utilisation in plants

Nitrogen is a major constituent of most important plant molecules including nucleic acids, proteins, chlorophyll and phytohormones (auxin, cytokinins). Although N_2 is the dominant gas in our atmosphere (~78 vol%) plants cannot use this source directly due to the lack of nitrogenase. This nitrogen fixing enzyme is present in various prokaryotes (e.g. some cyanobacteria strains), which are the only organisms capable of converting atmospheric nitrogen (N_2) into bioavailable ammonia (NH_3). Nonetheless, some plants, mainly from the legume family, evolved a symbiotic relationship with specific bacteria (*Rhizobia*). Within this symbiosis, distinct root structures, called nodules, are formed where the bacteria fix N_2, and in return are provided with other nutrients by the plant. Other plants, including crops, have not evolved this relationship and are dependent on N uptake from the soil through the roots, where nitrogenous compounds have to cross the plasma membrane to enter the cells. This process is mediated by substrate specific H^+ co-transport proteins that rely on a proton gradient. Although nitrogen can be taken up by the roots in the form of amino acids (Hirner *et al.*, 2006; Lee *et al.*, 2007), urea (Kojima *et al.*, 2007) or peptides (Komarova *et al.*, 2008), the most important soil nitrogen sources are ammonium and nitrate, which are taken up by transporters from the ammonium transporter (AMT) and nitrate transporter (NRT) families, respectively. In general nitrate levels are higher in comparison to ammonium, with average levels of 6.0 mM and 0.77 mM in agricultural soil samples (Crawford and Glass, 1998), respectively. These concentrations can heavily fluctuate due to biotic and abiotic factors (Crawford and Glass, 1998). In order to cope with the varying concentrations of nitrogenous compounds in the soil, transporters from the AMT and NRT families show different affinities and are also regulated by the availability of their respective substrates (see Nacry *et al.*, 2013, for a recent review). The NRTs can be divided into the two subgroups NRT2, which contains high affinity nitrate transporters and is represented by seven candidates in

Arabidopsis (Glass *et al.*, 2002) and the larger Nitrate/Peptide Transporter (NPF) family containing 53 members in Arabidopsis (Tsay *et al.*, 2007). Many NPF transporters have no, or no exclusive function, with respect to importing soil bound nitrogen into the roots, but also do participate in nitrogen distribution throughout the whole plant and will be presented in more detail in section 1.4..

Before being utilised for biosynthesis of different nitrogen containing molecules, nitrate has to be reduced to ammonium via the following reactions:

I) $NO_3^- + 2\ NADH(H^+) \rightarrow NO_2^- + 2\ NAD^+ + H_2O$

II) $NO_2^- + 6$ Ferredoxin (red.) $+ 8\ H^+ \rightarrow NH_4^+ + 2\ H_2O + 6$ Ferredoxin (ox.)

The first reaction is catalysed by nitrate reductase in the cytosol, while the second one is conferred by nitrite reductase within the plastids. Ammonium is the final inorganic form of nitrogen and is subsequently incorporated in all other molecules (Lea *et al.*, 1990), with glutamate (Glu) being the central metabolite for both the amination and the de-amination processes. The primary nitrogen incorporation into organic molecules is conferred by the GS/GOGAT cycle. First, ammonium is transferred to Glu by glutamine synthase (GS) forming glutamine (Gln), which can happen in the plastids or the cytosol by the activity of GS2 and GS1, respectively. In a second step glutamine oxoglutarate aminotransferase (GOGAT) in plastids catalyses the reaction of Gln and 2-oxo-glutarate to two molecules of Glu, so that one molecule can act as acceptor in the next round of ammonium fixation, while the second one can be used for the biosynthesis of other nitrogen containing molecules. Glu can also be generated by direct amination of 2-oxoglutarate through the activity of glutamate dehydrogenase (GDH), but experimental evidence rather supports a function for GDH in the de-amination processes and the role of GDH in primary nitrogen assimilation is still under discussion (Miflin and Habash, 2002). Glu can then be directly converted into alanine (Ala) and aspartate (Asp) through trans-amination reactions with pyruvate and oxaloacetate, respectively. Asp itself represents a precursor for the biosynthesis of asparagine (Asn) or lysine (Lys). Taken together, all nitrogenous compounds can be synthesised *in planta* from Glu through a series of biochemical reactions and conversions.

Depending on whether nitrogen is taken up as nitrate or ammonium the subsequent usage can differ. In most cases, ammonium is directly incorporated into Glu in the roots and either used to supply the nitrogen demand within the roots or transported to other sink tissues, while most nitrate is directly transported to above ground tissues, where it is reduced to ammonia.

1.3. Senescence – processes and regulation

During the lifecycle of annual plants all parental tissues undergo sequential developmental stages from initiation and growth, until full functionality. After a certain period of time ageing/senescence processes, accompanied by a reduction of functionality and changes on the transcriptional and metabolic level, become obvious and finally lead to the death of organs or the whole plant. The only surviving parts are the seeds, which represent the next generation of plants. Senescence processes in plants are particularly visible in leaves, where a gradual change in colour from green to yellow can be observed without any further devices. Looking at annual plants during their development, it is also obvious, that these processes do not happen in all tissues at the same time, but show a gradient from the level of the whole plant down to the organ level. For example, in barley the oldest leaves undergo senescence, before the plant reaches maturity and changes in colour first become obvious at the leaf tips, before gradually spreading to the petiole.

Despite leading to tissue deterioration and death, senescence is a highly regulated developmental programme that requires active transcription as well as translation of new, specific mRNAs and proteins, respectively (Smart, 1994). Leaf senescence involves a series of highly regulated events involving cessation of photosynthesis, chloroplast disintegration and degradation of proteins, chlorophyll, and nucleic acids (Buchanan-Wollaston, 1997). These catabolic processes lead to the release of high amounts of nutrients (e.g. N, C or minerals), which are subsequently transported to other parts of the plant (Buchanan-Wollaston, 1997).

Although senescence is an inherent step in the development of leaves, they cannot undergo senescence at every developmental stage, but need to acquire the competence (Hensel *et al.*, 1993; Weaver *et al.*, 1998). This competence might be conferred by age-related-changes, that are irreversible and strictly dependent on age and thus development (Jibran *et al.*, 2013). Even when this competence is acquired, execution and timing of the senescence programme is still dependent on various internal and external factors (Smart, 1994). Abiotic stresses including drought, pathogen attack or nutrient deprivation can induce or accelerate senescence processes (Navarre and Wolpert, 1999; Munné-Bosch and Alegre, 2004; Schildhauer *et al.*, 2008). Internal factors modulating senescence include levels of different hormones, as cytokinins or gibberelic acid retard, while ethylene and abscisic acid promote senescence (Schippers *et al.*, 2007). The onset of reproduction in annual plants is another important internal factor influencing senescence, as it leads to senescence of the whole plant (Noodén, 1988a, 1988b). All these senescence-associated changes/phenotypes are orchestrated through changes in the transcriptome and several hundred transcripts that are differentially expressed have been identified from different species (Smart, 1994; Buchanan-

Wollaston, 1997; Ay *et al.*, 2008; Breeze *et al.*, 2011). Based on their expression patterns the senescence-associated genes (SAG) can be grouped into different classes (Smart, 1994; Buchanan-Wollaston, 1997) that are involved in different aspects of initiation and progression of senescence. In accordance with reduced photosynthetic activity and yellowing of green tissues, photosynthesis-associated genes, such as chlorophyll-binding proteins, Ribulose-1,5-bisphosphate carboxylase/oxygenase (RuBisCO) or structural proteins of the photosystem, mainly show down-regulation during senescence. On the other hand transcripts involved in catabolism, transport processes and regulation of transcription are up-regulated.

This large scale reprogramming of the transcriptome requires the differential expression of different transcription factors (TFs) that can work synergistically or antagonistically in regulating developmental processes. Among the up-regulated TFs during senescence, the two plant-specific WRKY and NAC TFs represent the largest groups (Guo *et al.*, 2004). WRKY-TFs are zinc-finger-like TFs containing one or two conserved WRKY domains at their N-terminus, that confer DNA binding (Eulgem *et al.*, 2000). This family comprises 79 members in Arabidopsis (Rushton *et al.*, 2010) and most WRKY-TFs from Arabidopsis have been characterised as regulators of stress responses and senescence (Eulgem and Somssich, 2007). Especially AtWRKY53 has been subject to extensive studies since its discovery as early up-regulated during senescence (Hinderhofer and Zentgraf, 2001). The analysis of over-expressing and knock-out lines showed accelerated and delayed senescence phenotypes, respectively, revealing an important role for AtWRKY53 in regulating onset/progression of senescence (Miao *et al.*, 2004). It has also been shown that expression, as well as activity and degradation of AtWRKY53 are regulated on several levels, and this complex regulation of one TF might give a glimpse into the sophisticated regulatory network, that is involved in the execution of senescence (Zentgraf *et al.*, 2010).

NAC-TFs are named after the first characterised members of this group namely NAM (no apical meristem), ATAF1,2 (*Arabidopsis thaliana* activating factor) and CUC2 (cup-shaped cotyledon) and are involved in various developmental processes (reviewed in (Olsen et al., 2005)).They contain a highly conserved N-terminal NAC domain, that can bind both DNA and other proteins, accompanied by diverse C-terminal domains (Ernst *et al.*, 2004). AtORE1 was first identified as a positive regulator of leaf senescence (Aeong Oh *et al.*, 1997), and in recent years parts of a regulatory network involving AtORE1 was elucidated (Kim *et al.*, 2009; Balazadeh *et al.*, 2010; Matallana-Ramirez *et al.*, 2013). In barley several NAC TFs show differential co-regulation with senescence-associated genes during senescence of flag leaves, and putative NAC binding sites are over-represented in the promoters of SAGs (Christiansen and Gregersen, 2014). Further candidates seem to be directly involved in senescence-associated N (and mineral) remobilisation, like NAM-B1 from wheat that

accelerates senescence and increases nutrient remobilisation from leaves to developing grains (Uauy *et al.*, 2006; Waters *et al.*, 2009).

Protein degradation is a crucial process to release N for export from leaves, as up to 75% of nitrogen in leaf mesophyll cells is located in the chloroplasts, with stromal enzymes (mainly RuBisCo) accounting for the largest fraction (Peoples and Dalling, 1988). Protein degradation is dependent on the activity of proteases, that can be classified according to their mode of action and the structure of their catalytic centre (Rawlings *et al.*, 2014). Accordingly, a large number of proteases are up-regulated during leaf senescence in Arabidopsis (Buchanan-Wollaston *et al.*, 2003). Despite the importance of plastidial protein breakdown for nitrogen remobilisation, the underlying mechanisms are still not completely resolved and there are indications of degradation processes inside, as well as outside the plastids (Martínez et al., 2008). *In vitro* studies showed initial degradation of RuBisCo in isolated wheat chloroplasts, rendering 44 kDa and 51 kDa fragments of the large subunit, but no further degradation (Kokubun *et al.*, 2002; Zhang *et al.*, 2007). Further steps in the degradation of RuBisCo could be linked to small-senescence-associated vehicles, which emerge during leaf senescence and contain SAG12, a cysteine peptidase, specifically up-regulated during developmental senescence (Noh and Amasino, 1999; Otegui *et al.*, 2005).

After degradation of proteins the resulting products, amino acids and peptides, must be exported to other tissues. While the information about peptide remobilisation is still scarce, nitrogen remobilisation during leaf senescence has been analysed in more detail. In wheat free amino acids are transported via the phloem to developing seeds either directly or indirectly via glumes and/or roots (Simpson *et al.*, 1983). The major amino acids transported in the phloem of barley and wheat are Glu, Gln, Asp, threonine (Thr) and serine (Ser) (Winter *et al.*, 1992; Caputo *et al.*, 2001). While many genes involved in amino acid biosynthesis are down-regulated during senescence, other specific enzymes show increasing transcript abundances. Enzymes involved in primary nitrogen assimilation NR, GOGAT and, consistent with the dismantling of the chloroplasts, plastidial GS2 are down-regulated, while transcription of cytosolic GS1 and GDH is increasing (Masclaux *et al.*, 2000). During the course of senescence, Glu can be generated from the catabolism of other amino acids, and further de-aminated through GDH, producing 2-oxoglutarate and ammonia. 2-oxoglutarate can fuel energy generation through the TCA, while the released ammonia can be re-assimilated into Gln by GS1 and subsequently transported to sink tissues (Miyashita and Good, 2008a).

Most efforts characterising senescence so far have been focussing on processes happening in leaves. Considering the important role of glumes in providing C and N during grain filling in cereals (see 1.1.), a better understanding of glumes´ senescence could provide new insights in specific remobilisation processes and thus yield potentials for crop improvement.

1.4. Transporters for (remobilised) nitrogen

The efficient reallocation of nitrogenous compounds, such as amino acids and small peptides, from the place of primary acquisition or remobilisation to sink tissues is based on the activity of specialised transporters. These transporters allow their respective substrates to cross membranes in order to be transferred from cell to cell, or enter and leave the vasculature for long-distance transport. Candidates for uptake and distribution of amino acids and peptides can be found in the large groups of amino acid transporters (AAT), the nitrate/peptide transporters (NPF) and the oligopeptide transporters (OPT), that can be further subdivided based on their substrates and/or their similarity at the amino acid level (Table 1).

Table 1 Transporters for remobilised nitrogen

	Amino acid transporters		Nitrate/Peptide transporters (NPF)	Oligopeptide transporters
Subfamilies	Amino acid transporter family (ATF): Amino acid permeases (AAP), Proline transporters (ProT), Lysine histidine transporters (LHT), GABA transporters (GAT), Aromatic/neutral amino acid transporters (ANT), Auxin permease 1-like (AUX)	Amino acid-polyamine-choline-facilitators (APC): Cationic amino acid transporters (CAT), L-type amino acid transporters (LAT), GABA permeases (GAP)	8 clades	Oligopeptide transporters (OPT), Yellow-stripe-like transporters (YSL)
Structure	9 - 11 TMD	12 - 14 TMD	12 TMD	12 - 14 TMD
Energy source	Proton gradient	Proton gradient	Proton gradient	Proton gradient
Substrate	amino acids, auxin		nitrate, di- and tripeptides, ABA, glucosinolates	phytosiderophores, tetra- and pentapeptides

The AAT family contains 61 members in Arabidopsis and can be classified into 2 larger gene families and 9 subfamilies that can be distinguished by their substrate specificities and affinities (Rentsch *et al.*, 2007; Tegeder and Rentsch, 2010). Import of organic nitrogen, in the form of amino acids, into cells takes place throughout the entire development of plants in all tissues and is mediated by different candidates from different subfamilies: e.g. AtLHT1 and AtProT2 import amino acids in roots or leaf mesophyll cells (Hirner *et al.*, 2006; Lehmann *et al.*, 2011), while AtAAP2 confers long distance transport (Zhang *et al.*, 2010) or AtAAP1 and AtAAP8 which supply developing seeds (Schmidt *et al.*, 2007; Sanders *et al.*,

2009). Although AATs have overlapping substrates their expression shows tissue- and development-specific patterns, indicating distinct roles *in planta* for each candidate. On the other hand the overlapping substrates make it difficult to assign specific functions to certain transporters *in planta* through knock outs, as it is typical that more than one AAT is expressed in a certain tissue at a certain time point, and thus could compensate for the loss of function of another candidate.

Most transporters characterised so far are involved in amino acid uptake into cells. However, AtBAT1 has been recently described as bi-directional transporter, that mediates the import of Arg and Ala, and the export of Lys and Glu in yeast (Dündar and Bush, 2009), and the expression of AtBAT1 in the vasculature of sink tissues suggests a function in phloem unloading (Dündar, 2009). Another protein that can export amino acids from cells was found within the Arabidopsis Medicago truncatula NODULIN21 (MtN21) gene family belonging to the plant drug/metabolite exporter family. Based on its phenotype, accumulation of anthocyanins in the youngest siliques under constant light conditions, this protein was named Siliques Are Red1 (AtSIAR1), and confirmed to import as well as export amino acids from yeast cells and xenopus oocytes. Expression patterns suggest a function in the export of amino acids into the apoplast prior to long distance transport or an uptake by reproductive structures (Ladwig *et al.*, 2012).

The second large group harbouring transporters putatively involved in nitrogen cycling within plants is the NPF. Originally this group was named NRT1/PTR family after the identified substrates of different candidates, such as the dual affinity nitrate transporter AtCHL1/NRT1.1 (Tsay *et al.*, 1993), the low affinity nitrate transporter AtNRT1.2 (Huang *et al.*, 1999) or the peptide transporters HvPTR (West *et al.*, 1998) and AtPTR1 (Dietrich *et al.*, 2004). Further research within this family and across different species showed that possible substrates are not limited to nitrate or peptides, but could also include other substrates, e.g. amino acids (Zhou *et al.*, 1998) or abscisic acid (Kanno *et al.*, 2012). Nonetheless, this group was recently renamed to NPF, for NRT1/PTR Family and a phylogenetic analysis including all NPF members from 31 sequenced plant species identified eight unambiguous clades within this family (Léran *et al.*, 2014). This new grouping could hint to substrate specificities of certain candidates for future analyses. While nitrate transporters can be found in all clades, the ABA transporters (as functionally characterised at this time) are restricted to clade 4, the glucosinolate transporters to clade 2 and three out of four Arabidopsis peptide transporters can be found in clade 8 (Léran *et al.*, 2014).

After the genome sequence of Arabidopsis became available, nine putative OPTs were identified based on their sequence similarity to the respective yeast genes. Functionality of several transporters was verified *in vitro*, and tissue-specific expression patterns indicated distinct functions for each candidate (Koh *et al.*, 2002). Phylogenetic relationship analysis of

the Yellow-stripe-1 transporter from maize (ZmYS1), which imports Fe(III)-phytosiderophores in roots (Curie *et al.*, 2001), showed that ZmYS1 and its eight homologues from Arabidopsis clustered to the OPT family and the Yellow-stripe-like (YSL) subgroup was defined (Yen *et al.*, 2001). Although originally described as peptide transporters, the rice OPT OsGT1 was shown to transport glutathione (Zhang *et al.*, 2004) and AtOPT3 is important for whole-plant iron homeostasis and iron nutrition of developing seeds in Arabidopsis (Stacey *et al.*, 2008). These findings suggest alternative/additional roles, at least for certain members of the OPT family, and several putative functions during plant development are currently under discussion (Lubkowitz, 2011).

Despite their apparent importance for N remobilisation, and thus grain nutrition, the role of N transporters with respect to cereal grain development is still not well characterised. Recently Peng *et al.* (2014) showed that increased expression of OsAAP6 leads to higher grain protein content in rice without impairing yield, which hints at the potential of utilising N transporters as a mean to improve the nutritional quality of grains.

2. Aim of the project

Several studies have addressed specific aspects of nitrogen translocation from vegetative tissues to developing crop seeds, and changes in metabolite and transcript profiles during development of specific organs. Those studies have demonstrated important functions for flag leaves and glumes in nurturing developing grains, and showed transcriptional and/or metabolic changes occurring during the development of isolated organs. These results clearly show alterations in the metabolism of vegetative tissues that are timely correlated with the developmental status of the grains. However, a comprehensive approach, combining metabolic and transcriptional analyses using material from different organs of the same plants during development is still missing.

The general aim of this project is to close this gap, and analyse the influences of the developmental status of the grains on the adjacent vegetative tissues, the glumes and flag leaves. In order to elucidate the dynamic interactions between sink and source tissues, following questions will be addressed:

- What are the temporal and spatial patterns of N translocation?
- What adaptations in metabolism are induced by the increasing nutrient demand of developing grains?
- How is this demand signalled?
- Which transporters are transcriptionally up-regulated in sink and source tissues?
- What regulatory components are involved?
- Can alteration of sink-strength improve grain quality and/or affect yield?

Answering these questions will extend the current knowledge of N remobilisation processes that are essential for proper grain development. Furthermore, the identification of regulatory components of N remobilisation and involved N transporters will provide new starting-points for future works addressing crop improvement.

3. Experimental approaches

At the beginning of this project, the full genomic sequence for barley was not available, and although a large collection of barley cDNAs was summarised in the HarvEST35 assembly (H35), some considerations led to the decision to perform transcriptome sequencing (RNAseq) from flag leaves, glumes and grains. Despite the total number of 444,648 ESTs included in H35, only 264 sequences derived from glumes. In contrast, more sequence data originating from flag leaves or grains is included, but often representing only specific stages and no developmental series. The preparation method of the cDNA libraries via subcloning in *E. coli* harbours another problem, as it is not clear if the cloning of plant transcripts and especially of membrane proteins in *E. coli* works for every transcript with the same efficiency. Therefore specific transcripts might be under-represented or simply not present in the available libraries. RNA libraries were prepared separately for each tissue comprising material from -4 to 24 days after flowering (DAF) and pyrosequencing was done by GATC Biotech (Konstanz, Germany) using the Roche/454 GS-FLX Titanium technology.

The generated reads were assembled separately for each library, and analysed with respect to functional annotation and tissue-specificity. Based on sequence similarities to annotated N transporters, putative candidates from the RNAseq approach were extracted, complemented with H35 information and subjected to a phylogenetic analysis. This approach was also used to identify and characterise cysteine peptidases. This analysis was done by J. Hollmann and not the focus of our work, therefore this part was left out in the summary of the publication. Subsequently, the temporal expression patterns of 25 amino acid transporters were analysed via qRT-PCR. For this approach material was sampled in two day steps starting from -4 (flag leaves and glumes) and 4 (endosperm) until 24 DAF.

In order to identify interactions between glumes and grains during development, material was harvested from glumes and endosperm until 24 DAF, starting at 0 and 4 DAF, respectively. This material was sampled simultaneously and then subjected to physiological, transcript and metabolite analyses.

Accumulation of weight, total N and starch were measured and compared between glumes and the endosperm. The dynamics of free amino acid concentrations in glumes and endosperm during development were detected by UPLC. These profiles were analysed and then correlated with the respective profiles from the grain vasculature, which were derived from GC-MS measurements of micro-dissected material. Large scale metabolite profiling of complete organs was performed via GC-MS measurements and the results were analysed with respect to the corresponding transcriptional activities. For analysing the transcriptomes a new microarray was designed, because the commercially available ones were outdated. This was due to the increasing sequence information for barley transcripts in recent years,

provided by next generation sequencing approaches and new cDNA collections. In order to create this new microarray, transcript data from H35, two RNAseq experiments (Kohl *et al.*, 2012; Thiel *et al.*, 2012) and a full-length cDNA collection (Matsumoto *et al.*, 2011) were used. These sequences were assembled into 46,114 unique barley contigs, which were annotated against different databases and used for creating a customised 8x60k Agilent microarray. This array was then hybridised with time-course material from glumes and the endosperm.

For analysing the influence of increased grain sink-strength on grain development and nutrient composition of mature grains, a transgenic approach was chosen. The barley sucrose transporter 1 (HvSUT1, SUT) was over-expressed in the endosperm of winter wheat (cv Certo) during storage product accumulation. In order to ensure tissue- and time point-specific expression, the transporter was cloned between the promoter and terminator of the barley Hordein B1 storage protein (HO), and several independent HOSUT-lines were generated. Three lines (HOSUT10, 11 and 20), each containing one copy of the transgene, were selected for further analysis and compared to wild type (WT) plants.

Expression of the transgene and its physiological functionality were tested by qRT-PCR and *in vitro* uptake experiments, respectively. Growth parameters and ABA levels were determined between 6 and 34 DAF and compared to WT plants. In order to discover influences of the transgene expression on general and especially storage metabolism, the composition of mature grains and metabolite profiles during development (detected by GC-MS) were compared between HOSUT10 and WT plants.

Transcripts, which are differentially expressed during development in HOSUT10 and WT plants, were identified by cRNA hybridisation to the Affimetrix GeneChip Wheat Genome Array. Out of ~1,700 identified transcripts, 109 candidates with clear annotations in metabolic or physiological processes were selected for further analysis, and expression profiles between 6 and 34 DAF were validated by qRT-PCR.

The experiments, designed and conducted by me, did not contribute the substantial part to this publication, but as this work essentially extended the knowledge about the physiological consequences and the molecular mechanisms triggered by sink manipulation in cereal grains, the results will be presented and discussed in detail.

4. Results and discussion

4.1. RNA sequencing, identification of N transporters and their expression profiles

4.1.1. Global RNAseq analysis reveals differences in glumes transcriptome compared to flag leaf and grains

After adaptor and quality trimming, the sequencing approach yielded 615,568, 485,800, and 484,443 single reads from flag leaves, glumes and grains, respectively, with average lengths between 392 and 400 base pairs (Table 2).

Table 2 Large scale RNAseq output and HarvEST35 (H35) annotation

		Flag leaf	Glumes	Grain
Total output	Total reads	615,568	485,800	484,443
	Ø Read length	397	400	392
	Total contigs	43,467	31,022	37,790
	Ø Reads/contig	12	15	11
	Ø Contig size	688	835	791
	Total singletons	97,348	29,388	82,446
Contig annotation against H35	BlastN Hits (e^{-20})	33,743 (77.6%)	24,416 (78.7%)	30,077 (79.6%)
	No Hits	9,724 (22.4%)	6,606 (21.3%)	7,713 (20.4%)

adapted from Kohl *et al.*, 2012

Subsequently an assembly of the single reads was performed and 43,476 flag leaf (FL), 31,022 glumes (GL) and 37,790 grain (G) contigs were generated. The average lengths of these contigs varied from 688 base pairs in flag leaves to 835 base pairs in glumes. Additionally 97,348 flag leaf, 29,388 glumes and 82,446 grain reads could not be assembled (= singletons) and were not used for further analysis. High numbers of singletons or high contig numbers together with low contig lengths are an indication for a high number of low abundant transcripts while the opposite constellation hints to a lower number of highly expressed transcripts. The results of this assembly suggest either a low complexity or a high specificity of glumes transcriptome compared with grains and especially flag leaves. In order to identify the level of new information yielded by the RNAseq approach, contigs were compared against H35 and more than 20% represent new barley sequence information (Table 2).

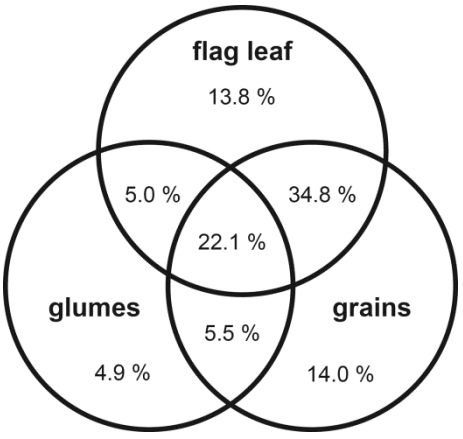

Figure 3 Venn diagram showing tissue specificity of the CAP3-contigs (Kohl, *et al.*, 2012).

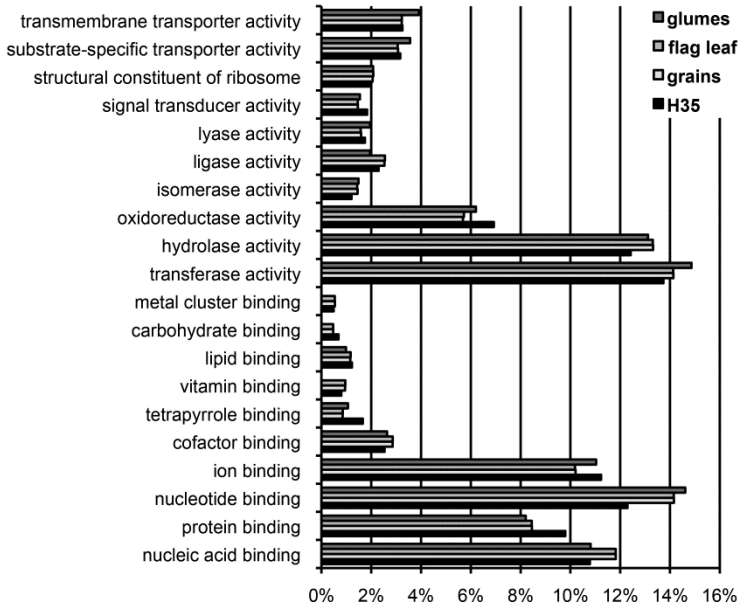

Figure 4 Blast2GO annotations of RNAseq contigs and H35 unigenes. The result is based on gene ontology terms level 3 of the category Molecular Function. 21,525 sequences from leaves, 10,361 sequences from glumes, 21,199 sequences from grains and 22,043 sequences from the H35 database were annotated (Kohl *et al.*, 2012).

A comparison between the tissues revealed that ~22% of transcripts were shared between all tissues, while ~5% (GL) and ~14% (FL and G) were specific for each tissue (Figure 3). Interestingly nearly 35% of transcripts overlap between flag leaves and grains, while glumes only share ~5% with one of the other tissues.

This result was approved by analysis of the functional annotation according to GO categories, where FL and G showed a comparable distribution within the categories, while GL showed a different distribution, that was more comparable with H35 (Figure 4). Taken together, these results show that the barley glumes´ transcriptome clearly differs from the transcriptome of flag leaves and grains, although glumes evolved as leave-like structures. Since the H35 assembly contains sequence information from different tissues collected over a broad range of developmental stages, it represents an average of various organs with specific functions. The comparable distribution of glumes contigs and H35 according to GO categories indicates that barley glumes have to fulfil a broad range of different functions during grain development. Whether these different functions are equally active throughout development, or if the role of glumes changes during the time line analysed cannot be clarified with the RNAseq approach, but was later resolved through microarray analysis.

4.1.2. RNAseq adds new and complements available sequence information of barley N transporters

When searching H35 for contigs annotated as transporters from the AAT, NPF, or OPT a high number in comparison to Arabidopsis, becomes evident (134 versus 63, 103 versus 52 and 42 versus 17, respectively). Together with the low level of sequence information with respect to the average amino acid (aa) length and full length sequences (191 aa and 12 full-length, 190 aa and 3 full-length, 192 aa and 0 full-length, respectively), this indicates missing sequence information, as well as a certain redundancy within H35. For identification of

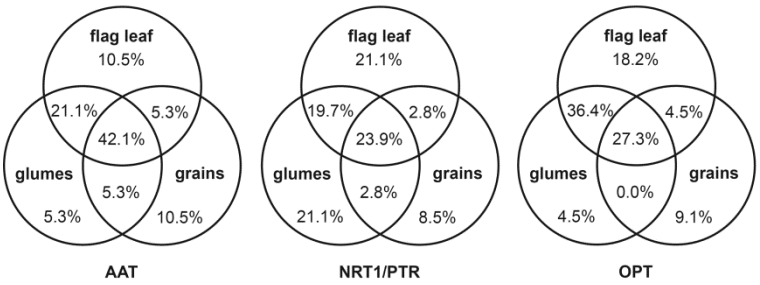

Figure 5 Venn diagrams showing tissue-specific expression of N transporters (adapted from Kohl *et al.*, 2012).

putative N transporters within the RNAseq dataset, a BlastN comparison with the candidates from H35 was performed and yielded 147, 165 and 59 contigs belonging to the AAT, NPF or OPT transporter families in all tissues, respectively. In case of the N transporters, the analysis of tissue-specificity (Figure 5) showed completely opposing trends compared to the distribution of functional categories between the tissues (Figure 4). The numbers of contigs shared between all tissues is higher than for the complete dataset. This observation is especially prominent for the AATs with more than 40%, indicating a general and important role for candidates from this group in different tissues. On the other hand more than 50% of NPFs show tissue-specific expression that can be explained by organ-specific transport demands for their respective substrates. Furthermore the overlap of contigs between flag leaves and glumes is always higher than the overlap between grains and one of the other tissues. That means that despite differences in their overall transcriptome flag leaves and glumes share common characteristics with respect to N transport, while grains rely on other specific mechanisms.

In order to complement the present information and evaluate the power of the RNAseq approach for N transporters the contigs from H35 and RNAseq were assembled. Although it was expected to reduce redundancy in H35 by applying the assembly, there was no clear tendency towards lower contig numbers afterwards, while the average contig length was

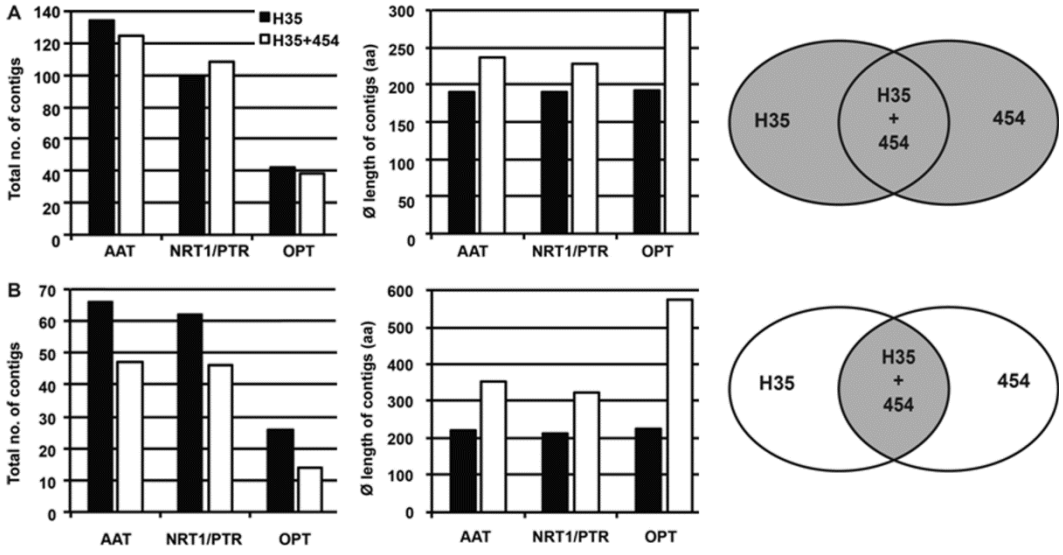

Figure 6 Number and average length of unigenes encoding putative N transporters. (A) Total number and average length of contigs after assembly of all N transporter unigenes available from RNAseq (454) and H35. (B) Number and length of N transporter contigs containing sequence information overlapping between the two sources. Black bars represent H35 information; white bars show results after combining H35 and RNAseq unigenes. Origin of sequences is represented by gray-shaded areas in the ellipses at the right-hand side (adapted from Kohl *et al.*, 2012).

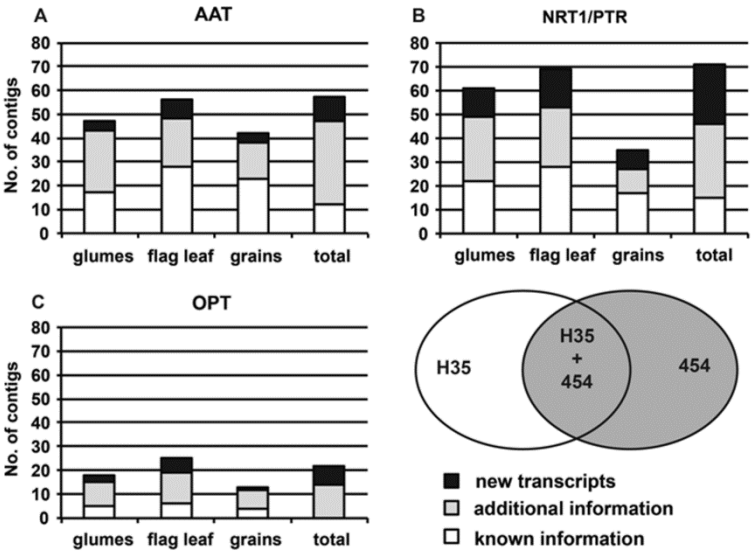

Figure 7 New sequence information for N transporter genes. Comparison of RNAseq (454) and H35 unigenes for (A) *AAT*, (B) *NPF* (*NRT1/PTR)* and (C) *OPT* transporter sequences. New information (black areas) from RNAseq showed less than 98% identity to H35 unigenes at amino acid level. Additional information (gray-shaded) matched H35 unigenes and extended information by more than 50 bp, or allowed to join unigenes. Known information (white areas) did not add new knowledge. Origin of sequences is represented by gray-shaded areas of the overlapping ellipses at the right side (adapted from Kohl *et al.*. 2012).

increased (Figure 6a).

This may be due to the presence of genomic sequences and chimeric clones within H35. Another factor that has to be taken into consideration when interpreting the H35 dataset is the presence of sequences deriving from various cultivars, that can vary in their untranslated regions and by that prevent a correct assembly. For further analysis only contigs containing either only RNAseq or RNAseq and H35 sequences were taken into consideration. Comparing the original H35 contig numbers and lengths, the numbers have been reduced between 23% (NPF) and 46% (OPT), while the average amino acid lengths increased from 47% to 157% depending on the transporter group (Figure 6b). This approach also showed that between 78% (NPF) and 100% (OPT) of RNAseq contigs extended existing H35 information or provided new sequences (Figure 7). Furthermore, the number of barley full-length cDNA sequences was increased from 12 to 25, 3 to 8 and 0 to 5 for AATs, NPFs and OPTs, respectively.

4.1.3. RNAseq derived barley N transporters can be classified according to annotated candidates from other plant species

The previous analysis yielded 57, 71 and 21 candidates from AAT, NPF and OPT, respectively, that are transcribed in vegetative and generative tissues during barley grain development. In order to classify them, alignments of the corresponding amino acid sequences were performed with transporters from Arabidopsis and rice annotated in the Aramemnon database (Schwacke *et al.*, 2003). Phylogenetic trees were calculated and all barley AAT and OPT sequences clustered within the groups described by Rentsch *et al.* (2007) and Zheng *et al.* (2011), respectively (Figure 8). Furthermore, the total numbers in the respective groups correspond to rice and Arabidopsis. From the 71 NPF sequences only 46 clustered into the four subgroups defined by Tsay *et al.* (2007), which might be due to limited

sequence information. The 46 candidates that clustered had an average length of 305 aa, while the 25 candidates that did not cluster only had an average length of 185 aa, which could have prevented a proper alignment.

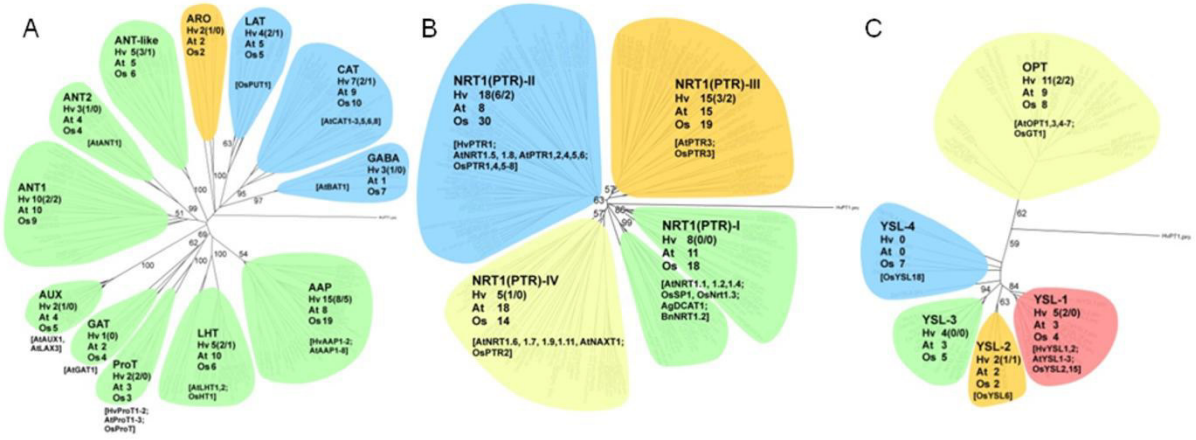

Figure 8 Phylogenetic trees of plant N transporters. (A) Clustering of 63 Arabidopsis, 80 rice and 59 unique barley AAT sequences with *H. vulgare* phosphate transporter 1 (HvPT1) as out-group. Colours indicate membership to different subgroups of ATF (green) and APC (blue) families, members of the aromatic amino acid transporters are shown in orange. Full-length barley sequences are given in brackets (total number/new from RNAseq). Sequences from Arabidopsis and rice, including their respective nomenclature, were extracted from Aramemnon, barley sequences derived from RNAseq, H35 (only full-length sequences), publications (HvProT, HvProT2) and previous unpublished work (HvAAP1+2). The phylogenetic tree was constructed using the neighbour-joining algorithm in the program PAUP* (Swofford, 2002). The tree was displayed and manipulated using FigTree (http://tree.bio.ed.ac.uk/software/figtree/). (B) Clustering of 52 Arabidopsis, 81 rice and 46 unique barley NPF sequences; for consolidation of the tree, sequences from *Alnus glutinosa* (AgDCAT1) and *Brassica napa* (BnNRT1) were included (according to Tsay *et al*., 2007). Colours indicate membership to subgroups I (green), II (blue), III (orange) and IV (yellow) as defined by Tsay *et al.* (2007). Barley sequences were derived from RNAseq, H35 (only full-length sequences), publications (HvPTR1) and previous unpublished work (IPK_HvPTR2, 3, 6). (C) Clustering of 17 Arabidopsis, 26 rice and 22 unique barley OPT sequences. Colours indicate membership to the OPT (yellow) and the yellow stripe-like (YSL) family. According to Zheng *et al*., 2011, YSL transporter sequences are subdivided into the subgroups YSL-1 (red), YSL-2 (orange), YSL-3 (green) and YSL-4 (blue). Barley sequences were derived from RNAseq and publications (HvYSL1+2) and previous unpublished work (IPK_HvPTR2, 3, 6) (adapted from Kohl *et al*., 2012).

4.1.4. qRT-PCR expression profiles of amino acid transporters indicate different developmental phases in glumes, flag leafs and endosperm

For the further characterisation of amino acid transport processes in flag leaves, glumes and grains, qRT-PCR was performed for the 25 full-length transporters derived from the previous analysis. The overall characteristic of the dataset with regard to tissue-specificity is represented by the candidates showing the highest expression in the respective tissues (Figure 9 and Table 3). Within the general amino acid permeases, HvAAP4 and 7 are ubiquitously expressed in all tissues, while other transporters show high expression only in sink (HvAAP3) or in source (HvAAP2 and 6) tissues. Transporters from other subfamilies seem to be more tissue-specific, as high expression of candidates from the LHT and ProT subfamilies is limited to source tissues (HvLHT1 in glumes and HvLHT2 and HvProT1 in flag leaves, respectively), while high transcript abundances of ANT and CAT transporters mainly

Table 3 *AAT* genes with high expression in flag leaves, glumes and developing grains*

	Flag leaf	Glumes	Grains
AAP	*HvAAP2*	*HvAAP2*	-
	-	-	*HvAAP3*
	HvAAP4	*HvAAP4*	*HvAAP4*
	HvAAP6	*HvAAP6*	-
	HvAAP7	*HvAAP7*	*HvAAP7*
others	-	*HvLHT1*	-
	HvLHT2	-	-
	HvProT1	-	-
	-	*HvAUX1*	-
	-	-	*HvCAT1*
	-	-	*HvANT3*
	-	-	*HvANT4*

*For each tissue the six AAT genes showing highest expression levels are presented (Kohl *et al.*, 2012).

occur in developing grains (Table 3). The selective expression of barley LHT and ProT transporters in vegetative tissues is consistent with the findings in Arabidopsis, where AtLHT1 is preferentially expressed in leaf mesophyll cells (Hirner *et al.*, 2006) and AtProT1-3 are expressed in different tissue types, but not in seeds (Grallath *et al.*, 2005). These two groups might harbour promising candidates for elucidating the role of amino acid transporters in source tissue N remobilisation during barley grain filling. Grain-specific HvCAT1 on the other hand is similar to vacuolar-localised AtCAT2 (Su et al., 2004) and high expression values during late grain filling indicates storage of amino acids in vacuoles during barley grain filling. Such general assumptions cannot be made for the broadband transporters from the AAP group, where candidates have shown ubiquitous, as well as tissue-specific expression. Nonetheless, comparison with functions of Arabidopsis AAPs can help to reveal possible roles for the barley candidates. HvAAP3 showed grain-specific expression and is homologous to AtAAP1 and 8 involved in seed loading (Schmidt *et al.*, 2007; Sanders *et al.*, 2009), indicating a role for HvAAP3 in supplying amino acids to developing barley grains. In contrast, HvAAP2 and 6, highly expressed in glumes and flag leaves, are related to AtAAP2, 3 and 5 with an assumed function in long distance transport, phloem loading or xylem to phloem transfer, respectively (Rentsch *et al.*, 2007).

Global expression analysis in grains distinguished distinct developmental stages of barley grain development, starting with the pre-storage phase (0 to 4 DAF), followed by an intermediate phase (6 and 8 DAF) and the storage phase (10 to 24 DAF), before desiccation starts (Sreenivasulu *et al.*, 2004). In order to find development-related patterns of AAT expression, PCA analysis and K-means clustering was performed on the transcript data (Figure 9). This approach identified three distinct phases in grains comprising DAF 4 and 6 (early), 8 to 14 (intermediate) and DAF 16 onwards (late). While the early phase was characterised by high expression of specific AATs (e.g. HvAAP4 and 7), the intermediate phase showed generally lower expression values, before most candidates had their highest expression in the late phase. The observed shift of the intermediate phase in comparison to Sreenivasulu et al. (2004) can be explained by the fact, that high AAT expression is expected to be associated with storage protein synthesis. While starch is the dominant storage product

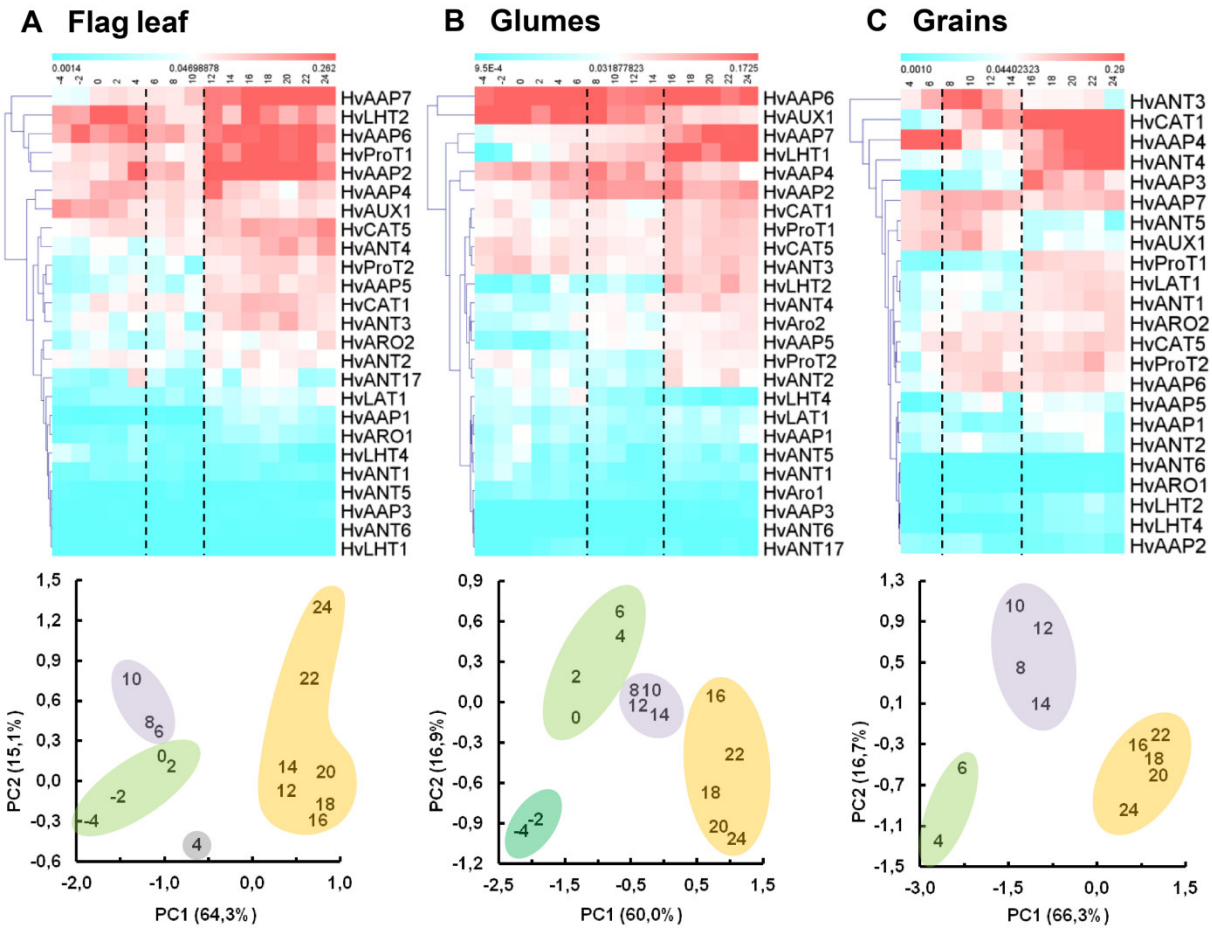

Figure 9 Transcript profiling, principle component analysis (PCA) and K-means clustering of 25 AAT genes. Distinct developmental phases were identified in flag leaves (A), glumes (B) and developing grains (C). Tissues were analysed in two-day steps starting at -4 DAF in flag leaves and glumes and at 4 DAF in developing grains until 24 DAF. The heat maps (upper panels) reflect relative transcript abundances (blue = low expression; red = high expression). Developmental phases as identified by PCA are given in the lower panels; numbers represent DAF. Results of K-means clustering are visualized by encircling of respective stages. Light violet areas represent the transition phase (Kohl *et al.*, 2012).

in barley and starts accumulating at 6 DAF (Radchuk *et al.*, 2009), storage protein deposition in the starchy endosperm begins at 10 DAF (Xiang and Bao, 1997).

Although highly expressed AATs differ between grains and glumes, expression clusters comprised identical time points. The additionally sampled stages in glumes either clustered to the pre-storage phase (DAF 0 and 2) or formed a separate cluster (DAF -4 and -2), which was marked by high expression of AATs. Therefore this pre-anthesis cluster could either supply glumes growth and/or flower development. As glumes dry weight and N content reach their maximum at 8 DAF (Figure 10) the two clusters comprising 8 to 14 and 16 to 24 DAF, respectively, likely resemble adaptations of glumes´ transport transcriptome to the changing demands of developing grains.

In flag leaves four different clusters are identified that were again characterised by high expression of specific candidates during early development, generally lower expression between 6 and 10 DAF and highest expression of most candidates during later development. Compared to glumes the patterns differ especially in early development, suggesting a

different function for flag leaves at this developmental stage. These differences might also be due to the different developmental status of the organs. While flag leaves are already completely developed, glumes are still growing and differentiating organs at anthesis. In flag leaves the late phase with high expression of AATs started at DAF 12, which was 4 days earlier, than in glumes or grains. This is remarkable as it indicates increasing amino acid transport activities before high nitrogen sink strength is established in developing grains.

4.2. Dissecting the development of glumes and its relationship to grain development

4.2.1. Accumulation dynamics of dry weight, starch, total N and free amino acids indicate a correlation between glumes development and grain storage protein synthesis

During early development, glumes´ (relative) dry weight (Dw) and total N (N) increased by about 40% between 0 and 8 DAF, which marked their maximum levels (Figures 10A and B). From 8 to 10 DAF a significant drop was observed for both parameters and was more pronounced for N (~30%) than for Dw (~20%). At 12 DAF the levels increased again, but while Dw was completely restored, N only reached ~80% of the maximum. Subsequently both values fluctuated at rather constant levels and decreased again between 18 and 24 DAF by ~10% (Dw) and ~20% (N). Starch content in glumes had its maximum at 0 DAF, before it decreased by ~60% and stayed constant until 24 DAF (Figure 10C). Endosperm Dw and N levels slowly increased in early development and entered the linear phase of accumulation at 8 (Dw) and 10 DAF (N), respectively (Figure 10A and B). While the linear increase in N continued until the end of the observation, Dw showed no significant increase after 18 DAF. Starch levels increased linear starting at 4 DAF and kept a constant level after 18 DAF (Figure 10C). These profiles were consistent with previous findings, e.g. Wobus et al. (2005), and underlined the temporal shift in the initial demand for C and N compounds, as well as the stability of the developmental programme for storage product accumulation in barley grains.

In glumes, summarised concentrations of free amino acids (FAA) increased from ~10 µmol/g (Fw) to more than 30 µmol/g (Fw) until 8 DAF, before a significant decrease of about ~50% was observed and levels were fluctuating at ~20 µmol/g (Fw) afterwards (Figure 11A). This strong decline in concentration between 8 and 10 DAF was reflected in most FAA, and especially pronounced for Asn, Pro and Glu (decrease of 86%, 74% and 71%, respectively). Asp on the other hand showed no major changes throughout development and levels for Glu stayed constant between 8 and 10 DAF, increasing afterwards.

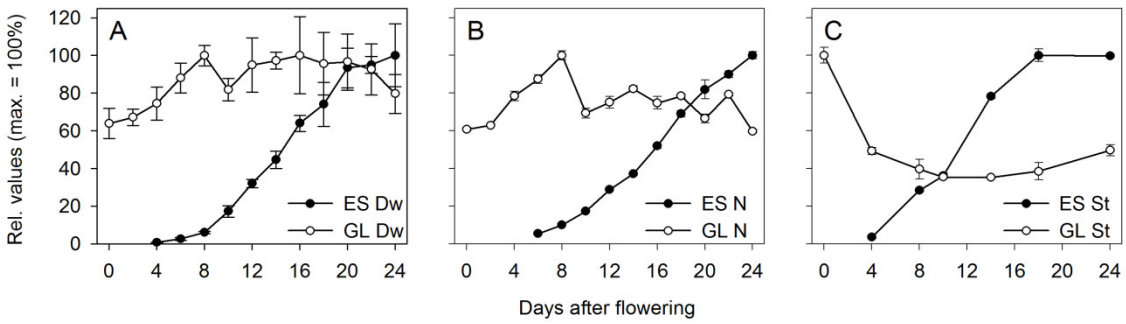

Figure 10 Changes of physiological parameters during endosperm (ES) and glumes (GL) development. Relative changes (maximum amount = 100%) of (A) dry weight (Dw); (B) total nitrogen (N) and (C) starch content (St) between 0 and 24 days after flowering (DAF). Data points represent three to five biological replicates +/-SD (Kohl *et al.*, 2015).

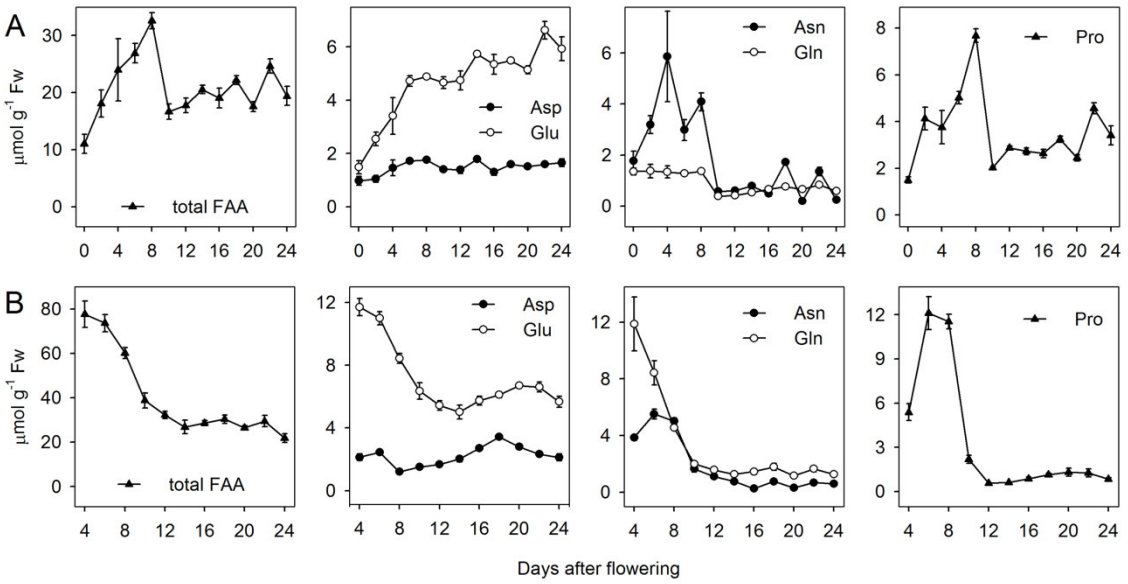

Figure 11 Concentrations of free amino acids in barley glumes (A) and endosperm (B) during development. Samples were measured via UPLC in two day steps from 0 (glumes) and 4 (endosperm) DAF, respectively. Each data point represents two (Arg, Gly) or three biological replicates +/-SD (adapted from Kohl *et al.*, 2015).

In the endosperm total concentrations of FAA declined from ~78 µmol/g (Fw) at 4 DAF to ~26 µmol/g (Fw) at 14 DAF, fluctuated then between 26 and 30 µmol/g (Fw) until 22 DAF, before decreasing to 22 µmol/g (Fw) at 24 DAF (Figure 11B). The strongest decline (~36%) was observed between 8 and 10 DAF and most pronounced for Pro, Gln and Asn (decreases of 81%, 67% and 56%, respectively).

Using a micro-dissection based approach, changes in FAA concentrations were determined in the vasculature of developing grains via GC-MS. All measured FAAs had their highest values at 4 or 8 DAF and low levels by the end of development (Figure 12, middle panel). In a next step, correlations between the relative FAA concentrations of glumes and vasculature as well as vasculature and the endosperm were determined (Figure 12). This comparison showed that levels of most determined FAA were positively and significantly correlated between vasculature and endosperm, with most $C_{Vc,Es}$>0.8. Comparison between vasculature and glumes on the other hand showed a mixture of positive and negative correlations and highest $C_{Vc,Gl}$ values were obtained for Gln (0.76) and Glu (-0.88).

Taken together these profiles showed that glumes were growing, N accumulating organs until 8 DAF, before N was relocated, while the endosperm was constantly accumulating dry weight and N, but starch accumulation ceased after 18 DAF. The decrease of total N content and free amino acid concentrations between 8 and 10 DAF in glumes coincided with the start of linear N accumulation in the developing endosperm and most likely represents a consequence of increasing N sink strength in grains.

In wheat, most N entering the grain, although not originally deriving from glumes, is cycled through the glumes (Simpson *et al.*, 1983). Therefore temporary increases and fluctuating N levels after 8 DAF in barley glumes was likely a result of the balance of N import from other

	Glumes							Vasculature							Endosperm					
	Days after flowering							Days after flowering							Days after flowering					
	4	8	10	14	18	24	$C_{Gl, Vc}$	4	8	10	14	18	24	$C_{Vc, Es}$	4	8	10	14	18	24
Alanine	60	100	68	72	82	75	-0.32	100	67	66	63	49	23	0.89*	100	55	54	25	21	18
Asparagine	100	70	10	14	30	4	0.73	100	95	81	72	49	31	0.81*	77	100	33	15	15	12
Glutamate	57	82	79	97	93	100	-0.88*	100	85	53	37	27	32	0.93*	100	72	54	43	52	48
Glutamine	98	100	29	39	56	43	0.76	100	68	60	54	62	48	0.98*	100	38	17	11	15	11
Isoleucine	72	94	48	67	100	65	0.12	54	100	57	34	18	27	0.61	100	84	29	28	43	31
Leucine	75	91	44	62	100	83	-0.03	69	100	61	44	29	44	0.53	100	58	26	24	33	28
Lysine	100	99	34	49	79	30	0.69	100	81	66	65	45	19	0.09	66	96	38	60	100	55
Phenylalanine	65	100	75	71	90	90	0.09	87	100	68	48	38	54	0.50	100	38	28	28	32	35
Proline	49	100	26	35	42	44	0.66	79	100	55	9	8	10	0.90*	47	100	19	5	10	7
Serine	54	100	55	63	52	44	0.71	87	100	84	70	43	31	0.96*	72	100	70	42	34	16
Threonine	63	100	66	83	92	66	0.10	100	99	81	69	46	29	0.92*	100	100	81	70	74	29
Valine	76	100	51	72	98	77	-0.02	100	98	70	60	38	48	0.84*	100	63	28	21	29	23

Figure 12 Relative concentrations of free amino acids in barley glumes (Gl), grain vasculature (Vc) and endosperm (Es). Measurements were done between 4 and 24 DAF via UPLC for glumes and endosperm with three biological replicates and via GC-MS for grain vasculature with eight biological replicates. Concentrations were normalised and colour coded from dark-red (low) to dark-blue (high) values (see Figure 13), before Pearson correlation (C) was determined for Vc and Gl, and Vc and Es, respectively. Correlations are shown in orange (negative) and green (positive); statistically significant correlations ($p<0.05$) are marked with an asterisk (Kohl *et al.*, 2015).

vegetative tissues and N export to developing grains. Although the total amount of free amino acids in the endosperm was constantly increasing (data not shown), the concentrations for most FAA decreased between 4 and 14 DAF. This decrease was most pronounced between 8 and 10 DAF underlining the rising demand of FAA for storage protein synthesis. The positive correlation between FAA concentrations between vasculature and endosperm indicates that the depletion of FAA was propagated through the vasculature to the glumes. FAA participate in signalling the N status of plants and influencing N uptake from the soil. Application of Gln and Asp in the phloem of beech led to reduced NO_3^- uptake (Geßler *et al.*, 1998) and feeding FAA to barley roots negatively regulated expression of high affinity NO_3^- uptake transporter (Vidmar *et al.*, 2000). Presuming a similar role for FAA in N status signalling in the ear, the depletion of FAA in the endosperm and vasculature could signal increasing FAA demand to glumes and trigger remobilisation processes. In accordance with this hypothesis, Glu levels in glumes were increasing after 10 DAF, indicating high N turnover, as the α-amino group of Glu is directly involved in the assimilation and dissimilation of ammonia and is transferred to all other amino acids (Forde and Lea, 2007). Taken together with the decreasing levels of most other FAA and total N these findings suggest high N remobilisation and subsequent transport to grains.

4.2.2. Metabolite profiling indicates changes in the cell wall structure of glumes during development

Polar central metabolites were measured via GC-MS and relative changes during development are shown in Figure 13 for selected pathways/metabolites. Levels of sucrose, maltose, raffinose, xylulose, rhamnose and fucose increased whereas xylose, arabinose and trehalose decreased in glumes with progressing development. Several sugars are involved in cell wall biosynthesis, indicating alterations in cell wall dynamics in glumes. These alterations might provide the infrastructure and be a prerequisite to render glumes into a tissue adapted to provide remobilised nutrients to the developing grains.

In the endosperm hexoses were highest at early development whereas sucrose peaked at 8 DAF. The levels of these sugars in grains and their ratios with respect to each other are involved in signalling developmental stages and the transition between them (Weschke *et al.*, 2000).

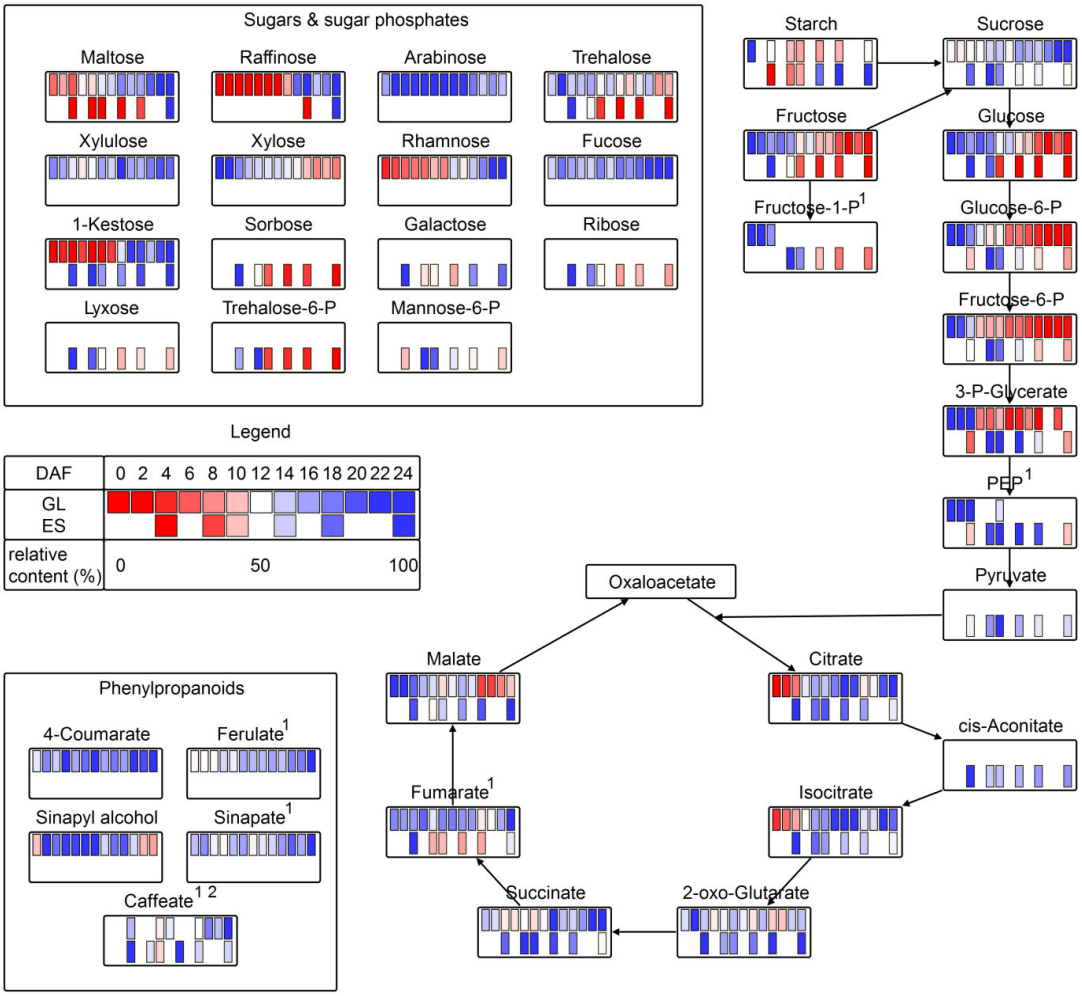

Figure 13 Changes in metabolite levels in barley glumes and endosperm during development. Samples were taken in two day steps between DAF 0 and 24 (glumes) and at DAF 4, 8, 10, 14, 18, 24 (endosperm). Metabolites were measured by GC-MS with six biological replicates per time point. Data was corrected by internal standard and fresh weight, subsequently maximum normalised and colour coded for each metabolite (maximum amount = 100%, values >90% coloured in dark-blue, values <10% in dark-red), as shown by the insert depicting a constant increase from 0 to 100% between DAF 0 and 24. Metabolites without significant changes in one of the tissues are marked by [1] for glumes and [2] for the endosperm (adapted from Kohl *et al.*, 2015).

In glumes, all metabolites from glycolysis had their maximum level at 0 and 4 DAF, followed by decreasing values, while corresponding endosperm values peaked at 8 and 10 DAF.
TCA intermediates, except 2-oxoglutarate and malate, increased in glumes, whereas the highest endosperm levels occurred at early and mid-development. Except caffeate, intermediates from the phenylpropanoid pathway were only detected in glumes and tended to increase during development. The metabolite data will be discussed together with the corresponding transcripts in the following section.

4.2.3. Expression profiles reveal three developmental phases in glumes and grains

A microarray-based expression analysis was performed with material from glumes (0 to 24 DAF) and the endosperm (4 to 24 DAF). After removing outliers and performing statistical analysis (with significant differences between at least two stages according to ANOVA with $p<0.005$ and FC>3), the transcriptome analysis yielded 8,998 and 3,999 differentially expressed transcripts in endosperm and glumes, respectively. The profiles of these transcripts during development revealed similarities between the two tissues and identified three different phases: I) high differential expression between 0 and 8/10 DAF in glumes and endosperm; II) low differential expression between 8/10 and 14 DAF for glumes and endosperm; III) high differential expression after 14 DAF (Figure 14). The deduced phases in the endosperm correspond to the cellularisation and intermediate phase (I) and show that the storage phase can be divided into early and main storage phase (II and III) with the latter one resembling the transition to the desiccation phase (Wobus et al., 2005). Interestingly, profiles of differential expression in glumes are highly correlated with the endosperm in time, indicating a coordinated regulation between the tissues. Furthermore, the end of phase I in glumes at 8 DAF coincides with the cease of Dw accumulation and the relocation of total N and free amino acids (Figures 10 and 11), implicating that the transcriptional changes lead to new functionalities within glumes.

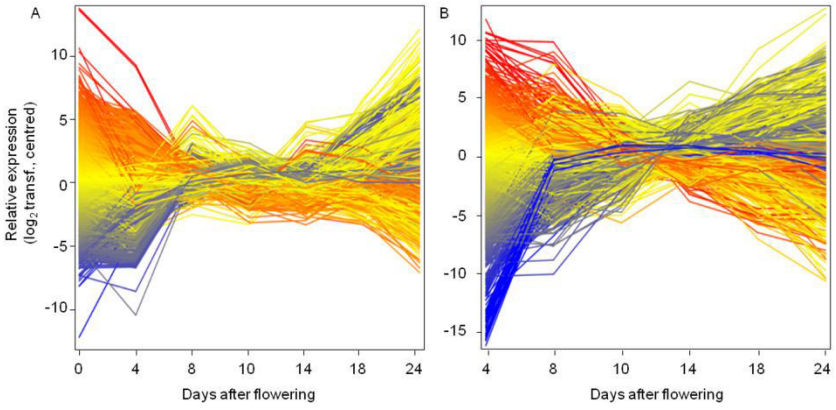

Figure 14 Expression profiles of 3,999 and 8,998 differentially expressed transcripts during development in barley glumes (A) and endosperm (B), respectively. Data was derived from microarray experiments (Agilent 8x60K customised barley array); each time point represents three biological replicates. Raw expression values were log_2 transformed, quantile normalised and centred. Differential expression was detected by ANOVA ($p<0.005$, FC>3); single profiles were coloured according to their values at 0 DAF (Kohl *et al.*, 2015).

4.2.4. Glumes and endosperm show opposing metabolic shifts at the beginning of grain filling

In glumes, the expression of transcripts involved in glycolysis and starch metabolism (e.g. Glc-6-P epimerase, cytosolic/plastidic pyruvate kinase, sucrose synthase and various starch synthases) strongly decreased between 0 and 8 DAF and slightly afterwards (Figure 15). These changes in transcriptional activity are consistent with the relative concentrations of starch and the intermediates of glycolysis that had their highest values at 0 and 4 DAF (Figure 13) and decreased afterwards. On the other hand, the expression of genes related to glycolysis and starch synthesis in the endosperm increased between 4 and 8 DAF, remained constant until 14 DAF and decreased afterwards (Figure 15). These transcriptional tendencies were also reflected at metabolite levels, which peaked at 8 to 10 DAF for glycolytic intermediates (Figure 13), while starch as the main storage compound increased steadily until 24 DAF. A comparable profile was also observed for endosperm storage protein synthesis, which was highly up-regulated between 4 and 8 DAF and remained constant until 24 DAF. Between 4 and 8 DAF genes related to the tricarboxylic acid cycle (TCA) and to the mitochondrial electron-transport chain (mETC), such as 2-OG dehydrogenase (DH), succinyl

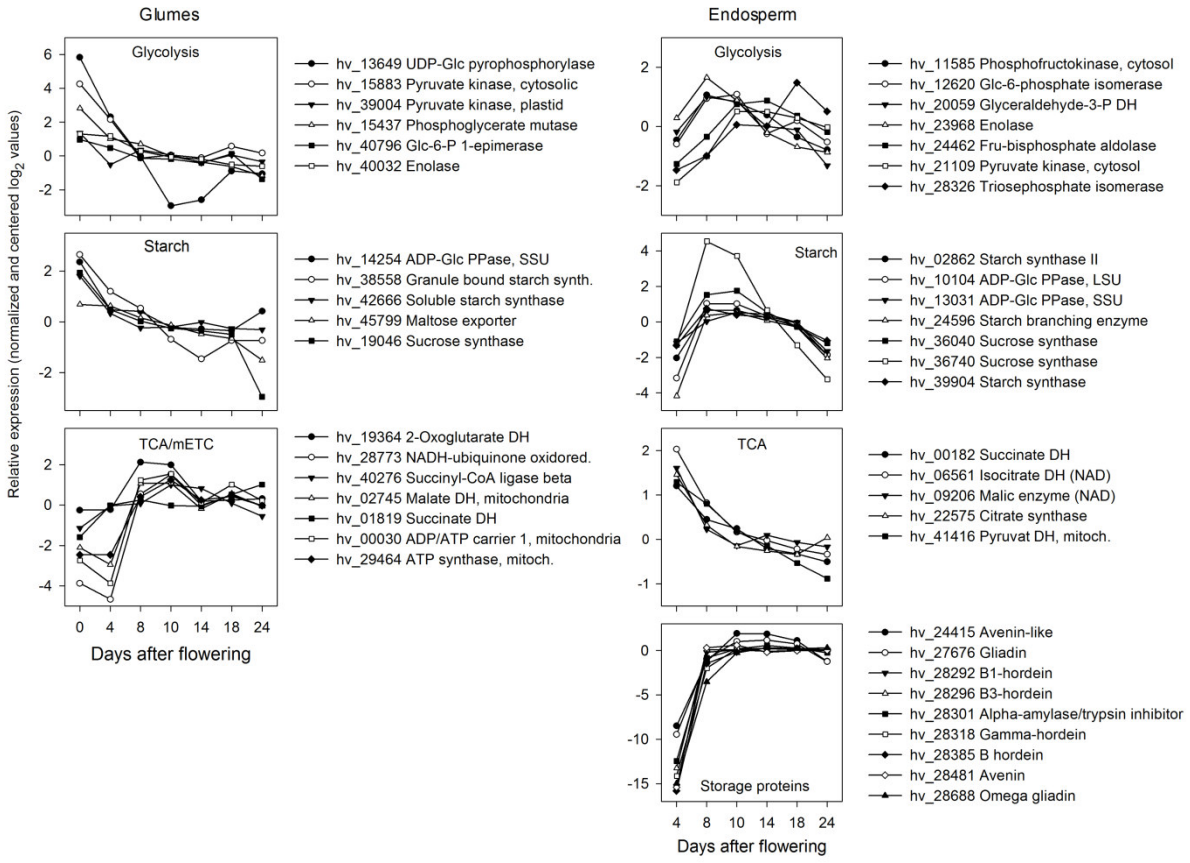

Figure 15 Comparison of transcripts involved in central metabolic pathways in glumes (left panel) and endosperm (right panel). Relative expression values (see Figure 14) are shown for array contigs (hv_number). DCX = decarboxylase; DH = dehydrogenase; LSU = large subunit; mETC = mitochondrial electron transport chain; PPase = pyrophosphorylase; SSU = small subunit, TCA = Citrate cycle (adapted from Kohl *et al,* 2015).

CoA ligase, malate and succinate DH, NAD:ubiquinone oxidoreductase or ATP-synthase, were steeply up-regulated in glumes. Expression of TCA cycle-related genes in the endosperm, e.g. citrate synthase, pyruvate DH or NAD-isocitrate DH, was highest at 4 DAF, then decreased steadily until 10 DAF and remained constant until 24 DAF (Figure 15). The transcript and metabolite analysis revealed opposing trends for glycolysis, starch synthesis, TCA cycle and mETC-activities. While glycolysis and starch synthesis were down-regulated in glumes and up-regulated in the endosperm during grain filling, TCA cycle and mETC-activities were strongly up-regulated in glumes at 8 DAF, while respective endosperm transcripts decreased until 10 DAF.

This indicates that the main energy generation in glumes is shifted from the usage of glucose in glycolysis to the usage of C skeletons, derived from the breakdown of other macromolecules, and their subsequent channelling into TCA and mETC.

This shift coincides with the beginning of storage product accumulation in the endosperm at 8 DAF and may be due to the reallocation of photosynthates from glumes to developing grains. This would also explain increasing sucrose levels in glumes (Figure 13), which indicates that photosynthetically acquired C was directly metabolised into the phloem-mobile transport form in order to support proper grain development.

4.2.5. Transition of glumes from sink to source tissue can be deduced from changes in the transcriptome

Until 8 DAF glumes accumulated dry weight, total N and free amino acids, before respective parameters decreased due to reallocation of resources to the developing grains (Figures 10 and 11). This transition from sink to source tissue was not only reflected in metabolite changes, but also became evident at the transcriptional level. Most transcripts involved in photosynthesis, such as various chlorophyll-binding proteins, photosystem 2 structural proteins and RuBisCO, were down-regulated between 0 and 8 DAF, retained their levels until 14 DAF and were further down-regulated afterwards (Figure 16). On the other hand, expression of pheophorbide a oxygenase, a chlorophyll-degrading enzyme active during senescence (Hörtensteiner, 2006), was up-regulated starting 14 DAF, which indicates that senescence-associated complete degradation of the photosynthetic apparatus did not occur before 14 DAF. Transcripts involved in plastidial protein synthesis, mainly ribosomal proteins and elongation factors, showed profiles comparable to ones promoting photosynthesis, while cytosolic protein synthesis was highly up-regulated from 4 to 10 DAF (Figure 16). This change is a further indication of glumes´ transition from a tissue with high photosynthetic activity to one fulfilling additional/alternative tasks.

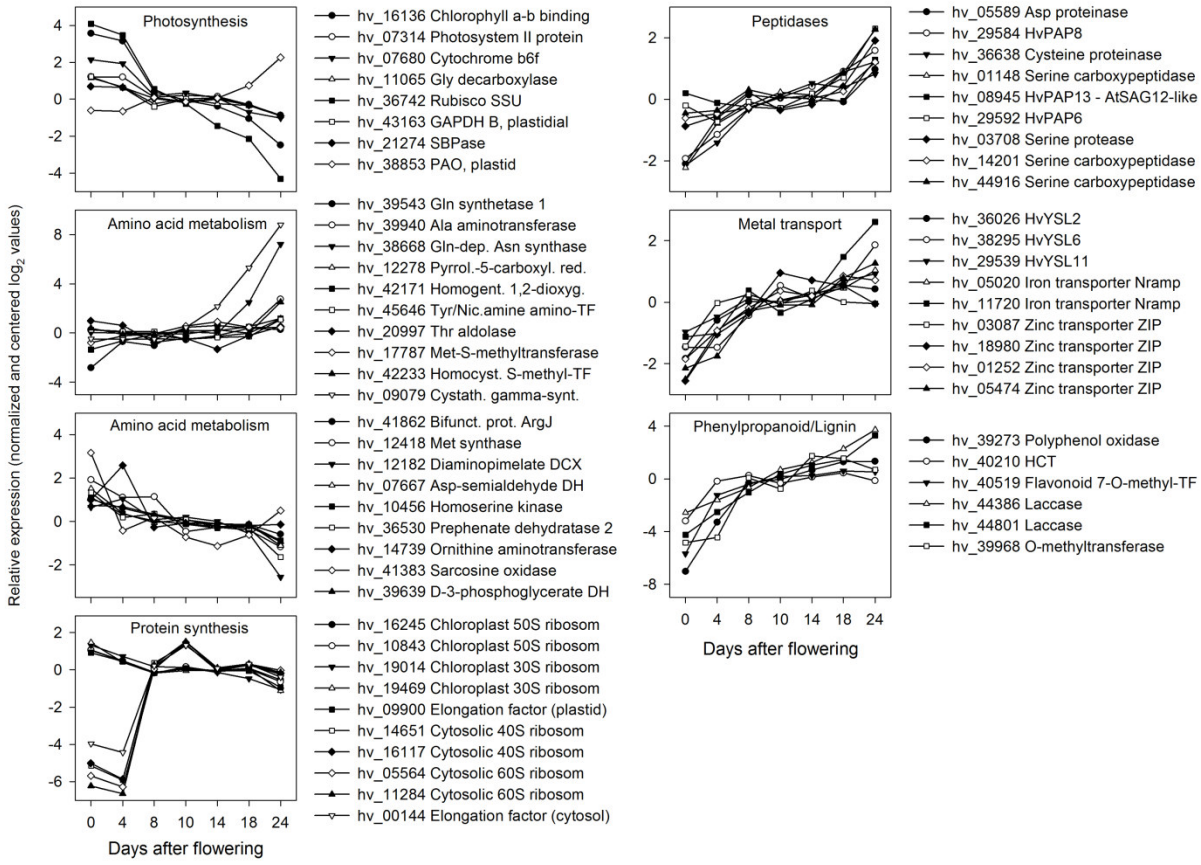

Figure 16 Expression patterns of components regulating transition in glumes from sink to source tissue. Relative expression values (see Figure 14) are shown for selected physiological processes. HCT = hydroxycinnamoyl-CoA shikimate/quinate hydroxycinnamoyl transferase; PAO = pheophorbide a oxygenase; PAP = papain-like cysteine peptidase; SBPase = sedoheptulose-1,7-bisphosphatase; TF = transferase (adapted from Kohl *et al.*, 2015).

Remobilisation of N is dependent on protein degradation, as up to 75% of N present in photosynthetic-active tissues is incorporated in (stromal) proteins (Peoples and Dalling, 1988). The expression profiles of up-regulated peptidases showed two major patterns, either up-regulated between 0 and 8 DAF or up-regulated after 14 DAF and contained members from aspartate, serine and cysteine peptidase subfamilies (Figure 16). Candidates from the first group might primarily support the transition of glumes to fulfil their function in supplying the developing grains. Among the peptidases showing only late up-regulation ~40% belonged to the cysteine peptidase family including a homologue to AtSAG12, which is specifically activated during developmental senescence, but not stress- or hormone-controlled (Noh and Amasino, 1999). This group is likely involved in senescence associated degradation processes and could work in combination with pheophorbide a oxygenase.

Changes in amino acid metabolism provided further insights into the changing characteristics of barley glumes. Several transcripts participating in amino acid biosynthesis, e.g. enzymes involved in the Asp pathway towards Lys, Met and Thr or Arg biosynthesis, showed highest expression at 0 and 4 DAF, before values decreased (Figure 16). On the other hand, enzymes participating in the degradation of aromatic amino acids and Pro, like homogentisate 1,2-dioxygenase and pyrroline-5-carboxylate reductase, were up-regulated

continuously or after 10 DAF, respectively. Furthermore, transcript profiles hinted to a conversion of amino N into Gln and Asn, presumably for export to developing grains. Cytosolic glutamine synthetase-1 (GS1) was up-regulated at 10 DAF and remained constant afterwards. Alanine aminotransferase (Ala-AT) together with glutamine-dependent asparagine synthase (Gln-ASN) showed strong increases in expression after 10 DAF. These enzymes can convert Ala to Glu (Ala-AT), and subsequently to Gln (GS1) and Asn (Gln-ASN). Concerted action of Ala-AT and GS1 has been postulated to generate Gln for export in barley endosperm transfer cells (Thiel *et al.*, 2009). Gln-ASN plays an important role in senescence induced N remobilisation in *M. truncatula* leaves (De Michele *et al.*, 2009). This model is summarised in Figure 17A and would lead to N remobilisation as Gln or Asn at the expense of alanine and amino N. Accordingly, levels of Gln and Asn decreased several fold from 8 to 10 DAF and remained low thereafter, while alanine and Glu levels remained high after 10 DAF (Figure 11).

A combined remobilisation of S and N was suggested to be involved in the transport of reduced sulphur out of senescing tissues into the developing endosperm (Thiel *et al.*, 2009). Transcript profiles of the respective enzymes indicate a similar mechanism taking place in barley glumes. Key enzymes of methionine and cysteine biosynthesis, cystathionine-γ-synthase (CGS), serine acetyl transferase (SAT) and cysteine synthase (OAS1), as well as methionine-S-methyltransferase are up-regulated during glumes development. Together these enzymes could generate phloem-mobile S-methyl-methionine and provide reduced

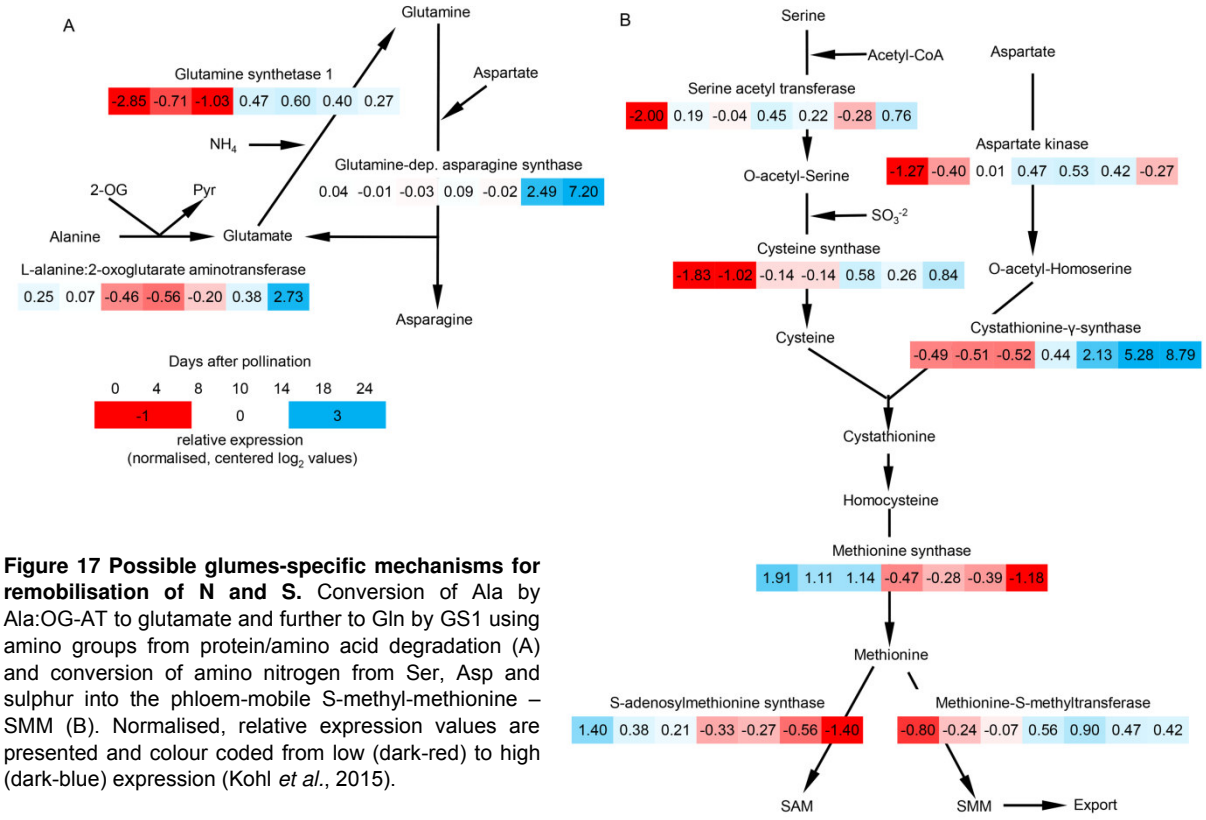

Figure 17 Possible glumes-specific mechanisms for remobilisation of N and S. Conversion of Ala by Ala:OG-AT to glutamate and further to Gln by GS1 using amino groups from protein/amino acid degradation (A) and conversion of amino nitrogen from Ser, Asp and sulphur into the phloem-mobile S-methyl-methionine – SMM (B). Normalised, relative expression values are presented and colour coded from low (dark-red) to high (dark-blue) expression (Kohl *et al.*, 2015).

sulphur for the developing grains (Bourgis *et al.*, 1999). The putative pathway including additional enzymes is shown in Figure 17B.

Lignification and secondary cell wall thickening play important roles in establishing (water) transport pathways (Zhao *et al.*, 2013), which are a prerequisite for efficient remobilisation processes. In barley glumes enzymes leading to lignin precursors, like polyphenol oxidase and hydroxycinnamoyl-CoA shikimate/quinate hydroxycinnamoyl transferase, as well as laccases, which catalyze the polymerisation of lignin from precursors (e.g. coniferyl- or sinapyl-alcohol), were up-regulated in glumes between 8 and 24 DAF (Figure 16). Concordant with these expression profiles, the respective metabolites increase during development (Figure 13), indicating the necessity of an extended transport system in glumes, especially during later development.

4.2.6. Sink to source transition in glumes is reflected in N transporter expression

During the pre-storage phase of grain development glumes represent a sink organ and accumulate N compounds. After the onset of storage protein synthesis in the grains, metabolism and transcriptome of glumes changes and they become remobilising organs nourishing the developing grains. This change from importing N compounds to efficiently remobilising them to the developing seeds is characterised by the differential expression of N transporters.

More than 72% and 56% of putative amino acid (AAT) and nitrate/peptide transporters (NPF), respectively, were at least transiently up-regulated in glumes and three major profiles became evident. Respective candidates were up-regulated either between 0 and 8 DAF (early, Figure 18), constantly up-regulated or only up-regulated starting at 14 DAF (late).

Among the early up-regulated transporters HvAAP2 is homologous to AtAAP2, which is involved in xylem to phloem transfer and important for sink N supply (Zhang *et al.*, 2010).

Early up-regulated NPF transporters included homologues to the tonoplast localized AtPTR2/AtNPF8.3 (hv_38962) with functions in flowering time and seed development (Song *et al.*, 1997) and the plasma membrane localized AtPTR5/AtNPF8.2 (hv_38267), which is important for peptide transport in generative tissue (Komarova *et al.*, 2008). Based on their expression patterns, these transporters are promising candidates for establishment of sink strength and intermediate storage of N in glumes during the pre-storage phase.

The constantly up-regulated transporters included two putative LHT transporters and their homologues AtLHT1 and 2 were shown to play a role in importing amino acids into cells, that are not directly associated with vascular tissue, like leaf mesophyll and tapetum cells (Lee and Tegeder, 2004; Hirner *et al.*, 2006). A similar function for nitrate distribution was deduced for AtNRT1.4/NPF6.2, where mutants showed lower accumulation of nitrate in leaf

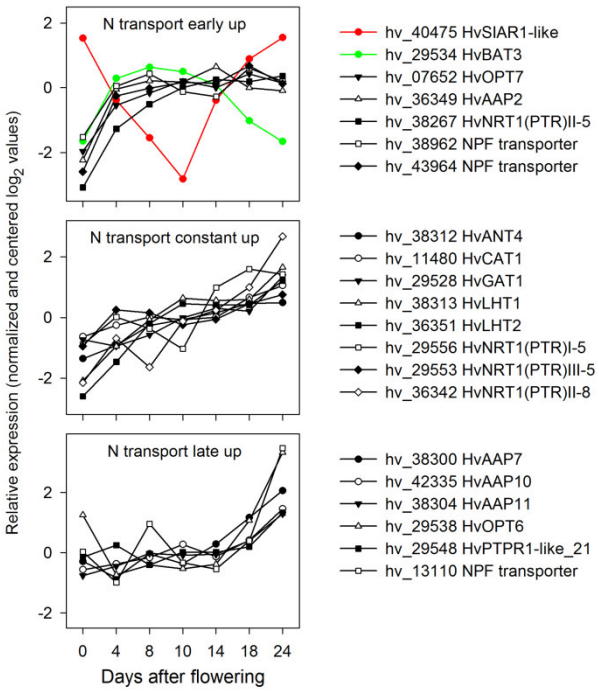

Figure 18 Expression patterns of putative nitrogen transporters in glumes. Relative expression values (see Fig. 14) are presented for nitrate/peptide (NRT/PTR – NPF transporter, respectively) and amino acid (aa) transporters including subgroups: AAP = general aa permease, ANT = aromatic and neutral aa transporter, BAT = bidirectional aa transporter, CAT = cationic aa transporter, GAT = GABA transporter, LHT = lysine/histidine transporter, PUT = polyamine uptake transporter, SIAR = siliques are red - MtN21-like transporter (adapted from Kohl *et al.*, 2015).

petioles and expression was not located adjacent to the xylem (Chiu *et al.*, 2004) and xylem unloading activity was demonstrated for AtNRT1.8/NPF7.2 (Li *et al.*, 2010). Two barley homologues, hv_29556 and hv_36342, were continuously up-regulated during glumes development. Presuming a similar function as their homologues, the constantly up-regulated barley N transporters might be responsible for importing and distributing amino acids and nitrate within the glumes. This may be for either supplying the intrinsic N demand or rendering N compounds available for conversion and subsequent transport to developing grains.

Four AAPs showed up-regulation only after 14 DAF, while no members of other ATF subfamilies followed this regulatory profile. HvAAP11 is related to AtAAP5, which is highly expressed in Arabidopsis source leaves with a supposed role in phloem loading (Fischer *et al.*, 1995). Thus HvAAP11 may be an interesting candidate for exporting amino acids derived from senescence dependent proteolysis in glumes. HvAAP10 on the other hand shows the highest homology to AtAAP6, involved in xylem to phloem transfer (Okumoto *et al.*, 2002) and is more likely to re-allocate amino acids deriving from other source tissues within the vascular system for transport to developing grains. Two candidates of the NPF transporters (hv_29548 and hv_13110) showed exclusive up-regulation at later development. The corresponding Arabidopsis homologues AtNRT1.5/NPF7.3 and AtNRT1.11/NPF1.2 are involved in xylem loading (Lin et al., 2008) and xylem-to-phloem transfer for redistributing nitrate from older leaves to sink tissues (Hsu and Tsay, 2013), respectively. This indicates a function for nitrate translocation from glumes to developing barley seeds.

Currently, only two transporters have been shown to export amino acids out of plant cells and were characterised to have opposing functions. While AtBAT1 is putatively involved in phloem unloading in sink tissues (Dündar and Bush, 2009), AtSIAR1 is implicated in remobilisation and homoeostasis of free amino acids in Arabidopsis source tissues (Ladwig *et al.*, 2012). Expression of corresponding barley homologues differed from the three main patterns occurring within the other N transporters (Figure 18, red and green profiles).

HvBAT3 was up-regulated between 0 and 8 DAF, before expression levels decreased. HvSIAR1-like on the other hand showed decreasing expression values until 10 DAF and was up-regulated afterwards. With respect to free amino acids these two candidates could represent markers for the transition of glumes from sink to source tissues.

4.2.7. Glumes development is governed by NAC and WRKY transcription factors, and influenced by ABA and JA

Metabolite and transcript analyses showed that glumes undergo developmental and metabolic transitions correlated to grain development. These phase changes are associated with mobilisation and import/export of assimilates and nutrients and are likely governed by the activities of TFs and hormonal influences.

NAC and WRKY TFs are frequently involved in general developmental processes, especially the signalling pathways of senescence. The functions of specific members on induction and execution of senescence and nutrient remobilisation were analysed in different plant species (Uauy *et al.*, 2006; Zentgraf *et al.*, 2010; Breeze *et al.*, 2011; Christiansen and Gregersen, 2014) and have highlighted the specific importance of NAC and WRKY TFs in regulating this developmental program. Most NAC and WRKY TFs were up-regulated showing three major profiles (Figure 19). One set showed high increases in transcript abundances until 8 DAF with constant levels afterwards, including HvNAC029 (HvNAM-1). This TF is associated with differences in grain protein content between cultivated and wild barley (Jamar *et al.*, 2010) and a homologue to TtNAM-1, an effector of senescence and remobilisation in wheat flag leaves (Uauy *et al.*, 2006; Distelfeld *et al.*, 2008). Up-regulation of these candidates stopped with the beginning storage protein accumulation in developing seeds, and they seem reasonable candidates to be involved in adjusting glumes metabolism in response to early seed development.

A second group showed strong increases in transcriptional activity starting at 14 DAF and contained only NAC TFs. All of these candidates were described as up regulated in senescing leaves and/or old ears. Furthermore, hormonal induced up regulation via methyl-jasmonate or ABA, respectively, has been demonstrated for HvNAC013 and HvNAC036 (Christiansen *et al.*, 2011). Functionally these TFs may contribute to the initiation of chlorophyll and subsequent chloroplast degradation, which is processed by actions of co-induced HvPAO and SAG12-like cysteine peptidases.

The largest group revealed a pattern of bi-phasic up-regulation with high increases in expression between 0 and 8 DAF, followed by constant transcript levels until 14 DAF before being further up-regulated. This group included HvNAC006 and HvNAC008, homologues to AtORE1, an important factor of the regulatory network controlling leaf senescence in

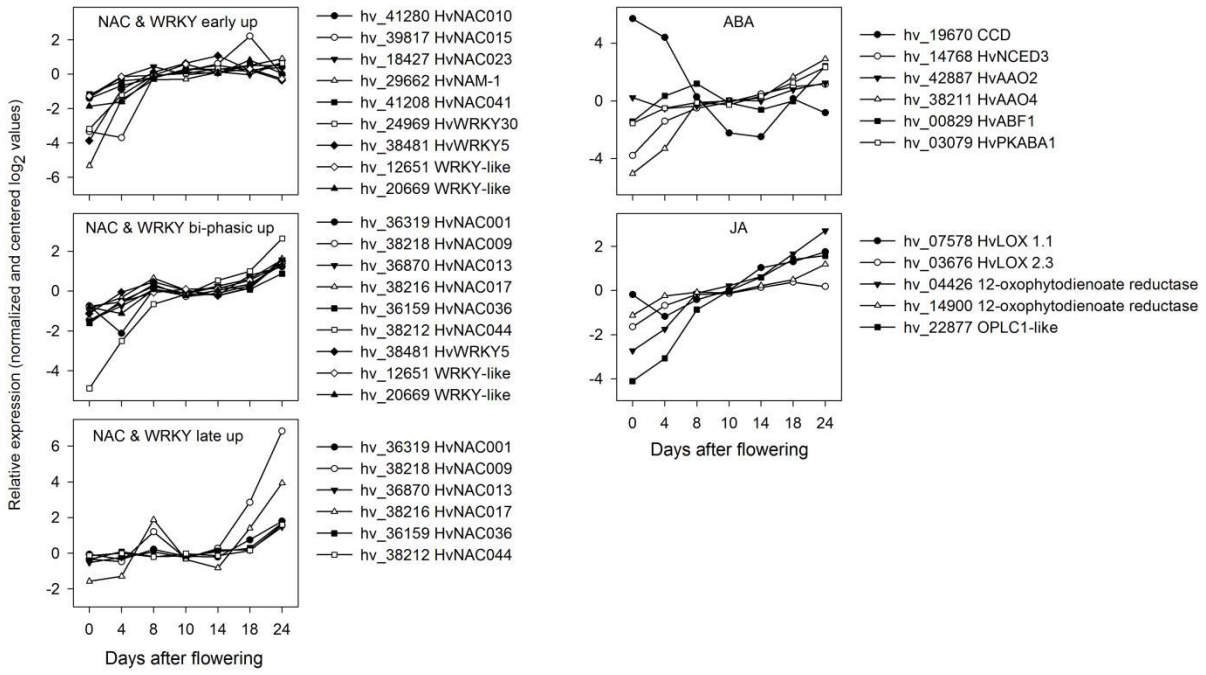

Figure 19 Expression patterns of components regulating transition in glumes from sink to source tissue. Relative expression values (see Fig. 14) are shown for selected transcripts. ABF = ABA-responsive element binding factor; AAO = aldehyde oxidase; CCD = carotenoid cleavage dioxygenase; LOX = lipoxygenase; NCED = 9-cis-epoxycarotenoid dioxygenase; PKABA = ABA-inducible protein kinase; (adapted from Kohl *et al.*, 2015).

Arabidopsis (Kim *et al.*, 2009; Balazadeh *et al.*, 2010), and AtATAF1, which, when over-expressed under 35S-Promotor, leads to several phenotypes including early-senescing leaves (Kleinow *et al.*, 2009). From this group, HvWRKY12 was recently identified as a candidate likely to be involved in age-dependent developmental processes rather than in N remobilisation (Hollmann *et al.*, 2014). The TFs showing bi-phasic up-regulation probably govern the whole progression of glumes development in three distinct phases.

Hormones are involved in all plant developmental processes and differently affect leaf senescence, which can be delayed by cytokinins (CKs) and gibberellic acids (GAs), and accelerated by abscisic acid (ABA) and jasmonates (JA) (Jibran *et al.*, 2013).

Transcripts associated with ABA biosynthesis and signalling are up regulated during senescence (van der Graaff et al., 2006) and increasing ABA levels in leaf development/senescence were reported and seemed to be correlated with grain filling in maize (He *et al.*, 2005) and the beginning of flowering in Arabidopsis (Breeze *et al.*, 2011).

In barley glumes transcripts for carotenoid cleavage dioxygenase (CCD), involved in early steps of ABA biosynthesis decreased until 10 DAF and increased from 14 DAF. Genes catalysing later steps of ABA biosynthesis, such as 9-cis-epoxycarotenoid dioxygenase (NCED) and aldehyde oxidase (AAO) were up-regulated, either continuously or bi-phasically at 8 DAF and after 14 DAF. ABA-inducible protein kinase (HvPKABA1) and ABA responsive element binding factor 1 (HvABF1) were similarly up-regulated in a bi-phasic manner (Figure 19). These results indicate an important role for ABA in the first phase of glumes

development until 8 DAF, as well as in late development from 14 DAF onwards. On the other hand transcripts showed constant (HvAAO4) or decreasing (HvABF1 and HvABAPK1) abundances between 8 and 14 DAF. HvABF1 can interact with HvPKABA1 and 14-3-3 proteins, which may be important regulators in the signaling crosstalk between ABA and GA (Schoonheim et al., 2007; Schoonheim et al., 2009). Decreasing expression levels may be important for delaying ABA regulated senescence-associated processes in order to maintain full functionality of barley glumes to support seed development.

During leaf senescence in Arabidopsis levels of JA increase, the application of JA can induce premature senescence (He *et al.*, 2002) and expression of senescence associated transcripts, like AtSEN4 and AtSAG12 (Xiao *et al.*, 2004) or AtCLH1/CORI1 and AtERD1/SAG15 (Jung *et al.*, 2007). JA biosynthesis depends on subsequent action of lipoxygenase (LOX), allene oxide synthase and cyclase, 12-oxophytodienoate reductase (OPR), followed by beta oxidation (Lyons *et al.*, 2013). Isoforms of LOXs, OPRs and a homologue to AtOPLC1, which is involved in ß oxidation (Koo *et al.*, 2006), were continuously up-regulated in glumes (Figure 19). In contrast to transcripts involved in ABA biosynthesis, bi-phasic up regulation is not evident for JA-related transcripts. These expression profiles indicate a role for JA in age dependent development; however a direct influence of seed development cannot be deduced.

4.3. Increasing seed sink strength in order to improve grain traits

4.3.1. Expression profiles and *in vitro* uptake capacity show functionality of HOSUT construct, but steady-state sucrose levels in developing grains stay unchanged

In order to analyse the influence of increased sink-strength in developing grains, the barley sucrose transporter HvSUT1 was over-expressed in the endosperm of wheat during storage product accumulation, and three independent lines were characterised.

Expression of HvSUT1 was validated using qRT-PCR and showed similar patterns for all three lines (Figure 20A). After an initial up-regulation between 6 and 12 DAF, transcript levels stayed constant (HOSUT20) or increased with different dynamics (HOSUT10 and 11). Between 22 and 26 DAF, transcript abundances increased in all lines, before the expression was down-regulated. Expression analysis showed that the barley Hordein B1 promoter is active in the wheat endosperm and led to increasing transcript abundances of HvSUT1 from the intermediate phase (6 DAF) until late grain filling (26 DAF).

In order to test the physiological functionality of the transgene, caryopses from WT and HOSUT10 and -20 plants were harvested at 19 DAF. Subsequently they were incubated in media containing ^{14}C-labeled sucrose for 10 minutes and, after multiple washing steps, the remaining ^{14}C label was measured. In a control experiment the grains were pre-incubated with diethylpyrocarbonate (DEPC), known to inhibit proton-coupled symport (Bush, 1989). HOSUT10 and -20 grains accumulated 30 to 40% more ^{14}C label compared to the WT, while adding DEPC reduced ^{14}C uptake in all tested samples and yielded comparable uptake rates in WT and HOSUT grains (Figure 20B). These results showed that HvSUT1 is physiologically functional in wheat grains during grain filling and increases sucrose uptake, at least *in vitro*.

Sucrose levels slightly increased between 6 and 12 DAF, before a strong increase occurred between 12 and 14 DAF. Levels decreased by ~50% between 14 and 18 DAF and stayed

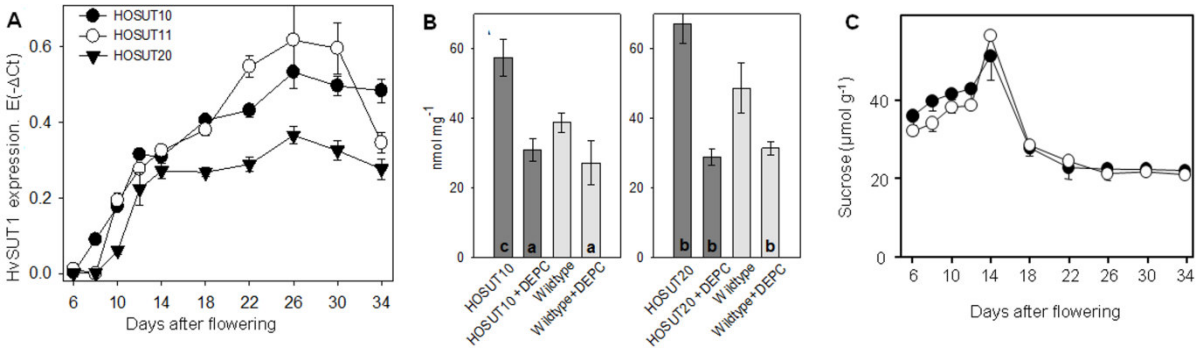

Figure 20 Characterisation of HvSUT1-overexpressing wheat lines. (A) qRT-PCR expression analysis of HvSUT1 in HOSUT grains during development. (B) *In vitro* sucrose uptake capacity of HOSUT and WT grains. ^{14}C label incorporation in WT and HOSUT grains, harvested at 19 DAF, was measured after 10 min incubation with ^{14}C sucrose. In a control experiment, grains were pre-incubated with diethylpyrocarbonate, which inhibits proton-coupled symport. Significant differences according to t-test are marked with (a) for $p<0.05$, (b) for $p<0.01$, and (c) for $p<0.001$. (C) Sucrose concentrations in caryopses during development. Values are means of three (A and B) and five (C) biological replicates ±SD (adapted from Weichert *et al.*, 2010).

constant until the end of development (Figure 20C). Interestingly, levels of sucrose were not changed between HOSUT10 and WT grains, indicating an influence of HvSUT1 expression rather on sucrose fluxes than on steady-state levels, which are tightly controlled in the wheat endosperm (Jenner *et al.*, 1991).

4.3.2. Analysis of growth parameters indicates prolonged grain filling in HOSUT lines and influences of ABA

The dynamics of fresh (Fw) and dry weight (Dw) accumulation showed no differences between HOSUT10 and WT grains during early development, when both parameters increased linearly from 6 to 18 DAF (Fw) and from 6 to 22 DAF (Dw). While both levels stayed constant in the WT afterwards, Dw continued to increase in a linear manner and Fw stayed constant before increasing again after 30 DAF in HOSUT10 (Figure 21A and B).

ABA is involved in the late stages of seed development and is crucial for acquiring desiccation tolerance and seed dormancy (Finkelstein *et al.*, 2002). WT and HOSUT grains showed no differences in ABA content during early development with fluctuating levels between 8 and 14 DAF, followed by an increase between 14 and 18 DAF. ABA contents in the WT increased by three fold at 22 DAF, stayed constant at 24 DAF and slightly decreased after 26 DAF. In HOSUT10 grains the ABA levels stayed constant until it decreased at 26 DAF and then linearly increased until 34 DAF, reaching approximately the same levels as in the WT (Figure 21C).

The prolonged phase of Dw and Fw accumulation suggests differences in the maturation behaviour of HOSUT10 grains leading to a longer grain filling period. This shift might be induced by the actions of ABA, which reaches its maximum at 26 DAF in WT grains, while accumulation is delayed in HOSUT10 grains with maximum amounts at 34 DAF.

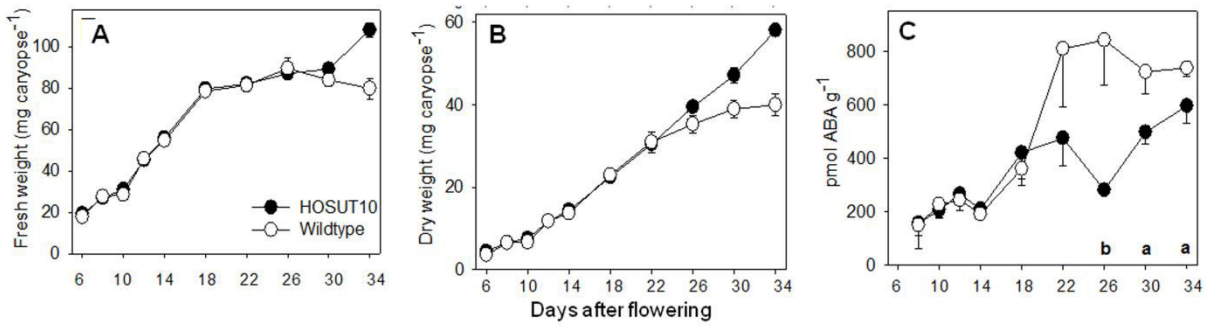

Figure 21 Growth parameters of HOSUT10 and WT grains. (A) Fresh weight and (B) dry weight accumulation during development. (C) Abscisic acid concentration during development, significant differences according to t-test are marked with (a) for $p<0.05$ and (b) for $p<0.01$. Values are means of 100 (A and B) and five (C) biological replicates ±SD (adapted from Weichert *et al.*, 2010).

4.3.3. Mature HOSUT grains have higher N content and changed storage product composition

Analysis of yield parameters and grain composition was performed for line HOSUT10 in field trials, under controlled, but field-like conditions, and in the greenhouse. Under all tested conditions, total N and grain protein content (GPC) were significantly increased by 5% to 16%, which also led to a higher N to C ratio (Table 4). Measuring the different storage proteins fractions (albumins, globulins and prolamins) showed that these increases were not due to generally higher storage protein synthesis, as the contents of albumins and globulins were not significantly changed in comparison to the WT. On the other hand, contents of the prolamin subfractions (gliadins and glutenins) increased by 9 to 15% for gliadins and 6 to 23% for glutenins, depending on the conditions.

Increasing GPC in cereals is (often) associated with decreasing yield (Simmonds, 1995) and although N fertilisation has stimulatory effects on GPC up to a certain limit (Barneix, 2007), wheat usually grows under saturated nutrient conditions, which suggests that sink limitation is an important factor restricting increases of yield parameters (Borrás *et al.*, 2004). Over-expression of HvSUT1 in wheat endosperm seems to overcome these limitations, at least partially, as HOSUT10 grains had higher GPC together with tendencies of increased thousand grain weight (TGW) and relative yield (seed mass per plant; Table 4).

Table 4 Compositional analysis of HOSUT10 and wild type grains grown under different conditions. Values are means ± SE; statistically significant differences according to Student's t-test are marked with (a) for $p<0.05$, (b) for $p<0.01$ and (c) for $p<0.001$ (adapted from Weichert *et al.*, 2010).

	Field trail 2006/2007		**Semi-controlled 2006/2007**		**Greenhouse 2006**	
	HOSUT10	**WT**	**HOSUT10**	**WT**	**HOSUT10**	**WT**
Total nitrogen (%)	**2.62 ± 0.05**^{a}	2.45 ± 0.04	**2.73 ± 0.01**^{b}	2.60 ± 0.03	**3.62 ± 0.05**^{c}	3.12 ± 0.05
Albumins/Globulins (%)	100.87 ± 1.82	100	98.68 ± 1.26	100	99.61 ± 1.02	100
Gliadins (%)	**112.67 ± 2.64**^{b}	100	**109.61 ± 2.24**^{b}	100	**115.26 ± 2.77**^{c}	100
Glutenins (%)	**106.32 ± 2.04**^{a}	100	**105.98 ± 1.88**^{a}	100	**123.93 ± 4.38**^{c}	100
Total carbon (%)	**44.81 ± 0.01**^{b}	44.67 ± 0.03	**44.78 ± 0.01**^{c}	44.58 ± 0.03	**45.06 ± 0.03**^{b}	44.88 ± 0.01
N/C ration	**0.058 ± 0.001**^{a}	0.055 ± 0.001	**0.061 ± 0.0003**^{b}	0.059 ± 0.001	**0.080 ± 0.001**^{c}	0.07 ± 0.001
Total grain protein (%)	**14.95 ± 0.29**^{a}	13.96 ± 0.2	**15.54 ± 0.07**^{b}	14.81 ± 0.18	**20.66 ± 0.3**^{c}	17.79 ± 0.28
Starch (%)	62.5 ± 0.8	64.1 ± 0.8	62.8 ± 0.2	64.3 ± 0.7	**60.3 ± 0.5**^{a}	64.1 ± 0.8
Thousand grain weight (g)	44.0 ± 1.6	41.2 ± 2	**51.0 ± 0.4**^{a}	46.4 ± 1.7	58.6 ± 0.5	57.4 ± 0.5
Yield impact (%)	112.1 ± 19.1	100	**129 ± 6.2**^{b}	100	100.21 ± 20.8	100
Protein yield impact (%)	120.6 ± 21	100	**136.3 ± 5.2**^{c}	100	116.4 ± 24.2	100

Specifically prolamin synthesis is enhanced and leads to a higher N to C ration compared to WT grains. Positive effects of sugar supply on storage protein synthesis has been reported at the transcript, as well as the protein level (Giroux *et al.*, 1994; Rosche *et al.*, 2005; Weigelt *et al.*, 2009), but the underlying mechanisms leading to increased N fluxes into the seeds remain unclear. In cereals, where most N entering the grains derives from pools stored during vegetative growth, effects on remobilisation processes in vegetative tissues seem likely.

4.3.4. HOSUT expression preferentially stimulates prolamin gene expression, alters transcription of central metabolic pathways, and hormone regulation and signalling

Differences in gene expression during development between HOSUT10 and WT grains were analysed via qRT-PCR for 109 candidates between 6 and 34 DAF.

Striking differences became obvious for storage proteins from the prolamin group. At 6 DAF, when storage protein expression is generally low, corresponding transcripts were down-regulated in HOSUT, before a strong up-regulation occurred at 8 and 10 DAF. After 14 DAF, the transcription levels showed only slight variations between HOSUT and WT (Figure 22A). This indicates that increased amounts of prolamins in mature grains (Table 4) were already initiated during the transition of grains from pre-storage into the storage phase. Higher grain prolamin synthesis is likely accompanied by alterations in amino acid metabolism and expression of the corresponding transcripts. In HOSUT grains eight transcripts were differentially expressed, without a clear tendency towards up- or down-regulation. Still, indications for prolonged amino acid anabolism in order to support longer grain filling could be deduced. Plastidial glutamine synthetase, involved in primary N fixation, and aspartate kinase, preceding the biosynthesis of Thr and Lys (Ben-Tzvi Tzchori *et al.*, 1996), were up-regulated at later development, while glutamate dehydrogenase, mainly associated with amino acid breakdown and induced under carbon-deficient conditions (Miyashita and Good, 2008, 2008), showed clearly decreasing transcript abundances at 30/34 DAF (Figure 22B). In order to find transcripts co-regulated with the prolamin genes, the dataset was screened for comparable expression profiles and ten candidates were identified (Figure 22C). AAA ATPase and phosphatidylinositol-3/4-kinase are involved in cell proliferation (Choi *et al.*, 2008; Park *et al.*, 2008) indicating higher cell numbers in HOSUT grains, which was supported by histological analysis (Andersch, unpublished results). Homologues of two sugar-inducible transcripts, flavonoid synthase (Lillo *et al.*, 2008) and AtABI5, a regulator of ABA signalling (Arroyo *et al.*, 2003), were also up-regulated between 8 and 14 DAF. Further transcripts identified in this cluster, homologues to His-Phosphotransferase from wheat (Ma

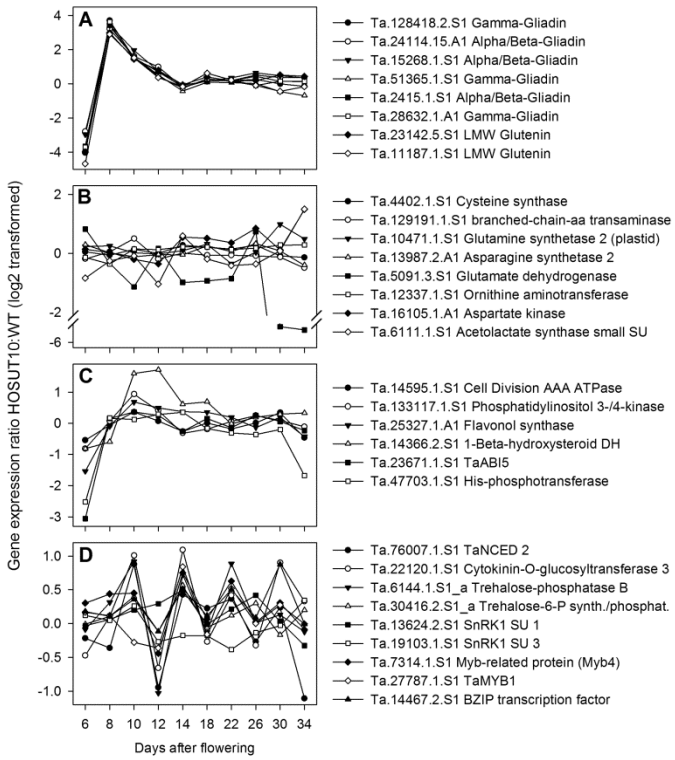

Figure 22 Ratios of gene expression between HOSUT10 and wild type. Gene expression was determined by qRT-PCR at 10 developmental stages with three biological replicates. Determined ΔΔct-values from HOSUT10 were related to WT plants at respective stages. (A) Storage proteins. (B) Amino acid metabolism. (C) Genes revealing a cluster similar to that presented in A. (D) Genes involved in regulatory processes showing deregulation between HOSUT10 and WT. Identifier numbers refer to the Affymetrix GeneChip (adapted from Weichert *et al.*, 2010).

and Tian, 2005) and 11-β-hydroxysteroid dehydrogenase, which effects seed development in Arabidopsis and canola (Li *et al.*, 2007), are involved in cytokinin and brassinosteroid responses. Hormone signalling pathways are deregulated in HOSUT plants during early development, which might lead to earlier initiation of prolamin transcription and biosynthesis.

In addition to the previously discussed candidates, transcript profiling indicated further deregulations of hormone and sugar signalling pathways. Interestingly, transcripts involved in different pathways followed a similar, oscillatory pattern of up-regulation at 10, 14, 22, and 30 DAF and down-regulation at 8, 12, 18, and 26 DAF (Figure 22D). Among these candidates, transcripts involved in ABA (9-cis-epoxycarotenoid dioxygenase) and cytokinin (cytokinin-O-glucosyltransferase) metabolism, as well as MYB and bZIP transcription factors, and members of the SnRK1 and trehalose pathways that regulate carbohydrate metabolism (Lunn *et al.*, 2006; Radchuk *et al.*, 2010) were identified.

Transcript analysis provided further indications for the physiological functionality of HvSUT1 in the wheat endosperm, as several sugar-inducible genes, including storage proteins from the prolamin subfraction, started to be up-regulated at 8 or 10 DAF, when HvSUT1 expression increased in a linear manner (Figure 20A). Additionally, transcripts involved in different signalling pathways, like transcription factors, hormone and sugar signalling, were deregulated and showed oscillatory patterns. Thus it is clear that the induced metabolic alterations are balanced by concerted actions of different signalling components.

4.3.5. Metabolite analysis reveals differences in early and late development between HOSUT and WT grains

Relative metabolite concentrations were determined via GC-MS in developing HOSUT and WT grains between 6 and 26 DAF.

Hierarchical clustering of all metabolite profiles allowed a clear separation between developmental stages, but not between the lines (data not shown). In order to identify the developmental stages with highest variation in metabolite composition between HOSUT and WT grains, independent component analysis was applied on the $\log_{10}$-transformed response ratios (Figure 23 A and B) and revealed major differences only for 8, 10, and 26 DAF.

In comparison to WT plants, HOSUT plants had higher prolamin contents in mature grains and prolamin expression is up-regulated at 8 and 10 DAF, which is likely reflected in differences of amino acid levels. Clustering of amino acid profiles measured via GC-MS yielded two major profiles. Both profiles showed similar behaviour during early development, when HOSUT levels were lower at 8 and 10 DAF and comparable to WT at 6, 12, 14, and 18 DAF. After 18 DAF, levels of Glu, Asp, Gly, Ser, and Val where lower in HOSUT grains, while levels of most other amino acids were higher in comparison to WT grains (Figure 23 C and D). These metabolic differences coincide with other major alterations between HOSUT and WT grains, as found using other experimental approaches.

At 8 and 10 DAF the transcription of prolamin genes is up-regulated in HOSUT grains (Figure 22A) and adaptations of metabolic processes seem a reasonable consequence. In order to provide components, especially free amino acids, for storage protein synthesis the respective metabolite levels temporarily decrease. Differences at 26 DAF might be induced by the differences in maturation behaviour and the prolonged seed filling period in HOSUT grains

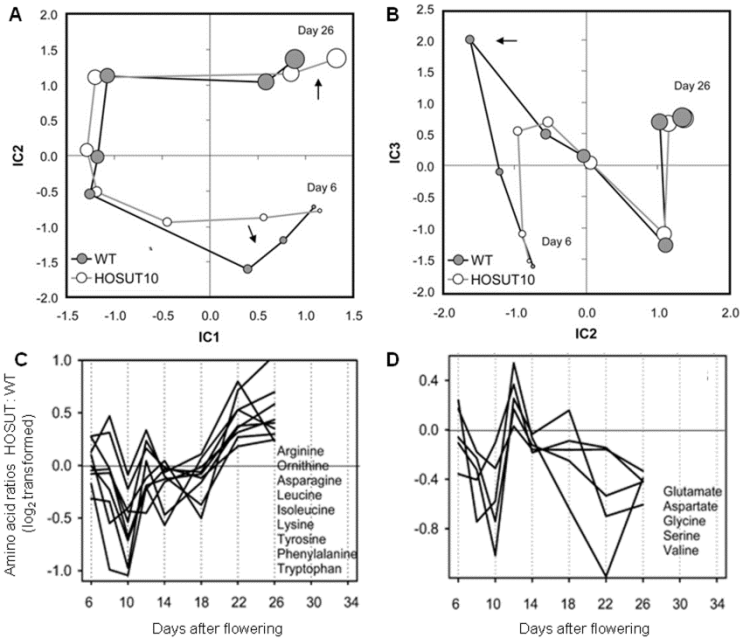

Figure 23 GC-MS based metabolite analysis in developing HOSUT and wild type (WT) grains. (A and B) Independent component (IC) analysis based on the median cantered and $\log_{10}$-transformed response ratios. The graphs show deviations of metabolite levels during grain development; major differences are indicated by arrows. The size of each circle represents the developmental stage from small (6 DAF) to large (26 DAF). (C and D) Ratios of amino acid levels between HOSUT10 and WT. Cluster with higher (C) and lower (D) amino acid levels at stages 22 and 26 DAF are separated (adapted from Weichert *et al.*, 2010).

(Figure 21). Up-regulation of glutamine synthetase and aspartate kinase at later developmental stages suggests prolonged synthesis of amino acids from the aspartate branch and indicates longer availability of the respective precursors.

5. Summary

Cereal grains develop as heterotrophic organs and depend on nutrient import from vegetative tissues. In order to ensure optimal development, timing and extent of nutrient flows have to be coordinated with the developmental status of the grains. While C is constantly provided by photosynthetic activity of vegetative tissues, N uptake from the soil after anthesis is lower than the demands of the grains, implying the need for remobilisation of previously accumulated N, and active transport from source to sink tissues.

In this work, newly generated RNAseq data and sequences from public databases were combined, which allowed identifying new barley N transporters and complementation of the present sequence information. Although RNAseq revealed large differences in the overall transciptome of flag leaves and glumes, which points to distinct functionalities for both organs, similarities with respect to N transport became obvious. qRT-PCR analysis revealed distinct phases of amino acid transporter expression in flag leaves, glumes and endosperm, indicating a strictly controlled timing of amino acid fluxes. Additionally, this analysis allowed distinguishing transporters specific for vegetative tissues from candidates with ubiquitous or grain-specific expression.

The parallel analyses of transcripts, metabolites and physiological parameters in glumes and endosperm showed that the development of glumes is separated into three phases, which are tightly correlated with grain development. These phases represent glumes´ transition from sink to source tissues and are likely coordinated by NAC and WRKY transcription factors and influenced by ABA. In the first 8 days after flowering (DAF), glumes acted as temporary nutrient buffers and accumulated biomass, total N and free amino acids. Coinciding with the beginning of storage protein synthesis in the grains, between 8 and 10 DAF, concentrations of most free amino acids drastically decreased in glumes. Increasing N demand in grains has led to high nutrient relocation from glumes, and might have been propagated via the vasculature, where a comparable depletion of free amino acids was observed. In accordance with proposed high N fluxes, the expression of specific transporters was up-regulated in glumes. Between 10 and 14 DAF, only minor changes in transcript and metabolite levels were observed, suggesting that glumes had to maintain their functionality to support optimal grain development. After 14 DAF, senescence-associated processes, such as degradation of chlorophyll and proteins, and nutrient transporters (N, S, and metals) were up-regulated in glumes.

In an approach to increase grain sink strength in wheat, a sucrose transporter (HvSUT1) was over-expressed in the endosperm during storage product accumulation, which led to higher prolamin contents in mature grains. Although steady-state sucrose levels were not changed, *in vitro* studies showed the functionality of the transporter, pointing to increased sucrose

fluxes. Metabolite and hormone analyses revealed differences in the maturation behaviour of transgenic grains, and transcript analysis indicated up-regulation of storage protein synthesis during early development and a prolonged amino acid biosynthesis. As expected, the expression of HvSUT1 in wheat grains generated an imbalance in the N to C ratio, which led to alterations in maturation and an extended seed filling period.

6. Zusammenfassung

Getreidekörner sind heterotrophe Organe und auf die Versorgung mit Nährstoffen durch die vegetativen Gewebe angewiesen. Für eine optimale Entwicklung, müssen die Nährstoffflüsse zeitlich und umfänglich an den Entwicklungsstatus des Korns angepasst werden. Während C permanent durch die Photosynthese grüner Gewebe bereit gestellt wird, kann der N-Bedarf der Körner nach Anthese nicht mehr durch die Aufnahme aus dem Boden gedeckt werden. Deshalb ist Remobilisierung und aktiver Transport pflanzlicher N-Reserven von Source- zu Sink-Geweben unerlässlich.

In dieser Arbeit wurden mittels neu generierter RNAseq-Daten, sowie deren Kombination mit Sequenzen aus öffentlichen Datenbanken, neue N-Transporter identifiziert und die vorhandenen Informationen deutlich erweitert. Die RNAseq-Daten zeigten, dass sich das Gesamt-Transkriptom von Fahnenblättern und Spelzen deutlich unterscheidet. Obwohl dies auf unterschiedliche Funktionen beider Organe hindeutete, zeigten sich bezüglich des N-Transports Gemeinsamkeiten. Die Expressionsprofile von Aminosäuretransportern wurden in Fahnenblatt, Spelzen und Endosperm mittels qRT-PCR Analyse ermittelt. Die jeweiligen Profile waren in klar abgegrenzte Phasen unterteilt, was auf eine strenge zeitliche Regulierung der Aminosäureflüsse hindeutete. Desweiteren konnten durch diese Analyse Transporter identifiziert werden, die entweder ubiquitär, samenspezifisch oder spezifisch in vegetativen Geweben exprimiert wurden.

Durch die parallelen Analysen von Transkripten, Metaboliten und physiologischen Parametern in Spelzen und Endosperm, konnte gezeigt werden, dass die Entwicklung der Spelzen in drei Phasen unterteilt und eng an die Kornentwicklung angepasst ist. Diese Phasen kennzeichnen den Übergang der Spelzen vom Sink- zum Source-Gewebe, welcher offensichtlich durch NAC- und WRKY-Transkriptionsfaktoren reguliert und von ABA beeinflusst wird.

In den ersten acht Tagen nach der Blüte (DAF) fungieren die Spelzen als temporäre Nährstoffspeicher und akkumulieren Biomasse, N und freien Aminosäuren. Mit dem Beginn der Speicherstoffsynthese im Korn (zwischen acht und 10 DAF), ging die Konzentration der meisten freien Aminosäuren in den Spelzen stark zurück. Vermutlich bewirkte der steigende N-Bedarf im Korn einen erhöhten Aminosäuretransport aus den Spelzen. Dabei könnte ein erhöhter N-Bedarf über das Leitgewebe kommuniziert werden, in welchem die Konzentrationen freier Aminosäuren ebenfalls deutlich abfielen.

Übereinstimmend mit potentiell erhöhten N-Flüssen, wurde die Genexpression spezifischer Transporter in den Spelzen erhöht. Zwischen 10 und 14 DAF veränderte sich das Transkriptom und Metabolom der Spelzen nur gering. Dies lässt darauf schließen, dass die Funktion der Spelzen für eine optimale Kornentwicklung aufrecht erhalten werden muss.

Ab 14 DAF wurde in den Spelzen die Genexpression Seneszenz-assoziierter Prozesse, wie Chlorophyll- und Proteindegradation, sowie die Expression von Transportern für N, S und Metallionen hochreguliert.

Um die Sink-Stärke während der Kornfüllung zu erhöhen, wurde ein Saccharose-Transporter aus Gerste (HvSUT1) im Endosperm von Weizen über-exprimiert. Die reifen Körner der transgenen Pflanzen enthielten erhöhte Prolamingehalte. *In vitro* Versuche bestätigten die Funktionalität des Transporters, jedoch blieben die steady-state Saccharosegehalte unverändert. Zusammen deutete dies auf erhöhte Saccharoseflüsse hin. Veränderte Metabolit- und Hormongehalte, sowie Expressionsanalysen lassen eine erhöhte Biosynthese von Speicherproteinen während der frühen Entwicklung, sowie eine verlängerte Biosynthese bestimmter Aminosäure vermuten. Erwartungsgemäß bewirkte die Expression von HvSUT1 ein Ungleichgewicht im N:C Verhältnis, und dadurch eine veränderte Kornreifung und eine verlängerte Kornfüllung.

7. Outlook

The analyses presented in this work provided new insights into the complex processes taking place in vegetative organs as a consequence of the changing demands of developing grains, and showed the potential of seed sink strength alteration as an approach to increase yield, as well as grain quality. Furthermore, the importance of amino acid transporters for nutrient remobilisation and grain filling was indicated, which will be used as basis for further investigations.

7.1. Down-regulation of amino acid transporters will clarify their importance for N remobilisation *in planta*

The expression profiles of amino acid transporters (Figure 9, pericarp data unpublished) were analysed with respect to tissue and time point specificity, and correlated (data not shown) with the profiles of free amino acid concentrations (Figure 11, pericarp and flag leaf data unpublished) in the respective tissues. Based on these results, seven candidates, putatively having an important function in N remobilisation from sink to source, were selected for further analysis (Table 5).

Table 5 Selection of amino acid transporters for generating RNAi-plants. Based on tissue specificity, timing of expression and correlation with profiles of free amino acids in the respective tissues, seven amino acid transporters were chosen to clarify their role for N remobilisation and grain filling *in planta*.

Transporter	Tissue	Expressed during	Putative function
HvAAP2	flag leaf, glumes	transition & storage phase	N remobilisation
HvAAP7	flag leaf, glumes	storage phase	N remobilisation
HvProT1	flag leaf	storage phase	N remobilisation
HvLHT1	glumes	storage phase	N remobilisation
HvAAP1	pericarp	pre-storage phase	early seed development
HvANT5	pericarp, endosperm	pre-storage phase	early seed development
HvAAP3	pericarp, endosperm	storage phase	seed filling

The promoter sequences of these amino acid transporter genes were extracted from the barley genome, and used to create transformation vectors that harbour RNAi-constructs for the respective transporters under their endogenous promoters. Down-regulation of these transporters is expected to impair N translocation efficiency and/or the uptake into developing grains, which would confirm their importance for grain N nutrition and provide candidates that can be utilised for crop improvement. All constructs were successfully

transformed in barley, and the T1 generation is currently being analysed with respect to copy number of the transgene. After generating homozygous lines, they will be screened for the efficiency of down-regulation and for yield-related parameters, such as grain weight and number, as well as starch and protein content. If phenotypes that are consistent with impaired N remobilisation are observed, a detailed transcript and metabolite analysis is planned, in order to further elucidate the underlying molecular mechanisms.

7.2. Analysis of the N transporter promoter region will be used to identify putative key regulators of N remobilisation

Microarray based analyses identified distinct expression patterns for N transporters and putative regulators, such as transcription factors (TF) and components of hormone metabolism and signalling pathways (Figure 18 and 19 for glumes; endosperm data published in Kohl *et al.*, 2015; pericarp and flag leaf unpublished). The derived patterns clearly indicate different functions, such as N remobilisation from vegetative tissues or establishment of sink-strength, for specific transporters from the AAT, NPF, and OPT group, respectively.

Since the barley genome is publicly available, a detailed analysis of the respective promoter regions will be addressed. After extracting the promoter sequences, they will be screened for cis-elements. The evaluation of this data will provide information whether specific elements (or combinations/enrichments of elements) are correlated with time point and/or tissue specificity of N transporter expression.

From this analysis, hints at certain TF groups with a pronounced importance for N nutrition of developing grains are expected. Candidates involved in the regulation of N transporter expression are expected to have similar profiles as the respective transporters. The microarray datasets will be checked for the expression of TFs from these groups and their correlation to N transporter expression. This combination of *in silico* and wet lab approaches will be used to identify putative key regulators of N remobilisation in source and sink tissues during grain development. Manipulation of these regulators might address the expression of several N transporters simultaneously, and thereby increase the efficiency of N remobilisation. This approach could possibly exert a greater positive influence on N nutrition of developing grains and thereby the nutritional quality, than the manipulation of single transporters.

8. References

Aeong Oh S, Park J-H, In Lee G, Hee Paek K, Ki Park S, Gil Nam H (1997) Identification of three genetic loci controlling leaf senescence in *Arabidopsis thaliana*. The Plant Journal **12:** 527-535

Araus JL, Brown HR, Febrero A, Bort J, Serret MD (1993) Ear photosynthesis, carbon isotope discrimination and the contribution of respiratory CO_2 to differences in grain mass in durum wheat. Plant, Cell & Environment **16:** 383-392

Arroyo A, Bossi F, Finkelstein RR, León P (2003) Three genes that affect sugar sensing (*Abscisic Acid Insensitive 4, Abscisic Acid Insensitive 5, and Constitutive Triple Response 1*) are differentially regulated by glucose in Arabidopsis. Plant Physiology **133:** 231-242

Ay N, Clauß K, Barth O, Humbeck K (2008) Identification and characterization of novel senescence-associated genes from barley (*Hordeum vulgare*) primary leaves. Plant Biology **10:** 121-135

Balazadeh S, Siddiqui H, Allu AD, Matallana-Ramirez LP, Caldana C, Mehrnia M, Zanor M-I, Köhler B, Mueller-Roeber B (2010) A gene regulatory network controlled by the NAC transcription factor ANAC092/AtNAC2/ORE1 during salt-promoted senescence. The Plant Journal **62:** 250-264

Barneix AJ (2007) Physiology and biochemistry of source-regulated protein accumulation in the wheat grain. Journal of Plant Physiology **164:** 581-590

Ben-Tzvi Tzchori I, Perl A, Galili G (1996) Lysine and threonine metabolism are subject to complex patterns of regulation in Arabidopsis. Plant Molecular Biology **32:** 727-734

Borrás L, Slafer GA, Otegui MaE (2004) Seed dry weight response to source–sink manipulations in wheat, maize and soybean: a quantitative reappraisal. Field Crops Research **86:** 131-146

Bourgis F, Roje S, Nuccio ML, Fisher DB, Tarczynski MC, Li C, Herschbach C, Rennenberg H, Pimenta MJ, Shen T-L, Gage DA, Hanson AD (1999) S-Methylmethionine plays a major role in phloem sulfur transport and is synthesized by a novel type of methyltransferase. The Plant Cell Online **11:** 1485-1497

Breeze E, Harrison E, McHattie S, Hughes L, Hickman R, Hill C, Kiddle S, Kim Y-s, Penfold CA, Jenkins D, Zhang C, Morris K, Jenner C, Jackson S, Thomas B, Tabrett A, Legaie R, Moore JD, Wild DL, Ott S, Rand D, Beynon J, Denby K, Mead A, Buchanan-Wollaston V (2011) High-resolution temporal profiling of transcripts during Arabidopsis leaf senescence reveals a distinct chronology of processes and regulation. The Plant Cell **23:** 873-894

Buchanan-Wollaston V (1997) The molecular biology of leaf senescence. Journal of Experimental Botany **48:** 181-199

Buchanan-Wollaston V, Earl S, Harrison E, Mathas E, Navabpour S, Page T, Pink D (2003) The molecular analysis of leaf senescence – a genomics approach. Plant Biotechnology Journal **1:** 3-22

Bush DR (1989) Proton-Coupled Sucrose Transport in Plasmalemma Vesicles Isolated from Sugar Beet (*Beta vulgaris* L. cv Great Western) Leaves. Plant Physiology **89:** 1318-1323

Caputo C, Fatta N, Barneix AJ (2001) The export of amino acid in the phloem is altered in wheat plants lacking the short arm of chromosome 7B. Journal of Experimental Botany **52:** 1761-1768

Chiu C-C, Lin C-S, Hsia A-P, Su R-C, Lin H-L, Tsay Y-F (2004) Mutation of a nitrate transporter, AtNRT1:4, results in a reduced petiole nitrate content and altered leaf development. Plant and Cell Physiology **45:** 1139-1148

Choi Y, Lee Y, Jeon BW, Staiger CJ, Lee Y (2008) Phosphatidylinositol 3- and 4-phosphate modulate actin filament reorganization in guard cells of day flower. Plant, Cell & Environment **31:** 366-377

Christiansen M, Holm P, Gregersen P (2011) Characterization of barley (*Hordeum vulgare L.*) NAC transcription factors suggests conserved functions compared to both monocots and dicots. BMC Research Notes **4:** 302
Christiansen MW, Gregersen PL (2014) Members of the barley NAC transcription factor gene family show differential co-regulation with senescence-associated genes during senescence of flag leaves. Journal of Experimental Botany **65:** 4009-4022
Cochrane MP, Duffus CM (1980) The nucellar projection and modified aleurone in the crease region of developing caryopses of barley (*Hordeum vulgare L.* var.distichum). Protoplasma **103:** 361-375
Crawford NM, Glass ADM (1998) Molecular and physiological aspects of nitrate uptake in plants. Trends in Plant Science **3:** 389-395
Curie C, Panaviene Z, Loulergue C, Dellaporta SL, Briat J-F, Walker EL (2001) Maize yellow stripe1 encodes a membrane protein directly involved in Fe(III) uptake. Nature **409:** 346-349
De Michele R, Formentin E, Todesco M, Toppo S, Carimi F, Zottini M, Barizza E, Ferrarini A, Delledonne M, Fontana P, Lo Schiavo F (2009) Transcriptome analysis of *Medicago truncatula* leaf senescence: similarities and differences in metabolic and transcriptional regulations as compared with Arabidopsis, nodule senescence and nitric oxide signalling. New Phytologist **181:** 563-575
Dietrich D, Hammes U, Thor K, Suter-Grotemeyer M, Flückiger R, Slusarenko AJ, Ward JM, Rentsch D (2004) AtPTR1, a plasma membrane peptide transporter expressed during seed germination and in vascular tissue of Arabidopsis. The Plant Journal **40:** 488-499
Distelfeld A, Korol A, Dubcovsky J, Uauy C, Blake T, Fahima T (2008) Colinearity between the barley grain protein content (GPC) QTL on chromosome arm 6HS and the wheat Gpc-B1 region. Molecular Breeding **22:** 25-38
Dündar E (2009) Multiple GUS expression patterns of a single Arabidopsis gene. Annals of Applied Biology **154:** 33-41
Dündar E, Bush D (2009) BAT1, a bidirectional amino acid transporter in Arabidopsis. Planta **229:** 1047-1056
Engell K (1989) Embryology of barley: Time course and analysis of controlled fertilization and early embryo formation based on serial sections. Nordic Journal of Botany **9:** 265-280
Ernst HA, Nina Olsen A, Skriver K, Larsen S, Lo Leggio L (2004) Structure of the conserved domain of ANAC, a member of the NAC family of transcription factors. EMBO Reports **5:** 297-303
Eulgem T, Rushton PJ, Robatzek S, Somssich IE (2000) The WRKY superfamily of plant transcription factors. Trends in Plant Science **5:** 199-206
Eulgem T, Somssich IE (2007) Networks of WRKY transcription factors in defense signaling. Current Opinion in Plant Biology **10:** 366-371
Finkelstein RR, Gampala SSL, Rock CD (2002) Abscisic acid signaling in seeds and seedlings. The Plant Cell Online **14:** S15-S45
Fischer W-N, Kwart M, Hummel S, Frommer WB (1995) Substrate specificity and expression profile of amino acid transporters (AAPs) in Arabidopsis. Journal of Biological Chemistry **270:** 16315-16320
Forde BG, Lea PJ (2007) Glutamate in plants: metabolism, regulation, and signalling. Journal of Experimental Botany **58:** 2339-2358
Geßler A, Schultze M, Schrempp S, Rennenberg H (1998) Interaction of phloem-translocated amino compounds with nitrate net uptake by the roots of beech (*Fagus sylvatica*) seedlings. Journal of Experimental Botany **49:** 1529-1537
Giroux MJ, Boyer C, Feix G, Hannah LC (1994) Coordinated transcriptional regulation of storage product genes in the maize endosperm. Plant Physiology **106:** 713-722
Glass ADM, Britto DT, Kaiser BN, Kinghorn JR, Kronzucker HJ, Kumar A, Okamoto M, Rawat S, Siddiqi MY, Unkles SE, Vidmar JJ (2002) The regulation of nitrate and ammonium transport systems in plants. Journal of Experimental Botany **53:** 855-864

Grallath S, Weimar T, Meyer A, Gumy C, Suter-Grotemeyer M, Neuhaus J-M, Rentsch D (2005) The AtProT Family. Compatible solute transporters with similar substrate specificity but differential expression patterns. Plant Physiology **137:** 117-126
Grundbacher FJ (1963) The physiological function of the cereal awn. The Botanical Review **29:** 366-381
Guo Y, Cai Z, Gan S (2004) Transcriptome of Arabidopsis leaf senescence. Plant, Cell & Environment **27:** 521-549
He P, Osaki M, Takebe M, Shinano T, Wasaki J (2005) Endogenous hormones and expression of senescence-related genes in different senescent types of maize. Journal of Experimental Botany **56:** 1117-1128
He Y, Fukushige H, Hildebrand DF, Gan S (2002) Evidence supporting a role of jasmonic acid in Arabidopsis leaf senescence. Plant Physiology **128:** 876-884
Hensel LL, Grbić V, Baumgarten DA, Bleecker AB (1993) Developmental and age-related processes that influence the longevity and senescence of photosynthetic tissues in arabidopsis. The Plant Cell Online **5:** 553-564
Hinderhofer K, Zentgraf U (2001) Identification of a transcription factor specifically expressed at the onset of leaf senescence. Planta **213:** 469-473
Hirel B, Le Gouis J, Ney B, Gallais A (2007) The challenge of improving nitrogen use efficiency in crop plants: towards a more central role for genetic variability and quantitative genetics within integrated approaches. Journal of Experimental Botany **58:** 2369-2387
Hirner A, Ladwig F, Stransky H, Okumoto S, Keinath M, Harms A, Frommer WB, Koch W (2006) Arabidopsis LHT1 is a high-affinity transporter for cellular amino acid uptake in both root epidermis and leaf mesophyll. The Plant Cell Online **18:** 1931-1946
Hollmann J, Gregersen PL, Krupinska K (2014) Identification of predominant genes involved in regulation and execution of senescence-associated nitrogen remobilization in flag leaves of field grown barley. Journal of Experimental Botany **65:** 3963-3973
Hörtensteiner S (2006) Chlorophyll degradation during senescence. Annual Review of Plant Biology **57:** 55-77
Hsu P-K, Tsay Y-F (2013) Two phloem nitrate transporters, NRT1.11 and NRT1.12, are important for redistributing xylem-borne nitrate to enhance plant growth. Plant Physiology **163:** 844-856
Huang N-C, Liu K-H, Lo H-J, Tsay Y-F (1999) Cloning and functional characterization of an Arabidopsis nitrate transporter gene that encodes a constitutive component of low-affinity uptake. The Plant Cell Online **11:** 1381-1392
Jamar C, Loffet F, Frettinger P, Ramsay L, Fauconnier M-L, du Jardin P (2010) NAM-1 gene polymorphism and grain protein content in *Hordeum*. Journal of Plant Physiology **167:** 497-501
Jenner C, Ugalde T, Aspinall D (1991) The physiology of starch and protein deposition in the endosperm of wheat. Functional Plant Biology **18:** 211-226
Jibran R, Hunter D, Dijkwel P (2013) Hormonal regulation of leaf senescence through integration of developmental and stress signals. Plant Molecular Biology **82:** 547-561
Jung C, Lyou S, Yeu S, Kim M, Rhee S, Kim M, Lee J, Choi Y, Cheong J-J (2007) Microarray-based screening of jasmonate-responsive genes in *Arabidopsis thaliana*. Plant Cell Reports **26:** 1053-1063
Kanno Y, Hanada A, Chiba Y, Ichikawa T, Nakazawa M, Matsui M, Koshiba T, Kamiya Y, Seo M (2012) Identification of an abscisic acid transporter by functional screening using the receptor complex as a sensor. Proceedings of the National Academy of Sciences **109:** 9653-9658
Kim JH, Woo HR, Kim J, Lim PO, Lee IC, Choi SH, Hwang D, Nam HG (2009) Trifurcate feed-forward regulation of age-dependent cell death involving miR164 in Arabidopsis. Science **323:** 1053-1057

Kleinow T, Himbert S, Krenz B, Jeske H, Koncz C (2009) NAC domain transcription factor ATAF1 interacts with SNF1-related kinases and silencing of its subfamily causes severe developmental defects in Arabidopsis. Plant Science **177:** 360-370
Koh S, Wiles AM, Sharp JS, Naider FR, Becker JM, Stacey G (2002) An oligopeptide transporter gene family in Arabidopsis. Plant Physiology **128:** 21-29
Kohl S, Hollmann J, Blattner F, Radchuk V, Andersch F, Steuernagel B, Schmutzer T, Scholz U, Krupinska K, Weber H, Weschke W (2012) A putative role for amino acid permeases in sink-source communication of barley tissues uncovered by RNA-seq. BMC Plant Biology **12:** 154
Kojima S, Bohner A, Gassert B, Yuan L, Wirén Nv (2007) AtDUR3 represents the major transporter for high-affinity urea transport across the plasma membrane of nitrogen-deficient Arabidopsis roots. The Plant Journal **52:** 30-40
Kokubun N, Ishida H, Makino A, Mae T (2002) The degradation of the large subunit of ribulose-1,5-bisphosphate carboxylase/oxygenase into the 44-kDa fragment in the lysates of chloroplasts incubated in darkness. Plant and Cell Physiology **43:** 1390-1395
Komarova NY, Thor K, Gubler A, Meier S, Dietrich D, Weichert A, Suter Grotemeyer M, Tegeder M, Rentsch D (2008) AtPTR1 and AtPTR5 transport dipeptides in planta. Plant Physiology **148:** 856-869
Koo AJ, Chung HS, Kobayashi Y, Howe GA (2006) Identification of a peroxisomal acyl-activating enzyme involved in the biosynthesis of jasmonic acid in Arabidopsis. The Journal of Biological Chemistry **281:** 33511-33520
Ladwig F, Stahl M, Ludewig U, Hirner AA, Hammes UZ, Stadler R, Harter K, Koch W (2012) *Siliques Are Red1* from Arabidopsis acts as a bidirectional amino acid transporter that is crucial for the amino acid homeostasis of siliques. Plant Physiology **158:** 1643-1655
Lea PJ, Robinson SA, Stewart GR (1990) The enzymology and metabolism of glutamine, glutamate, and asparagine. The biochemistry of plants **16:** 121-159
Lee Y-H, Foster J, Chen J, Voll LM, Weber APM, Tegeder M (2007) AAP1 transports uncharged amino acids into roots of Arabidopsis. The Plant Journal **50:** 305-319
Lee Y-H, Tegeder M (2004) Selective expression of a novel high-affinity transport system for acidic and neutral amino acids in the tapetum cells of Arabidopsis flowers. The Plant Journal **40:** 60-74
Lehmann S, Gumy C, Blatter E, Boeffel S, Fricke W, Rentsch D (2011) In planta function of compatible solute transporters of the AtProT family. Journal of Experimental Botany **62:** 787-796
Leprince O, Hendry GAF, McKersie BD (1993) The mechanisms of desiccation tolerance in developing seeds. Seed Science Research **3:** 231-246
Léran S, Varala K, Boyer J-C, Chiurazzi M, Crawford N, Daniel-Vedele F, David L, Dickstein R, Fernandez E, Forde B, Gassmann W, Geiger D, Gojon A, Gong J-M, Halkier BA, Harris JM, Hedrich R, Limami AM, Rentsch D, Seo M, Tsay Y-F, Zhang M, Coruzzi G, Lacombe B (2014) A unified nomenclature of NITRATE TRANSPORTER 1/PEPTIDE TRANSPORTER family members in plants. Trends in Plant Science **19:** 5-9
Li F, Asami T, Wu X, Tsang EWT, Cutler AJ (2007) A putative hydroxysteroid dehydrogenase involved in regulating plant growth and development. Plant Physiology **145:** 87-97
Li J-Y, Fu Y-L, Pike SM, Bao J, Tian W, Zhang Y, Chen C-Z, Zhang Y, Li H-M, Huang J, Li L-G, Schroeder JI, Gassmann W, Gong J-M (2010) The Arabidopsis nitrate transporter NRT1.8 functions in nitrate removal from the xylem sap and mediates cadmium tolerance. The Plant Cell Online **22:** 1633-1646
Lillo C, Lea US, Ruoff P (2008) Nutrient depletion as a key factor for manipulating gene expression and product formation in different branches of the flavonoid pathway. Plant, Cell & Environment **31:** 587-601

Lin S-H, Kuo H-F, Canivenc G, Lin C-S, Lepetit M, Hsu P-K, Tillard P, Lin H-L, Wang Y-Y, Tsai C-B, Gojon A, Tsay Y-F (2008) Mutation of the Arabidopsis NRT1.5 nitrate transporter causes defective root-to-shoot nitrate transport. The Plant Cell Online **20:** 2514-2528

Lubkowitz M (2011) The Oligopeptide Transporters: A small gene family with a diverse group of substrates and functions? Molecular Plant **4:** 407-415

Lunn JE, Feil R, Hendriks JH, Gibon Y, Morcuende R, Osuna D, Scheible WR, Carillo P, Hajirezaei MR, Stitt M (2006) Sugar-induced increases in trehalose 6-phosphate are correlated with redox activation of ADPglucose pyrophosphorylase and higher rates of starch synthesis in *Arabidopsis thaliana*. Biochem J **397:** 139-148

Lyons R, Manners JM, Kazan K (2013) Jasmonate biosynthesis and signaling in monocots: a comparative overview. Plant Cell Reports **32:** 815-827

Ma Q-H, Tian B (2005) Characterization of a wheat histidine-containing phosphotransfer protein (HP) that is regulated by cytokinin-mediated inhibition of leaf senescence. Plant Science **168:** 1507-1514

Martínez DE, Costa ML, Guiamet JJ (2008) Senescence-associated degradation of chloroplast proteins inside and outside the organelle. Plant Biology **10:** 15-22

Masclaux C, Valadier M-H, Brugière N, Morot-Gaudry J-F, Hirel B (2000) Characterization of the sink/source transition in tobacco (*Nicotiana tabacum* L.) shoots in relation to nitrogen management and leaf senescence. Planta **211:** 510-518

Matallana-Ramirez LP, Rauf M, Farage-Barhom S, Dortay H, Xue G-P, Dröge-Laser W, Lers A, Balazadeh S, Mueller-Roeber B (2013) NAC transcription factor ORE1 and senescence-induced BIFUNCTIONAL NUCLEASE1 (BFN1) constitute a regulatory cascade in Arabidopsis. Molecular Plant **6:** 1438-1452

Matsumoto T, Tanaka T, Sakai H, Amano N, Kanamori H, Kurita K, Kikuta A, Kamiya K, Yamamoto M, Ikawa H, Fujii N, Hori K, Itoh T, Sato K (2011) Comprehensive sequence analysis of 24,783 barley full-length cDNAs derived from 12 clone libraries. Plant Physiology **156:** 20-28

Melkus G, Rolletschek H, Fuchs J, Radchuk V, Grafahrend-Belau E, Sreenivasulu N, Rutten T, Weier D, Heinzel N, Schreiber F, Altmann T, Jakob PM, Borisjuk L (2011) Dynamic 13C/1H NMR imaging uncovers sugar allocation in the living seed. Plant Biotechnology Journal **9:** 1022-1037

Miao Y, Laun T, Zimmermann P, Zentgraf U (2004) Targets of the WRKY53 transcription factor and its role during leaf senescence in Arabidopsis. Plant Molecular Biology **55:** 853-867

Miflin BJ, Habash DZ (2002) The role of glutamine synthetase and glutamate dehydrogenase in nitrogen assimilation and possibilities for improvement in the nitrogen utilization of crops. Journal of Experimental Botany **53:** 979-987

Miyashita Y, Good AG (2008a) Glutamate deamination by glutamate dehydrogenase plays a central role in amino acid catabolism in plants. Plant Signaling & Behavior **3:** 842-843

Miyashita Y, Good AG (2008b) NAD(H)-dependent glutamate dehydrogenase is essential for the survival of Arabidopsis thaliana during dark-induced carbon starvation. Journal of Experimental Botany **59:** 667-680

Munné-Bosch S, Alegre L (2004) Die and let live: leaf senescence contributes to plant survival under drought stress. Functional Plant Biology **31:** 203-216

Myers SS, Zanobetti A, Kloog I, Huybers P, Leakey ADB, Bloom AJ, Carlisle E, Dietterich LH, Fitzgerald G, Hasegawa T, Holbrook NM, Nelson RL, Ottman MJ, Raboy V, Sakai H, Sartor KA, Schwartz J, Seneweera S, Tausz M, Usui Y (2014) Increasing CO_2 threatens human nutrition. Nature **510:** 139-142

Nacry P, Bouguyon E, Gojon A (2013) Nitrogen acquisition by roots: physiological and developmental mechanisms ensuring plant adaptation to a fluctuating resource. Plant and Soil **370:** 1-29

Navarre DA, Wolpert TJ (1999) Victorin induction of an apoptotic/senescence–like response in oats. The Plant Cell Online **11:** 237-249

Noh Y-S, Amasino R (1999) Identification of a promoter region responsible for the senescence-specific expression of SAG12. Plant Molecular Biology **41:** 181-194
Noodén LD (1988a) The phenomena of senescence and aging. In "Senescence and Aging in Plants"; Noodén, L.D., Leopold, A.C., Eds.; Academic Press: San Diego, CA, USA, 1988; pp 1-50
Noodén LD (1988b) Whole plant senescence. In "Senescence and Aging in Plants"; Noodén, L.D., Leopold, A.C., Eds.; Academic Press: San Diego, CA, USA, 1988; pp 392-439
Offler CE, McCurdy DW, Patrick JW, Talbot MJ (2003) Transfer cells: Cells specialized for a special purpose. Annual Review of Plant Biology **54:** 431-454
Okumoto S, Schmidt R, Tegeder M, Fischer WN, Rentsch D, Frommer WB, Koch W (2002) High affinity amino acid transporters specifically expressed in xylem parenchyma and developing seeds of Arabidopsis. Journal of Biological Chemistry **277:** 45338-45346
Olsen AN, Ernst HA, Leggio LL, Skriver K (2005) NAC transcription factors: structurally distinct, functionally diverse. Trends in Plant Science **10:** 79-87
Olsen O-A (2001) Endosperm development: Cellularization and cell fate specification. Annual Review of Plant Physiology and Plant Molecular Biology **52:** 233-267
Otegui MS, Noh Y-S, Martínez DE, Vila Petroff MG, Andrew Staehelin L, Amasino RM, Guiamet JJ (2005) Senescence-associated vacuoles with intense proteolytic activity develop in leaves of Arabidopsis and soybean. The Plant Journal **41:** 831-844
Park S, Rancour DM, Bednarek SY (2008) In planta analysis of the cell cycle-dependent localization of AtCDC48A and its critical roles in cell division, expansion, and differentiation. Plant Physiology **148:** 246-258
Patrick JW, Offler CE (2001) Compartmentation of transport and transfer events in developing seeds. Journal of Experimental Botany **52:** 551-564
Peng B, Kong H, Li Y, Wang L, Zhong M, Sun L, Gao G, Zhang Q, Luo L, Wang G, Xie W, Chen J, Yao W, Peng Y, Lei L, Lian X, Xiao J, Xu C, Li X, He Y (2014) OsAAP6 functions as an important regulator of grain protein content and nutritional quality in rice. Nature Communications **5:** Article number: 4847
Peoples MB, Dalling MJ (1988) The interlplay between proteolysis and amino acid metabolism during senescence and aging in plants. In "Senescence and Aging in Plants"; Noodén, L.D., Leopold, A.C., Eds.; Academic Press: San Diego, CA, USA, 1988; pp. 182-218
Radchuk R, Emery RJN, Weier D, Vigeolas H, Geigenberger P, Lunn JE, Feil R, Weschke W, Weber H (2010) Sucrose non-fermenting kinase 1 (SnRK1) coordinates metabolic and hormonal signals during pea cotyledon growth and differentiation. The Plant Journal **61:** 324-338
Radchuk VV, Borisjuk L, Sreenivasulu N, Merx K, Mock H-P, Rolletschek H, Wobus U, Weschke W (2009) Spatiotemporal profiling of starch biosynthesis and degradation in the developing barley grain. Plant Physiology **150:** 190-204
Rawlings ND, Waller M, Barrett AJ, Bateman A (2014) MEROPS: the database of proteolytic enzymes, their substrates and inhibitors. Nucleic Acids Research **42:** D503-D509
Rentsch D, Schmidt S, Tegeder M (2007) Transporters for uptake and allocation of organic nitrogen compounds in plants. FEBS Letters **581:** 2281-2289
Rosche EG, Blackmore D, Offler CE, Patrick JW (2005) Increased capacity for sucrose uptake leads to earlier onset of protein accumulation in developing pea seeds. Functional Plant Biology **32:** 997-1007
Rushton PJ, Somssich IE, Ringler P, Shen QJ (2010) WRKY transcription factors. Trends in Plant Science **15:** 247-258
Sanchez-Bragado R, Molero G, Reynolds MP, Araus JL (2014) Relative contribution of shoot and ear photosynthesis to grain filling in wheat under good agronomical conditions assessed by differential organ δ13C. Journal of Experimental Botany **65:** 5401-5413

Sanders A, Collier R, Trethewy A, Gould G, Sieker R, Tegeder M (2009) AAP1 regulates import of amino acids into developing Arabidopsis embryos. The Plant Journal **59:** 540-552

Schildhauer J, Wiedemuth K, Humbeck K (2008) Supply of nitrogen can reverse senescence processes and affect expression of genes coding for plastidic glutamine synthetase and lysine-ketoglutarate reductase/saccharopine dehydrogenase. Plant Biology **10:** 76-84

Schippers JHM, Jing H-C, Hille J, Dijkwel PP (2007) Developmental and hormonal control of leaf senescence. *In* Annual Plant Reviews Volume 26: Senescence Processes in Plants. Blackwell Publishing Ltd, pp 145-170

Schmidt R, Stransky H, Koch W (2007) The amino acid permease AAP8 is important for early seed development in *Arabidopsis thaliana*. Planta **226:** 805-813

Schoonheim PJ, Costa Pereira DD, De Boer AH (2009) Dual role for 14-3-3 proteins and ABF transcription factors in gibberellic acid and abscisic acid signalling in barley (*Hordeum vulgare*) aleurone cells. Plant, Cell & Environment **32:** 439-447

Schoonheim PJ, Sinnige MP, Casaretto JA, Veiga H, Bunney TD, Quatrano RS, de Boer AH (2007) 14-3-3 adaptor proteins are intermediates in ABA signal transduction during barley seed germination. The Plant Journal **49:** 289-301

Schwacke R, Schneider A, van der Graaff E, Fischer K, Catoni E, Desimone M, Frommer WB, Flügge U-I, Kunze R (2003) ARAMEMNON, a novel database for Arabidopsis integral membrane proteins. Plant Physiology **131:** 16-26

Shewry PR, Halford NG (2002) Cereal seed storage proteins: structures, properties and role in grain utilization. Journal of Experimental Botany **53:** 947-958

Simmonds NW (1995) The relation between yield and protein in cereal grain. Journal of the Science of Food and Agriculture **67:** 309-315

Simpson RJ, Lambers H, Dalling MJ (1983) Nitrogen redistribution during grain growth in wheat (*Triticum aestivum L.*) : IV. Development of a quantitative model of the translocation of nitrogen to the grain. Plant Physiology **71:** 7-14

Smart CM (1994) Gene expression during leaf senescence. New Phytologist **126:** 419-448

Song W, Koh S, Czako M, Marton L, Drenkard E, Becker JM, Stacey G (1997) Antisense expression of the peptide transport gene *AtPTR2-B* delays flowering and arrests seed development in transgenic Arabidopsis plants. Plant Physiology **114:** 927-935

Sreenivasulu N, Altschmied L, Radchuk V, Gubatz S, Wobus U, Weschke W (2004) Transcript profiles and deduced changes of metabolic pathways in maternal and filial tissues of developing barley grains. The Plant Journal **37:** 539-553

Stacey MG, Patel A, McClain WE, Mathieu M, Remley M, Rogers EE, Gassmann W, Blevins DG, Stacey G (2008) The Arabidopsis AtOPT3 Protein Functions in Metal Homeostasis and Movement of Iron to Developing Seeds. Plant Physiology **146:** 589-601

Su Y-H, Frommer WB, Ludewig U (2004) Molecular and functional characterization of a family of amino acid transporters from Arabidopsis. Plant Physiology **136:** 3104-3113

Swofford DL (2002) PAUP*: Phylogenetic Analysis Using Parsimony (and Other Methods) 4.0 Beta. Sinauer Associates, Inc., Publishers, Florida State University

Tegeder M, Rentsch D (2010) Uptake and partitioning of amino acids and peptides. Molecular Plant **3:** 997-1011

Thiel J, Hollmann J, Rutten T, Weber H, Scholz U, Weschke W (2012) 454 transcriptome sequencing suggests a role for two-component signalling in cellularization and differentiation of barley endosperm transfer cells. PLoS ONE **7:** e41867

Thiel J, Müller M, Weschke W, Weber H (2009) Amino acid metabolism at the maternal–filial boundary of young barley seeds: a microdissection-based study. Planta **230:** 205-213

Thiel J, Weier D, Sreenivasulu N, Strickert M, Weichert N, Melzer M, Czauderna T, Wobus U, Weber H, Weschke W (2008) Different hormonal regulation of cellular differentiation and function in nucellar projection and endosperm transfer cells: a microdissection-based transcriptome study of young barley grains. Plant Physiology **148:** 1436-1452

Tsay Y-F, Chiu C-C, Tsai C-B, Ho C-H, Hsu P-K (2007) Nitrate transporters and peptide transporters. FEBS Letters **581:** 2290-2300

Tsay Y-F, Schroeder JI, Feldmann KA, Crawford NM (1993) The herbicide sensitivity gene CHL1 of arabidopsis encodes a nitrate-inducible nitrate transporter. Cell **72:** 705-713

Uauy C, Distelfeld A, Fahima T, Blechl A, Dubcovsky J (2006) A NAC gene regulating senescence improves grain protein, zinc, and iron content in wheat. Science **314:** 1298-1301

van der Graaff E, Schwacke R, Schneider A, Desimone M, Flügge U-I, Kunze R (2006) Transcription analysis of Arabidopsis membrane transporters and hormone pathways during developmental and induced leaf senescence. Plant Physiology **141:** 776-792

Vidmar JJ, Zhuo D, Siddiqi MY, Schjoerring JK, Touraine B, Glass ADM (2000) Regulation of high-affinity nitrate transporter genes and high-affinity nitrate influx by nitrogen pools in roots of barley. Plant Physiology **123:** 307-318

Waters BM, Uauy C, Dubcovsky J, Grusak MA (2009) Wheat (*Triticum aestivum*) NAM proteins regulate the translocation of iron, zinc, and nitrogen compounds from vegetative tissues to grain. Journal of Experimental Botany **60:** 4263-4274

Waters SP, Peoples MB, Simpson RJ, Dalling MJ (1980) Nitrogen redistribution during grain growth in wheat (*Triticum aestivum* L.) I. Peptide hydrolase activity and protein breakdown. Planta **148:** 422-428

Weaver L, Gan S, Quirino B, Amasino R (1998) A comparison of the expression patterns of several senescence-associated genes in response to stress and hormone treatment. Plant Molecular Biology **37:** 455-469

Weigelt K, Küster H, Rutten T, Fait A, Fernie AR, Miersch O, Wasternack C, Emery RJN, Desel C, Hosein F, Müller M, Saalbach I, Weber H (2009) ADP-Glucose pyrophosphorylase-deficient pea embryos reveal specific transcriptional and metabolic changes of carbon-nitrogen metabolism and stress responses. Plant Physiology **149:** 395-411

Weschke W, Panitz R, Sauer N, Wang Q, Neubohn B, Weber H, Wobus U (2000) Sucrose transport into barley seeds: molecular characterization of two transporters and implications for seed development and starch accumulation. The Plant Journal **21:** 455-467

West CE, Waterworth WM, Stephens SM, Smith CP, Bray CM (1998) Cloning and functional characterisation of a peptide transporter expressed in the scutellum of barley grain during the early stages of germination. The Plant Journal **15:** 221-229

Winter H, Lohaus G, Heldt HW (1992) Phloem transport of amino acids in relation to their cytosolic levels in barley leaves. Plant Physiology **99:** 996-1004

Wobus U, Sreenivasulu N, Borisjuk L, Rolletschek H, Panitz R, Gubatz S, Weschke W (2005) Molecular physiology and genomics of developing barley grains. *In* SG Pandalai, ed, Recent Research Developments in Plant Molecular Biology, Vol 2. Research Signpost, Trivandrum, pp 1-29

Xiang X, Bao Y (1997) Relationship between embryo and endosperm development and accumulation of storage reserves in barley. Acta Botanica Sinica **39:** 905–913

Xiao S, Dai L, Liu F, Wang Z, Peng W, Xie D (2004) COS1: An Arabidopsis coronatine insensitive1 suppressor essential for regulation of jasmonate-mediated plant defense and senescence. The Plant Cell Online **16:** 1132-1142

Yen M-R, Tseng Y-H, Saier MH (2001) Maize Yellow Stripe1, an iron-phytosiderophore uptake transporter, is a member of the oligopeptide transporter (OPT) family. Microbiology **147:** 2881-2883

Zentgraf U, Laun T, Miao Y (2010) The complex regulation of WRKY53 during leaf senescence of *Arabidopsis thaliana*. European Journal of Cell Biology **89:** 133-137

Zhang L-F, Rui Q, Zhang P, Wang X-y, Xu L-L (2007) A novel 51-kDa fragment of the large subunit of ribulose-1,5-bisphosphate carboxylase/oxygenase formed in the stroma of chloroplasts in dark-induced senescing wheat leaves. Physiologia Plantarum **131:** 64-71

Zhang L, Tan Q, Lee R, Trethewy A, Lee Y-H, Tegeder M (2010) Altered xylem-phloem transfer of amino acids affects metabolism and leads to increased seed yield and oil content in Arabidopsis. The Plant Cell Online **22:** 3603-3620

Zhang M-Y, Bourbouloux A, Cagnac O, Srikanth CV, Rentsch D, Bachhawat AK, Delrot S (2004) A novel family of transporters mediating the transport of glutathione derivatives in plants. Plant Physiology **134:** 482-491

Zhao Q, Nakashima J, Chen F, Yin Y, Fu C, Yun J, Shao H, Wang X, Wang ZY, Dixon RA (2013) Laccase is necessary and nonredundant with peroxidase for lignin polymerization during vascular development in Arabidopsis. Plant Cell **25:** 3976-3987

Zheng L, Fujii M, Yamaji N, Sasaki A, Yamane M, Sakurai I, Sato K, Ma JF (2011) Isolation and characterization of a barley Yellow Stripe-Like Gene, *HvYSL5*. Plant and Cell Physiology **52:** 765-774

Zhou J-J, Theodoulou FL, Muldin I, Ingemarsson B, Miller AJ (1998) Cloning and functional characterization of a *Brassica napus* transporter that is able to transport nitrate and histidine. Journal of Biological Chemistry **273:** 12017-12023

9. Acknowledgements

I want to express my gratitude to Dr. Weschke and Dr. Weber for giving me the opportunity to work on this project, providing the prerequisites for a successful scientific work within the Seed Development Group, and the fruitful discussions concerning the scientific interpretation of the results deriving from this work.
For excellent technical assistance with everyday lab work, as well as for the support on many different levels throughout all the years, I want to specially thank Angela Stegmann.
I would like to thank our technicians at the IPK, Elsa Fessel, Gabriele Einert, Uta Siebert, Heiko Weichert, Kathrin Blaschek, and Angela Schwarz, as well as Dr. Martin Müller for their excellent assistance in harvesting, preparing and analysing the plant material. Furthermore, I want to thank all the postdocs at the IPK who shared their knowledge with me, especially Dr. Ruslana Radchuk for discussing all matters of expression analyses.
Special thanks to all the authors for their input to the publications this thesis is based on, especially to Julien Hollmann (University of Kiel) whose bioinformatics work laid the basis for the evaluation of the RNAseq data and the array design.
I want to thank Dr. Weschke, Dr. Weber, Dr. Hart Poskar and Dr. Hardy Rolletschek for their critical revisions of the thesis, and the suggestions to improve content and style.

Finally, I want to express my gratitude to the persons without whom I would have never been able to come to this point. My special thanks go to my mother and Sigi, to my father, Tanja and Sergej, who supported me throughout my life and always believed in me.
Thank you for everything!

This work was funded by the Deutsche Forschungsgemeinschaft (DFG) in the frame of Research Unit 948 “Nitrogen uptake, metabolism and remobilisation in leaves during plant senescence” (Grant Number: WE 1641/13-2).

10. Eidesstattliche Erklärung

Hiermit erkläre ich, Stefan Kohl, geboren am 04.06.1975 in Augsburg, dass diese Arbeit von mir bisher weder der Naturwissenschaftlichen Fakultät I – Biowissenschaften – der Martin-Luther-Universität Halle-Wittenberg, noch einer anderen wissenschaftlichen Einrichtung zum Zweck der Promotion eingereicht wurde und ich noch keine vergeblichen Promotionsversuche unternommen habe.
Ich erkläre ferner, dass ich diese Arbeit selbstständig, ohne fremde Hilfe und nur unter zur Zuhilfenahme der angegebenen Hilfsmittel und Literatur angefertigt habe und weiterhin keine anderen als die von mir angegebenen Quellen und Hilfsmittel benutzt habe, sowie die den benutzten Werken wörtlich oder inhaltlich entnommenen Stellen als solche kenntlich gemacht habe.

Gatersleben, 12.03.2015

(S. Kohl)

11. *Curriculum vitae*

Personal details

Name:	Stefan Kohl
Sex:	Male
Nationality:	German
Present address	Valentina-Tereschkova-Str. 1, 06449 Aschersleben, Germany
Date of birth:	4th of June, 1975
Place of birth:	Augsburg, Germany

Contact information

Telephone:	+49(0)394825772 (office) / +49(0)3473979931 (private)
E-mail:	kohl@ipk-gatersleben.de

Education

09/1981 – 06/1985	Basic primary school, Königsbrunn, Germany
09/1985 – 07/1994	Secondary school, Königsbrunn, Germany Graduated with the general qualification for university entrance
08/1994 – 09/1995	Applied for Studies in Business Engineering; part-time jobs
10/1995 – 08/1996	Studies of Economics, Fachhochschule Augsburg, Germany
09/1996 – 02/1999	Vocational educations as Industrial Management Assistant IBA Hartmann GmbH & Co. KG, Augsburg, Germany Graduated as Industrial Management Assistant (Chamber of Industry and Commerce)
03/1999 – 09/2003	Employed as Industrial Management Assistant IBA Hartmann GmbH & Co. KG, Augsburg, Germany
10/2003 – 10/2008	Studies of Biology, University of Kassel, Germany Graduated as Biologist (Diploma)
03/2008 – 10/2008	Diploma thesis at the Leibniz Institute of Plant Genetics and Crop Plant Research (IPK), Gatersleben, Seed Development Group: „Modifikation der Saccharoseaufnahme in Erbsenembryonen: Genotypische und phänotypische Analyse transgener Samen und Pflanzen“
01/2009 – 02/2009	Research assistant at the IPK, Gatersleben (Seed Development Group)
Since 03/2009	PhD student at the IPK, Gatersleben (Seed Development Group) Title: “N remobilisation during barley grain filling and the influences of sink-strength alteration in developing wheat grains”

List of publications

Weichert N, Saalbach I, Weichert H, Kohl S, Erban A, Kopka J, Hause B, Varshney A, Sreenivasulu N, Strickert M, Kumlehn J, Weschke W, Weber H. 2010. Increasing Sucrose Uptake Capacity of Wheat Grains Stimulates Storage Protein Synthesis. *Plant Physiology* **152**, 698-710.

Kohl S, Hollmann J, Blattner F, Radchuk V, Andersch F, Steuernagel B, Schmutzer T, Scholz U, Krupinska K, Weber H, Weschke W. 2012. A putative role for amino acid permeases in sink-source communication of barley tissues uncovered by RNA-seq. BMC Plant Biology 12, 154.

Weier D, Thiel J, Kohl S, Tarkowská D, Strnad M, Schaarschmidt S, Weschke W, Weber H, Hause B. 2014. Gibberellin-to-abscisic acid balances govern development and differentiation of the nucellar projection of barley grains. Journal of Experimental Botany 65, 5291-5304.

Kohl S, Hollmann J, Erban A, Kopka J, Riewe D, Weschke W, Weber H. 2015. Metabolic and transcriptional transitions in barley glumes reveal a role as transitory resource buffers during endosperm filling. Journal of Experimental Botany Journal of Experimental Botany 66, 1397-1411.

Pielot R, Kohl S, Manz B, Rutten T, Weier D, Tarkowská D, Rolčík J, Strnad M, Volke F, Weber H, Weschke W. 2015. Hormone-mediated growth dynamics of the barley pericarp as revealed by Magnetic Resonance Imaging and transcript profiling. Plant Physiology. Submitted 01/2015

Poster presentations

Kohl S, Hollmann J, Radchuk V, Steuernagel B, Schmutzer T, Scholz U, Weber H, Weschke W. Title: New 454 sequence information reflecting N-remobilization and N-supply for grain filling in barley. November 23rd to 24th, 2010, 10th Gatersleben Research Conference (GCRX), Leibniz Institute of Plant Genetics and Crop Plant Research (IPK), Gatersleben

Kohl S, Hollmann J, Blattner FR, Radchuk V, F Andersch, Steuernagel B, Schmutzer T, Scholz U, Krupinska K, Weber H, Weschke W. Title: A putative role for amino acid permeases in sink-source communication of barley tissues uncovered by RNA-seq. September 24th to 25th, 2012, Institutes Day, IPK, Gatersleben

Kohl S, Hollmann J, Erban A, Kopka J, Riewe D, Weber H, Weschke W. Title: Barley glumes: a transitory buffer of resources during endosperm filling. September 17th to 18th, 2014, Institutes Day, IPK, Gatersleben

Conferences and meetings attended

10th Gatersleben Research Conference (GCRX), Leibniz Institute of Plant Genetics and Crop Plant Research (IPK), Gatersleben, Germany.

Status meetings of the DFG Research Group 948 "Nitrogen uptake, metabolism and remobilization in leaves during plant senescence" (* Oral presentation)

07.10.2009	IPK Gatersleben, Germany*
06. – 07.05.2010	Norddeutsche Pflanzenzucht Hans-Georg Lembke KG, Hohenlieth, Germany*
13. – 14.10.2010	Universität Hohenheim, Germany*
12. – 13.05.2011	Universität Graz, Austria*
23. – 24.09.2011	Freie Universität Berlin, Germany
01. – 02.11.2012	Universität Potsdam, Germany*
03. – 04.10.2013	Universität Tübingen, Germany*
17. – 18.07.2014	Freie Universität Berlin, Germany*

Workshops attended and stays at other research centres

22. – 26.02.2010	Institute of Botany, University of Kiel, Germany; Workshop: "Cell imaging-techniques of electron and fluorescence microscopy in the context of wound-induced cellular changes of barley (*Hordeum vulgare*) leaves"
15. – 20.08.2010	MPI Golm, Germany; Scientific collaboration: Sample preparation and introduction into large-scale metabolite analysis via GC-MS
10. – 11.11.2010	IPK Gatersleben, Germany; Workshop: "Scientific Writing"
05. – 11.06.2011	MPI Golm, Germany; Workshop: "qRT-PCR and microarray based transcriptome analysis"

Teaching activities

03/2013	IPK Gatersleben, Germany; Lecture and practical course during the workshop “Microdissection and expression analysis” of the Leibniz Graduate School
2012 & 2014	IPK Gatersleben, Germany; Supervision of PhD students from the universities of Halle and Kiel performing microarray experiments

12. Publications on which this thesis is based on

12.1. Declaration on the contributions

12.1.1. Kohl S, Hollmann J, Blattner F, Radchuk V, Andersch F, Steuernagel B, Schmutzer T, Scholz U, Krupinska K, Weber H, Weschke W. 2012. A putative role for amino acid permeases in sink-source communication of barley tissues uncovered by RNA-seq. BMC Plant Biology 12 (1), 154.

My contribution to the work corresponds to ~40%:

- Identification of putative barley N transporters from public databases and RNAseq data
- Evaluation, comparison, and phylogenetic analyses of datasets
- Experimental planning, set-up and data analysis for qRT-PCR
- Manuscript and figure preparation

Gatersleben, 12.03.2015 Gatersleben, 12.03.2015

(S. Kohl) (W. Weschke)

12.1.2. Kohl S, Hollmann J, Erban A, Kopka J, Riewe D, Weschke W, Weber H. 2015. Metabolic and transcriptional transitions in barley glumes reveal a role as transitory resource buffers during endosperm filling. Journal of Experimental Botany, 66(5): 1397-1411.

My contribution to the work corresponds to ~70%:

- All experimental work (except derivatisation steps of chromatography analyses and micro-dissection of vascular tissues)
- All data evaluations and statistical analyses
- Manuscript and figure preparation

Gatersleben, 12.03.2015 Gatersleben, 12.03.2015

(S. Kohl) (H. Weber)

12.1.3. Weichert N, Saalbach I, Weichert H, **Kohl S**, Erban A, Kopka J, Hause B, Varshney A, Sreenivasulu N, Strickert M, Kumlehn J, Weschke W, Weber H. 2010. Increasing sucrose uptake capacity of wheat grains stimulates storage protein synthesis. Plant Physiology 152, 698-710.

My contribution to the work corresponds to ~10%:

- Establishing sucrose uptake experiments in wheat grains
- Data evaluation and figure preparation

Gatersleben, 12.03.2015 Gatersleben, 12.03.2015

(S. Kohl) (H. Weber)

Kohl et al. BMC Plant Biology 2012, 12:154
http://www.biomedcentral.com/1471-2229/12/154

BMC Plant Biology

RESEARCH ARTICLE Open Access

A putative role for amino acid permeases in sink-source communication of barley tissues uncovered by RNA-seq

Stefan Kohl[1*†], Julien Hollmann[2†], Frank R Blattner[1], Volodymyr Radchuk[1], Franka Andersch[1], Burkhard Steuernagel[1], Thomas Schmutzer[1], Uwe Scholz[1], Karin Krupinska[2], Hans Weber[1] and Winfriede Weschke[1*]

Abstract

Background: The majority of nitrogen accumulating in cereal grains originates from proteins remobilised from vegetative organs. However, interactions between grain filling and remobilisation are poorly understood. We used transcriptome large-scale pyrosequencing of flag leaves, glumes and developing grains to identify cysteine peptidase and N transporter genes playing a role in remobilisation and accumulation of nitrogen in barley.

Results: Combination of already known and newly derived sequence information reduced redundancy, increased contig length and identified new members of cysteine peptidase and N transporter gene families. The dataset for N transporter genes was aligned with N transporter amino acid sequences of rice and Arabidopsis derived from Aramemnon database. 57 *AAT*, 45 *NRT1/PTR* and 22 *OPT* unigenes identified by this approach cluster to defined subgroups in the respective phylogenetic trees, among them 25 *AAT*, 8 *NRT1/PTR* and 5 *OPT* full-length sequences. Besides, 59 unigenes encoding cysteine peptidases were identified and subdivided into different families of the papain cysteine peptidase clade. Expression profiling of full-length *AAT* genes highlighted amino acid permeases as the group showing highest transcriptional activity. *HvAAP2* and *HvAAP6* are highly expressed in vegetative organs whereas HvAAP3 is grain-specific. Sequence similarities cluster HvAAP2 and the putative transporter HvAAP6 together with Arabidopsis transporters, which are involved in long-distance transfer of amino acids. HvAAP3 is closely related to AtAAP1 and AtAAP8 playing a role in supplying N to developing seeds. An important role in amino acid re-translocation can be considered for HvLHT1 and HvLHT2 which are specifically expressed in glumes and flag leaves, respectively. PCA and K-means clustering of *AAT* transcript data revealed coordinate developmental stages in flag leaves, glumes and grains. Phloem-specific metabolic compounds are proposed that might signal high grain demands for N to distantly located plant organs.

Conclusions: The approach identified cysteine peptidases and specific N transporters of the AAT family as obviously relevant for grain filling and thus, grain yield and quality in barley. Up to now, information is based only on transcript data. To make it relevant for application, the role of identified candidates in sink-source communication has to be analysed in more detail.

Keywords: Barley, Vegetative organs, Developing grains, N remobilisation, N accumulation, RNA-seq, Cysteine peptidases, N transporter genes, Source-sink communication

* Correspondence: kohl@ipk-gatersleben.de; weschke@ipk-gatersleben.de
†Equal contributors
[1]Leibniz-Institut für Pflanzengenetik und Kulturpflanzenforschung (IPK), Gatersleben D-06466, Germany
Full list of author information is available at the end of the article

Background

In crop plants more than 70% of seed nitrogen is remobilised and translocated from vegetative tissues such as stems and senescing leaves [1]. Remobilisation of N follows different time courses, and contributions of various organs and tissues to N economy of developing seeds differ [2]. In cereals, flag leaves and glumes maintain their metabolic activity longer than other vegetative tissues, and their contribution to the final grain yield is high [3].

Up to 75% of reduced nitrogen in photosynthetically active leaf cells is located in the chloroplasts. Ribulose-1,5-bisphosphate carboxylase/oxygenase (Rubisco) represents the major fraction of chloroplast nitrogen [4]. Before nitrogen is exported to the phloem, Rubisco must be degraded to peptides and amino acids [5]. Gene expression analysis in wheat and barley identified several cysteine protease genes with enhanced transcript levels during leaf senescence [6-8]. Certain C1A-type (papain-type) cysteine proteases and possibly also S10-type serine carboxypeptidases are involved in bulk degradation of stromal proteins during leaf senescence [8]. Both types of proteases are potentially synthesised at the endoplasmatic reticulum and channelled by the secretory pathway, which suggests routing to the lytic vacuolar compartment such as small senescence-associated vacuoles [9]. High expression and strong upregulation of genes encoding papain-like cysteine peptidases suggests an important role for especially those family members in naturally senescing barley leaves between 7 and 21 DAF [7].

During senescence, cellular proteins are degraded into peptides and amino acids. Efficient partitioning of amino acids or peptides within the plant requires active transporters to transfer N compounds across cellular membranes [10]. For plants with fully sequenced genomes (e.g. Arabidopsis and rice), the Aramemnon database [11,12] provides annotation and further information for the complete collection of putative N transporter genes, whereas to date only four sequences for putative barley N transporters are listed. Based on sequence similarity, amino acid transporters were grouped into members of the ATF (amino acid transporter family) and the APC (amino acid-polyamine-choline) families. The ATF family can be further divided into AAPs (general amino acid permeases), LHTs (lysine-histidine transporters), proline transporters (ProTs) as well as into transporters with substrates like γ-aminobutyric acid (GATs), aromatic and neutral amino acids (ANTs) and indole-3-acetic acid (AUXs) [10,13,14]. Subdivision of the APC family reveals transporters for cationic (CATs) and L-type amino acids (LATs), as well as the GABA permeases (GAP). Overall 63 (Arabidopsis) and 80 (rice) candidates cluster into these groups.

Peptide transport in plants is accomplished by two gene families, the oligopeptide transporters (OPTs) transporting tetra- and pentapeptides and transporters for di- and tripeptides belonging to the nitrate/peptide transporter family (NRT1/PTR) [14]. In Arabidopsis and rice, 53 and 81 members belong to this group, while 9 and 8 transporters are annotated as OPTs. Whereas a relatively high number of Arabidopsis amino acid and NRT1/PTR transporters are functionally characterized (for reviews see [10,13]) the information for monocots, especially for barley is scarce. The best characterised monocot peptide transporter is HvPTR1 localized in the scutellum of barley grains and responsible for mobilisation of peptides from endosperm into germinating embryos [15,16]. OsPTR6 was shown to transport Gly-His-Gly [17]. From the OPT family, only one monocot sequence (OsGT1) has been functionally characterised so far [18].

Numerous transporters contributing to iron trafficking in plants are described and were functionally characterised for grasses. This is due to the fact that grasses evolved a distinct mechanism to acquire Fe from the soil best described as 'chelation' strategy [19]. Strong Fe chelators called phytosiderophores (PS), are synthesised by the plant and secreted into the rhizosphere, where they bind Fe(III). The Fe(III)-PS complex is than taken up by Fe(III)–PS uptake proteins [20,21] called Yellow Stripe-Like (YSL) transporters. Several YSL transporters have been identified and characterised (see for instance [22-25]), among them the barley transporters HvYSL5 [26], HvYSL2 [25] and HvYS1 [27]. The role of YSL transporters in remobilisation and grain filling is unclear yet. YSL transporters are distantly related to the OPT family [28]. In Arabidopsis and rice, 8 and 18 sequences belong to the YSL group.

Although numerous plant amino acid and peptide transporters have been identified and some of them functionally characterised, it is difficult to determine which are the most important for plant N recycling on both the source and the sink side. For barley, this situation is even more complicated as the genomic sequence is only partially assembled [29]. Furthermore, only 0.06% (264 ESTs) from 444,652 barley ESTs in assembly 35 of HarvEST:Barley v1.83 (H35, [30]) represent sequences expressed in glumes and those 33,376 ESTs (7.47%) derived from leaf cDNA libraries are not representative for remobilising flag leaves. Sequence information from EST collections might also be reduced for membrane-associated compounds because of high instability of respective *E. coli* clones.

Next generation sequencing (NGS) technologies offer new opportunities to analyse plants without fully sequenced genomes. Transcriptome large-scale parallel

pyrosequencing was addressed to flag leaves, glumes and developing grains in order to analyse remobilisation and import of N compounds immediately before and after seed set. Data evaluation was focussed on two specific groups of genes responsible for remobilisation and accumulation of nitrogen, cysteine peptidases and N transporters. Combination of publicly available and RNA-seq data reduced redundancy, increased length of gene-specific contigs and identified new members within the respective gene families. Members of the *AAT* gene family were over-represented in the set of RNA-seq N transporter sequences. Sequence alignment allowed to reconstruct 25 full-length *AAT* genes. Based on temporal expression profiling of these genes we hypothesise that establishment of high N-sink strength in developing grains is perceived in flag leaf and glumes, the tissues in close proximity to developing seeds. We postulate that metabolites communicate the increasing sink strength to the remobilising tissues by modulating transcript amounts as shown here for amino acid permeases. Thus, *AAT* gene activities might be involved in source/sink communication in barley. In addition, fluctuating transcript abundances of *AAT* genes especially in flag leaves might reflect tissue-specific regulation of sink/source transition.

Results

RNA-seq and sequence assembly

mRNA was prepared from barley flag leaves, glumes and caryopses collected at different stages of grain development. Equal amounts of RNA were combined from each stage at 2 day intervals, from 4 days before anthesis up to 24 days after flowering (DAF) for flag leaves and glumes, between anthesis and 24 DAF for caryopses.

After quantification and quality control of the samples, reverse transcription and normalisation of the three libraries as well as transcriptome sequencing was performed by GATC Biotech (Konstanz, Germany). One half Roche/454 GS-FLX run was performed for each library. From a total of 1,806,025 reads 701,026 distribute to flag leaves (FL), 557,505 to glumes (GL) and 547,494 to grains (G). Adaptor and quality trimming reduced read-yield to 1,585,811 (615,568 + 485,800 + 484,443, see Table 1). Average read length was 397 bp (FL), 400 bp (GL) and 392 bp (G). For each organ, reads were clustered and assembled into contigs and singletons (Table 1). Flag leaves showed highest contig number (43,467) but lowest contig length (688 bp). Glumes revealed lowest contig number (31,022) and highest contig length (835 bp). Grains showed moderate levels (37,790 and 791, Table 1). On average, each contig was covered by 11 to 15 reads. Whereas contig numbers were comparable between the three organs, numbers of singletons vary from high values in FL and G (97,348 and 82,446) to low values in GL (29,388). This suggests high numbers of lowly expressed genes in flag leaves and grains and low numbers of highly expressed genes in glumes, indicating lower complexity of the glumes transcriptome.

Table 1 Output of large scale RNA-seq and sequence assembly

	Flag leaf	Glumes	Grains
Total reads	615,568	485,800	484,443
Ø Read length	397	400	392
Total contigs	43,467	31,022	37,790
Ø Reads/contig	12	15	11
Ø Contig size	688	835	791
Total singletons	97,348	29,388	82,446

Annotation

Contigs and singletons obtained after sequence assembly were characterised by a multilevel process of filtering from barley-specific to more general data sets as well as from high to low stringency using the different databases in the following order: (1) H35 [30], (2) UniProtKB/Swiss-Prot [31], (3) UniProtKB/TrEMBL [31] and (4) non-redundant dataset from NCBI [32] with E-value cut-offs of $<1E^{-20}$, $<1E^{-20}$, $<1E^{-10}$ and $<1E^{-5}$, respectively. Sequences without a match in one database were compared to the next one. The output of annotation is given in Table 2.

Percentages of total contig hits are comparable between glumes and grains (88.73% and 88.56%) but are higher for flag leaves (90.34%). BLAST searches against the different databases revealed 14.1% (FL), 11.3% (GL) and 10.1% (G) of new contig sequences as not functionally described in H35. For the total no hit category, results for flag leaves are different from those of glumes

Table 2 Annotation of RNA-seq contigs and singletons

BLASTn vs	Flag leaf	Glumes	Grains
		No. of contigs	
HarvEST35 (e^{-20})	33,743	24,416	30,077
UniProtKB/Swiss-Prot (e^{-20})	1,196	542	635
UniProtKB/TrEMBL (e^{-10})	3,573	2,183	2,302
non-redundant (e^{-5})	754	386	453
Total hits	39,266	27,527	33,467
Total no hits	4,201	3,495	4,323
		No. of singletons	
HarvEST35 (e^{-20})	38,119	16,200	32,390
UniProtKB/Swiss-Prot (e^{-20})	843	509	611
UniProtKB/TrEMBL (e^{-10})	5,809	2,840	4,892
non-redundant (e^{-5})	4,986	887	3,992
Total hits	49,757	20,436	41,885
Total no hits	47,591	8,952	40,561

and grains (9.7%, 11.3% and 11.4%, respectively). Percentages of total-hit singletons are comparable for flag leaves and grains (51.1% and 50.8%) but higher for glumes (69.5%). This result coincides with the observed low number of glumes singletons (Table 1) and indicates lower complexity of the glumes transcriptome compared to flag leaves and grains.

The sum of contigs and singletons annotated from flag leaves (33,743 + 38,119) yields 71,862 expressed genes, which is clearly higher than the number of unigenes from H35 (50,938). This may reflect high redundancy of the flag leaf dataset, which is also obvious for grains (62,467 annotated sequences) but not for glumes (40,616 annotated sequences). This can be explained by the fact that only RNA-seq reads were used for the assembly process. Obviously, some of the RNA-seq singletons and/or contigs represent the same gene, but do not overlap and thus increase the numbers within the total hit category. The contribution of contigs should be lower than that of singletons.

Tissue-specificity of contigs

Figure 1 shows tissue-specificity of CAP3 contigs. The percentage of contigs expressed exclusively in glumes (4.9%) is remarkably lower than that expressed specifically in flag leaves (13.8%) or grains (14.0%). The transcriptome of the glumes contains a low number of sequences identical with those expressed in flag leaves (5.0%) and grains (5.5%). In contrast, a high percentage of sequences (34.8%) is shared between flag leaves and grains.

For an overview on the tissue specificity of molecular functions, pyrosequence contigs and H35 unigenes were annotated based on gene ontology terms [33] and analysed by Blast2GO software [34,35]. The results from level 3 of the category Molecular Function are depicted in Figure 2.

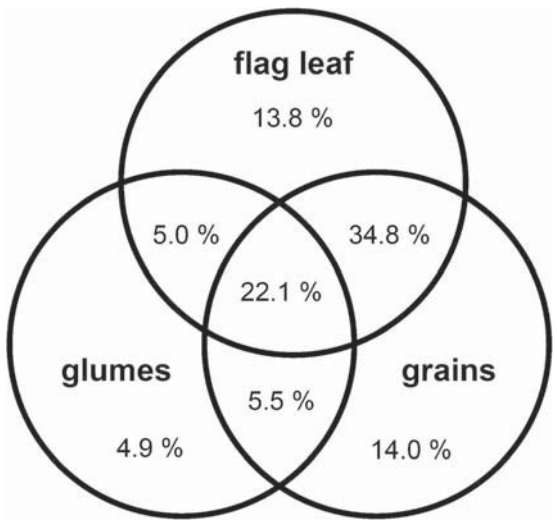

Figure 1 Venn diagram showing tissue specificity of the CAP3-contigs.

There are two main findings: (i) flag leaf and grain transcriptomes are highly similar in all depicted categories and (ii) the glumes transcriptome differs from flag leaves and grains, but is comparable to H35. Categories "trans-membrane transporter activity", "substrate-specific transport activity" and to lesser extent "transferase-activity" and "nucleotide binding" are enriched in glumes. Especially for "ion binding", "nucleic acid binding", "lyase and ligase activities", "oxidoreductase activity" and "cofactor binding", the glumes transcriptome is more similar to that of H35 than to those of flag leaves and grains.

RNA-seq gained new sequence information for N transporters and cysteine peptidases

Based on annotation, sequences encoding putative N transporters and cysteine peptidases were selected from H35 unigenes and independent BLAST searches were performed within RNA-seq contigs. Combining H35 and RNA-seq information, new sets of N transporter and cysteine peptidase unigenes were created and manually revised for each tissue (tissue-specificity is summarised in Figure 3).

To evaluate the power of the RNA-seq approach for N transporter and cysteine peptidase gene families, the contigs were compared with H35 (Figure 4). After combining information from all three organs, between 67% (CPEP) to 100% (OPT) of pyrosequencing contigs extend known or add new sequence information in comparison to H35.

Results from assembling all candidate sequences from the three libraries and H35 are summarised in Figure 5A and show a clearly increased average contig length (right panel), whereas for total contig number no general tendency was found (left panel). In the subset of contigs containing information from both sources (Figure 5B) the contig number is reduced for all gene groups and the increase in average contig length is more pronounced than for the overall dataset.

RNA-seq contigs of N transporters and cysteine peptidases cluster with annotated homologs from Arabidopsis and rice and enlarge available full-length sequences

Papain-like cysteine peptidases

For all further analyses, sequences derived from the combination of pyrosequencing and H35 as well as unique pyrosequences were considered.

59 genes encoding putative papain-like cysteine peptidases of the CA clan were assembled (Table 3). Based on sequence similarities, the resulting contigs were

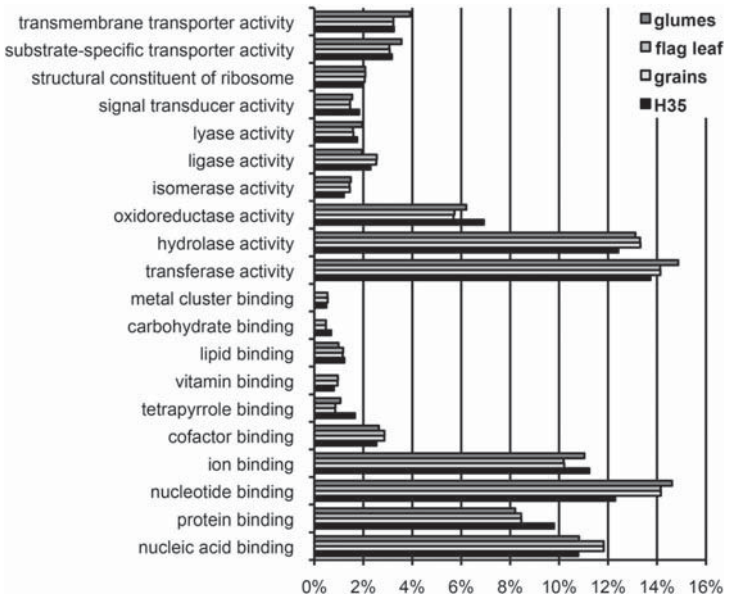

Figure 2 Blast2GO annotation of RNA-seq contigs and H35 unigenes. The result is based on gene ontology terms level 3 of the category Molecular Function. 21,525 sequences from flag leaves, 10,361 sequences from glumes, 21,199 sequences from grains and 22,043 sequences from the H35 database were annotated.

subdivided into different families of the CA clan (Merops database, [36,37]). In general, numbers of barley unigenes defined after sequence assembly were lower than numbers of full-length genes in Arabidopsis and rice except for the families C02, C85 and C88. The C02 cysteine peptidase of Arabidopsis and rice is encoded by a single copy gene. In contrast, two full-length genes and one additional contig were identified for barley, reflecting at least three gene family members. Despite the unclear situation for C85, this subfamily might harbour promising candidates for further investigation, as the high contig number suggests implication for this type of cysteine peptidases in remobilisation processes taking place in at least one analysed tissue.

N transporters

The new dataset was aligned with all N transporter amino acid sequences of rice and Arabidopsis derived from Aramemnon [12] and phylogenetic trees were constructed.

All putative members of the AAT family from barley cluster into the subgroups described for *A. thaliana* by Rentsch et al. [13]. We furthermore included the group of transporters related to EcTyrP, a tyrosine-specific permease of *E. col*. [38]. The phylogenetic tree of AAT sequences (Figure 6, Additional file 1: Figure S1) contains 33 functionally characterised transporters (Additional file 2: Table S2). 26 of them reside in the ATF clade and seven are APC transporters. Most genes with proven functionality (27) are from Arabidopsis, only three from rice, and four from barley. These transporters are listed in Additional file 2: Table S2 and include two barley transporters (HvAAP1 and 2) that were characterised in the author's lab.

From 71 RNA-seq contigs of the barley NRT1/PTR family only 45 cluster into the four subfamilies defined

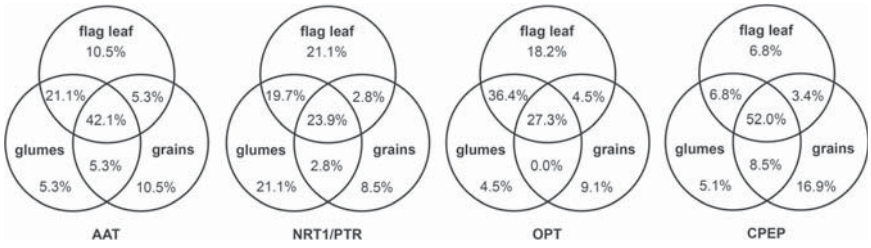

Figure 3 Venn diagrams showing organ-specific expression of N transporters and cysteine peptidases.

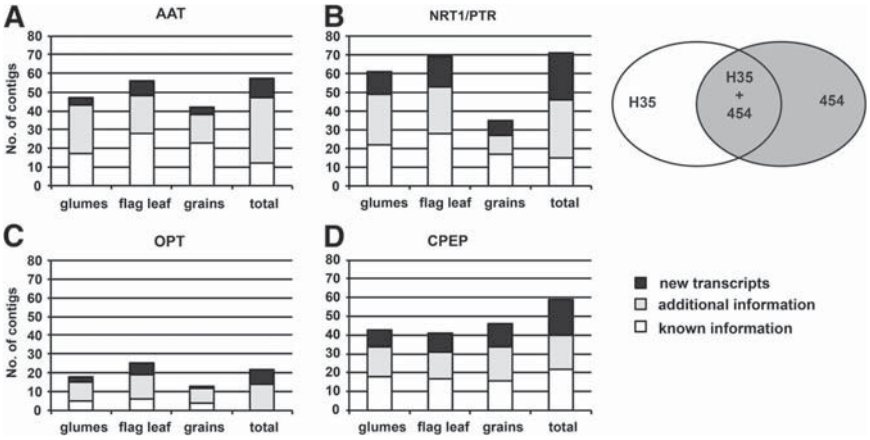

Figure 4 New sequence information for N transporter and cysteine peptidase genes. Comparison of RNA-seq and H35 unigenes for (**A**) *AAT*, (**B**) *NRT1/PTR* and (**C**) *OPT* transporter sequences and for (**D**) cysteine peptidase unigenes. New information (black areas) from RNA-seq shows less than 98% identity to H35 unigenes at amino acid level. Additional information (gray-shaded) matches H35 unigenes, but extends information by more than 50 bp or closes gaps between unigenes. Known information (white areas) did not add new knowledge. Origin of sequences is represented by gray-shaded areas of the overlapping ellipses at the right side.

by Tsay et al. [14], while 26 sequences form a separate branch (data not shown). As BLAST analysis showed no obvious differences between these 26 and the other 45 candidates in sequence similarity to the clustering rice sequences (data not shown), a unique group in barley seems unlikely and these sequences were omitted from the tree. This deviant behaviour might be explained by the overall heterogeneity within this group or the limited sequence information of these outliers (average length of 184 aa compared to 305 aa for sequences that clustered).

According to Tsay et al. [14] the subgroups are named NRT1/PTR-I, II, III and IV (Figure 7, Additional file 4: Figure S3) although our data would suggest an adjustment of this classification, as the members of the NRT1/PTR-I group are not monophyletic. The high heterogeneity within subgroup I is also reflected by the sequence

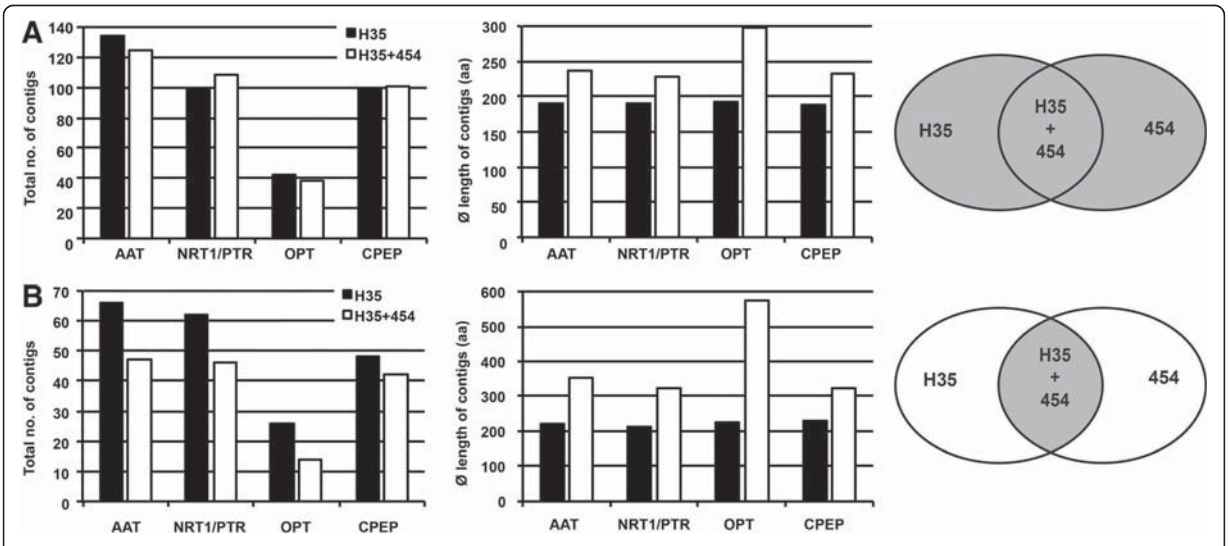

Figure 5 Number and average length of unigenes encoding putative N transporters and cysteine peptidases. (**A**) Total number and average length of contigs after assembly of all N transporter and cysteine peptidase unigenes available from RNA-seq and H35. (**B**) Number and length of N transporter and cysteine peptidase contigs containing sequence information overlapping between the two sources. Black bars represent H35 information, white bars show results after combining H35 and RNA-seq unigenes. Gray-shaded areas in the ellipses at the right-hand side represent the origin of the sequences.

Table 3 Putative papain type cysteine peptidases in different plant species

Clan	Family	*H.v.**	*A.t.*	*O.s.*
	C01	26 (15/4)	40	51
	C02	3 (2/1)	1	1
	C19	7 (1/1)	37	22
CA	C54	1 (0/0)	2	2
	C65	1 (0/0)	1	3
	C85	17 (2/2)	6	7
	C88	4 (1/0)	1	2
	total	59	88	88

* full-length barley sequences are given in brackets (total number/new from RNA-seq).

distance matrix data (Additional file 5: Figure S4) showing similarities of 39.1% for subgroup I in comparison to 44.6% and 42.3% for subgroup II and III, respectively. Although percentages of similarity are even lower for subgroup IV (37.9%), this branch is monophyletic confirming the basic structure presented by Tsay et al. [14]. 30 of the presented NRT1/PTR sequences are functionally characterised (Additional file 2: Table S2), 18 of them are coming from Arabidopsis, eleven from rice. From barley, only HvPTR1 belonging to subgroup II is functionally characterised so far [15].

All 22 barley sequences functionally annotated as putative OPT transporters cluster into the phylogenetic tree presented in Figure 8. Phylogenetic analysis clearly separates sequences of the OPT type from yellow stripe-like (YSL) transporters. Also the classification within the YSLs according to Zheng et al. [26] was reproduced. Transporters of the YSL groups 1, 2 and 3 show a high degree of sequence similarity whereas the YSL-4 group is more diverse (Additional file 6: Figure S6) and not monophyletic (Figure 8, Additional file 7: Figure S5). Furthermore, this group is rice specific with only OsYSL18 functionally characterised [24]. NGS transcriptome data from the rice genome annotation project [39] point to pollen-specificity of this YSL-transporter group. Sequences of putative HvYSL-transporters belonging to subgroups 1, 2 and 3 might be starting points to analyse micronutrient transport into developing barley grains. The highest number of functionally characterised OPTs resides within the OPT and the YSL-1 groups (10 and 8 sequences) while no YSL-3 transporter is functionally characterised so far.

Additional contribution from sequence analysis of barley full-length cDNAs

The H35 and pyrosequencing output was compared with 24,783 barley full-length cDNAs [40]. Combining information from these datasets reduced the number of RNA-seq unigenes for all three N transporter classes and *CPEP* genes (see Table 4), but also revealed redundancy within the full-length cDNA approach. Thus, a fraction of these sequences are redundant, at least with regard to N transporters and *CPEP genes*.

Both approaches identified additional and so far unknown sequences. Matsumoto et al. [40] identified 36 novel putative N transporter and *CPEP* genes, 36 novel genes were detected by pyrosequencing. In summary, sequence information of expressed barley N transporters and cysteine peptidases comprises 78 *AAT*, 71 *NRT1/PTR*, 29 *OPT* and 120 *CPEP* unigenes (Table 4). All RNA-seq unigenes can be considered as expressed in flag leaves, glumes or grains and are barley-specific as checked against the barley genome sequence [41].

Expression profiling of AAT genes revealed coordinate distinct developmental stages in flag leaves, glumes and grains

RNA-seq and H35 sequences were assembled into 57 *AAT*, 71 *NRT1/PTR* and 22 *OPT* unigenes (Table 5) and, except 26 NRT1/PTR sequences, they cluster into defined subgroups in the respective phylogenetic trees (Figures 6, 7, 8, Additional file 1: Figure S1, Additional file 4: Figure S3, Additional file 7: Figure S5). This unigene set represents 25 *AAT*, 8 *NRT1/PTR* and 5 *OPT* full-length sequences and shows a considerably higher percentage of full-length *AAT* genes compared to putative *NRT1/PTR* and *OPT* genes (42.3% versus 15.7% and 22.7%, respectively). To exclude a predominant bias of H35 leading to these numbers, we compared RNA-seq read numbers contributing to *AAT*, *NRT1/PTR* and *OPT* contigs. Table 5 shows the number of *AAT*, *NRT1/PTR* and *OPT* reads representing a ratio of 3:2:1. After normalising read numbers against the average length of annotated rice N transporters a ratio of 4.0:2.3:1.0 is obtained (data not shown). So both, the raw and normalised read numbers point to higher transcriptional activity of *AAT* genes in comparison to that of the *NRT1/PTR* and *OPT* group. Because of their over-representation in the set of RNA-seq N transporter sequences we suggested that this group of N transporters might play an important role in N retranslocation and grain filling. Because remobilisation related to increasing grain sink strength might be reflected by changing transcript levels of associated N transporters we decided to compare expression of the full-length *AAT* genes in the three organs.

qRT-PCR analysis was used to estimate transcript amounts in two-day intervals starting 4 days before anthesis in vegetative tissues and at anthesis in grains until 24 DAF, when grain desiccation starts (Figure 9, upper panel). Among the group of 6 *AAT* genes showing highest expression in each of the three organs, *AAPs* are clearly overrepresented (Table 6). Besides, LHT

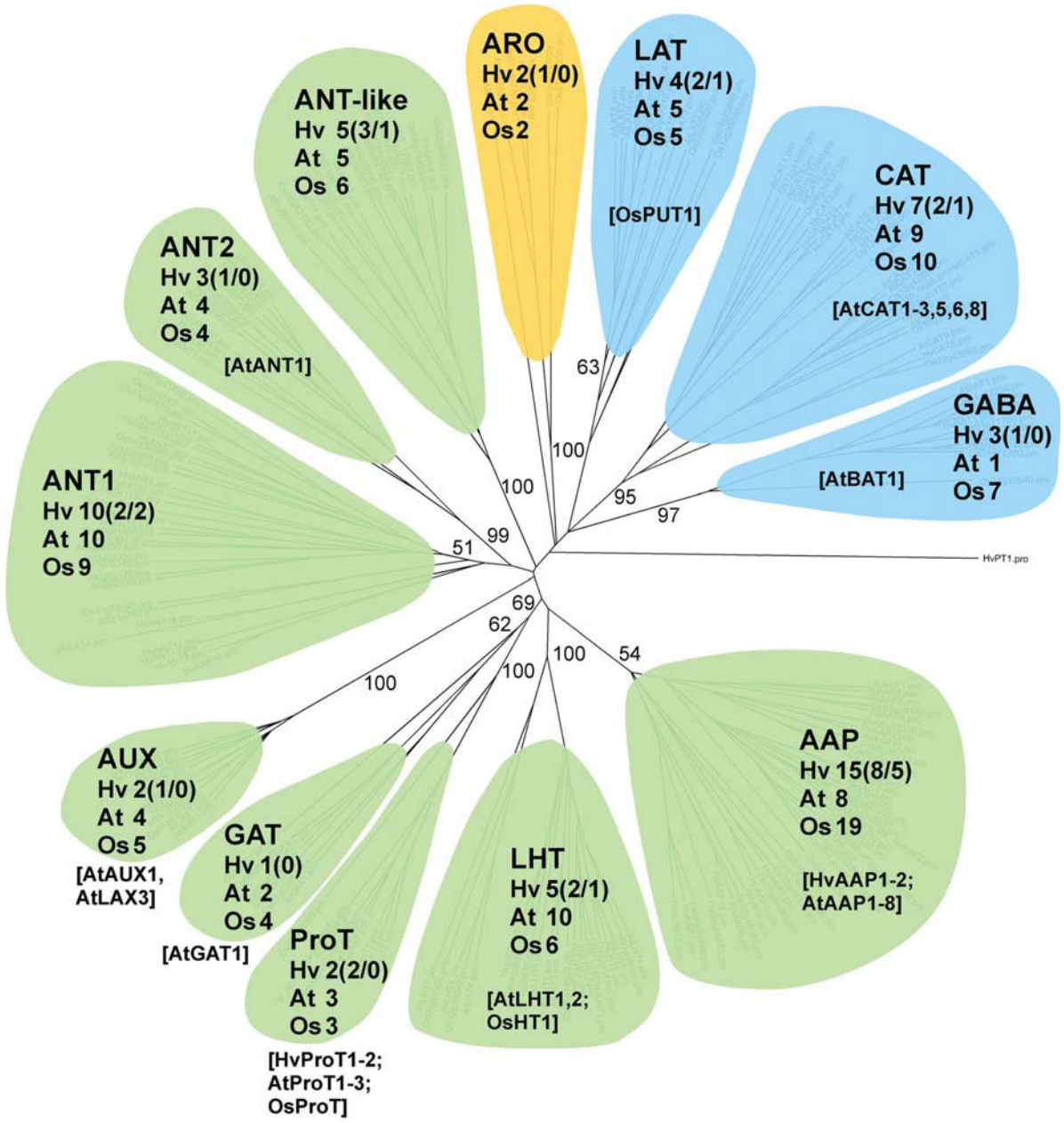

Figure 6 Phylogenetic tree of plant AATs. Clustering of 63 Arabidopsis, 80 rice and 59 unique barley sequences with *H. vulgare* phosphate transporter 1 (HvPT1) as outgroup. Colours indicate membership to different subgroups of ATF (green) and APC (blue) families, members of the aromatic amino acid transporters are shown in orange. Full-length barley sequences are given in brackets (total number/new from RNA-seq), functionally characterized transporters are given in square brackets and mentioned in Additional file 2: Table S2. Sequences from Arabidopsis and rice, including their respective nomenclature, were extracted from Aramemnon, barley sequences derived from RNA-seq, H35 (only full-length sequences), publications (HvProT, HvProT2) and previous unpublished work (HvAAP1 + 2) - see also Additional file 2: Table S2. The phylogenetic tree was constructed using the neighbor-joining algorithm in the program PAUP* [78]. The tree was displayed and manipulated using FigTree [79]. Clustering of AAT sequences into different subgroups is supported by the sequence distance matrices (Additional file 3: Figure S2). Detailed version of the phylogenetic tree including ID-numbers of all sequences is given in Additional file 1: Figure S1.

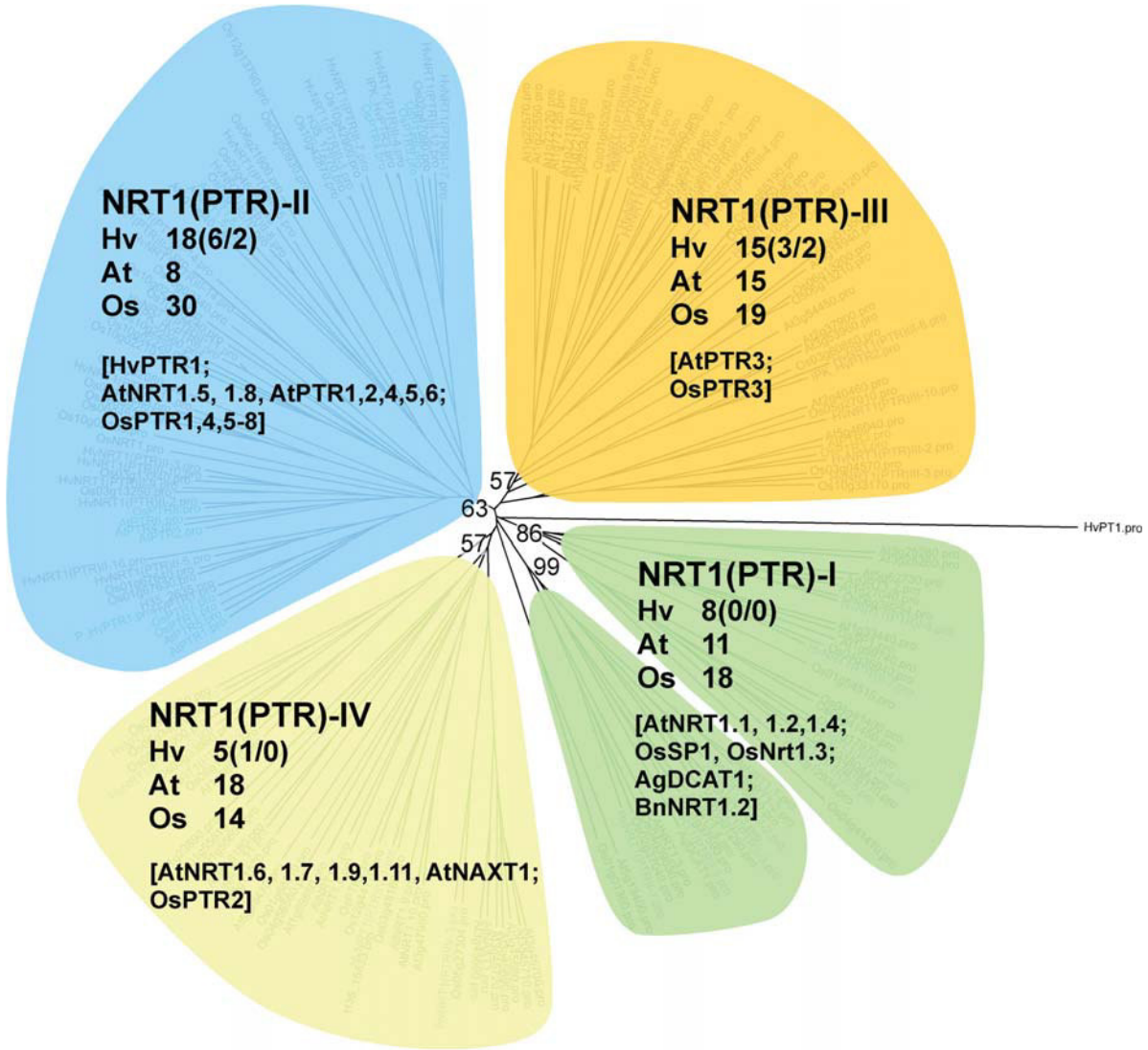

Figure 7 Phylogenetic tree of plant NRT1/PTRs. Clustering of 52 Arabidopsis, 81 rice and 46 unique barley sequences; for consolidation of the tree, sequences from *Alnus glutinosa* (AgDCAT1) and *Brassica napus* (BnNRT1) were included (according to Tsay et al. [14]). Colours indicate membership to subgroups I (green), II (blue), III (orange) and IV (yellow) as defined by Tsay et al. [14]. Barley sequences were derived from RNA-seq, H35 (only full-length sequences), publications (HvPTR1) and previous unpublished work (IPK_HvPTR2, 3, 6). Clustering of NRT1/PTR sequences into different subgroups is supported by the sequence distance matrices (Additional file 5: Figure S4). Detailed version of the phylogenetic tree including ID-numbers of all sequences is given in Additional file 4: Figure S3. For further explanations see legend of Figure 6.

transporters seem to be important for remobilisation. *HvLHT2* and *HvLHT1* are highly expressed in flag leaves and glumes, respectively. In developing grains their expression is either very low or not detectable. There, specific members of the ANT group are highly expressed, *HvANT3* between 6 and 8 DAF and *HvANT4* during early as well as late grain development (Figure 9, upper panel).

To visualise relationships between the three tissues, principle component analysis (PCA) was applied to the tissue-specific qRT-PCR results. Then, K-means clustering was used to identify developmental stages that might be related to each other. The results of the two-step procedure are depicted in the lower panels of Figure 9. In each panel, coloured areas represent related stages. For all three organs, a group including stages 8 and 10 DAF was identified (violet areas). Besides, developmental stages representing the late phase of grain development form separate groups (areas coloured in yellow). K-means clusters

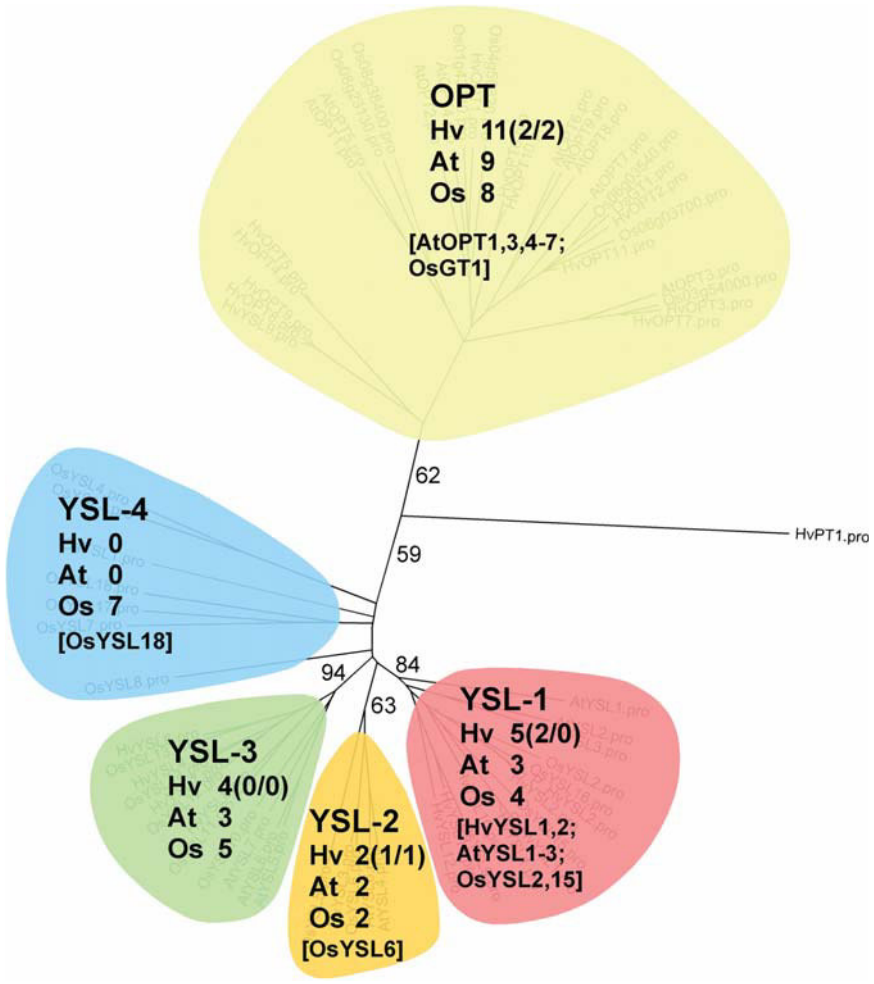

Figure 8 Phylogenetic tree of plant OPTs. Clustering of 17 Arabidopsis, 26 rice and 22 unique barley sequences. Colours indicate membership to the OPT (yellow) and the yellow stripe-like (YSL) family. According to Zheng et al. [26] YSL transporter sequences are subdivided into the subgroups YSL-1 (red), YSL-2 (orange), YSL-3 (green) and YSL-4 (blue). Barley sequences were derived from RNA-seq and publications (HvYSL1 + 2). Clustering of OPT sequences into different subgroups is supported by the sequence distance matrices (Additional file 6: Figure S6). Detailed version of the phylogenetic tree including ID-numbers of all sequences is given in Additional file 7: Figure S5. For further explanations see legend of Figure 6.

coloured in green represent stages of early development. They are highly dispersed, especially between flag leaves and glumes (lower panels of Figure 9A, B).

Discussion

The majority of N accumulating in cereal grains originates from proteins remobilised from vegetative organs, but interactions of grain filling and remobilisation are only poorly understood. Here we used large-scale transcriptome pyrosequencing of flag leaves, glumes and developing grains to identify putative cysteine peptidases and transporters of amino acids, peptides and oligopeptides involved in N remobilisation and retranslocation into developing grains. This approach suggests that distinct amino acid transporters might be important in sink-source communication between remobilising organs and accumulating grains.

RNA-seq revealed the specific character of the glumes transcriptome

The read numbers gained by transcriptome sequencing are similar with about 0.5 million for each organ with higher values for flag leaves (Table 1). Also average length and number of reads per contig are comparable between the three organs. In glumes lower contig numbers but higher read numbers per contig were found

Table 4 Comparison of N transporter and cysteine peptidases (CPEP) sequence information from full-length cDNA* and RNA-seq data

Gene family	Raw data		After assembly		Found in H35		New				Overall
	cDNA	RNA- seq	cDNA	RNA- seq	cDNA	RNA- seq	cDNA	Excl.	RNA- seq	Excl.	
AAT	99	57	69	55	54	46	15	9	9	3	78
NRT1/PTR	98	71	55	56	42	42	13	8	14	9	71
OPT	27	22	19	20	14	14	9	8	6	5	29
CPEP	120	59	89	59	78	40	11	11	19	19	120

*Matsumoto et al. [40]; numbers of unigenes shown.

and furthermore the number of singletons in the glume transcriptome is only one third compared to flag leaves and grains. This suggests either higher specificity or lower complexity of the glumes transcriptome.

Comparison of the three transcript sets as visualised in Figure 1 revealed high similarity between flag leaf and grain contigs (34.8% of identical sequences). On the other hand, only about 5% of glumes sequences are identical with those in flag leaves or grains, pointing again to either higher specificity or lower complexity of the glumes transcriptome.

Another argument underlining the specific character of the glumes transcriptome comes from annotation of organ-specific RNA-seq contigs and its comparison to H35 based on gene ontology terms (Figure 2). These results suggest a different function of the glumes transcriptome compared to the two other tissues especially regarding transport activity. Potential functions of the glumes transcriptome are more similar to these of H35 than to those of flag leaves and grains. H35 contigs consist of ESTs derived from several different tissues. Thus, functional annotation of the glumes transcriptome points to expression patterns representing an average of many tissues. This indicates that annotated functions in glumes are less tissue-specific, whereas transcriptomes of flag leaves and grains seem to be tissue-specific and functional annotation indicates similarity between the two organs.

In summary, comparisons between the transcriptomes of flag leaves, glumes and grains indicates that gene expression in glumes is less tissue-specific and might be characterised by higher activity of a lower number of genes. The glumes transcriptome seems to be different from those of flag leaves and grains whereas the latter two organs reveal functional similarity to each other.

Table 5 Overview of sequence information on N transporter genes

N transporter group	Reads	Unigenes	Full-length	% full-length
AAT	2,973	57	25	42.3
NRT1/PTR	2,040	71	8	15.7
OPT	1,016	22	5	22.7

Glumes might function as mediator between remobilising vegetative tissues and accumulating grains

Relative to grains, both flag leaves and glumes are source organs. Nitrogen mobilisation during grain filling and the role of flag leaves and glumes have been studied predominantly in wheat [3,42,43]. These studies revealed different cellular organisation and distribution of glumes compared to leaves of the same developmental stage [43]. Glumes have more sclerenchyma cells, which serve as a supporting structure for the grain. Compared to flag leaves, glumes contain less green tissue and, consequently, fewer chloroplasts and less Rubisco [44,45].

During grain development, a decline in the content of soluble proteins is detected in both flag leaves and glumes but patterns of remobilisation differ. Protein content in flag leaves remains constant up to anthesis and declines when grains develop. Glumes continue to accumulate protein until 5 DAF before remobilisation starts. The different initiation time of remobilisation suggests that glumes act as a transient sink for N derived from flag leaves and senescing vegetative organs. These studies indicate that glumes are supplying nitrogen to the grains during later developmental stages [43].

Glumes contain high percentages of Gln, Pro, Lys, Arg and His [43]. Considerable high contents of Gln, Lys, Arg and His also occur in the nucellar projection (NP) compared to endosperm transfer cells (ETC) at the beginning of grain filling [46]. The NP/ETC complex represents the transfer path between maternal and filial grain tissues and also functions as a metabolic interface to precondition amino acid supply to the developing endosperm. In NP cells, gene expression of different cytosolic isoforms of Gln synthetase (GS) could be involved in re-assimilation of ammonia from protein breakdown and production of N transport compounds [46]. Such a function has been suggested also for GS present in glumes [43].

In summary, flag leaves and glumes obviously function differently, at least during early grain development when sink strength of the endosperm is still low. Analogies can be observed between glumes and supplying maternal grain tissues. This suggests that the glumes metabolism is adjusted to the changing demands of developing

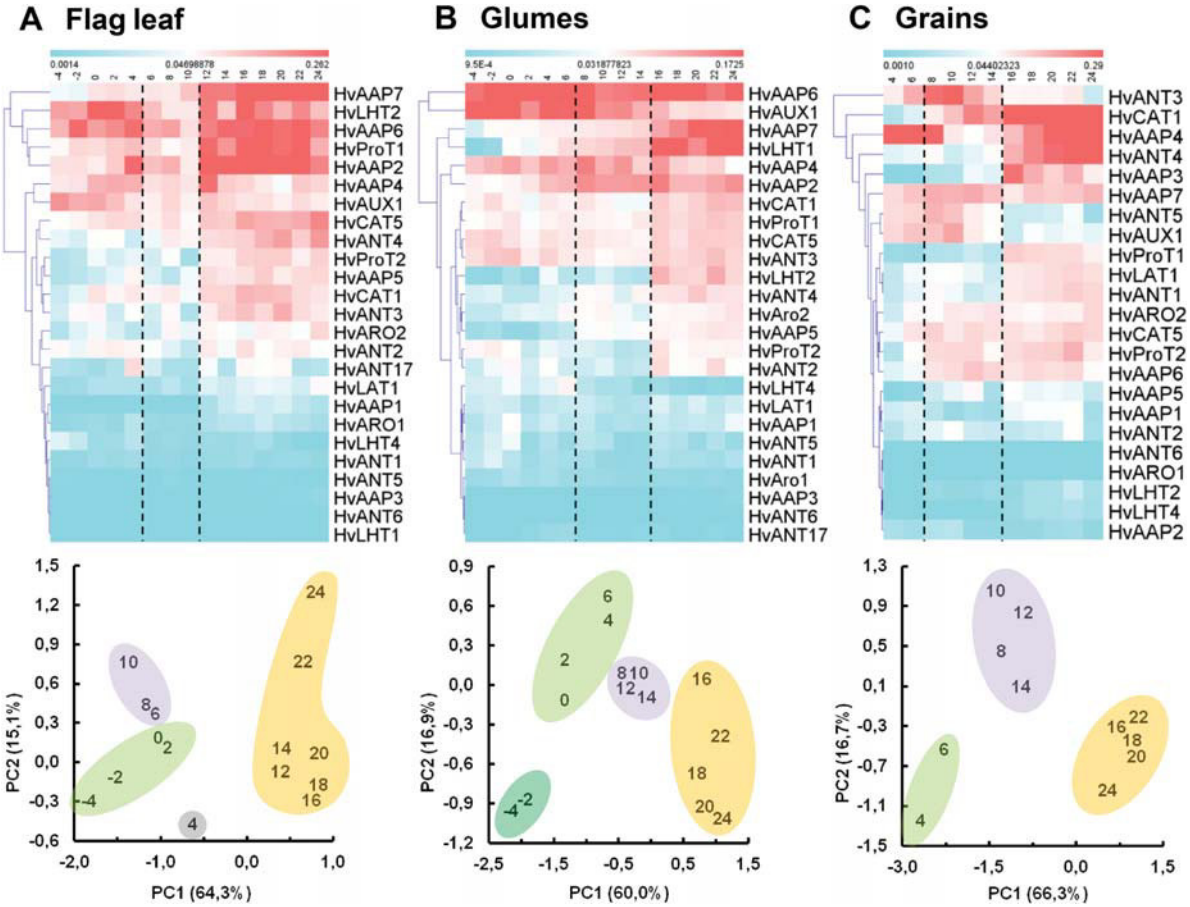

Figure 9 Transcript profiling, principle component analysis (PCA) and K-means clustering of 25 AAT genes. Distinct developmental phases were identified in flag leaves (**A**), glumes (**B**) and developing grains (**C**). Tissues were analysed in two-day steps starting 4 days before anthesis (-4) in flag leaves and glumes and at 4 DAF in developing grains until 24 DAF. The heat maps (upper panels) reflect relative transcript abundances after normalisation against *actin* expression (blue = low expression; red = high expression). Developmental phases as identified by PCA are given in the lower panels, numbers represent DAF. Results of K-means clustering are visualized by encircling of respective stages. Light violet areas represent the transition phase.

grains and points to a putative function of the glumes as mediator between (remobilising) vegetative tissues and (accumulating) grains.

RNA-seq identified a set of putative cysteine peptidase and N transporter genes possibly involved in remobilising and accumulating of nitrogen

RNA-seq provided new sequence information for cysteine peptidases and N transporter genes compared to H35 (Figure 4), reduced redundancy and increased unigene length within H35 data (Figure 5B). With respect to full-length cDNAs published by Matsumoto et al. [40], 36 contigs were identified as unique in the collection of pyrosequences (Table 4). While these new sequences might be involved in degradation and retranslocation of N compounds during grain development those cDNAs present only in the H35 or Matsumoto collections should be less relevant for such functions.

Cysteine peptidases

Papain-like cysteine peptidases play an important role in naturally senescing barley tissues [8,9], especially between 7 and 21 days post anthesis [47]. Although several genes encoding cysteine proteases are upregulated during senescence [6,8,48-50], direct evidence for the implication of specific members from this class of proteases in protein degradation is lacking.

Combination of H35 and RNA-seq sequence information identified a set of 59 unigenes that encode Papain-like cysteine peptidases (Table 4). This set represents 21 full-length sequences and 38 unigenes that belong to an unknown number of genes. Some of these sequences

Table 6 *AAT* genes with high expression in flag leaves, glumes and developing grains*

	Flag leaf	Glumes	Grains
AAP	*HvAAP2*	*HvAAP2*	-
	-	-	*HvAAP3*
	HvAAP4	*HvAAP4*	*HvAAP4*
	HvAAP6	*HvAAP6*	-
	HvAAP7	*HvAAP7*	*HvAAP7*
others	-	*HvLHT1*	-
	HvLHT2	-	-
	HvProT1	-	-
	-	*HvAUX1*	-
	-	-	*HvCAT1*
	-	-	*HvANT3*
	-	-	*HvANT4*

*For each tissue the six AAT genes showing highest expression levels are presented.

might belong to the same gene but cannot be aligned (redundancy problem). These candidates can be considered as active between anthesis and DAF 24 in at least one of the three tissues. In comparison, the total number of cysteine peptidase genes from the same peptidase family of rice and Arabidopsis is high (88 candidate genes in both species) pointing to a certain degree of specificity of the newly assembled contigs for remobilisation. In the C01 and C85 families most unigenes (26 and 17), as well as most new full-length sequences (4 and 2) were found (Table 4), predestining their members as promising candidates. Analysis of tissue-specificity and localisation of the respective gene products to defined cellular compartments remain to be done.

Amino acid permeases seem to be predominant in N retranslocation and grain filling

AAPs seem to be predominant in N retranslocation and grain filling. This conclusion was derived from over-representation of this gene family in the set of RNA-seq derived N transporter sequences (Table 5) and from its very strong expression in both, source and sink tissues (upper panel of Figure 9, Table 6). Two of the highly expressed putative *AAP* genes (*HvAAP2, HvAAP6*) are active only in the source tissues flag leaves and glumes, two others (*HvAAP4* and *HvAAP7*) are expressed in source as well as sink tissues. Among the putative transporter genes listed in Table 6, *HvAAP3* is specific for grains. HvAAP3 but also HvAAP4 show high sequence similarity to AtAAP1 and AtAAP8 (Additional file 1: Figure S1). The two Arabidopsis transporters play a role in supplying developing seeds with nitrogen [51,52]. HvAAP2 and HvAAP6 are closely related to AtAAP2 and AtAAP5 (Additional file 1: Figure S1). AtAAP5 is expressed in mature leaves, stems and flowers and involved in long-distance transfer of amino acids, especially glutamine, the predominant amino acid found in the phloem [53]. Promoter-reporter gene fusions showed that *AtAAP2* is expressed in vascular tissues of stems and siliques. Furthermore, *AtAAP*2 expression is tightly associated with phloem strands that connect to fruits. Thus, AtAAP2 seems to be an excellent candidate for xylem-phloem transfer along this path [54,55], a role that might also be assumed for HvAAP2 and HvAAP6. HvAAP7 is a member of a separated branch of the AAT tree harbouring only uncharacterised rice and barley sequences (Additional file 1: Figure S1). Because of its high expression in flag leaves and glumes during grain filling, *HvAAP7* can be considered as being an interesting candidate for functional studies in barley.

Besides members of the AAP family, the two putative transporters HvLHT1 and HvLHT2 seem to be specifically important for N retranslocation in flag leaves (HvLHT2) and glumes (HvLHT1). At the sequence level, the two proteins are closely related to each other and to the functionally characterised OsHT1 [56]. Because of its high expression and strong tissues-specificity (see upper panels of Figure 9), *HvLHT1* might be an excellent candidate to elucidate the specific role of glumes for N supply to the developing grains. Two members of the ANT gene family (*HvANT3*, *HvANT4*, Table 6) are highly expressed in developing grains (Figure 9, upper right panel). Because only one member of the large ANT family is functionally characterised so far (AtANT1, [57]), any hint to possible functions of HvANT3 and HvANT4 in grain filling is missing.

A putative role for amino acid transporters in sink-source communication

Seed sink strength for N, which means the ability of the grain to attract and import N compounds, is due to high storage protein synthesis and high demand and/or intensity of active uptake via membrane-localised transporters [58]. Recent work in our lab demonstrated that increasing sink strength due to overexpression of an amino acid transporter in legume seeds increases amino acid supply, total seed N and protein content [59,60].

In barley grains, highest expression of storage protein genes occurs between 10 and 12 DAF [61]. Storage protein accumulation starts two days later in aleurone and starchy endosperm cells [62]. Simultaneously, when high N sink strength is initiated a set of AAT genes is transcriptionally activated in grains (Figure 9C, upper panel). Remarkably, expression of these genes is low between 8 and 14 DAF, but higher during early development. PCA and K-means clustering of AAT gene expression data, clearly separate three groups of data points belonging to stages 4 and 6 DAF, 8 to 14 DAF and 16 to 24 DAF

(lower panel of Figure 9C). These groups have been assigned to pre-storage, intermediate (transition) and storage phases of barley grain development, respectively. This staging of grain development has been deduced from transcript profiling of 12,000 grain-expressed unigenes. Data evaluation justified the intermediate phase between 6 and 10 DAF [61]. Considering expression profiles of AAT genes alone, the intermediate phase would start two days later and would be prolonged to 14 DAF (lower panel of Figure 9C). This reflects the interval between beginning starch accumulation in the differentiated caryopsis centre (6 DAF, [63]) and high storage protein synthesis in the peripheral parts of the grain. Such difference in the beginning of the transition phase reflects delayed beginning of protein accumulation compared to starch biosynthesis, and also reveals the internal gradient of caryopsis differentiation.

The highly expressed members of the AAT gene family in flag leaves and glumes differ from those in filling grains (upper panels of Figure 9), but phases of grain development are also reflected in the supplying organs flag leaves and glumes (lower panels of Figure 9). In grains and glumes, transition phase and grain filling include the same stages (8 to 14 DAF and 16 to 24 DAF, respectively). This supports the hypothesis that glumes adjust metabolism according to the specific demands of the grains. Remarkably, expression of *AAT* genes in flag leaves is elevated four days earlier than in glumes and grains (upper panels of Figure 9). Thus, flag leaves seem to respond to the expected demand for amino acids before sink strength is established in grains and respectively, the transition phase starts two days earlier. Striking differences are visible between flag leaves and glumes during pre-anthesis and early grain development (–4 to 6 DAF). This strengthens the assumption that glumes function in a distinctive way compared to flag leaves, at least during early grain development.

Increasing N demand can generate long-distance signals within the plant [64]. Possibly certain N compounds or amino acids could be translocated through the phloem and its fluctuating levels might signal the nitrogen status of the plant. Especially glutamate has been suggested to function as an evolutionary conserved long-distance signal in plants as well as in animals [65]. Cytokinins can also be involved in signalling the N status of the plant [66,67]. The phloem might be important in delivering signals to distantly located plant organs. In this way, high grain demands for N might decrease assimilate levels in the phloem which could generate signals for remobilisation in the source.

We hypothesise that in such a way phases of grain developmen could be perceived in the ear-near tissues flag leaf and glumes. This would suggest development-specific signalling which mediates sink-source communication during grain development and which also might regulate *AAT* gene expression. Tissue-specific regulation of sink/source transition can also play a role as observed from fluctuating transcript abundances of *AAT* genes especially in flag leaves. Overall, such hypothetical relationship in sink-source communication has been derived from expression profiles of a collection of genes which transcripts are over-represented in a specific set of pyrosequences which demonstrates the power of this approach.

Conclusions

Analysis of the overall dataset showed, that flag leaves and glumes obviously have different functions during early grain development when endosperm sink strength is low. Analogies in gene expression observed between glumes and the supplying maternal tissues indicate that glumes function as mediators between remobilising vegetative tissues and accumulating grains. Combination of already known and newly derived sequence information reduced redundancy, increased contig length and identified new members of cysteine peptidase and N transporter gene families. Participation of the respective gene products in either N remobilisation or accumulation can be expected. Amino acid permeases (AAPs), a sub-group of the AAT family of N transporters seem to be predominant in N retranslocation and grain filling. In phylogenetic trees, putative *HvAAP* genes which are highly expressed in remobilising tissues cluster together with functionally characterised Arabidopsis transporters responsible for long-distance transport of amino acids. In contrast, grain-specific AAPs are most similar to Arabidopsis transporters active in developing embryos. Based on expression profiling of *AAT* genes and subsequent statistical data analysis we hypothesise that high grain demands for N might decrease assimilate levels in the phloem which could generate signals for remobilisation in the source. Our future scientific work will be focussed on identification of metabolic/hormonal phloem components, which signal the grain N status to the plant.

Overall, cysteine peptidase and N transporter sequences as identified in this study might be of high interest for applied research because of their obvious role in N partitioning for grain filling. Up to now, information is based only on transcript data. For application of this knowledge in development of new breeding strategies, the specific role of individual candidates (for instance specific cysteine peptidases, LHT, AAP and ANT genes) in N remobilisation and accumulation has to be clarified.

Methods

Plant growth and RNA preparation

Barley (*Hordeum vulgare* L.) plants of cv. Barke were grown in pots with Substrat2 (Klasmann-Deilmann GmbH, Germany) and fertilized with 10 g Osmocote

(Scotts Ind BV, Netherlands) and 0.2% solution of Hakaphos red (Compo GmbH & Co KG, Germany) at 3 leaf and at heading stage, respectively. The plants grew in the greenhouse at 18°C with 16 h of light. Developmental stages for barley grains were determined as described by Weschke et al. [63]. Flag leaves, glume fractions (including palea, lemma and awn) and grain tissues were collected based on grain developmental stages. For flag leaves and glumes, samples were collected in two day intervals starting from 4 days before anthesis until 24 days after flowering (DAF). Grains from 0, 4, 8, 10, 12, 14 DAF were manually dissected into maternal and filial parts and whole caryopses were sampled at 16, 20 and 24 DAF. Total RNA was isolated separately from each tissue at different stages using Purescript RNA isolation kit (Biozym, Hamburg, Germany). To prepare RNA samples for transcriptome sequencing, equal amounts of RNA from all stages were united for each tissue to achieve 27 μg of RNA for each organ. Pyrosequencing of the three libraries using the Roche/454 GS-FLX Titanium technology was done by GATC Biotech (Konstanz, Germany).

Sequence analysis

Generated raw reads are accessible at EMBL/EBI, European Nucleotide Archive (ENA Project ERP001286, [68]). All reads were adaptor and quality trimmed using SeqClean [69]. Clustering and assembling was done separately for each library using the TGICL pipeline [70]. The pipeline uses megablast [71] for pre-clustering and CAP3 [72] for sequence assembly. The overlap settings for assembly were 95% identity and 35 bp overlap (all other parameters were set to default). The best BLASTn [73] hit of individual reads against all contigs was used to determine read numbers per contig. To cross-check these results, a second assembly has been generated using Newbler [74], (data not shown).

Comparisons of assembled sequences to public databases and each other were done by BLAST similarity searches [73] with different E-values. For stepwise blast, a perl script [75] using several BioPerl packages [76] was written. To determine Gene Ontology (GO) terms, sequences were analysed using Blast2GO [34,35].

To obtain *in silico* expression levels numbers of all single reads matching one contig in the BLASTn query (E-value $>1E^{-20}$) and derived from the same tissue were summarized.

Identification of N transporter sequences

BLASTn of all contigs from the tissue-specific assemblies was done against N transporter collections (AAT, OPT, NTR1/PTR) selected from H35 [30]. Setting blast E-value to $<1E^{-10}$ we considered sequences beyond that cut-off as putative candidates. Candidates were assembled with H35 sequences using the standard algorithm of Lasergene 8 (DNAStar Inc, Madison, USA). Newly created contigs and remaining RNA-seq singletons were used for further analysis.

Confirmation of the amino acid sequences was done by BLASTp against Aramemnon [12] and comparison to rice homologs. Identities between 30-94% (AAT), 59-92% (OPT) and 51-94% (NRT1/PTR) were observed. To exclude contaminations, a BLASTn of these sequences was done against the available barley genomic sequence [41] and verified the barley specificity with identities between 97 and 100% on nucleotide level.

Phylogenetic trees

Basic alignments for tree construction and corresponding sequence distance matrices were calculated using the ClustalW algorithm with Blosum protein weight matrix in Lasergene 8 (DNAStar Inc, Madison, USA) with HvPT1 [77] included as outgroup. For each dataset (AAT, OPT, and NRT1/PTR) mean pairwise distances between sequences were calculated and clustered with the neighbor-joining algorithm in PAUP* [78]. Bootstrap support values were calculated by 1000 bootstrap resamples for each dataset. Phylogenetic trees were visualised with FigTree v1.3.1 [79]. The EMBL accessions of RNA-seq N transporter sequences and IPK previously unpublished sequences (HvAAP1, HvAAP2, HvPTR2, HvPTR3, HvPTR6) are summarised in Additional file 8: Table S3, the additionally used EST-sequences are available at H35 [30].

Identification of cysteine peptidase sequences

Cysteine peptidases were identified by BLASTn searches (E-value $<1E^{-10}$) against known cysteine peptidases sequences from H35 and by BLASTx (E-value $<1E^{-10}$) searches against cysteine peptidases from *Arabidopsis thaliana* and *Oryza sativa* [80,81]. Candidates from the three tissue libraries were assembled with H35 sequences using the standard algorithm of Lasergene 8 (DNAStar Inc, Madison, USA). The created contigs and remaining RNA-seq singletons were used for further analysis. For annotation and classification of the cysteine peptidases the translated amino acid sequences were compared by BLASTp to those of known cysteine peptidases from barley and homologs from Arabidopsis and rice in the MEROPS database [37]. To exclude contaminations, sequences were blasted against the available barley genomic sequence [41] and were verified with identities between 93 and 100% at nucleotide level.

qRT-PCR analysis

Plant material was collected in two day steps (flag leaf −4 – 24 DAF, glumes −4 – 24 DAF, filial grain tissue 4 – 24 DAF) and homogenised at −80°C.

Total RNA was extracted using Spektrum Plant Total RNA Kit (Sigma Aldrich, Steinheim, Germany) and treated with RNase-free TURBO™ DNase (Ambion, Life Technologies, Darmstadt, Germany). cDNA was synthesized from 2 μg of total RNA with Superscript™ III (Invitrogen, Life Technologies, Darmstadt, Germany) using poly(dT) and random hexamer primers according to the manufacturer's instructions. 1 μg diluted cDNA (1:32) was used for qRT-PCR with gene-specific primers (Additional file 9: Table S1). Real time PCR was performed using ABI Prism 7900HT Sequence Detection System and Power SybrGreen PCR Mastermix reagent; data was analysed with SDS 2.2.1 Software (all Applied Biosystems, Darmstadt, Germany). Determination of a suitable reference gene, test of PCR efficiencies and determination of CT values were done according to Radchuk et al. [82]. The CT values were determined for three biological replicates, with three technical replicates for each value, and normalized against *actin* expression (ΔCT). The arithmetic averages of the ΔCT values were calculated and $2^{-\Delta CT}$ values were used for clustering and visualization of data with Multiple Experiment Viewer v4.7 [83].

PCA and K-means clustering

The entire set of qRT-PCR data was subjected to principle component analysis (PCA) and analysed using the J-Express software 2011 [84]. Thereby, the first axis was placed in the direction of the largest variance component, the second orthogonal axis in direction of the second largest variance. As about 60% of the total variance is represented along the first axis, and more than 12% along the second, coordinates on these two axes which together represent nearly two third of the total variance are plotted in Figure 9. To center the given data set and to define number of clusters representative for each tissue K-means clustering [85] was performed using OriginPro 8.1 [86].

Additional files

Additional file 1: Figure S1. Detailed phylogentic tree of plant AATs. Clustering of 63 Arabidopsis, 80 rice and 72 barley sequences (accounting for 59 unique sequences). To support the tree, barley full-length sequences from H35 and publications were included. Barley sequences are written in violet, functionally characterised transporters in dark green (see Additional file 2: Table S2).

Additional file 2: Table S2. Functionally characterised N transporters in phylogentic trees.

Additional file 3: Figure S2. Sequence distance matrices of AAT genes from Lasergene data. Only percent similarity is shown.

Additional file 4: Figure S3. Detailed phylogentic tree of plant NRT1/PTRs. Clustering of 52 Arabidopsis, 81 rice,1 *Brassica napus*, 1 *Alnus glutinosa* and 52 barley sequences (accounting for 46 unique sequences). To support the tree, barley full-length sequences from H35 and publications were included. Barley sequences are written in violet, functionally characterised transporters in dark green (see Additional file 2: Table S2).

Additional file 5: Figure S4. Sequence distance matrices of NRT1/PTR genes from Lasergene data. Only percent similarity is shown.

Additional file 6: Figure S6. Sequence distance matrices of OPT genes from DNAStar data. Only percent similarity is shown.

Additional file 7: Figure S5. Detailed phylogentic tree of plant OPTs. Clustering of 17 Arabidopsis, 26 rice and 24 barley sequences (accounting for 22 unique sequences). To support the tree, barley full-length sequences from H35 and publications were included. Barley sequences are written in violet, functionally characterised transporters in dark green (see Additional file 2: Table S2).

Additional file 8: Table S3. EMBL accessions of N Transporters.

Additional file 9: Table S1. Primers used in qRT-PCR.

Abbreviations

AAP: Amino acid permeases; AAT: Amino acid transporters; DAF: Days after flowering; ETC: Endosperm transfer cells; FL: Flag leaf; G: Grain; GL: Glumes; GS: Glutamine synthetase; H35: Assembly 35 of HarvEST:Barley v1.83 [30]; NP: Nucellar projection; NRT1/PTR: Nitrate/peptide transporters; OPT: Oligopeptide transporters; PCA: Principle component analysis; PS: Phytosiderophores.

Competing interests

The authors declare that they have no competing interests.

Authors' contributions

SK: RNA preparation, analysis of qRT-PCR raw data, comparison between RNA-seq, H35 and Aramemnon data, alignment of N transporter sequences. JH, BS, TS, US: read quality trimming, sequence assembly and annotation, comparison to barley genome sequences. JH: alignment and annotation of cysteine peptidase sequences, clustering to the MEROPS clades. FRB: construction of phylogenetic trees. VR: RNA preparation. FA: qRT-PCR analysis. KK: critical revising of intellectual content. HW: substantial contribution to the concept, critical revising of intellectual content. WW: substantial contribution to the concept, interpretation of data. All authors read and approved the final manuscript.

Acknowledgements

We are grateful to Ruslana Radchuk for support in qRT-PCR analysis and to Angela Stegmann, Elsa Fessel and Gabriele Einert for excellent technical assistance. This work was supported by Deutsche Forschungsgemeinschaft (FOR948, WE 1641/13-1).

Author details

[1]Leibniz-Institut für Pflanzengenetik und Kulturpflanzenforschung (IPK), Gatersleben D-06466, Germany. [2]Christian-Albrechts-Universität (CAU), Kiel D-24118, Germany.

Received: 28 March 2012 Accepted: 22 August 2012
Published: 30 August 2012

References

1. Peoples MBDM: *The interlplay between proteolysis and amino acid metabolism during senescence and aging in plants*. New York: AcademicPress Inc; 1988.
2. Peeters KMU, Van Laere AJ: **Amino acid metabolism associated with N-mobilization from the flag leaf of wheat (*Triticum aestivum L.*) during grain development.** *Plant Cell Environ* 1994, **17**(2):131–141.
3. Simpson RJ, Lambers H, Dalling MJ: **Nitrogen Redistribution during Grain Growth in Wheat (*Triticum aestivum L.*): IV. Development of a Quantitative Model of the Translocation of Nitrogen to the Grain.** *Plant Physiol* 1983, **71**(1):7–14.
4. Hörtensteiner S, Feller U: **Nitrogen metabolism and remobilization during senescence.** *J Exp Bot* 2002, **53**(370):927–937.
5. Masclaux-Daubresse C, Reisdorf-Cren M, Orsel M: **Leaf nitrogen remobilisation for plant development and grain filling.** *Plant Biology* 2008, **10**:23–36.

6. Gregersen PL, Holm PB: **Transcriptome analysis of senescence in the flag leaf of wheat (*Triticum aestivum L.*).** *Plant Biotechnol J* 2007, **5**(1):192–206.
7. Parrott DL, McInnerney K, Feller U, Fischer AM: **Steam-girdling of barley (*Hordeum vulgare*) leaves leads to carbohydrate accumulation and accelerated leaf senescence, facilitating transcriptomic analysis of senescence-associated genes.** *New Phytol* 2007, **176**(1):56–69.
8. Parrott DL, Martin JM, Fischer AM: **Analysis of barley (*Hordeum vulgare*) leaf senescence and protease gene expression: a family C1A cysteine protease is specifically induced under conditions characterized by high carbohydrate, but low to moderate nitrogen levels.** *New Phytol* 2010, **187**(2):313–331.
9. Martínez DE, Costa ML, Guiamet JJ: **Senescence-associated degradation of chloroplast proteins inside and outside the organelle.** *Plant Biology* 2008, **10:**15–22.
10. Tegeder M, Rentsch D: **Uptake and Partitioning of Amino Acids and Peptides.** *Molecular Plant* 2010, **3**(6):997–1011.
11. Schwacke R, Schneider A, van der Graaff E, Fischer K, Catoni E, Desimone M, Frommer WB, Flügge U-I, Kunze R: **ARAMEMNON, a Novel Database for Arabidopsis Integral Membrane Proteins.** *Plant Physiol* 2003, **131**(1):16–26.
12. *ARAMEMNON - Plant Membrane Protein Database.* [http://aramemnon.uni-koeln.de]
13. Rentsch D, Schmidt S, Tegeder M: **Transporters for uptake and allocation of organic nitrogen compounds in plants.** *FEBS Lett* 2007, **581**(12):2281–2289.
14. Tsay Y-F, Chiu C-C, Tsai C-B, Ho C-H, Hsu P-K: **Nitrate transporters and peptide transporters.** *FEBS Lett* 2007, **581**(12):2290–2300.
15. West CE, Waterworth WM, Stephens SM, Smith CP, Bray CM: **Cloning and functional characterisation of a peptide transporter expressed in the scutellum of barley grain during the early stages of germination.** *The Plant Journal* 1998, **15**(2):221–229.
16. Waterworth WM, West CE, Bray CM: **The barley scutellar peptide transporter: biochemical characterization and localization to the plasma membrane.** *J Exp Bot* 2000, **51**(348):1201–1209.
17. Ouyang J, Cai Z, Xia K, Wang Y, Duan J, Zhang M: **Identification and analysis of eight peptide transporter homologs in rice.** *Plant Science* 2010, **179**(4):374–382.
18. Zhang M-Y, Bourbouloux A, Cagnac O, Srikanth CV, Rentsch D, Bachhawat AK, Delrot S: **A Novel Family of Transporters Mediating the Transport of Glutathione Derivatives in Plants.** *Plant Physiol* 2004, **134**(1):482–491.
19. Conte SS, Walker EL: **Transporters Contributing to Iron Trafficking in Plants.** *Molecular Plant* 2011, **4**(3):464–476.
20. Römheld V, Marschner H: **Evidence for a Specific Uptake System for Iron Phytosiderophores in Roots of Grasses.** *Plant Physiol* 1986, **80**(1):175–180.
21. von Wiren N, Mori S, Marschner H, Romheld V: **Iron Inefficiency in Maize Mutant ys1 (*Zea mays L.* cv Yellow-Stripe) Is Caused by a Defect in Uptake of Iron Phytosiderophores.** *Plant Physiol* 1994, **106**(1):71–77.
22. Inoue H, Kobayashi T, Nozoye T, Takahashi M, Kakei Y, Suzuki K, Nakazono M, Nakanishi H, Mori S, Nishizawa NK: **Rice OsYSL15 Is an Iron-regulated Iron(III)-Deoxymugineic Acid Transporter Expressed in the Roots and Is Essential for Iron Uptake in Early Growth of the Seedlings.** *J Biol Chem* 2009, **284**(6):3470–3479.
23. Lee S, Chiecko JC, Kim SA, Walker EL, Lee Y, Guerinot ML, An G: **Disruption of OsYSL15 Leads to Iron Inefficiency in Rice Plants.** *Plant Physiol* 2009, **150**(2):786–800.
24. Aoyama T, Kobayashi T, Takahashi M, Nagasaka S, Usuda K, Kakei Y, Ishimaru Y, Nakanishi H, Mori S, Nishizawa N: **OsYSL18 is a rice iron(III)–deoxymugineic acid transporter specifically expressed in reproductive organs and phloem of lamina joints.** *Plant Mol Biol* 2009, **70**(6):681–692.
25. Araki R, Murata J, Murata Y: **A Novel Barley Yellow Stripe 1-Like Transporter (HvYSL2) Localized to the Root Endodermis Transports Metal–Phytosiderophore Complexes.** *Plant and Cell Physiology* 2011, **52**(11):1931–1940.
26. Zheng L, Fujii M, Yamaji N, Sasaki A, Yamane M, Sakurai I, Sato K, Feng Ma J: **Isolation and Characterization of a Barley Yellow Stripe-like Gene, HvYSL5.** *Plant and Cell Physiology* 2011, **52**(5):765–774.
27. Ueno D, Yamaji N, Ma JF: **Further characterization of ferric—phytosiderophore transporters ZmYS1 and HvYS1 in maize and barley.** *J Exp Bot* 2009, **60**(12):3513–3520.
28. Yen M-R, Tseng Y-H, Saier MH: **Maize Yellow Stripe1, an iron-phytosiderophore uptake transporter, is a member of the oligopeptide transporter (OPT) family.** *Microbiology* 2001, **147**(11):2881–2883.
29. Mayer KFX, Martis M, Hedley PE, Šimková H, Liu H, Morris JA, Steuernagel B, Taudien S, Roessner S, Gundlach H, *et al*: **Unlocking the Barley Genome by Chromosomal and Comparative Genomics.** *The Plant Cell Online* 2011, **23**(4):1249–1263.
30. *HarvEST:Barley.* [http://harvest.ucr.edu]
31. *UniProtKB/Swiss-Prot.* [http://www.ebi.ac.uk/swissprot]
32. *NCBI non-redundant dataset.* [ftp://ftp.ncbi.nlm.nih.gov/blast/db/]
33. *Geneontology.* [www.geneontology.org]
34. Conesa A, Götz S, García-Gómez JM, Terol J, Talón M, Robles M: **Blast2GO: a universal tool for annotation, visualization and analysis in functional genomics research.** *Bioinformatics* 2005, **21**(18):3674–3676.
35. *Blast2GO.* [http://www.blast2go.com]
36. Rawlings ND, Barrett AJ, Bateman A: **MEROPS: the database of proteolytic enzymes, their substrates and inhibitors.** *Nucleic Acids Res* 2012, **40**(D1):D343–D350.
37. *MEROPS - The Peptidase Database.* [http://merops.sanger.ac.uk/]
38. Wookey PJ, Pittard J, Forrest SM, Davidson BE: **Cloning of the tyrP gene and further characterization of the tyrosine-specific transport system in Escherichia coli K-12.** *J Bacteriol* 1984, **160**(1):169–174.
39. *The TIGR Rice Genome Annotation Resource: improvements and new features.* [http://rice.plantbiology.msu.edu/index.shtml]
40. Matsumoto T, Tanaka T, Sakai H, Amano N, Kanamori H, Kurita K, Kikuta A, Kamiya K, Yamamoto M, Ikawa H, *et al*: **Comprehensive Sequence Analysis of 24,783 Barley Full-Length cDNAs Derived from 12 Clone Libraries.** *Plant Physiol* 2011, **156**(1):20–28.
41. *IPK Barley Viroblast.* [http://webblast.ipk-gatersleben.de/barley/viroblast.php]
42. Waters SP, Peoples MB, Simpson RJ, Dalling MJ: **Nitrogen redistribution during grain growth in wheat (*Triticum aestivum L.*).** *Planta* 1980, **148**(5):422–428.
43. Lopes M, Cortadellas N, Kichey T, Dubois F, Habash D, Araus J: **Wheat nitrogen metabolism during grain filling: comparative role of glumes and the flag leaf.** *Planta* 2006, **225**(1):165–181.
44. Araus JL, Brown HR, Febrero A, Bort J, Serret MD: **Ear photosynthesis, carbon isotope discrimination and the contribution of respiratory CO2 to differences in grain mass in durum wheat.** *Plant Cell Environ* 1993, **16**(4):383–392.
45. Tambussi EA, Nogués S, Araus JL: **Ear of durum wheat under water stress: water relations and photosynthetic metabolism.** *Planta* 2005, **221**(3):446–458.
46. Thiel J, Müller M, Weschke W, Weber H: **Amino acid metabolism at the maternal–filial boundary of young barley seeds: a microdissection-based study.** *Planta* 2009, **230**(1):205–213.
47. Jukanti AK, Heidlebaugh NM, Parrott DL, Fischer IA, McInnerney K, Fischer AM: **Comparative transcriptome profiling of near-isogenic barley (*Hordeum vulgare*) lines differing in the allelic state of a major grain protein content locus identifies genes with possible roles in leaf senescence and nitrogen reallocation.** *New Phytol* 2008, **177**(2):333–349.
48. Buchanan-Wollaston V, Earl S, Harrison E, Mathas E, Navabpour S, Page T, Pink D: **The molecular analysis of leaf senescence – a genomics approach.** *Plant Biotechnology Journal* 2003, **1**(1):3–22.
49. Buchanan-Wollaston V, Page T, Harrison E, Breeze E, Lim PO, Nam HG, Lin J-F, Wu S-H, Swidzinski J, Ishizaki K, *et al*: **Comparative transcriptome analysis reveals significant differences in gene expression and signalling pathways between developmental and dark/starvation-induced senescence in Arabidopsis.** *The Plant Journal* 2005, **42**(4):567–585.
50. Gregersen PL, Holm PB, Krupinska K: **Leaf senescence and nutrient remobilisation in barley and wheat.** *Plant Biology* 2008, **10:**37–49.
51. Sanders A, Collier R, Trethewy A, Gould G, Sieker R, Tegeder M: **AAP1 regulates import of amino acids into developing Arabidopsis embryos.** *The Plant Journal* 2009, **59**(4):540–552.
52. Okumoto S, Schmidt R, Tegeder M, Fischer WN, Rentsch D, Frommer WB, Koch W: **High Affinity Amino Acid Transporters Specifically Expressed in Xylem Parenchyma and Developing Seeds of Arabidopsis.** *J Biol Chem* 2002, **277**(47):45338–45346.
53. Fischer W-N, Loo DDF, Koch W, Ludewig U, Boorer KJ, Tegeder M, Rentsch D, Wright EM, Frommer WB: **Low and high affinity amino acid**

H + −cotransporters for cellular import of neutral and charged amino acids. *The Plant Journal* 2002, **29**(6):717–731.
54. Hirner B, Fischer WN, Rentsch D, Kwart M, Frommer WB: **Developmental control of H+/amino acid permease gene expression during seed development of Arabidopsis.** *The Plant Journal* 1998, **14**(5):535–544.
55. Van Bel AJE: **Quantification of the xylem-to-phloem transfer of amino acids by use of inulin [14C]carboxylic acid as xylem transport marker.** *Plant Science Letters* 1984, **35**(1):81–85.
56. Liu D, Gong W, Bai Y, Luo J-C, Zhu Y-X: **OsHT, a Rice Gene Encoding for a Plasma-Membrane Localized Histidine Transporter.** *Journal of Integrative Plant Biology* 2005, **47**(1):92–99.
57. Chen L, Ortiz-Lopez A, Jung A, Bush DR: **ANT1, an Aromatic and Neutral Amino Acid Transporter in Arabidopsis.** *Plant Physiol* 2001, **125**(4):1813–1820.
58. Weber H, Borisjuk L, Wobus U: **Molecular physiology of legume seed development.** *Annual Review of Plant Biology* 2005, **56**(1):253–279.
59. Rolletschek H, Hosein F, Miranda M, Heim U, Götz K-P, Schlereth A, Borisjuk L, Saalbach I, Wobus U, Weber H: **Ectopic Expression of an Amino Acid Transporter (VfAAP1) in Seeds of *Vicia narbonensis* and Pea Increases Storage Proteins.** *Plant Physiol* 2005, **137**(4):1236–1249.
60. Weigelt K, Küster H, Radchuk R, Müller M, Weichert H, Fait A, Fernie AR, Saalbach I, Weber H: **Increasing amino acid supply in pea embryos reveals specific interactions of N and C metabolism, and highlights the importance of mitochondrial metabolism.** *The Plant Journal* 2008, **55**(6):909–926.
61. Sreenivasulu N, Altschmied L, Radchuk V, Gubatz S, Wobus U, Weschke W: **Transcript profiles and deduced changes of metabolic pathways in maternal and filial tissues of developing barley grains.** *The Plant Journal* 2004, **37**(4):539–553.
62. Xiang X, Bao Y: **Relationship between embryo and endosperm development and accumulation of storage reserves in barley.** *Acta Botanica Sinica* 1997, **39:**905–913.
63. Weschke W, Panitz R, Sauer N, Wang Q, Neubohn B, Weber H, Wobus U: **Sucrose transport into barley seeds: molecular characterization of two transporters and implications for seed development and starch accumulation.** *The Plant Journal* 2000, **21**(5):455–467.
64. Gansel X, Muños S, Tillard P, Gojon A: **Differential regulation of the NO3– and NH4+ transporter genes AtNrt2.1 and AtAmt1.1 in Arabidopsis: relation with long-distance and local controls by N status of the plant.** *The Plant Journal* 2001, **26**(2):143–155.
65. Forde BG, Lea PJ: **Glutamate in plants: metabolism, regulation, and signalling.** *J Exp Bot* 2007, **58**(9):2339–2358.
66. Sakakibara H: **Nitrate-specific and cytokinin-mediated nitrogen signaling pathways in plants.** *Journal of Plant Research* 2003, **116**(3):253–257.
67. Sakakibara H, Takei K, Hirose N: **Interactions between nitrogen and cytokinin in the regulation of metabolism and development.** *Trends Plant Sci* 2006, **11**(9):440–448.
68. *The European Nucleotide Archive (ENA).* [http://www.ebi.ac.uk/ena/]
69. *SeqClean.* [http://compbio.dfci.harvard.edu/tgi/software/]
70. *TGICL.* [http://compbio.dfci.harvard.edu/tgi/software/]
71. Zhang Z, Schwartz S, Wagner L, Miller W: **A Greedy Algorithm for Aligning DNA Sequences.** *J Comput Biol* 2000, **7**(1–2):203–214.
72. Huang X, Madan A: **CAP3: A DNA Sequence Assembly Program.** *Genome Res* 1999, **9**(9):868–877.
73. Altschul SF, Gish W, Miller W, Myers EW, Lipman DJ: **Basic local alignment search tool.** *J Mol Biol* 1990, **215**(3):403–410.
74. Margulies M, Egholm M, Altman WE, Attiya S, Bader JS, Bemben LA, Berka J, Braverman MS, Chen Y-J, Chen Z, *et al*: **Genome sequencing in microfabricated high-density picolitre reactors.** *Nature* 2005, **437**(7057):376–380.
75. *Perl - version 5.8.8.* [http://perl.org]
76. *BioPerl version 1.6.0.* [http://bioperl.org/]
77. Rae AL, Cybinski DH, Jarmey JM, Smith FW: **Characterization of two phosphate transporters from barley; evidence for diverse function and kinetic properties among members of the Pht1 family.** *Plant Mol Biol* 2003, **53**(1):27–36.
78. Swofford DL: *PAUP*: Phylogenetic Analysis Using Parsimony (and Other Methods) 4.0 Beta.* Florida State University: Sinauer Associates, Inc., Publishers; 2002.
79. *Figtree.* [http://tree.bio.ed.ac.uk/software/figtree]
80. Beers EP, Woffenden BJ, Zhao C: **Plant proteolytic enzymes: possible roles during programmed cell death.** *Plant Mol Biol* 2000, **44**(3):399–415.
81. Martinez M, Diaz I: **The origin and evolution of plant cystatins and their target cysteine proteinases indicate a complex functional relationship.** *BMC Evol Biol* 2008, **8**(1):198.
82. Radchuk R, Emery RJN, Weier D, Vigeolas H, Geigenberger P, Lunn JE, Feil R, Weschke W, Weber H: **Sucrose non-fermenting kinase 1 (SnRK1) coordinates metabolic and hormonal signals during pea cotyledon growth and differentiation.** *The Plant Journal* 2010, **61**(2):324–338.
83. Saeed AI, Bhagabati NK, Braisted JC, Liang W, Sharov V, Howe EA, Li J, Thiagarajan M, White JA, Quackenbush J: **TM4 Microarray Software Suite.** In *Methods in Enzymology*, Volume 411. Edited by Alan K, Brian O. San Diego, Calif: Elsevier/Academic Press; 2006:134–193.
84. *J-Express.* [http://jexpress.bioinfo.no/site/]
85. MacQueen J: *Some methods for classification and analysis of multivariate observations. In: Proceedings of the Fifth Berkeley Symposium on Mathematical Statistics and Probability: June 21-July 18, 1965 and December 27, 1965-January 7, 1966 1965; Berkeley, California, USA. Proceedings of the Fifth Berkeley Symposium on Mathematical Statistics and Probability*, Volume 1. Berkeley, California: Statistics: University of California Press; 1967:281–297.
86. *OriginPro 8.1.* [http://www.originlab.com/]

doi:10.1186/1471-2229-12-154
Cite this article as: Kohl *et al.*: A putative role for amino acid permeases in sink-source communication of barley tissues uncovered by RNA-seq. *BMC Plant Biology* 2012 **12**:154.

Journal of Experimental Botany, Vol. 66, No. 5 pp. 1397–1411, 2015
doi:10.1093/jxb/eru492 Advance Access publication 22 January 2015
This paper is available online free of all access charges (see http://jxb.oxfordjournals.org/open_access.html for further details)

RESEARCH PAPER

Metabolic and transcriptional transitions in barley glumes reveal a role as transitory resource buffers during endosperm filling

Stefan Kohl[1,*], Julien Hollmann[2], Alexander Erban[3], Joachim Kopka[3], David Riewe[1], Winfriede Weschke[1] and Hans Weber[1]

[1] Leibniz Institute of Plant Genetics and Crop Plant Research, 06466 Gatersleben, Germany
[2] Christian-Albrechts-Universität zu Kiel, 24118 Kiel, Germany
[3] Max-Planck-Institute of Molecular Plant Physiology, 14476 Potsdam-Golm, Germany

* To whom correspondence should be addressed. E-mail: kohl@ipk-gatersleben.de

Received 26 July 2014; Revised 24 October 2014; Accepted 18 November 2014

Abstract

During grain filling in barley (*Hordeum vulgare* L. cv. Barke) reserves are remobilized from vegetative organs. Glumes represent the vegetative tissues closest to grains, senesce late, and are involved in the conversion of assimilates. To analyse glume development and metabolism related to grain filling, parallel transcript and metabolite profiling in glumes and endosperm were performed, showing that glume metabolism and development adjusts to changing grain demands, reflected by specific signatures of metabolite and transcript abundances. Before high endosperm sink strength is established by storage product accumulation, glumes form early, intermediary sink organs, shifting then to remobilizing and exporting source organs. Metabolic and transcriptional transitions occur at two phases: first, at the onset of endosperm filling, as a consequence of endosperm sink activity and assimilate depletion in endosperm and vascular tissues; second, at late grain filling, by developmental ageing and senescence. Regulation of and transition between phases are probably governed by specific NAC and WRKY transcription factors, and both abscisic and jasmonic acid, and are accompanied by changed expression of specific nitrogen transporters. Expression and metabolite profiling suggest glume-specific mechanisms of assimilate conversion and translocation. In summary, grain filling and endosperm sink strength coordinate phase changes in glumes via metabolic, hormonal, and transcriptional control. This study provides a comprehensive view of barley glume development and metabolism, and identifies candidate genes and associated pathways, potentially important for breeding improved grain traits.

Key words: ABA, barley (*Hordeum vulgare* L. cv. Barke), glumes, jasmonic acid, NAC transcription factors, nitrogen (N) remobilization, N transport, seed development, WRKY transcription factors.

Introduction

During seed filling carbon (C) and nitrogen (N) compounds are remobilized from vegetative organs and transported to the seeds. Vegetative organs in barley and wheat are photosynthetically active, providing carbohydrates until late grain filling. By contrast, 60–90% of grain N originates from remobilization out of vegetative organs (Hirel *et al.*, 2007). Among the photosynthetically active tissues, glumes hold an exceptional role, as the organs nearest the grains. In wheat, glumes have a unique cellular and chloroplast distribution associated with their particular metabolism and supporting

grain maturation (Waters *et al.*, 1980; Lopes *et al.*, 2006). Up to 30% of photosynthates imported into grains derive from photosynthetic activity of glumes (Grundbacher, 1963).

Most N derived from other source tissues is not directly transported into developing grains, but instead transported through and eventually converted within glumes (Waters *et al.*, 1980; Simpson *et al.*, 1983).

Compared to flag leaves, glumes senesce late and thus could be important for N translocation during later grain filling. Thereby, the capacity of glumes to convert and translocate N during senescence is an important trait to assess in breeding for higher grain protein content.

To fulfil these tasks, glume metabolism must be coordinated with the different phases of grain development. In barley endosperm, cellularization begins around 4 days after pollination (DAP) and is completed 1–2 days later. The prestorage/cellularization phase, from anthesis to 6 DAP, and the storage phase, starting at 8–10 DAP, are separated by a transition stage characterized by transcriptional reprogramming and a switch into storage mode (Sreenivasulu *et al.*, 2004). Between 8 and 10 DAP, the endosperm starts accumulating storage products, develops high sink strength for sucrose and N, and enters the linear phase of dry matter accumulation between 10 and 20 DAP (Weschke *et al.*, 2000). Physiological maturity is reached around 24 DAP followed by desiccation.

Endosperm phase changes are accompanied by differences in sink strength, which affect metabolism, remobilization, and transport of resources into and from vegetative organs. As would be expected, central metabolism in glumes is coordinated with such changes during grain filling (Lopes *et al.*, 2006). There is a lack of detailed knowledge about this cross-talk at the molecular level, and of metabolic and transcriptional adjustments according to the specific demands of grains. The remobilization of assimilates and reserves during seed filling is highly regulated (Watanabe *et al.*, 2013). The WRKY (contains the WRKY amino acid signature at the N-terminus and zinc-finger structure at the C-terminus) and NAC (*N*AM, *A*TAF1,2, *C*UC) transcription factors are involved in regulating remobilization and senescence (Balazadeh *et al.*, 2010; Breeze *et al.*, 2011; Fischer, 2012). In barley, specific members of the NAC transcription factor gene family are co-regulated with senescence-associated genes in senescing flag leaves (Gregersen and Holm, 2007; Christiansen and Gregersen, 2014). In wheat the NAC transcription factor Gpc-B1 accelerates senescence and increases nutrient remobilization from leaves (Uauy *et al.*, 2006).

Remobilized N from protein degradation has to be transported across membranes by specific transporters (Tegeder and Rentsch, 2010). Members of the amino acid transporter family (ATF) and nitrate/peptide transporter family (NPF) are key components in remobilization, and functionally characterized transporters are expressed in tissue and development specific-manners. AtAAP1 is involved in amino acid uptake into embryos (Hirner *et al.*, 1998; Sanders *et al.*, 2009), AtAAP8 is involved in amino acid uptake into endosperm (Schmidt *et al.*, 2007), and AtPTR5 is preferentially expressed during early seed development (Komarova *et al.*, 2008). Barley HvPTR1 transports peptides from endosperm to growing embryos during germination (West *et al.*, 1998). Transporters involved in amino acid uptake into cells have mainly been characterized (Tegeder, 2012), but recently AtBAT1 (Dündar and Bush, 2009) and AtSIAR1 (Ladwig *et al.*, 2012) have been shown to export amino acids out of cells with apparently opposing functions. While AtBAT1 shows preferential expression in sink tissues (Dündar, 2009), AtSIAR1 expression is associated with source tissues, and *Arabidopsis* mutants have lower contents and disturbed homeostasis of amino acids in siliques (Ladwig *et al.*, 2012).

The aim of this study was to analyse temporal changes of transcript and metabolite abundances in glumes and endosperm during barley grain development. Such parallel profiling allows a correlation of shifts in glume metabolism and remobilization events with distinct phases of grain development. Furthermore, possible signals and transporters involved in coordinating metabolism and N translocation between glumes and endosperm are presented and discussed.

Material and methods

Plant growth and harvest

Barley (*Hordeum vulgare* L. cv. Barke) was grown in greenhouses with 16 h light/8 h dark. Stages of grain development were determined as described previously (Weschke *et al.*, 2000). Glumes and endosperm tissue were collected between 10am and 12pm in 2- or 4-day intervals starting at anthesis (glumes) and 4 DAP (endosperm) until 24 DAP. Endosperm was manually separated from pericarp between 4 and 14 DAP, and whole caryopses were sampled between 16 and 24 DAP.

Array design

Transcript data from HarvEST assembly 35 (www.harvest.ucr.edu), two RNAseq experiments (Kohl *et al.*, 2012; Thiel *et al.*, 2012*a*), and a full-length cDNA collection (Matsumoto *et al.*, 2011) were assembled to 46 114 unique barley contigs using TGICL pipeline (http://compbio.dfci.harvard.edu/tgi/) as described previously (Kohl *et al.*, 2012). Sequences were annotated using Blast2go (Gene Ontology terms) (Conesa *et al.*, 2005), Mercator (bincodes) (Thimm *et al.*, 2004), and BLAST (Altschul *et al.*, 1990). Best hits were obtained from BLASTx similarity searches against UniRef90 (www.uniprot.org), TAIR10 (www.arabidopsis.org), *Oryza sativa* (http://rice.plantbiology.msu.edu/, last accessed 31 December 2014), and UniProtKB/Swiss-Prot (www.uniprot.org). Unambiguous 60 bp oligomer probes were derived using eArray (Agilent Technologies, Santa Clara, USA) and a part of this probe set was replicated. Microarray design and expression data is available at EMBL-EBI ArrayExpress, accession E-MTAB-3040.

RNA isolation, labelling, and array hybridization

Glume and endosperm material for three biological replicates was harvested from 0 (only glumes), 4, 8, 10, 14, 18, and 24 (glumes and endosperm) DAP; and total RNA was extracted with a Spectrum™ Plant Total RNA Kit (Sigma Aldrich, Steinheim, Germany). RNA integrity was confirmed using the Bioanalyser system (Agilent Technologies). 100 ng RNA was used for cRNA synthesis and Cy3-labelling with a Low Input Quick Amp Labelling Kit (Agilent Technologies). Labelling efficiency, and amount and quality of cRNA, were assured using an ND-1000 Spectrophotometer (NanoDrop Technologies, Wilmington, USA) and Bioanalyser system. 600 ng labelled cRNA was used for fragmentation and array loading (Gene Expression Hybridization Kit, Agilent Technologies). Hybridization was done for 17 h at 65°C. After washing (Gene

Expression Wash Buffer Kit, Agilent Technologies) and drying, arrays were scanned at 5 µm resolution using an Agilent Technologies Scanner G2505C. Resulting images were evaluated (determination of spot intensities, background correction) with Feature Extraction V11.5 (Agilent Technologies).

Data evaluation

Data evaluation was done with Genespring V12.5 (Agilent Technologies). Values were $\log_2$ transformed and quantile normalized, before relative expression values were calculated by subtracting the median expression of each probe from the other values of this specific probe (baseline transformation). After removing outliers and transcripts without significant expression at any time point, ANOVA ($P \leq 0.005$, $FC \geq 3$) and FDR correction (Benjamini-Hochberg) was performed. These stringent parameters were chosen in order to identify important transcripts without (unnecessarily) expanding the data set.

Preparation of vascular tissue

Seeds were harvested (eight biological replicates) at 4, 8, 10, 14, 18, and 24 DAP according to Thiel *et al.* (2009). Vascular tissues were micro-dissected from the middle of the grain with 30 µm thickness per section (Supplementary Figure S1).

UPLC measurements

Extraction and measurement are described in Thiel *et al.* (2009), with the following changes: 10 mg of dried material was used; before extraction, 5 µl Norvalin (5mM) were added; 100 µl aliquots of extract were concentrated under vacuum and dissolved in 200 µl water.

C/N and starch measurements

Total C and N were determined from dried and ground material using a Vario EL Elementar analyser (Elementar Analysensysteme GmbH, Hanau, Germany). Starch was measured as described (Weschke *et al.*, 2000).

Metabolite profiling by GC-MS

For GC-MS measurements of polar central metabolites, 100 mg (glumes) and 10 mg (endosperm) fresh material from six biological replicates was collected in 2-day steps (0–24 DAP) for glumes and at 4, 8, 10, 14, 18, and 24 DAP for endosperm. Sample preparation, extraction and data evaluation were done as described by Weichert *et al.* (2010). Data was visualised with the VANTED software package (Junker *et al.*, 2006). To analyse micro-dissected grain vascular tissue, 9 nl material for eight biological replicates was collected at 4, 8, 10, 14, 18, and 24 DAP, extracted, and evaluated as described previously (Riewe *et al.*, 2012; Thiel *et al.*, 2012*b*).

Results

Growth parameters, starch and N content

Growth parameters were analysed for glumes between 0 and 24 DAP and for endosperm from 4 to 24 DAP. Glume dry weight increased steadily by 40% from 0 to 8 DAP followed by a transient decrease of 20% between 8 and 10 DAP. Thereafter, dry weight rose slightly, remained constant until 20 DAP and declined thereafter (Fig. 1A). Total N in glumes increased until 8 DAP, followed by a sharp decline at 8 DAP without further changes until 20 DAP and a slight decrease thereafter (Fig. 1B). Starch content in glumes was generally low compared to endosperm (Supplementary Table S1) and decreased by 65% between 0 and 10 DAP, before increasing by 15% from 18 to 24 DAP (Fig. 1C). Endosperm dry weight and starch content rose at ~8 DAP followed by linear accumulation during the main storage phase (10 to 20 DAP), levelling off afterwards (Fig. 1A, C). Total N increased linearly from 8 DAP until around 20 DAP (Fig. 1B).

The results show that from anthesis glumes accumulated dry weight and N until approximately 8 DAP, followed by a considerable decrease, coinciding with the start of starch and dry weight accumulation in the endosperm.

Comparative gene expression analysis in glumes and endosperm

Comparative transcript analysis was performed in glumes and endosperm to analyse changes in central metabolic pathways, remobilization, and transport processes, as well as putative regulatory elements. Labelled cRNA from glume (0–24 DAP) and endosperm (4–24 DAP) fractions were hybridized to Agilent microarrays. In endosperm and glumes, 8998 and 3999 transcripts were identified as differentially expressed (significant differences between at least two stages; Supplementary Tables S2, S3). General profiles for both tissues are similar, revealing three distinct phases: (i) high differential expression between 0 and 8–10 DAP in glumes and endosperm; (ii) low differential expression between 8–10 and 14 DAP for glumes and endosperm; (iii) high differential expression after 14 DAP (Fig. 2A, B).

Central carbohydrate and N metabolism

In glumes, gene expression related to glycolysis (e.g. Glc-6-P epimerase, enolase, cytosolic/plastidic pyruvate kinase, and

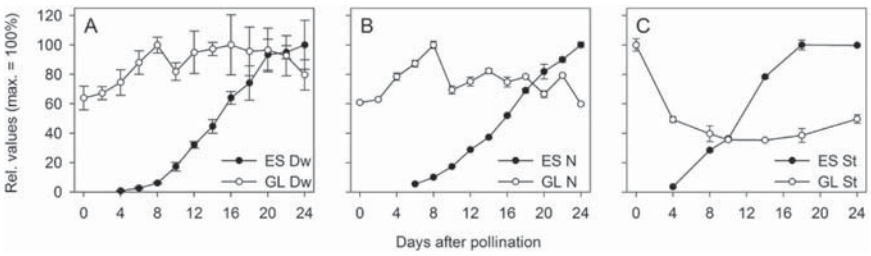

Fig. 1. Changes of physiological parameters during endosperm (ES) and glume (GL) development. Relative changes (maximum amount = 100%) are shown for (A) dry weight (Dw), (B) total N, and (C) starch content (St) between 0 and 24 DAP. Data points represent three to five biological replicates ±SD.

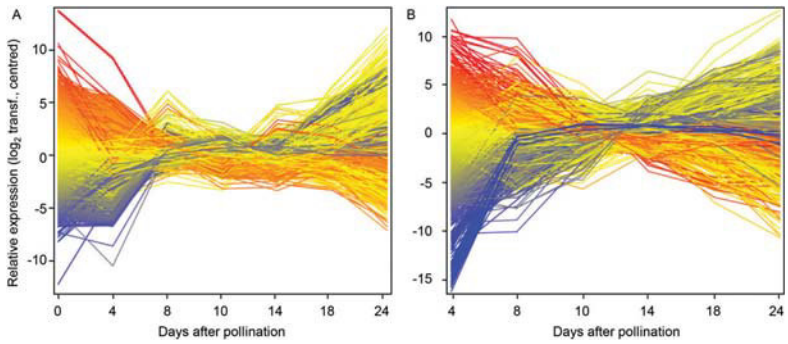

Fig. 2. Expression profiles of 3999 and 8998 differentially expressed transcripts during development in (A) barley glumes and (B) endosperm, respectively. Data was derived from microarray experiments (Agilent 8 × 60K customized barley array); each time point represents three biological replicates. Raw expression values were $\log_2$ transformed, quantile normalized, and centred. Differential expression was detected by ANOVA ($P < 0.005$, $FC > 3$); single profiles were coloured according to their values at 0 DAP.

phosphoglycerate mutase) decreased steeply from 0 to 8 DAP and slightly thereafter. This was similar to the expression of the main starch metabolism genes, such as sucrose synthase, various starch synthases, and ADP-Glc pyrophosphorylase. By contrast, expression of seven genes related to glycolysis and seven associated with starch biosynthesis strongly increased in endosperm from 4 to 8 DAP, remained constantly high up to 14 DAP, and declined thereafter (Fig. 3).

In glumes between 4 and 8 DAP genes related to the tricarboxylic acid (TCA) cycle (2-OG dehydrogenase, succinyl CoA ligase, and malate dehydrogenase) and to the mitochondrial electron-transport chain (mETC) (succinate dehydrogenase, NAD:ubiquinone oxidoreductase, and ATP synthase), were steeply upregulated. In endosperm, expression of TCA cycle-related genes, such as citrate synthase, pyruvate dehydrogenase or NAD-isocitrate dehydrogenase, was highest at 4 DAP, decreased steadily until 10 DAP, and remained constant until 24 DAP (Fig. 3).

In glumes, nine genes associated with amino acid biosynthesis were most highly expressed at 0 and 4 DAP, followed by decreasing expression. Four are involved in the aspartate pathway towards lysine, methionine, and threonine biosynthesis; two others are involved in arginine biosynthesis. By contrast, endosperm expression of nine genes related to amino acid biosynthesis increased at 8 DAP and decreased after 18 DAP (Fig. 3). Endosperm expression of storage protein genes increased strongly from 4 to 8 DAP, and remained at a high level until 24 DAP (Fig. 3).

Transcript analysis revealed opposing trends for certain metabolic pathways such as glycolysis, and starch and amino acid synthesis, these being downregulated in glumes but upregulated in the endosperm during grain filling. TCA cycle and mETC-activities were strongly upregulated in glumes at 8 DAP, the beginning of grain filling.

Carbohydrate and N transporters

Remobilization of reserves from glumes and accumulation in the endosperm depends on efficient transport from sink to source. In glumes, expression of several carbohydrate transporter genes increased at 8 DAP and then further until 24 DAP. This involved hexose/sugar transporters and members of the SWEET family, which potentially export sugars from *Arabidopsis* leaves (Chen *et al.*, 2012). In the endosperm, solute transporters related to storage product synthesis (e.g. HvSUT1, plastidic translocators for ADP-Glc and phosphoenol pyruvate) were upregulated at 8 DAP with decreasing expression levels towards 24 DAP (Fig. 4).

In glumes, more than 72% of putative amino acid transporters were at least transiently upregulated (Supplementary Table S4). Three major profiles were evident, early upregulated (between 0 and 8 DAP), constantly upregulated, and late upregulated (after 14 DAP) (Fig. 4).

HvAAP2 was upregulated between 0 and 8 DAP and is homologous to *AtAAP2*, which is involved in xylem to phloem transfer and is important for sink N supply (Zhang *et al.*, 2010). *HvAAP7* and *HvAAP11* were upregulated from 14 and 18 DAP and are possibly involved in senescence-related remobilization. The second group contained members from other ATF subgroups like *HvLHT1*, specifically expressed in glumes and probably important for amino acid re-translocation (Kohl *et al.*, 2012), *HvCAT1*, *HvANT4*, and *HvGAT1*. Barley homologues of AtBAT1 (Dündar and Bush, 2009) and AtSIAR1 (Ladwig *et al.*, 2012) showed opposing expression profiles. *HvBAT3* was upregulated between 0 and 14 DAP followed by downregulation, while *HvSIAR1-like* was downregulated between 0 and 10 DAP followed by strong upregulation.

Bias towards upregulation is less pronounced for putative nitrate/peptide transporters, where 13 from 30 candidates showed decreasing expression (Supplementary Table S4). Within upregulated candidates, three major profiles present in the ATF transporters could be observed (Fig. 4). Endosperm-expressed N transporters probably facilitate N import or distribution. 80% and >73% of ATF and NPF transporters, respectively, were upregulated during development (Supplementary Table S5). Major patterns showed upregulation until 14 DAP, transient upregulation at 8 or 10 DAP, and constant upregulation after 8 DAP (Fig. 4).

Among transiently upregulated transcripts, *HvAAP3* is closely related to *AtAAP8* and *AtAAP1*, importing amino acids into seeds (Schmidt *et al.*, 2007; Sanders *et al.*, 2009).

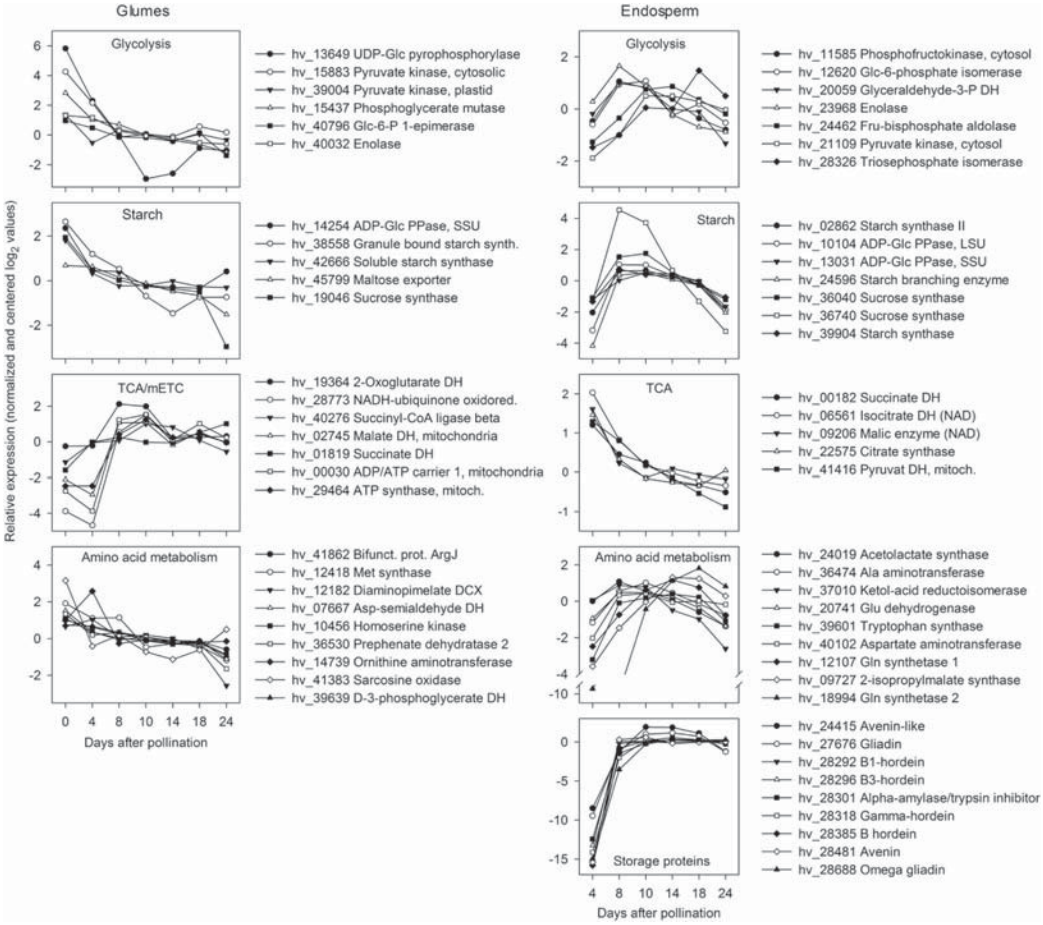

Fig. 3. Comparison of transcript profiles between glumes (left panel) and endosperm (right panel) fractions. Relative expression values (means of three biological replicates, quantile normalized and baseline transformed) are shown for array contigs (hv_number) involved in central C and N metabolism, energy balance, and storage proteins (endosperm only). DCX, decarboxylase; DH, dehydrogenase; LSU, large subunit; PPase, pyrophosphorylase; SSU, small subunit.

Expression of a *BAT-like* transcript was also steadily increasing during development, and is possibly involved in phloem unloading (Dündar, 2009), while increasing expression of *OsPUT1-like* after 8 DAP indicates polyamine import into grains (Mulangi *et al.*, 2012).

Transcriptional transitions in glume metabolism during grain filling

Photosynthesis-associated transcripts in glumes were highly expressed at 0–4 DAP, with decreasing levels after 8 DAP (Fig. 5A). Chlorophyll is degraded during leaf senescence by a pathway involving pheophorbide a oxygenase (PAO) (Hörtensteiner, 2006). In glumes, *HvPAO* was upregulated from 14 DAP onwards (Fig. 5A), indicating chlorophyll degradation only at late seed filling. Protein degradation is a prerequisite for N remobilization, and several proteases were transcriptionally upregulated in glumes at two distinct phases, between 0 and 8 DAP and from 14 DAP onwards. This involved several serine-, aspartyl-, and cysteine-like proteinases including a homologue to *Arabidopsis senescence-associated gene-12* (*SAG12*), which is specifically activated by developmentally controlled senescence but is not stress- or hormone-controlled (Noh and Amasino, 1999).

Whereas several amino acid biosynthesis genes were downregulated (Fig. 3), others involved in different parts of amino acid metabolism (e.g. homogentisate 1,2-dioxygenase and pyrroline-5-carboxylate reductase) were upregulated in glumes and may participate in aromatic amino acid and proline degradation. Alanine aminotransferase and glutamine synthetase-1 (GS1) could be involved in glutamine biosynthesis for export (Thiel *et al.*, 2009). Thus, expression patterns indicate interconversion and/or degradation of certain amino acid species in glumes during later grain filling. Transcripts of glutamine-dependent asparagine synthase (Gln-ASN) increased by 150-fold between 14 and 24 DAP, indicating an important role for remobilization (Fig. 5).

Potential metal transporters, like members of natural resistance-associated macrophage proteins (NRAMP), zinc transporters, yellow stripe-like (YSL), and oligopeptide transporters (OPT) were transcriptionally upregulated at 8 DAP and/or at 24 DAP. Specific genes of lipid biosynthesis/

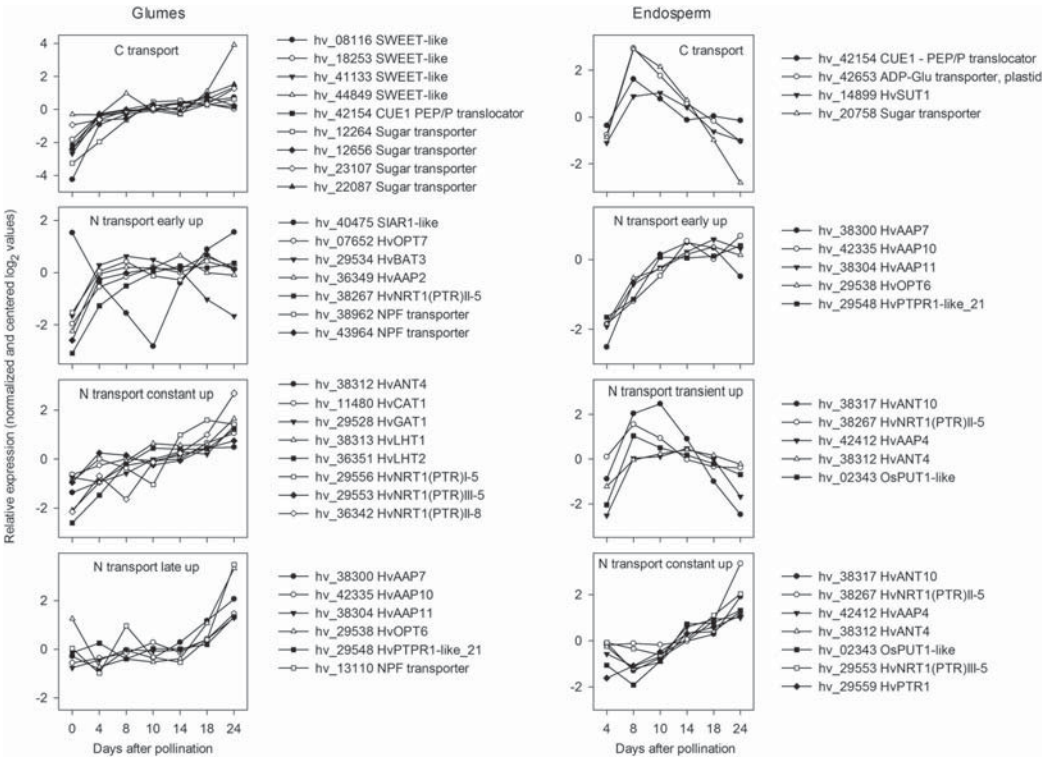

Fig. 4. Expression patterns of putative C and N transporters in glumes (left panel) and endosperm (right panel). Relative expression values (see Fig. 3) are presented for putative carbohydrate, nitrate/peptide (NRT/PTR – NPF transporter, respectively), and amino acid (aa) transporters (subgroups: AAP, general aa permease; ANT, aromatic and neutral aa transporter; BAT, bidirectional aa transporter; CAT; cationic aa transporter; GAT, GABA transporter; LHT, lysine/histidine transporter; PUT, polyamine uptake transporter; SIAR, siliques are red – MtN21-like transporter).

degradation were differently expressed during glume development. Two members degrading phospholipids, phosphatidylcholine phospholipase D, and glycero-P-diesterase were strongly upregulated between 0 and 8/10 DAP. Candidates involved in degradation of mono- and triacylglycerides, like enoyl-CoA hydratase, palmitoyl protein thioesterase, and mono- and triacylglycerol lipase were upregulated after 14 DAP. Enzymes synthesizing long-chain fatty acids, acyl-activating enzyme, very-long-chain fatty acid-condensing enzyme, and 3-ketoacyl-acyl carrier protein were most highly expressed at 18 and 24 DAP.

Genes involved in the phenylpropanoid/lignin pathway were upregulated in glumes from 8 to 24 DAP, including polyphenol oxidase, flavonoid 7-O-methyltransferase, and hydroxycinnamoyl-CoA shikimate/quinate hydroxycinnamoyl transferase. Two genes encoding laccases were constantly upregulated during development. Laccases catalyse lignin polymerization from the precursors coniferyl- and sinapyl-alcohol, and respective knockouts in *Arabidopsis* drastically reduce the lignin content (Zhao *et al.*, 2013), indicating an important role for lignification and secondary cell wall thickening in mechanical support and water transport (Zhao *et al.*, 2013).

Whereas mitochondrial activity was transcriptionally activated at 8 DAP (Fig. 3), specific genes encoding TCA-cycle and mETC-enzymes, such as pyruvate and NADH dehydrogenases, electrontransfer flavoprotein, and alternative oxidase, were upregulated only after 14 DAP.

Results from transcript profiling suggest metabolic transitions in glumes from sink to source in accordance to grain filling, namely downregulated photosynthesis and upregulated proteolysis, lipid and phenylpropanoid metabolism, and mitochondrial activities and metal transport.

Transcriptional and hormonal control of remobilization in glumes

NAC and WRKY transcription factors are frequently involved in senescence signalling (Zentgraf *et al.*, 2010; Breeze *et al.*, 2011; Christiansen and Gregersen, 2014). Most NAC transcription factors were upregulated, showing three major profiles: (i) upregulation until 8 DAP, with constant levels afterwards, including *HvNAM-1*, homologous to *TtNAM-1*, a regulator of senescence and remobilization in wheat flag leaves (Uauy *et al.*, 2006; Distelfeld *et al.*, 2008); (ii) bi-phasic upregulation, with increasing transcript abundances between 0 and 8 DAP and after 14 DAP, including *HvNAC006* and *HvNAC008*, homologous to *AtORE1* and *AtATAF1*, controlling leaf senescence in *Arabidopsis* (Kim *et al.*, 2009; Kleinow *et al.*, 2009; Balazadeh *et al.*, 2010); (iii) upregulation after 14 DAP obviously associated with developmental senescence (Fig. 5B). The latter group includes *HvNAC009* and

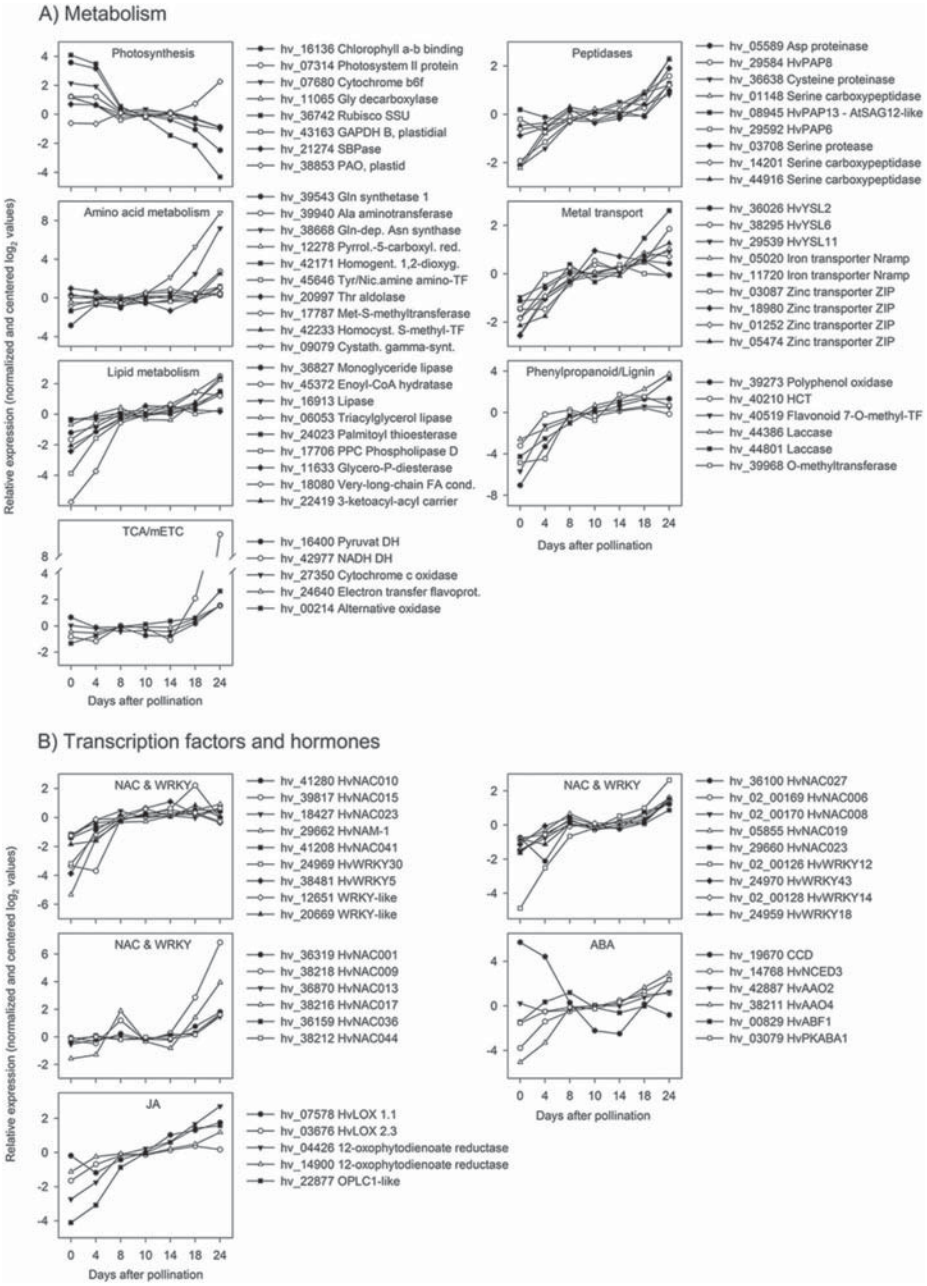

Fig. 5. Expression patterns of components regulating transition in glumes from sink to source tissue. Relative expression values (see Fig. 3) are shown for selected transcripts: (A) metabolism; (B) transcription factors and hormones. ABF, ABA-responsive element binding factor; AAO, aldehyde oxidase; CCD, carotenoid cleavage dioxygenase; HCT, hydroxycinnamoyl-CoA shikimate/quinate hydroxycinnamoyl transferase; LOX, lipoxygenase; NCED, 9-*cis*-epoxycarotenoid dioxygenase; PAO, pheophorbide a oxygenase; PAP, papain-like cysteine peptidase; PC, phosphatidylcholine; PKABA, ABA-inducible protein kinase; SBPase, sedoheptulose-1,7-bisphosphatase; TF, transferase; YSL, yellow-stripe-like transporter.

HvNAC013, upregulated in old ears and grains and old leaves, and inducible by methyl-jasmonate (Christiansen *et al.*, 2011).

Nineteen out of 22 WRKY transcription factors showed profiles according to (i) and (ii). The latter includes *HvWRKY12*, which is probably involved in age-dependent senescence rather than N remobilization (Hollmann *et al.*, 2014).

Hormones affect leaf senescence differently; senescence is delayed by cytokinins (CKs) and gibberellic acids (GAs), and accelerated by abscisic acid (ABA) and jasmonates (JA) (Jibran *et al.*, 2013). Transcripts for carotenoid cleavage dioxygenase, involved in early ABA biosynthesis, decreased until 10 DAP and increased after 14 DAP. Genes involved in late ABA biosynthesis, 9-*cis*-epoxycarotenoid dioxygenase

(*HvNCED3*) and aldehyde oxidase (*HvAAO*), were upregulated bi-phasically between 0 and 8 DAP and after 14 DAP. ABA-inducible protein kinase (*HvPKABA1*) and ABA-responsive element binding factor 1 (*HvABF1*) were similarly upregulated bi-phasically and are possibly involved in mediating GA/ABA responses (Yamauchi *et al.*, 2002; Schoonheim *et al.*, 2009).

JA biosynthesis depends on the subsequent action of lipoxygenase (LOX), allene oxide synthase and cyclase, 12-oxophytodienoate reductase (OPR), followed by beta oxidation (Lyons *et al.*, 2013). In glumes, continuously upregulated genes encode specific LOX isoforms and enzymes involved in late steps of JA biosynthesis (OPRs) and a homologue to AtOPLC1, involved in beta oxidation (Koo *et al.*, 2006).

Metabolite contents in developing glumes and endosperm

Metabolite levels were measured in glumes and endosperm (Fig. 6, Supplementary Table S6), while free amino acids were analysed by UPLC (Supplementary Table S7). Levels of sucrose, maltose, raffinose, xylulose, rhamnose, and fucose increased whereas xylose, arabinose, and trehalose decreased in glumes with progressing development. Several sugars are involved in cell wall biosynthesis, indicating alterations in cell wall dynamics in glumes. In endosperm, hexoses were highest during early development whereas sucrose peaked at 8 DAP (Weschke *et al.*, 2000).

In glumes, almost all metabolites within the glycolytic, pentose phosphate, and shikimate pathways, like hexoses and their phosphates, 6-phospho-gluconate and 3-phospho-glycerate, decreased whereas endosperm levels were highest at 8 and 10 DAP. Inositol and inositol-1-phosphate and sugar alcohols, except glycerol, decreased during glume development.

TCA intermediates, except 2-oxoglutarate and malate, increased in glumes, while the highest endosperm levels occurred at early and mid-development. Phenylpropanoid intermediates 4-coumarate, caffeate, ferulate, and sinapate also rose during glume development. Metabolites related to glycerophospholipid metabolism (ethanolamine, glycerol-3-P) increased in glumes whereas ethanolaminephosphate decreased. In the endosperm all these metabolites decreased over time. Fatty acids (stearate, palmitate) rose in glumes while endosperm levels declined. GABA, putrescine, 1, 3-diaminopropane, and β-alanine increased in glumes from 0 DAP to 18 DAP, while spermidine decreased. In the endosperm all these metabolites decreased (Fig. 6).

Free amino acid concentrations in glumes, endosperm, and vascular tissue

In glumes between pollination and 8 DAP, the summarized concentrations of all free amino acids increased from 11 to 32 µmol g^{-1} fresh weight, followed by a drastic decrease between 8 and 10 DAP (~50%; Fig. 7A; Supplementary Table S7). Thereafter, levels fluctuated at around 20 µmol g^{-1}. Most amino acids behaved similarly, showing distinct declines between 8 and 10 DAP, except Asp and Glu. Asp was generally low without larger changes, whereas Glu increased throughout. Ser was always higher by 10- to 15-fold compared to Gly. Asn was 2 to 3-fold higher than Gln between 2 and 10 DAP but not different later on.

In the endosperm, free amino acid levels decreased from 80 µmol g^{-1} fresh weight at 4 DAP to 25 µmol g^{-1} at 14 DAP, showing the largest decline between 8 and 10 DAP (Fig. 7B). Between 16 and 22 DAP levels remained constant, before decreasing at 24 DAP. While Ala, Gln, Glu, and Val followed this pattern, Arg, Asn, Pro, Ser, and Thr accumulated between 4 and 6 DAP, before their levels declined.

Concentrations of Gln and Pro most strongly declined (by ~80%) between 4 and 12 DAP. In contrast to Ser, Gly increased from 8 to 12 DAP, marking a switch from high to low Ser:Gly ratios during grain filling. Asp largely did not change. The results indicate a sudden decrease of most free amino acids (especially of Pro and Asn) in glumes at 8 DAP. This coincides with extensive use for storage protein synthesis in the endosperm.

As expected, high endosperm demand for amino acids due to storage activity is transmitted to the glumes, initiating remobilization. To analyse possible metabolic signals, GC-MS-based metabolic profiling was performed on microdissected regions comprising the main vascular bundles of grains between 4 and 24 DAP (Supplementary Figure S1). Thirty-two unambiguous metabolites were detected (Supplementary Table S8). Temporal profiles of 12 amino acids were compared between glumes, endosperm, and vascular regions (Fig. 8). Amino acid profiles were highly correlated (Pearson correlation) between vasculature and endosperm with $C_{vc,\,en}$ between 0.98 and 0.81 for Gln, Ser, Glu, Thr, Pro, Ala, Val, and Asn. Less positive ($C_{vc,\,en}$ <0.76) or even negative correlation (Ala, Glu) occurred between vasculature and glumes. This indicates that endosperm amino acid demand is propagated via the vasculature. In beech, increased Gln and Asp levels in the phloem lead to reduced root NO_3^- uptake (Geßler *et al.*, 1998) and amino acid feeding negatively regulates expression of high-affinity NO_3^--uptake transporters in barley roots (Vidmar *et al.*, 2000). In a reciprocal manner, depletion of certain amino acids such as Gln ($C_{vc,\,en}$ = 0.98) within the vasculature could signal and communicate endosperm demand to vegetative organs.

Discussion

Glumes are the vegetative organs closest to grains and are important for converting and translocating assimilates to them (Waters *et al.*, 1980; Simpson *et al.*, 1983; Lopes *et al.*, 2006). Phase changes during endosperm development are accompanied by large variations of sink strength that greatly affect metabolism in and assimilate fluxes from glumes. Parallel transcript and metabolite profiling in glumes and endosperm during grain filling showed that glume metabolism was adjusted to the changing demands of the grains, reflected by specific signatures of metabolite and transcript abundances. Obviously, grain filling and filial sink strength coordinate phase changes in glumes via metabolic, hormonal, and transcriptional control.

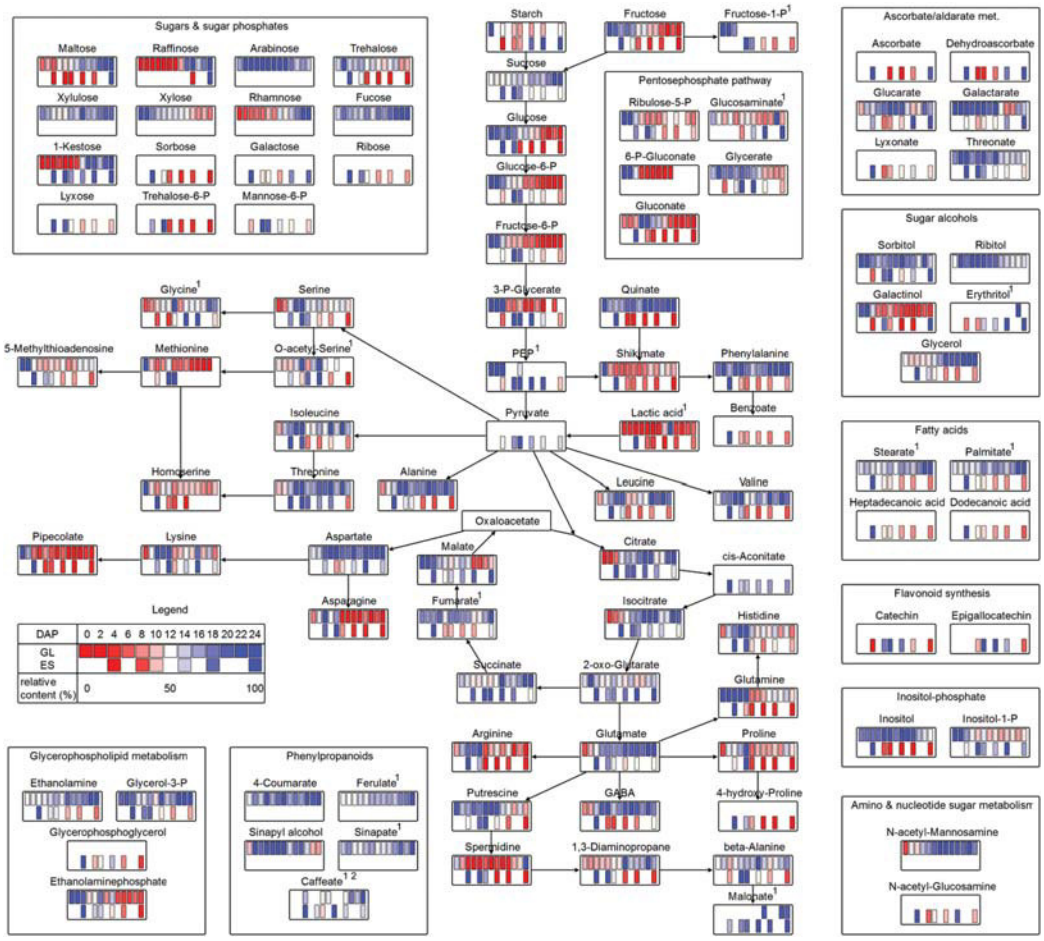

Fig. 6. Changes in metabolite levels in barley glumes and endosperm during development. Samples were taken in 2-day steps between 0 and 24 DAP (glumes) and at 4, 8, 10, 14, 18, and 24 DAP (endosperm). Levels of proteogenic amino acids and GABA were measured using UPLC with two (Arg, Gly) and three biological replicates, respectively. All other metabolites were measured by GC-MS with six biological replicates per time point. Data were corrected by internal standard and fresh weight, subsequently maximum normalized and colour coded for each metabolite (maximum amount = 100%, values >90% coloured in dark blue, values <10% in dark red), as shown by the insert depicting a constant increase from 0 to 100% between 0 and 24 DAP. Metabolites without significant changes in one of the tissues are marked (1) for glumes and (2) for endosperm.

Glumes are photosynthetically active sinks during the pre-storage phase

Transcript profiling in glumes at 0 and 4 DAP revealed high activity of photosynthesis, glycolysis, and starch and amino acid biosynthesis, but low mitochondrial activity and transport of sugars, peptides and metals. Accordingly, levels of hexoses, their phosphates, glycolytic intermediates, and starch were highest. By contrast, endosperm gene expression was low for central pathways glycolysis, and starch and amino acid biosynthesis, but high for mitochondrial activity before 8 DAP (Figs 3–5). Thus, during the pre-storage phase, glumes are photosynthetically active organs with a high level of biosynthesis, while the endosperm is a sink with high respiratory and mitochondrial activities.

During the pre-storage phase, glumes accumulated dry matter, total N, and free amino acids, with concentrations increasing nearly 3-fold between 0 and 8 DAP (Fig. 7). Likewise, α-amino N content in wheat glumes increases significantly until 5 DAP (Waters *et al.*, 1980). This demonstrates that during the pre-storage phase glumes generate early and intermediary sinks before high endosperm sink strength is established.

Glumes and endosperm display opposed metabolic shifts at the beginning of grain filling

At 8–10 DAP metabolic shifts occurred in glumes, indicated by decreasing dry matter, starch, total N, and most amino acids. At the transcript level this was reflected by downregulated photosynthesis, starch and amino acid biosynthesis, and glycolysis, but upregulated TCA cycle, mETC activities, and transport (Figs 3–5). Endosperm dry weight and starch increased linearly after 8 DAP together with storage-associated/sink-strength-related gene expression such as sucrose and amino acid transporters *HvSUT1*, *HvAAP3*, sucrose synthase, ADP-Glc pyrophosphorylase, and hordeins (Figs 3 and 4). Accordingly, levels of sucrose, glycolytic intermediates,

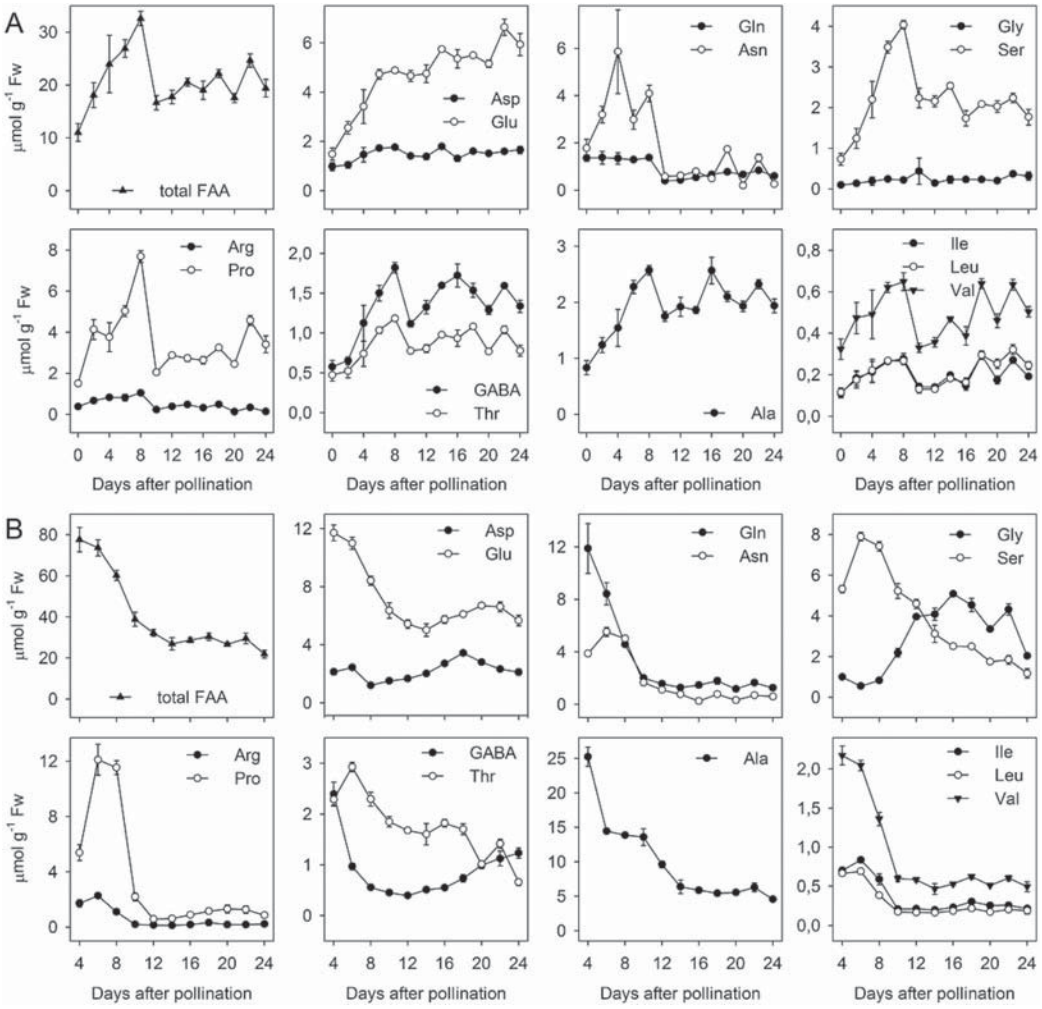

Fig. 7. Concentrations of free amino acids in (A) barley glumes and (B) endosperm during development. Samples were measured via UPLC in 2- day steps from 0 DAP (glumes) and 4 DAP (endosperm), respectively, before data were corrected by internal standard and fresh weight. Each data point represents two (Arg, Gly) or three biological replicates ±SD.

and amino acids were highest at 8–10 DAP in endosperm but decreased in glumes (Fig. 6). To conclude, metabolic shifts implicate opposing trends for central pathways glycolysis, and starch and amino acid biosynthesis, namely downregulation in glumes but upregulation in endosperm at early grain filling.

Glumes undergo transition into remobilizing and exporting organs coinciding with the beginning of storage activity in the endosperm. Phase changes in glumes may be initiated by emerging endosperm sink strength. This is supported by the fact that removal of sink organs generally prevents remobilization and delays senescence. Amino acid concentrations (especially Gln) decrease upon grain filling in wheat flag leaves, but increase in response to ear excision (Peeters and Van Laere, 1994), indicating that grain sink strength induces this drain. Senescence is also delayed by diverse crop manipulations such as inhibiting kernel set in maize and depodding (Miceli *et al.*, 1995; Borrás *et al.*, 2003). Instead, senescence in spinach plants is induced by exhaustive reallocation of nutrients from leaves to flowers (Sklensky and Davies, 2011).

Metabolic transition of glumes occurs in two phases

Gene expression in glumes suggested metabolic transitions at two phases. The first, at around 8 DAP, is consistent with the onset of endosperm storage activity and is probably a consequence of increasing endosperm sink activity. Amino acid profiles in the grain vasculature were highly correlated to those of the endosperm, but differed from glumes (Fig. 8). Although the total amount of free amino acids in the endosperm increased until 18 DAP (data not shown), concentrations of most members decreased during early grain filling. Such depletion might be transmitted via the vasculature and specific amino acids could function as metabolic signals communicating endosperm demand to vegetative organs. Chlorophyll breakdown, regarded as a senescence marker (Hörtensteiner, 2006), did not occur at 8

	Glumes							Vasculature							Endosperm					
	Days after pollination							Days after pollination							Days after pollination					
	4	8	10	14	18	24	$C_{Gl, Vc}$	4	8	10	14	18	24	$C_{Vc, Es}$	4	8	10	14	18	24
Alanine	60	100	68	72	82	75	-0.32	100	67	66	63	49	23	0.89*	100	55	54	25	21	18
Asparagine	100	70	10	14	30	4	0.73	100	95	81	72	49	31	0.81*	77	100	33	15	15	12
Glutamate	57	82	79	97	93	100	-0.88*	100	85	53	37	27	32	0.93*	100	72	54	43	52	48
Glutamine	98	100	29	39	56	43	0.76	100	68	60	54	62	48	0.98*	100	38	17	11	15	11
Isoleucine	72	94	48	67	100	65	0.12	54	100	57	34	18	27	0.61	100	84	29	28	43	31
Leucine	75	91	44	62	100	83	-0.03	69	100	61	44	29	44	0.53	100	58	26	24	33	28
Lysine	100	99	34	49	79	30	0.69	100	81	66	65	45	19	0.09	66	96	38	60	100	55
Phenylalanine	65	100	75	71	90	90	0.09	87	100	68	48	38	54	0.50	100	38	28	28	32	35
Proline	49	100	26	35	42	44	0.66	79	100	55	9	8	10	0.90*	47	100	19	5	10	7
Serine	54	100	55	63	52	44	0.71	87	100	84	70	43	31	0.96*	72	100	70	42	34	16
Threonine	63	100	66	83	92	66	0.10	100	99	81	69	46	29	0.92*	100	100	81	70	74	29
Valine	76	100	51	72	98	77	-0.02	100	98	70	60	38	48	0.84*	100	63	28	21	29	23

Fig. 8. Relative concentrations of free amino acids in barley glumes (Gl), grain vasculature (Vc), and endosperm (Es). Measurements were taken between 4 and 24 DAP using UPLC for glumes and endosperm, with three biological replicates, and using GC-MS for grain vasculature, with eight biological replicates. Concentrations were normalized and colour coded from dark red (low) to dark blue (high) values (see Fig. 6), before Pearson correlation (C) was determined for Vc and Gl and Vc and Es, respectively. Correlations are shown in orange (negative) and green (positive); statistically significant correlations ($P < 0.05$) are marked with an asterisk.

DAP since pheophorbide a oxygenase (PAO) was transcriptionally activated after 14 DAP. Senescence-associated genes, like cysteine proteinase, homologous to *Arabidopsis* SAG12 (Guo and Gan, 2005) and an AtSWEET15 homologue (AtSAG29), a potential sugar exporter and senescence-related protein that accelerates senescence when overexpressed in *Arabidopsis* (Seo *et al.*, 2011), were also not upregulated before 14 DAP. To conclude, developmental senescence in glumes was not initiated before 18 DAP (Fig. 5).

The second phase comprised developmental ageing and senescence denoting later grain filling. At transcript levels it was characterized by a further decrease of photosynthesis, glycolysis, and starch biosynthesis, whereas chlorophyll, lipid, and amino acid degradation increased together with proteolysis, mETC activity, and transport processes. Several genes involved in the final steps of amino acid biosynthesis were steadily downregulated, while others were upregulated, especially at later stages, such as homogentisate 1,2-dioxygenase and pyrroline-5-carboxylate reductase, which are probably engaged in Tyr, Phe, and Pro degradation.

To conclude, upon the first metabolic transition (8 DAP), glumes are converted into remobilizing and transporting organs for assimilates, providing for grain filling. The second transition (18 DAP) assigns developmental ageing and senescence. The period between is the main storage phase. It is obviously important that glumes remain fully functional at this stage. Sequential arrangements reflect the cascades of sink-induced remobilization at 8 DAP and developmental ageing after 14 DAP.

Regulation of glume metabolic transitions

NAC and WRKY transcription factors are frequently involved in signalling senescence (Uauy *et al.*, 2006; Zentgraf *et al.*, 2010; Breeze *et al.*, 2011; Christiansen and Gregersen, 2014). In glumes, three major patterns of upregulation are evident.

HvNAM-1 was upregulated at 8/10 DAP and influences grain protein content (Jamar *et al.*, 2010), while the wheat homologue, TtNAM-1, effects senescence and remobilization in flag leaves (Uauy *et al.*, 2006; Distelfeld *et al.*, 2008). Thus, *HvNAM-1* could be involved in adjusting glume metabolism in response to grain filling. *HvNAC001*, *HvNAC013*, *HvNAC036*, and *HvNAC044* were upregulated after 14 DAP and are induced during leaf senescence (Christiansen *et al.*, 2011). In glumes, these four NACs could initiate chloroplast degeneration, executed by co-induced HvPAO and SAG12-like proteinase. Twenty-one NACs and WRKYs were bi-phasically upregulated between 0 and 8 DAP and after 14 DAP. *HvNAC006* and *HvNAC008* are homologous to *AtORE1* and *AtATAF1*, controlling *Arabidopsis* leaf senescence (Kim *et al.*, 2009; Balazadeh *et al.*, 2010), and initiating early senescence upon overexpression (Kleinow *et al.*, 2009), respectively.

Biosynthesis and signalling of ABA are upregulated during senescence (van der Graaff *et al.*, 2006). *HvNCED3* was continuously upregulated and *HvAAO4* expression increased from 0 to 8 DAP and after 14 DAP, indicating that late steps of ABA biosynthesis are upregulated in glumes. Accordingly, ABA signalling, *HvPKABA1*, and *HvABF1* were bi-phasically upregulated, supporting ABA functions in glume phase transition. JA generally accelerates leaf senescence (Ueda *et al.*, 1981), although mechanisms are still unclear. MeJA induces senescence-associated transcripts *AtSAG12* (Xiao *et al.*, 2004), *AtCLH1*/*CORI1*, and *AtERD1*/*SAG15* (Jung *et al.*, 2007). Enzymes involved in JA biosynthesis, OPRs, lipoxygenases, and the AtOPLC1-homologue, involved in JA-related β-oxidation (Koo *et al.*, 2006), were continuously upregulated in glumes. In contrast to ABA, JA-related transcripts were not bi-phasically upregulated, indicating effects only on age-dependent senescence.

Glume transition from sink to source is accompanied by changed expression of N transporters

Switching from import to remobilization/export requires transport/re-translocation of N. *HvAAP2*, upregulated at 8/10 DAP, is homologous to *AtAAP2*, and involved in *Arabidopsis* xylem-to-phloem transfer and sink N supply (Zhang *et al.*, 2010). NPF-members hv_38962 (array contig) and hv_38267 were also upregulated at 8/10 DAP and are similar to tonoplast-localized AtPTR2/AtNPF8.3, functioning in flowering and seed development (Song *et al.*, 1997), and to plasma membrane-localized AtPTR5/AtNPF8.2, important for peptide transport in seeds (Komarova *et al.*, 2008). These transporters could potentially establish sink strength and intermediate storage in glumes (Fig. 4).

Three putative LHTs were upregulated and potentially involved in amino acid remobilization within glumes (Fig. 4). Their homologues, AtLHT1 and AtLHT2, import amino acids into *Arabidopsis* leaf mesophyll and tapetum cells (Lee and Tegeder, 2004; Hirner *et al.*, 2006). Constantly upregulated NPF transporters hv_29556 and hv_36342 (Fig. 4) could import nitrate into glumes similarly to *Arabidopsis* homologues AtNRT1.4/NPF6.2, which accumulates nitrate in leaf petioles (Chiu *et al.*, 2004), and AtNRT1.8/NPF7.2, involved in xylem unloading (Li *et al.*, 2010).

Four AAPs were upregulated in glumes after 14 DAP (Fig. 4). HvAAP11 is related to AtAAP5, involved in phloem loading (Fischer *et al.*, 1995). Thus, HvAAP11 is probably exporting amino acids during senescence-associated proteolysis in glumes. HvAAP10 is homologous to AtAAP6, involved in xylem-to-phloem transfer (Okumoto *et al.*, 2002). HvAAP10 probably relocates amino acids to vascular tissue and developing grains.

NPF-like transporters hv_29548 and hv_13110 were upregulated only after 14 DAP. Corresponding *Arabidopsis* homologues AtNRT1.5/NPF7.3 and AtNRT1.11/NPF1.2 are involved in xylem loading (Lin *et al.*, 2008) and xylem-to-phloem transfer of nitrate (Hsu and Tsay, 2013), respectively. These transporters could translocate nitrate in glumes.

Putative amino acid exporters *HvBAT3* and *HvSIAR1-like* were opposingly expressed (Fig. 4). *HvBAT3*, downregulated after 10 DAP, is homologous to *AtBAT1*, putatively involved in sink phloem unloading (Dündar and Bush, 2009). *HvSIAR1-like*, upregulated after 14 DAP, is homologous to *AtSIAR1*, and involved in amino acid remobilization and homoeostasis of *Arabidopsis* leaves (Ladwig *et al.*, 2012). Switching activities of *HvBAT3* and *HvSIAR1-like* could reflect the transition of glumes from sink to source.

HvOPT6, with unique expression among oligopeptide transporters, was downregulated at 4 DAP and upregulated after 14 DAP, and is homologous to glutathione transporter *OsGT1* (Zhang *et al.*, 2004), suggesting combined N and sulphur remobilization.

Glume-specific remobilization of assimilates and resources

Gene expression and metabolite profiles indicate glume-specific mechanisms of assimilate conversion and translocation towards grains. Induced L-alanine:2-oxoglutarate aminotransferase (Ala:OG-AT) and GS1 together may convert Ala by Ala:OG-AT to Glu and further to Gln by GS1 using amino groups from protein/amino acid degradation. Gln could then either be exported or converted to Asn by Gln-ASN, one of the most upregulated genes at 24 DAP (150-fold). This would mobilize N as Asn at the expense of Ala and amino N. Gln-ASN is important for remobilizing N during senescence of *Medicago truncatula* leaves (De Michele *et al.*, 2009). In rice and tobacco, Gln-ASN is located in vascular tissues (Gaufichon *et al.*, 2010). Assuming such a location in glumes suggests that Asn is preferentially synthesized in vascular tissue for export (Fig. 9A). Accordingly, levels of Ala and Glu remain high in glumes during grain filling, whereas Asn decreases 5-fold with similar profiles in glumes, vasculature, and endosperm.

Cystathionine-γ-synthase (CGS), involved in Met biosynthesis (Hacham *et al.*, 2013), was upregulated at 24 DAP in glumes (100-fold) together with serine acetyl transferase (SAT) and cysteine synthase (OAS1), involved in Cys biosynthesis from Ser. Upregulated Cys and Met biosynthesis contributes to possible conversion of amino N from Ser, Asp, and sulphur to phloem-mobile *S*-methyl-methionine (SMM), (Bourgis *et al.*, 1999). The pathway (Fig. 9B), involves additional enzymes, like aspartate kinase and methionine-*S*-methyltransferase, which were also upregulated in glumes. Similar mechanisms are suggested for synthesis and transport of SMM within barley nucellar projections to translocate reduced sulphur from senescing tissue into endosperm (Thiel *et al.*, 2009).

Differential transcription indicated degradation of phospholipids by phosphatidylcholine phospholipase D and glycero-*P*-diesterase, in glumes already at 8 DAP, together with biosynthesis of long-chain fatty acids by acyl-activating enzyme and very-long-chain fatty acid-condensing enzyme. However, degradation of mono- and triacylglycerides (TCGs) did not occur before 18 DAP, indicated by upregulated mono- and triacylglycerol lipases. These processes are probably involved in mobilizing C from membrane lipids into phloem-mobile sucrose (Kaup *et al.*, 2002; Troncoso-Ponce *et al.*, 2013). To conclude, in glumes, phospholipids from chloroplasts are degraded early, accompanied by *de novo* biosynthesis of TCGs. Accordingly, levels of stearate and palmitate increased in glumes (Fig. 6). During developmental senescence TCGs are degraded and C is converted to phloem-mobile sucrose or respired by mETC. Alternatively, acetyl-CoA could be converted into amino acids and to SMM for export (Fig. 9B).

In glumes, mitochondrial metabolism was upregulated at early grain filling involving TCA cycle activity, mETC, and ATP synthesis and transport, consistent with increased levels of citrate, isocitrate, and succinate. As expected, most ATP generated in mitochondria is needed to energize transport of sugars, amino acids, and peptides. Accordingly, respective transporters were co-induced (Fig. 4). Similarly, in senescing *Arabidopsis* leaves, mitochondrial respiration has to supply ATP and C skeletons to redistribute N (Hörtensteiner and Feller, 2002). Several mitochondrial genes were only upregulated later on, involving respiration and mETC (cytochrome c oxidase, electron transfer flavoprotein, NADH dehydrogenase) and energy dissipation (alternative oxidase). These genes are probably involved in developmental senescence and amino acid degradation, also upregulated at the transcript level at

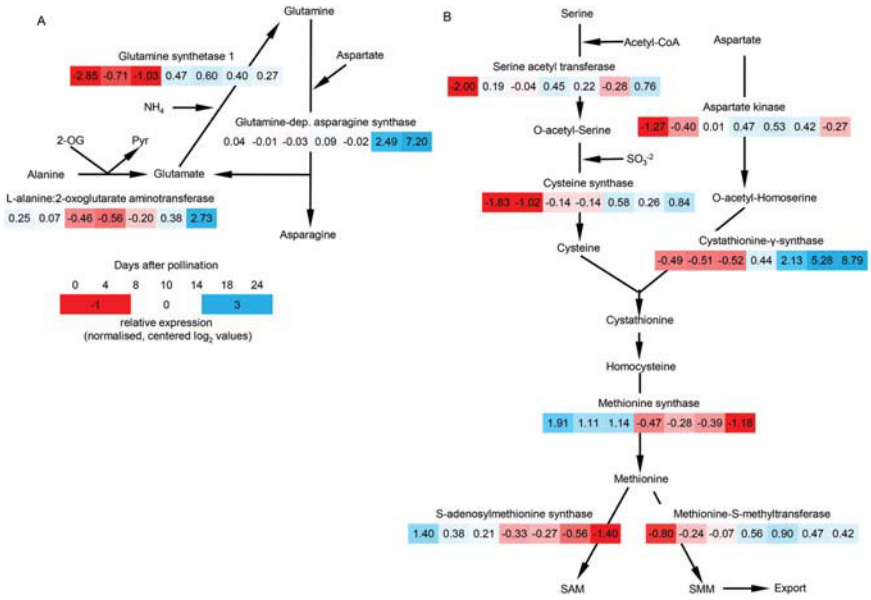

Fig. 9. Possible glume-specific mechanisms for remobilization of N and S. This shows conversion of alanine by Ala:OG-AT to glutamate and further to glutamine by GS1 using amino groups from protein/amino acid degradation (A) and conversion of amino N from serine, aspartate, and sulphur into the phloem-mobile SMM (B). Normalized, relative expression values are presented and colour coded from low (dark red) to high (dark blue) expression.

24 DAP. Mitochondrial alternative oxidase could balance senescence-related stress responses from excess degradation of sugars and/or amino acids as shown in legume embryos with perturbed metabolism (Gregersen and Holm, 2007; Weigelt *et al.*, 2008; Weigelt *et al.*, 2009; Araújo *et al.*, 2014).

Our results show that development of barley glumes after anthesis is separated into three phases associated with grain development, and these mark the transition from sink to source tissue. Until 8 DAP, glumes are growing and photosynthetically active tissues accumulating dry weight, total N, and free amino acids. Furthermore, decreasing levels of starch and glycolytic metabolites as well as the corresponding transcripts are observed. Between 8 and 10 DAP, coinciding with the beginning of storage protein synthesis in grains, total N and free amino acids decrease significantly, which probably represents relocation of nutrients to meet the demands of developing grains. Concentrations of free amino acids in endosperm and grain vasculature decrease at this stage, which could signal increasing N demand to glumes and trigger remobilization. Accordingly, expression of specific transporters in glumes is upregulated together with enzymes from the TCA cycle and mETC providing energy for transport. After 18 DAP, glumes undergo developmental ageing and senescence, involving chlorophyll degradation by PAO, specific proteases, and N transporters. Transition between these phases is probably governed by transcription factors from the NAC and WRKY families and influenced by ABA.

Supplementary material

Supplementary data can be found at *JXB* online.

Supplementary Table 1. Profiles for dry weight, total N, and starch.

Supplementary Table 2. Differentially expressed transcripts in glumes.

Supplementary Table 3. Differentially expressed transcripts in endosperm.

Supplementary Table 4. Differentially expressed N transporters in glumes.

Supplementary Table 5. Differentially expressed N transporters in endosperm.

Supplementary Table 6. Metabolite profiles (GC-MS) in glumes and endosperm.

Supplementary Table 7. Amino acid profiles (UPLC) in glumes and endosperm.

Supplementary Table 8. Metabolite profiles (GC-MS) in grain vasculature.

Supplementary Figure 1. Light microscopic images showing micro-dissection of vascular tissue.

Funding

This work was supported by the Deutsche Forschungsgemeinschaft (DFG) in the frame of Research Group 948: Nitrogen uptake, metabolism, and remobilization in leaves during plant senescence (Grant Number: WE 1641/13-2)

Acknowledgements

The authors want to thank Angela Stegmann, Elsa Fessel, Uta Siebert, Franka Andersch, Heiko Weichert, and Andrea Apelt at IPK Gatersleben, as well as Ines Fehrle at MPI Golm, for their excellent technical assistance.

References

Altschul SF, Gish W, Miller W, Myers EW, Lipman DJ. 1990. Basic local alignment search tool. *Journal of Molecular Biology* **215,** 403–410.

Araújo W, Nunes-Nesi A, Fernie A. 2014. On the role of plant mitochondrial metabolism and its impact on photosynthesis in both optimal and sub-optimal growth conditions. *Photosynthesis Research* **119,** 141–156.

Balazadeh S, Siddiqui H, Allu AD, Matallana-Ramirez LP, Caldana C, Mehrnia M, Zanor M-I, Köhler B, Mueller-Roeber B. 2010. A gene regulatory network controlled by the NAC transcription factor ANAC092/AtNAC2/ORE1 during salt-promoted senescence. *The Plant Journal* **62,** 250–264.

Borrás L, Maddonni GA, Otegui ME. 2003. Leaf senescence in maize hybrids: plant population, row spacing and kernel set effects. *Field Crops Research* **82,** 13–26.

Bourgis F, Roje S, Nuccio ML, *et al.* 1999 S-methylmethionine plays a major role in phloem sulfur transport and is synthesized by a novel type of methyltransferase. *The Plant Cell* **11,** 1485–1498.

Breeze E, Harrison E, McHattie S, *et al*. 2011. High-resolution temporal profiling of transcripts during Arabidopsis leaf senescence reveals a distinct chronology of processes and regulation. *The Plant Cell* **23,** 873–894.

Chen L-Q, Qu X-Q, Hou B-H, Sosso D, Osorio S, Fernie AR, Frommer WB. 2012. Sucrose efflux mediated by SWEET proteins as a key step for phloem transport. *Science* **335,** 207–211.

Chiu C-C, Lin C-S, Hsia A-P, Su R-C, Lin H-L, Tsay Y-F. 2004. Mutation of a nitrate transporter, AtNRT1:4, results in a reduced petiole nitrate content and altered leaf development. *Plant and Cell Physiology* **45,** 1139–1148.

Christiansen M, Holm P, Gregersen P. 2011. Characterization of barley (*Hordeum vulgare L*.) NAC transcription factors suggests conserved functions compared to both monocots and dicots. *BMC Research Notes* **4,** 302.

Christiansen MW, Gregersen PL. 2014. Members of the barley NAC transcription factor gene family show differential co-regulation with senescence-associated genes during senescence of flag leaves. *Journal of Experimental Botany* **65,** 4009–4022.

Conesa A, Götz S, García-Gómez JM, Terol J, Talón M, Robles M. 2005. Blast2GO: a universal tool for annotation, visualization and analysis in functional genomics research. *Bioinformatics* **21,** 3674–3676.

De Michele R, Formentin E, Todesco M, *et al*. 2009. Transcriptome analysis of *Medicago truncatula* leaf senescence: similarities and differences in metabolic and transcriptional regulations as compared with Arabidopsis, nodule senescence and nitric oxide signalling. *New Phytologist* **181,** 563–575.

Distelfeld A, Korol A, Dubcovsky J, Uauy C, Blake T, Fahima T. 2008. Colinearity between the barley grain protein content (GPC) QTL on chromosome arm 6HS and the wheat Gpc-B1 region. *Molecular Breeding* **22,** 25–38.

Dündar E. 2009. Multiple GUS expression patterns of a single Arabidopsis gene. *Annals of Applied Biology* **154,** 33–41.

Dündar E, Bush D. 2009. BAT1, a bidirectional amino acid transporter in *Arabidopsis*. *Planta* **229,** 1047–1056.

Fischer AM. 2012. The complex regulation of senescence. *Critical Reviews in Plant Sciences* **31,** 124–147.

Fischer W-N, Kwart M, Hummel S, Frommer WB. 1995. Substrate specificity and expression profile of amino acid transporters (AAPs) in Arabidopsis. *The Journal of Biological Chemistry* **270,** 16315–16320.

Gaufichon L, Reisdorf-Cren M, Rothstein SJ, Chardon F, Suzuki A. 2010. Biological functions of asparagine synthetase in plants. *Plant Science* **179,** 141–153.

Geßler A, Schultze M, Schrempp S, Rennenberg H. 1998. Interaction of phloem-translocated amino compounds with nitrate net uptake by the roots of beech (*Fagus sylvatica*) seedlings. *Journal of Experimental Botany* **49,** 1529–1537.

Gregersen PL, Holm PB. 2007. Transcriptome analysis of senescence in the flag leaf of wheat (*Triticum aestivum L*.). *Plant Biotechnology Journal* **5,** 192–206.

Grundbacher FJ. 1963. The physiological function of the cereal awn. *Botanical Review* **29,** 366–381.

Guo Y, Gan S. 2005. Leaf senescence: signals, execution, and regulation. *Current Topics in Developmental Biology* **71,** 83–112.

Hacham Y, Matityahu I, Amir R. 2013. Light and sucrose up-regulate the expression level of Arabidopsis cystathionine γ-synthase, the key enzyme of methionine biosynthesis pathway. *Amino Acids* **45,** 1179–1190.

Hirel B, Le Gouis J, Ney B, Gallais A. 2007. The challenge of improving nitrogen use efficiency in crop plants: towards a more central role for genetic variability and quantitative genetics within integrated approaches. *Journal of Experimental Botany* **58,** 2369–2387.

Hirner A, Ladwig F, Stransky H, Okumoto S, Keinath M, Harms A, Frommer WB, Koch W. 2006. Arabidopsis LHT1 is a high-affinity transporter for cellular amino acid uptake in both root epidermis and leaf mesophyll. *The Plant Cell Online* **18,** 1931–1946.

Hirner B, Fischer WN, Rentsch D, Kwart M, Frommer WB. 1998. Developmental control of H+/amino acid permease gene expression during seed development of Arabidopsis. *The Plant Journal* **14,** 535–544.

Hollmann J, Gregersen PL, Krupinska K. 2014. Identification of predominant genes involved in regulation and execution of senescence-associated nitrogen remobilization in flag leaves of field grown barley. *Journal of Experimental Botany* **65,** 3963–3973.

Hörtensteiner S. 2006. Chlorophyll degradation during senescence. *Annual Review of Plant Biology* **57,** 55–77.

Hörtensteiner S, Feller U. 2002. Nitrogen metabolism and remobilization during senescence. *Journal of Experimental Botany* **53,** 927–937.

Hsu P-K, Tsay Y-F. 2013. Two phloem nitrate transporters, NRT1.11 and NRT1.12, are important for redistributing xylem-borne nitrate to enhance plant growth. *Plant Physiology* **163,** 844–856.

Jamar C, Loffet F, Frettinger P, Ramsay L, Fauconnier M-L, du Jardin P. 2010. NAM-1 gene polymorphism and grain protein content in *Hordeum*. *Journal of Plant Physiology* **167,** 497–501.

Jibran R, Hunter D, Dijkwel P. 2013. Hormonal regulation of leaf senescence through integration of developmental and stress signals. *Plant Molecular Biology* **82,** 547–561.

Jung C, Lyou S, Yeu S, Kim M, Rhee S, Kim M, Lee J, Choi Y, Cheong J-J. 2007. Microarray-based screening of jasmonate-responsive genes in *Arabidopsis thaliana*. *Plant Cell Reports* **26,** 1053–1063.

Junker B, Klukas C, Schreiber F. 2006. VANTED: A system for advanced data analysis and visualization in the context of biological networks. *BMC Bioinformatics* **7,** 109.

Kaup MT, Froese CD, Thompson JE. 2002. A role for diacylglycerol acyltransferase during leaf senescence. *Plant Physiology* **129,** 1616–1626.

Kim JH, Woo HR, Kim J, Lim PO, Lee IC, Choi SH, Hwang D, Nam HG. 2009. Trifurcate feed-forward regulation of age-dependent cell death involving miR164 in Arabidopsis. *Science* **323,** 1053–1057.

Kleinow T, Himbert S, Krenz B, Jeske H, Koncz C. 2009. NAC domain transcription factor ATAF1 interacts with SNF1-related kinases and silencing of its subfamily causes severe developmental defects in Arabidopsis. *Plant Science* **177,** 360–370.

Kohl S, Hollmann J, Blattner F, *et al*. 2012. A putative role for amino acid permeases in sink-source communication of barley tissues uncovered by RNA-seq. *BMC Plant Biology* **12,** 154.

Komarova NY, Thor K, Gubler A, Meier S, Dietrich D, Weichert A, Suter Grotemeyer M, Tegeder M, Rentsch D. 2008. AtPTR1 and AtPTR5 transport dipeptides in planta. *Plant Physiology* **148,** 856–869.

Koo AJ, Chung HS, Kobayashi Y, Howe GA. 2006. Identification of a peroxisomal acyl-activating enzyme involved in the biosynthesis of jasmonic acid in Arabidopsis. *The Journal of Biological Chemistry* **281,** 33511–33520.

Ladwig F, Stahl M, Ludewig U, Hirner AA, Hammes UZ, Stadler R, Harter K, Koch W. 2012. Siliques are Red1 from Arabidopsis acts as a bidirectional amino acid transporter that is crucial for the amino acid homeostasis of siliques. *Plant Physiology* **158,** 1643–1655.

Lee Y-H, Tegeder M. 2004. Selective expression of a novel high-affinity transport system for acidic and neutral amino acids in the tapetum cells of Arabidopsis flowers. *The Plant Journal* **40,** 60–74.

Li J-Y, Fu Y-L, Pike SM, *et al*. 2010. The Arabidopsis nitrate transporter NRT1.8 functions in nitrate removal from the xylem sap and mediates cadmium tolerance. *The Plant Cell Online* **22,** 1633–1646.

Lin S-H, Kuo H-F, Canivenc G, *et al*. 2008. Mutation of the Arabidopsis NRT1.5 nitrate transporter causes defective root-to-shoot nitrate transport. *The Plant Cell Online* **20,** 2514–2528.

Lopes M, Cortadellas N, Kichey T, Dubois F, Habash D, Araus J. 2006. Wheat nitrogen metabolism during grain filling: comparative role of glumes and the flag leaf. *Planta* **225,** 165–181.

Lyons R, Manners JM, Kazan K. 2013. Jasmonate biosynthesis and signaling in monocots: a comparative overview. *Plant Cell Reports* **32,** 815–827.

Matsumoto T, Tanaka T, Sakai H, *et al*. 2011. Comprehensive sequence analysis of 24,783 barley full-length cDNAs derived from 12 clone libraries. *Plant Physiology* **156,** 20–28.

Miceli F, Crafts-Brandner SJ, Egli DB. 1995. Physical restriction of pod growth alters development of soybean plants. *Crop Science* **35,** 1080–1085.

Mulangi V, Phuntumart V, Aouida M, Ramotar D, Morris P. 2012. Functional analysis of *OsPUT1*, a rice polyamine uptake transporter. *Planta* **235,** 1–11.

Noh Y-S, Amasino R. 1999. Identification of a promoter region responsible for the senescence-specific expression of SAG12. *Plant Molecular Biology* **41,** 181–194.

Okumoto S, Schmidt R, Tegeder M, Fischer WN, Rentsch D, Frommer WB, Koch W. 2002. High affinity amino acid transporters specifically expressed in xylem parenchyma and developing seeds of Arabidopsis. *The Journal of Biological Chemistry* **277,** 45338–45346.

Peeters KMU, Van Laere AJ. 1994. Amino acid metabolism associated with N-mobilization from the flag leaf of wheat (*Triticum aestivum* L.) during grain development. *Plant, Cell and Environment* **17,** 131–141.

Riewe D, Koohi M, Lisec J, Pfeiffer M, Lippmann R, Schmeichel J, Willmitzer L, Altmann T. 2012. A tyrosine aminotransferase involved in tocopherol synthesis in Arabidopsis. *The Plant Journal* **71,** 850–859.

Sanders A, Collier R, Trethewy A, Gould G, Sieker R, Tegeder M. 2009. AAP1 regulates import of amino acids into developing Arabidopsis embryos. *The Plant Journal* **59,** 540–552.

Schmidt R, Stransky H, Koch W. 2007. The amino acid permease AAP8 is important for early seed development in *Arabidopsis thaliana*. *Planta* **226,** 805–813.

Schoonheim PJ, Costa Pereira DD, De Boer AH. 2009. Dual role for 14-3-3 proteins and ABF transcription factors in gibberellic acid and abscisic acid signalling in barley (*Hordeum vulgare*) aleurone cells. *Plant, Cell and Environment* **32,** 439–447.

Seo PJ, Park JM, Kang SK, Kim SG, Park CM. 2011. An Arabidopsis senescence-associated protein SAG29 regulates cell viability under high salinity. *Planta* **233,** 189–200.

Simpson RJ, Lambers H, Dalling MJ. 1983. Nitrogen redistribution during grain growth in wheat (*Triticum aestivum L.*): IV. Development of a quantitative model of the translocation of nitrogen to the grain. *Plant Physiology* **71,** 7–14.

Sklensky DE, Davies PJ. 2011. Resource partitioning to male and female flowers of *Spinacia oleracea L.* in relation to whole-plant monocarpic senescence. *Journal of Experimental Botany* **62,** 4323–4336.

Song W, Koh S, Czako M, Marton L, Drenkard E, Becker JM, Stacey G. 1997. Antisense expression of the peptide transport gene AtPTR2-B delays flowering and arrests seed development in transgenic Arabidopsis plants. *Plant Physiology* **114,** 927–935.

Sreenivasulu N, Altschmied L, Radchuk V, Gubatz S, Wobus U, Weschke W. 2004. Transcript profiles and deduced changes of metabolic pathways in maternal and filial tissues of developing barley grains. *The Plant Journal* **37,** 539–553.

Tegeder M. 2012. Transporters for amino acids in plant cells: some functions and many unknowns. *Current Opinion in Plant Biology* **15,** 315–321.

Tegeder M, Rentsch D. 2010. Uptake and partitioning of amino acids and peptides. *Molecular Plant*. **3,** 997–1011.

Thiel J, Hollmann J, Rutten T, Weber H, Scholz U, Weschke W. 2012*a*. 454 Transcriptome sequencing suggests a role for two-component signalling in cellularization and differentiation of barley endosperm transfer cells. *PLoS ONE* **7,** e41867.

Thiel J, Müller M, Weschke W, Weber H. 2009. Amino acid metabolism at the maternal–filial boundary of young barley seeds: a microdissection-based study. *Planta* **230,** 205–213.

Thiel J, Riewe D, Rutten T, Melzer M, Friedel S, Bollenbeck F, Weschke W, Weber H. 2012*b*. Differentiation of endosperm transfer cells of barley: a comprehensive analysis at the micro-scale. *The Plant Journal* **71,** 639–655.

Thimm O, Bläsing O, Gibon Y, Nagel A, Meyer S, Krüger P, Selbig J, Müller LA, Rhee SY, Stitt M. 2004. Mapman: a user-driven tool to display genomics data sets onto diagrams of metabolic pathways and other biological processes. *The Plant Journal* **37,** 914–939.

Troncoso-Ponce MA, Cao X, Yang Z, Ohlrogge JB. 2013. Lipid turnover during senescence. *Plant Science* **205–206,** 13–19.

Uauy C, Distelfeld A, Fahima T, Blechl A, Dubcovsky J. 2006. A NAC gene regulating senescence improves grain protein, zinc, and iron content in wheat. *Science* **314,** 1298–1301.

Ueda J, Kato J, Yamane H, Takahashi N. 1981. Inhibitory effect of methyl jasmonate and its related compounds on kinetin-induced retardation of oat leaf senescence. *Physiologia Plantarum* **52,** 305–309.

van der Graaff E, Schwacke R, Schneider A, Desimone M, Flügge U-I, Kunze R. 2006. Transcription analysis of Arabidopsis membrane transporters and hormone pathways during developmental and induced leaf senescence. *Plant Physiology* **141,** 776–792.

Vidmar JJ, Zhuo D, Siddiqi MY, Schjoerring JK, Touraine B, Glass ADM. 2000. Regulation of high-affinity nitrate transporter genes and high-affinity nitrate influx by nitrogen pools in roots of barley. *Plant Physiology* **123,** 307–318.

Watanabe M, Balazadeh S, Tohge T, Erban A, Giavalisco P, Kopka J, Mueller-Roeber B, Fernie AR, Hoefgen R. 2013. Comprehensive dissection of spatiotemporal metabolic shifts in primary, secondary, and lipid metabolism during developmental senescence in Arabidopsis. *Plant Physiology* **162,** 1290–1310.

Waters SP, Peoples MB, Simpson RJ, Dalling MJ. 1980. Nitrogen redistribution during grain growth in wheat (*Triticum aestivum* L.) I. Peptide hydrolase activity and protein breakdown. *Planta* **148,** 422–428.

Weichert N, Saalbach I, Weichert H, *et al*. 2010. Increasing sucrose uptake capacity of wheat grains stimulates storage protein synthesis. *Plant Physiology* **152,** 698–710.

Weigelt K, Küster H, Radchuk R, Müller M, Weichert H, Fait A, Fernie AR, Saalbach I, Weber H. 2008. Increasing amino acid supply in pea embryos reveals specific interactions of N and C metabolism, and highlights the importance of mitochondrial metabolism. *The Plant Journal* **55,** 909–926.

Weigelt K, Küster H, Rutten T, *et al*. 2009. ADP-glucose pyrophosphorylase-deficient pea embryos reveal specific transcriptional and metabolic changes of carbon-nitrogen metabolism and stress responses. *Plant Physiology* **149,** 395–411.

Weschke W, Panitz R, Sauer N, Wang Q, Neubohn B, Weber H, Wobus U. 2000. Sucrose transport into barley seeds: molecular characterization of two transporters and implications for seed development and starch accumulation. *The Plant Journal* **21,** 455–467.

West CE, Waterworth WM, Stephens SM, Smith CP, Bray CM. 1998. Cloning and functional characterisation of a peptide transporter expressed in the scutellum of barley grain during the early stages of germination. *The Plant Journal* **15,** 221–229.

Xiao S, Dai L, Liu F, Wang Z, Peng W, Xie D. 2004. COS1: An Arabidopsis coronatine insensitive1 suppressor essential for regulation of jasmonate-mediated plant defense and senescence. *The Plant Cell Online* **16,** 1132–1142.

Yamauchi D, Zentella R, Ho T-H. 2002. Molecular analysis of the barley (*Hordeum vulgare L.*) gene encoding the protein kinase PKABA1 capable of suppressing gibberellin action in aleurone layers. *Planta* **215,** 319–326.

Zentgraf U, Laun T, Miao Y. 2010. The complex regulation of WRKY53 during leaf senescence of *Arabidopsis thaliana*. *European Journal of Cell Biology* **89,** 133–137.

Zhang L, Tan Q, Lee R, Trethewy A, Lee Y-H, Tegeder M. 2010. Altered Xylem-Phloem transfer of amino acids affects metabolism and leads to increased seed yield and oil content in Arabidopsis. *The Plant Cell Online* **22,** 3603–3620.

Zhang M-Y, Bourbouloux A, Cagnac O, Srikanth CV, Rentsch D, Bachhawat AK, Delrot S. 2004. A novel family of transporters mediating the transport of glutathione derivatives in plants. *Plant Physiology* **134,** 482–491.

Zhao Q, Nakashima J, Chen F, Yin Y, Fu C, Yun J, Shao H, Wang X, Wang ZY, Dixon RA. 2013. Laccase is necessary and nonredundant with peroxidase for lignin polymerization during vascular development in Arabidopsis. *The Plant Cell* **25,** 3976–3987.

Increasing Sucrose Uptake Capacity of Wheat Grains Stimulates Storage Protein Synthesis[1][W]

Nicola Weichert, Isolde Saalbach, Heiko Weichert, Stefan Kohl, Alexander Erban, Joachim Kopka, Bettina Hause, Alok Varshney, Nese Sreenivasulu, Marc Strickert, Jochen Kumlehn, Winfriede Weschke, and Hans Weber*

Leibniz-Institut für Pflanzengenetik und Kulturpflanzenforschung, D–06466 Gatersleben, Germany (N.W., I.S., H.W., S.K., A.V., N.S., M.S., J.K., W.W., H.W.); Max-Planck-Institut für Molekulare Pflanzenphysiologie, D–14476 Potsdam-Golm, Germany (A.E., J.K.); and Leibniz-Institut für Pflanzenbiochemie, D–06120 Halle (Saale), Germany (B.H.)

Increasing grain sink strength by improving assimilate uptake capacity could be a promising approach toward getting higher yield. The barley (*Hordeum vulgare*) sucrose transporter HvSUT1 (SUT) was expressed under control of the endosperm-specific Hordein B1 promoter (HO). Compared with the wild type, transgenic HOSUT grains take up more sucrose (Suc) in vitro, showing that the transgene is functional. Grain Suc levels are not altered, indicating that Suc fluxes are influenced rather than steady-state levels. HOSUT grains have increased percentages of total nitrogen and prolamins, which is reflected in increased levels of phenylalanine, tyrosine, tryptophan, isoleucine, and leucine at late grain development. Transcript profiling indicates specific stimulation of prolamin gene expression at the onset of storage phase. Changes in gene expression and metabolite levels related to carbon metabolism and amino acid biosynthesis suggest deregulated carbon-nitrogen balance, which together indicate carbon sufficiency and relative depletion of nitrogen. Genes, deregulated together with prolamin genes, might represent candidates, which respond positively to assimilate supply and are related to sugar-starch metabolism, cytokinin and brassinosteroid functions, cell proliferation, and sugar/abscisic acid signaling. Genes showing inverse expression patterns represent potential negative regulators. It is concluded that HvSUT1 overexpression increases grain protein content but also deregulates the metabolic status of wheat (*Triticum aestivum*) grains, accompanied by up-regulated gene expression of positive and negative regulators related to sugar signaling and assimilate supply. In HOSUT grains, alternating stimulation of positive and negative regulators causes oscillatory patterns of gene expression and highlights the capacity and great flexibility to adjust wheat grain storage metabolism in response to metabolic alterations.

The protein content of wheat (*Triticum aestivum*) grains is a crucial determinant of bread and pasta quality and as such is an important economic factor. Breeding for high protein content is a main goal of wheat breeders. However, this seems to be difficult because of the well-known negative correlation between yield and grain protein content (Simmonds, 1995; Sinclair, 1998; Barneix, 2007). Because of the high starch levels of wheat grains, this compound is nearly exclusively yield determinant. Moreover, the required carbon costs per gram of seed yield is lower for starch than for protein, given that seed protein production is energetically more expensive (Vertregt and de Vries, 1987).

There is ample evidence that wheat grains grow under saturated assimilate supply, indicating that yield is mainly sink limited. Thus, grain sink strength seems to be a critical yield-limiting factor (Borrás et al., 2003; Reynolds et al., 2009). It is anticipated that modulating the balance between source and sink may result in increased yield (Reynolds et al., 2009).

Grain filling is largely dependent on assimilate supply and metabolic regulation (Weber et al., 1997b, 2005). Seeds take up Suc and nitrogen in the form of amino acids from the apoplast surrounding the filial tissue (Weber et al., 2005). While seed storage protein biosynthesis is in general dependent on nitrogen in pea (*Pisum sativum*), soybean (*Glycine max*), maize (*Zea mays*), and barley (*Hordeum vulgare*; Balconi et al., 1991; Müller and Knudsen, 1993; Salon et al., 2001; Hernández-Sebastià et al., 2005), Suc also has specific functions as a transport and nutrient sugar and as a signal molecule (Smeekens, 2000; Koch, 2004). In legume cotyledons and barley endosperm, Suc level increases at the onset of maturation, marks the switch from maternal to filial control of seed growth, and is associated with maturation (Weber et al., 2005). Suc is taken up by transporters within epidermal/endospermal transfer cells and is degraded by Suc synthase and invertases toward starch production (Weber et al., 1997a; Tegeder

[1] This work was supported by the Federal Ministry of Education and Research (grant nos. 0310610 and 0310638A) and the Ministry for Cultural Affairs (grant no. 0045KL/0805T).

* Corresponding author; e-mail weber@ipk-gatersleben.de.

The author responsible for distribution of materials integral to the findings presented in this article in accordance with the policy described in the Instructions for Authors (www.plantphysiol.org) is: Hans Weber (weber@ipk-gatersleben.de).

[W] The online version of this article contains Web-only data.
www.plantphysiol.org/cgi/doi/10.1104/pp.109.150854

et al., 1999; Weschke et al., 2000). Three Suc transporter genes are expressed in the developing grain of hexaploid wheat (Aoki et al., 2002). Although gene expression was detected in the maternal nucellar projection, in the filial aleurone/subaleurone transfer cells it has been suggested that Suc transport is restricted only to filial tissues (Bagnall et al., 2000). In legume and barley seeds, Suc induces storage-associated gene expression at the transcript level and up-regulates enzymes like Suc synthase and ADP-Glc pyrophosphorylase (Heim et al., 1993; Weber et al., 1998; Weschke et al., 2000). In legume seeds, Suc feeding disrupts the meristematic state, induces cell expansion and endopolyploidization (Weber et al., 1996), and promotes cotyledonary storage activity at the transcript level (Ambrose et al., 1987; Corke et al., 1990). In Arabidopsis (*Arabidopsis thaliana*), Suc induces a number of storage-related genes, among them oleosins, 2S and 12S globulins, as well as *leafy cotyledon* (*Lec*)- and *fusca* (*Fus*)-like transcription factors (Tsukagoshi et al., 2007). Seed protein content is partially regulated by increased availability of carbon acceptors in the form of organic acids (Miflin and Lea, 1977), which indicates general carbon limitation for amino acid/seed protein synthesis (Weigelt et al., 2008). Taken together, Suc initiates maturation, signals the transition into the storage mode, thereby acting on transcriptional and metabolic levels, and is thus a key player within the regulatory network controlling seed maturation (Weber et al., 2005).

We have previously shown that overexpression of an amino acid permease, VfAAP1, in pea embryos increases amino acid supply and total seed nitrogen and protein content but leads to deregulation of carbon-nitrogen balance (Weigelt et al., 2008). Moreover, Suc transporter overexpression in pea cotyledons also increases seed proteins (Rosche et al., 2002, 2005). The rate-limiting role of Suc transporters has been shown for rice (*Oryza sativa*). Here, suppression of OsSUT1 reduces grain starch and leads to a wrinkled phenotype (Scofield et al., 2002).

Here, we present an in-depth analysis of wheat lines overexpressing the barley Suc transporter HvSUT1 (Weschke et al., 2000) under the control of an endosperm-specific promoter using phenotypical analysis together with combined transcript and metabolite profiling. The aims of this study were 2-fold: first, to evaluate the potential of improved Suc uptake capacity on wheat grain quality and yield; second, to analyze assimilate and sugar effects on grain storage metabolism. The most pronounced finding was an increase of individual grain protein content, especially of prolamins. Suc transporter overexpression obviously modified metabolic flux potential, with only subtle changes of metabolite steady-state concentrations. Such an effect could be important during specific stages when Suc uptake becomes limited due to insufficient activity of endogenous transporter. On the other hand, HvSUT1-overexpression deregulates the metabolic status of wheat grains. We found that such metabolic alterations can effectively be balanced by activation of different signaling components, having the capacity to adjust grain storage metabolism in response to metabolic alterations and showing high flexibility of wheat grain storage.

RESULTS

Generation of Wheat Lines Overexpressing HvSUT1 in the Grain

The cDNA of the barley Suc transporter HvSUT1 (Weschke et al., 2000) was fused to the Hordein B1 promoter (HO; Heim et al., 1995), which is highly active in maturing cereal endosperm. Wheat transformation was performed by biolistic (Varshney and Altpeter, 2001) and *Agrobacterium tumefaciens*-mediated (Hensel et al., 2009) gene transfer. Three independent, PCR-positive homozygous lines (HOSUT10, -11, and -20) were chosen and analyzed by Southern hybridization for copy number. Compared with wild-type wheat, one or two additional bands appear in lines HOSUT11, -20, and -10, indicating single insertions (Fig. 1A). Quantitative reverse transcription (RT)-PCR revealed similar transgene expression in grains of all three lines, with increasing levels between 6 and 14 d after fertilization (DAF), a plateau phase between 14 and 18 DAF, and a further increase from 18 to 26 DAF (Fig. 1B). Overexpression of HvSUT1 is directed to endosperm cells, which are normally not engaged in Suc uptake. Suc uptake is mediated by a SUT within the modified aleurone/subaleurone transfer cells (Bagnall et al., 2000). Levels of total nitrogen were found to be increased in mature seeds of all three homozygous lines of the T2 (HOSUT11 and -20) and T4 (HOSUT10) generations by 5% to 13% compared with the wild type. Thousand grain weight was significantly increased for HOSUT20 and -10 (Fig. 1C). Levels of starch were not different on a per gram basis (data not shown).

HvSUT1 Overexpression Increases Suc Uptake into Grains

To prove the function of HvSUT1 overexpression, we measured ^{14}C label incorporation after short-term labeling with [^{14}C]Suc of immature grains of wild-type wheat and lines HOSUT10 and -20 at 19 DAF. Preincubation with the covalent protein modifier diethylpyrocarbonate, which is known to inhibit proton-coupled symport (Bush, 1989), led to 30% to 50% inhibition of label incorporation. Compared with the wild type, HOSUT10 (Fig. 2A) and HOSUT20 (Fig. 2B) grains incorporated about 30% to 40% more ^{14}C, indicating that endosperm-specific HvSUT1 expression increased Suc uptake into grains.

HvSUT1 Seeds Have Higher Grain Nitrogen and Prolamin Contents

Line HOSUT10 (T4 generation) was chosen for further analysis. To study whether ectopic expression

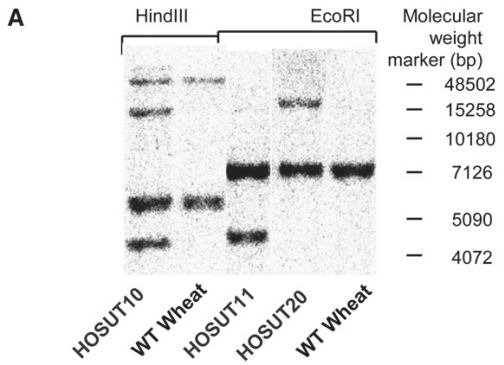

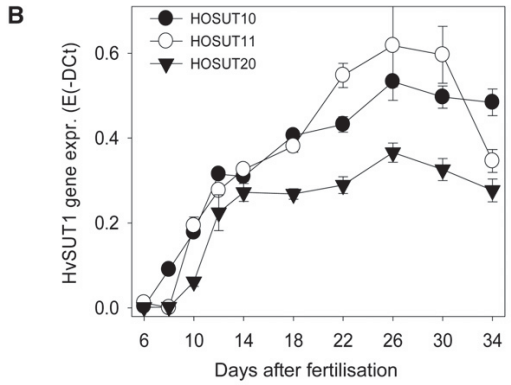

C

HOSUT Line	Total N (% of WT)	Thousand grain weight (% of W)
HOSUT20	**113 ± 1.9[b]**	**114.9 ± 3.7[b]**
HOSUT11	**105 ± 1.5[a]**	97 ± 2.6
HOSUT10	**107 ± 0.05[b]**	**107 ± 1.6[a]**

Figure 1. Characterization of HvSUT1-overexpressing wheat lines. A, Independent lines HOSUT10 (T4 generation), -11, and -20 (T2 generation) were analyzed for transgene integration by DNA gel-blot analysis. WT, Wild type. B, Quantitative real-time PCR analysis of HOSUT caryopses for transgene expression. Values are means of three biological replicates ± SD. C, Total nitrogen (N) and thousand grain weight of mature HOSUT grains (greenhouse grown). $n = 5$ to 10 ± SD. Significant differences according to t test are as follows: $^{a}P < 0.05$, $^{b}P < 0.01$. W, Wild type.

of HvSUT1 changes gene expression of endogenous Suc transporters, we performed quantitative real-time PCR on growing endosperms, showing that gene expression of the three endogenous wheat transporters TaSUT1A, -1B, and -1D (Aoki et al., 2002) was not different between HOSUT10 and the wild type (Fig. 2C).

To analyze the impact of Suc transporter overexpression on seed quality characteristics, plants were grown in greenhouses, in soil beds under semicontrolled conditions, and in field trials. Compositional analysis of mature HOSUT10 grains demonstrated that compared with wild-type seeds, total nitrogen content, which reflects grain protein content, was increased. To analyze the accumulation of different storage protein classes, seed protein was extracted from mature grains and separated into the fractions albumins/globulins and the prolamin classes gliadins and glutenins. Under all growth conditions, there was a significant increase of gliadins and glutenins, whereas the albumin/globulin fraction was unchanged, indicating a specific stimulation of prolamin synthesis in SUT1-overexpressing grains (Table I). There was a slight but significant increase in total seed carbon, whereas starch content was unchanged under semicontrolled and field conditions and slightly decreased for the greenhouse-grown material. Compared with

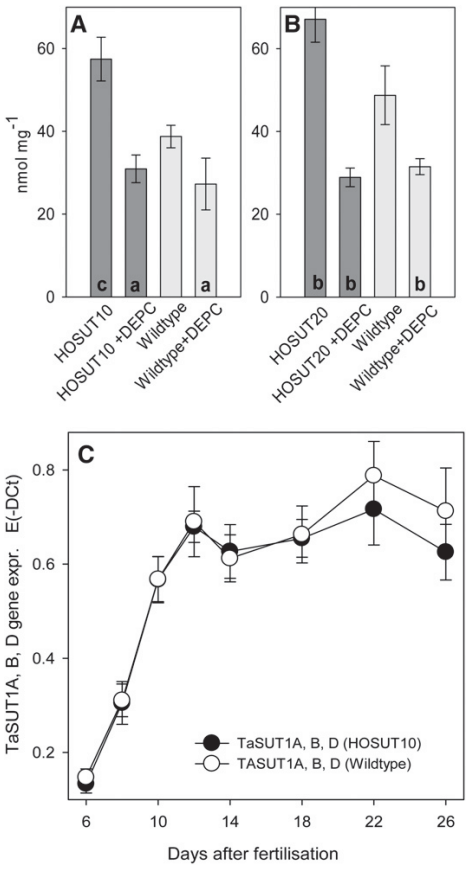

Figure 2. Suc uptake and TaSUT gene expression. A and B, ^{14}C label incorporation was measured after 10 min of labeling with [^{14}C]Suc of immature grains of wild-type Certo and lines HOSUT10 (A) and HOSUT20 (B) at 19 DAF. Thirty-minute preincubation was done with the covalent protein modifier diethylpyrocarbonate (DEPC), known to inhibit proton-coupled symport. Significant differences according to t test are as follows: $^{a}P < 0.05$, $^{b}P < 0.01$, $^{c}P < 0.001$. C, Quantitative RT-PCR of gene expression of endogenous wheat Suc transporters in HOSUT10 and wild-type endosperm. Values shown are means of at least three replicates ± SD.

Table I. *Compositional analysis of mature grains of line HOSUT10 grown under different conditions*

Values are means ± SE. Statistically significant differences according to Student's *t* test are as follows: [a]$P < 0.05$, [b]$P < 0.01$, [c]$P < 0.001$.

Variable	Field Trial 2006/2007		Semicontrolled 2006/2007		Greenhouse 2006	
	HOSUT10	Wild Type	HOSUT10	Wild Type	HOSUT10	Wild Type
Nitrogen (% of total mass)	2.62 ± 0.05[a]	2.45 ± 0.04	2.73 ± 0.01[b]	2.60 ± 0.03	3.62 ± 0.05[c]	3.12 ± 0.05
Albumins/globulins (%)	100.87 ± 1.82	100	98.68 ± 1.26	100	99.61 ± 1.02	100
Gliadins (%)	112.67 ± 2.64[b]	100	109.61 ± 2.24[b]	100	115.26 ± 2.77[c]	100
Glutenins (%)	106.32 ± 2.04[a]	100	105.98 ± 1.88[a]	100	123.93 ± 4.38[c]	100
Carbon (% of total mass)	44.81 ± 0.01[b]	44.67 ± 0.03	44.78 ± 0.01[c]	44.58 ± 0.03	45.06 ± 0.03[b]	44.88 ± 0.01
Nitrogen-carbon ratio	0.058 ± 0.001[a]	0.055 ± 0.001	0.061 ± 0.0003[b]	0.059 ± 0.001	0.080 ± 0.001[c]	0.07 ± 0.001
Grain protein (% of total mass)	14.95 ± 0.29[a]	13.96 ± 0.2	15.54 ± 0.07[b]	14.81 ± 0.18	20.66 ± 0.3[c]	17.79 ± 0.28
Starch (% of total mass)	62.5 ± 0.8	64.1 ± 0.8	62.8 ± 0.2	64.3 ± 0.7	60.3 ± 0.5[a]	64.1 ± 0.8
Thousand grain weight (g)	44.0 ± 1.6	41.2 ± 2	51.0 ± 0.4[a]	46.4 ± 1.7	58.6 ± 0.5	57.4 ± 0.5
Yield impact (%)	112.1 ± 19.1	100	129 ± 6.2[b]	100	100.21 ± 20.8	100
Protein yield impact (%)	120.6 ± 21	100	136.3 ± 5.2[c]	100	116.4 ± 24.2	100

the wild type, thousand grain weight was significantly higher in HOSUT10 by 10% and 6.8% under semicontrolled and field conditions. Overall, from measured parameters, an increase was observed in relative yield (seed mass per plant) and in protein yield in HOSUT10 grains. However, this was significant only when plants were grown under semicontrolled conditions (Table I).

HOSUT10 Grains Display Altered Development

Grain developmental parameters were analyzed for line HOSUT10 and wild-type grains. Unexpectedly, there was no change in Suc levels between 6 and 34 DAF (Fig. 3A) and in mature grains (data not shown). Fresh and dry weight accumulation of HOSUT10 and wild-type caryopses was similar only at early and mid development. However, at later stages, from 26 DAF onward, accumulation in HOSUT10 grains further increased. In contrast, the wild-type fresh and dry weight accumulation curve became flattened between 26 and 30 DAF (Fig. 3, B and C). This indicates a prolonged filling phase due to HvSUT1 overexpression. However, there was no apparent difference between the timing when HOSUT10 and wild-type grains reached maturity.

Abscisic acid (ABA) is the major hormone required for the initiation of seed maturation as well as for seed dormancy and desiccation tolerance (Finkelstein et al., 2002). ABA levels, measured on a fresh weight basis, during caryopses development were similar between 8 and 22 DAF but significantly lower in HOSUT10 grains between 26 and 34 DAF (Fig. 3D), which may also indicate altered maturation behavior of HOSUT10 grains, as seen from the dry/fresh weight accumulation curve.

Transcriptional Changes in HOSUT10 Grains Compared with the Wild Type

In order to compare gene expression between HOSUT10 and wild-type grains during development, we isolated mRNA from grains at 6, 8, 10, 12, 14, 18, 22, and 26 DAF for hybridization to an Affymetrix GeneChip Wheat Genome Array representing 55,052 transcripts from the hexaploid wheat genome (http://www.affymetrix.com/products_services/arrays/specific/wheat.affx). In a first screen, 1,700 sequences were selected with altered gene expression between HOSUT10 and wild-type grains. Approximately 50% of these candidates revealed no annotation and were designated as "unknown." A subset of 109 sequences was further selected with clear annotations that represent members of functional groups: amino acid metabolism, cell proliferation, nitrogen-carbon signaling, transcription factors, mitochondrial metabolism, hormone functions and development, primary and secondary metabolism, seed maturation, and transport (Supplemental Table S1). From this collection, altered gene expression between HOSUT10 and wild-type grains was verified by quantitative RT-PCR at 10 stages between 6 and 34 DAF using three biological replicates. Supplemental Table S2 shows those genes that are differentially expressed, based on quantitative RT-PCR in HOSUT10 grains ($P < 0.05$) in at least one developmental stage.

HvSUT1 Overexpression Preferentially Stimulates Prolamin Gene Expression

Strikingly, altered gene expression was observed for 10 sequences encoding members of the prolamin class of storage protein genes. Together with an oleosin gene, these candidates show a characteristically altered pattern. At the very early stage (6 DAF), gene expression was down-regulated in HOSUT10. However, at this stage, absolute gene expression levels of prolamins are still very low. This was followed immediately by a strong up-regulation between 8 and 14 DAF. At later stages, there were less distinct changes within this group, with at best slight up-regulation at 18 DAF (Fig. 4A). Such a pattern indicates that SUT1 overexpression strongly stimulates prolamin gene expression, especially at the transition from prestorage and storage phase. The collection of genes with altered expression (Supplemental Table S2) was screened for other members with a pattern similar to that of pro-

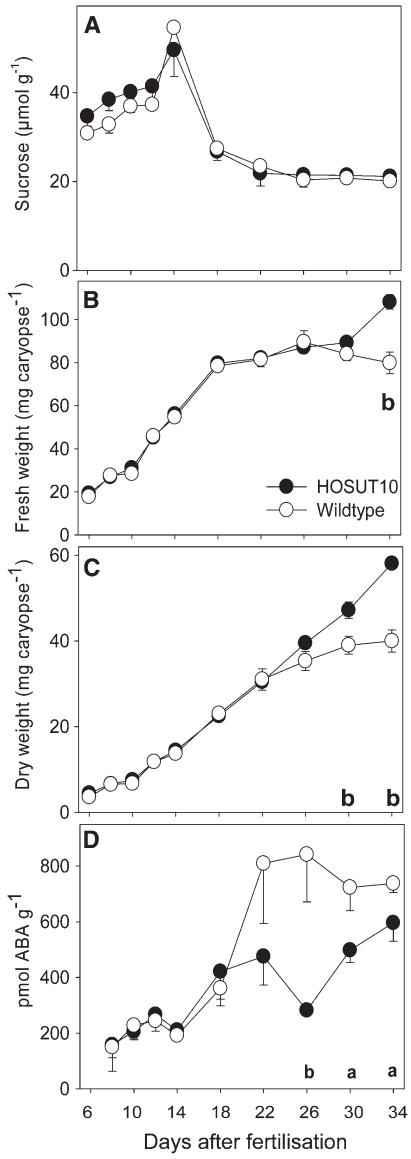

Figure 3. Growth parameters of HOSUT10 grains. A, Suc concentration in caryopses ± SD ($n = 5$). B, Fresh weight accumulation ($n = 100$). C, Dry weight accumulation ($n = 100$). D, ABA concentration (pmol g^{-1} fresh weight) ± SD ($n = 5$). Significant differences according to *t* test are as follows: $^{a}P < 0.05$, $^{b}P < 0.01$.

lamin genes, explicitly distinct up-regulation between 8 and 14 DAF. Thereby, a group of 10 members was identified (Fig. 4B), among them three from sugar-starch metabolism, Suc synthase, granule-bound starch synthase 1, and starch-branching enzyme, and a His-containing phosphotransfer protein, which is potentially involved in cytokinin signaling in wheat (Ma and Tian, 2005). Two other genes have putative roles in cell proliferation, cell division protein AAA ATPase (Park et al., 2008) and phosphatidylinositol 3- and 4-kinase (Choi et al., 2008). Other sequences have homologies to *Early flowering4* involved in oscillatory properties, circadian rhythm, and light signaling (McWatters et al., 2007), and to *flavonol synthase*, which is inducible by Suc supply and nitrogen depletion (Lillo et al., 2008). One gene encodes 11-β-hydroxysteroid dehydrogenase with a potential role to promote or mediate brassinosteroid effects. Its overexpression in Arabidopsis and canola (*Brassica napus*) improved growth and seed yield (Li et al., 2007). Finally, one sequence encodes an ABI5 homolog, which in Arabidopsis is involved in ABA signaling and is transcriptionally activated in response to sugars (Arroyo et al., 2003).

Altered Gene Expression in HOSUT10 Grains Related to Metabolism

Increased protein content indicates possible stimulatory effects on amino acid metabolism. Eight genes encoding enzymes of amino acid metabolism were differentially expressed in HOSUT grains (Supplemental Table S2), although without a clear overall tendency. Plastidial Gln synthetase and Asp kinase were strongly up-regulated, especially at later stages (Supplemental Table S2). Asp kinase catalyzes the synthesis of Thr and Lys and is strongly feedback inhibited by these end products (Ben-Tzvi Tzchori et al., 1996). On the other hand, glutamate dehydrogenase (GDH) was clearly down-regulated, especially at 30 and 34 DAF. GDH catalyzes amino acid breakdown and is induced under carbon-deficient conditions (Miyashita and Good, 2008). Its strong down-regulation in HOSUT10 grains may indicate carbon sufficiency. Accumulation of 2-oxoglutarate at DAF 22 to 26 together with decreased Glu but not Gln may also support this assumption (Supplemental Table S2).

Furthermore, there was a preferential up-regulation in HOSUT10 grains of genes encoding mitochondrial enzymes involved in carbohydrate metabolism and respiration, especially during mid and late development, such as uncoupling protein (34 DAF), ATP synthase F1 (22 and 26 DAF), pyruvate dehydrogenase E1 (30 DAF), alternative oxidase (10, 14, and 18 DAF), and malate dehydrogenase (30 and 34 DAF). This may indicate increased usage and respiration of carbohydrates within mitochondria of HOSUT10 grains. There is also a striking up-regulation of pyruvate decarboxylase (PDC), which is normally involved in fermentation pathways. However, under conditions of high sugars and glycolytic fluxes, PDC may bypass pyruvate dehydrogenase toward acetyl-CoA synthesis and therefore could support mitochondrial energy production (Gass et al., 2005).

Deregulated Gene Expression in HOSUT10 Grains Related to Hormonal and Signaling Functions

A subset of genes deregulated in HOSUT10 grains revealed a striking inverse pattern with up-regulation

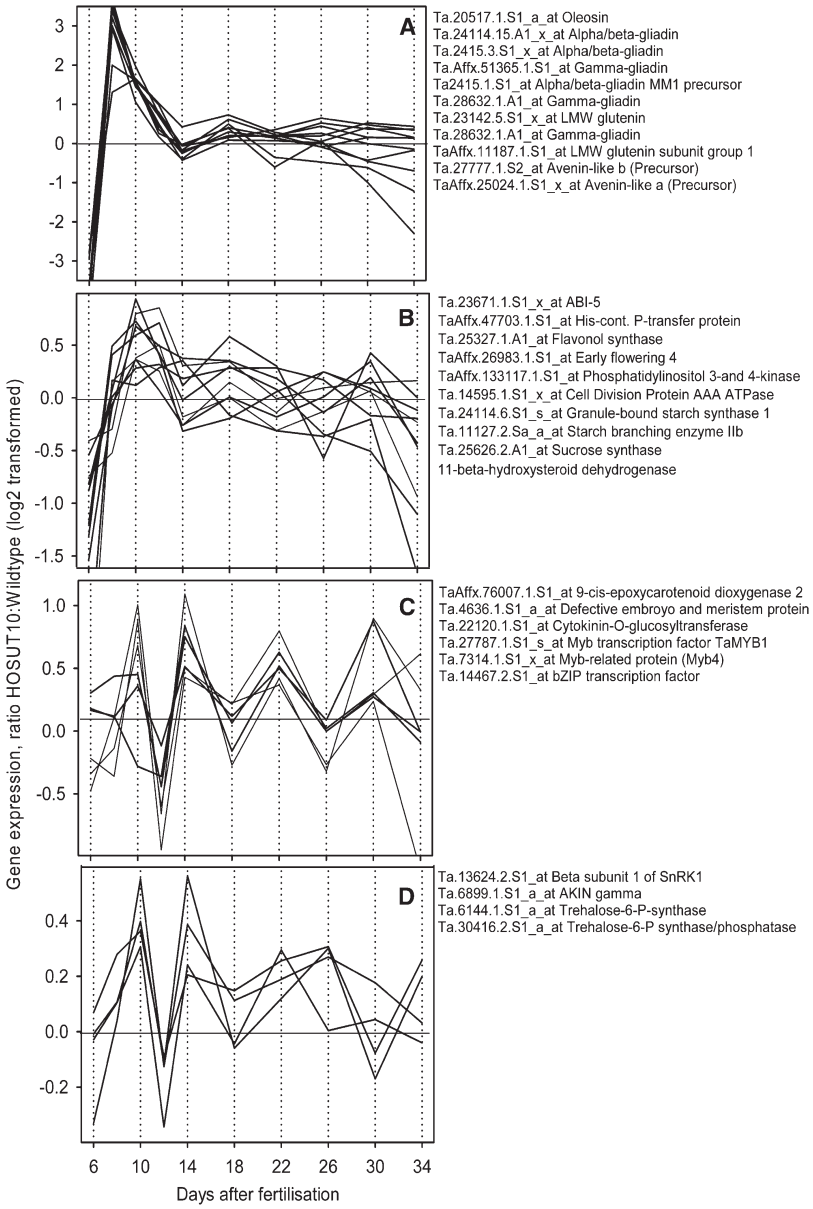

Figure 4. Ratios of gene expression, HOSUT10:wild type. Gene expression was determined by quantitative real-time PCR at 10 stages of development with three biological replicates. Data were extracted from Supplemental Table S2 and are $\log_2$ transformed. A, Storage protein and storage-associated genes. B, Genes revealing a cluster similar to that presented in A. C and D, Genes revealing a cluster inverse to that presented in B. For full description of genes, see Supplemental Table S2. Identifier numbers refer to the Affymetrix GeneChip.

at 10, 14, 22, and 30 DAF and with down-regulation at 8, 12, 18, and 26 DAF (Fig. 4C). Two of these genes encode key enzymes of ABA and cytokinin metabolism, 9-cis-epoxycarotenoid dioxygenase 2 and protein cytokinin-*O*-glucosyltransferase. Three others encode transcription factors, TaMyb1 and bZIP-like, both with unknown functions in wheat, and Myb4, with possible roles in stress response (Vannini et al., 2004). A set of four genes encoding two proteins, each of the trehalose and the SnRK1 pathways, show a very similar oscillating pattern (Fig. 4D). Signaling pathways of SnRK1 and of trehalose are known to be involved in the regulation of carbohydrate metabolism (Lunn et al., 2006; Radchuk et al., 2006). In summary, these genes, which in HOSUT10 grains show the particular pattern of an oscillatory up- and down-regulation mode inversely to the prolamin genes, mainly encode transcription factors and regulatory genes of hormonal and carbohydrate pathways.

Metabolite Profiling

Metabolite profiling was performed from HOSUT10 and wild-type grains at stages 6, 8, 10, 12, 14, 18, 22,

and 26 DAF (Supplemental Table S3). Hierarchical clustering of all metabolites (Supplemental Fig. S1) illustrates clusters according to their developmental behavior and clearly distinguishes minor (top) from major (bottom) changes. Steady decreases are more common than steady increases. To identify those stages showing major differences of metabolite composition between HOSUT10 and wild-type grains, we performed an independent component analysis based on median-centered and $\log_{10}$-transformed response ratios (Fig. 5). Major deviations in metabolite steady-state levels occur in early (6–8 DAF) and late (26 DAF) stages. Overall, there were not many differences in the ratios of metabolite contents. Although Suc transporter activity is apparently enhanced in HOSUT10 grains, there was no change in Suc levels in HOSUT10 grains compared with the wild type (Supplemental Table S3). On the contrary, there was a trend to lower levels from 8 DAF onward, although not statistically significant. There were also very little changes in the levels of hexoses and hexose phosphates. We found an increase of malate and 2-oxoglutarate levels at mid and later stages, indicating that carbohydrate acceptors for amino acid biosynthesis are not limited. However, citrate levels were lower in HOSUT grains at 12 and 26 DAF. Changes in amino acid levels were more pronounced. There was a clear trend for higher levels, specifically in later stages, 22 and 26 DAF, for Lys, Leu, Ile, Phe, Tyr, and Trp. On the other hand, levels of Cys, Asp, and Glu were decreased at these later stages. Because Asp and Glu are precursors of a range of other amino acids, such a pattern would indicate a stimulation of amino acid biosynthesis at later stages in HOSUT10 grains. Cluster analysis revealed that changed amino acid profiles roughly fall into two clusters. Levels of group 1 members (Arg, Orn, Asn, Leu, Ile, Lys, Tyr, Phe, Trp) were relatively lower in HOSUT10 grains between 8 and 12 DAF but displayed higher levels at later stages between 22 and 26 DAF (Fig. 6A). Levels of group 2 members (Glu, Asp, Gly, Ser, Val) were relatively decreased in HOSUT10 grains between 8 and 12 DAF and again between 20 and 26 DAF (Fig. 6B). This pattern suggest that most amino acid levels show a relative depression in HOSUT10 grains between 8 and 14 DAF, which coincides with the developmental period when prolamin gene expression is stimulated (Fig. 4A). This is in agreement with the independent component analysis results (Fig. 5).

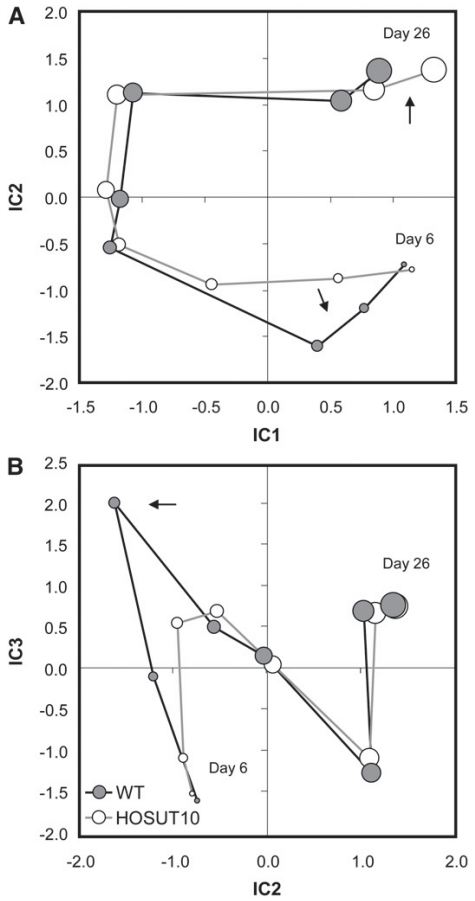

Figure 5. Independent component (IC) analysis based on the median centered and $\log_{10}$-transformed response ratios. The graph shows that deviations of metabolite levels during grain development occur in the early phase DAF 8 to 10 (arrow in B) and the late phase (26 DAF), indicating a continued development in transgenic grains at day 26 (arrow in A). The size of each circle indicates its developmental stage: smallest circle, 6 DAF; largest circle, 26 DAF. WT, Wild type.

DISCUSSION

Conventional breeding for yield increase in wheat seems to approach an upper limit. Especially grain protein content, although economically important, is difficult to improve because of negative correlations between yield and grain protein content (Sinclair, 1998; Barneix, 2007). Increasing grain sink strength could be a promising approach to overcome this constraint (Reynolds et al., 2009). We here show that overexpression of a Suc transporter increases Suc uptake capacity. We speculate that such changes, via a network of metabolic and hormonal signals, leads to higher grain protein content.

Protein Increase in HOSUT Grains Is Not Compromising Yield

Wheat grains overexpressing *HvSUT1* in the endosperm significantly take up more Suc in vitro (Fig. 2, A and B). This indicates that the transgene is functional. Surprisingly, grain Suc as well as hexose levels, as measured by HPLC (Fig. 3A) and gas chromatography-mass spectroscopy (GC-MS; Supplemental Table S3), are not altered, indicating tight control of Suc levels within the endosperm (Jenner et al., 1991). Thus, we

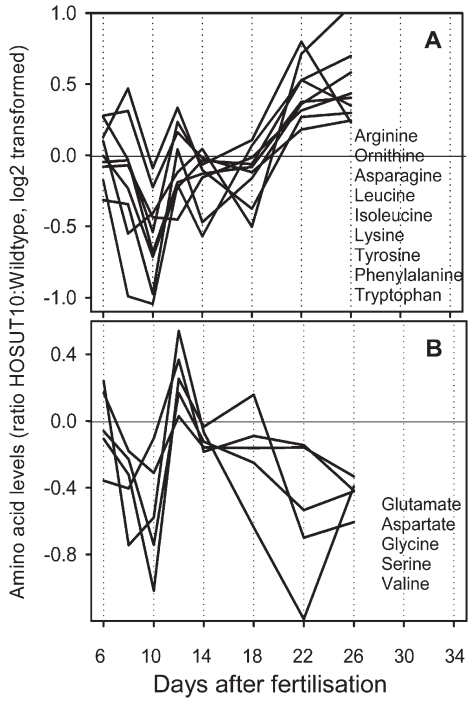

Figure 6. Ratios of amino acid levels, HOSUT10:wild type. Amino acids were determined by GC-MS, and data were extracted from Supplemental Table S3. A, Cluster with amino acid levels lower at 8 to 12 DAF and higher at later stages, 22 to 26 DAF. B, Cluster with amino acid levels lower at 8 to 12 DAF and lower at later stages, 22 to 26 DAF.

speculate that HvSUT1 modifies Suc flux potential rather than metabolite steady-state levels.

Notably, mature grains of three lines show increased percentages of total nitrogen (Fig. 1C), which reflects a higher grain protein content. Starch concentration, on the other hand, was unchanged but was increased on the per seed level due to higher thousand grain weight. Likewise, line HOSUT10, grown in different locations, greenhouses, semicontrolled conditions (Hensel et al., 2009), and in field trails, always displayed higher percentages of total nitrogen, grain protein content, and nitrogen-carbon ratios compared with the wild type (Table I). These data indicate that *HvSUT1* expression specifically stimulates grain protein accumulation. Under different growth conditions, there was no evidence for decreased yield of HOSUT lines. Thus, increases in grain protein content seem not to be correlated to lower yield (Table I). This has often been observed and is explained by the fact that high starch content of wheat grains (75%–85%) is almost completely dependent on starch accumulation (Sinclair, 1998). That means that every increase in yield should relatively decrease protein content (Barneix, 2007). Furthermore, because protein biosynthesis is energetically more expensive than that of starch (Vertregt and deVries, 1987), any yield increase would primarily apply to starch content.

Also, for HOSUT lines, a positive impact on yield cannot be supported definitely. Despite the higher protein content of individual seeds, higher seed size, and significant yield increases when grown under semicontrolled conditions, we found no clear overall higher protein yield (milligrams of seed protein per plant) that was statistically significant. A positive impact of HvSUT1 expression on protein yield under field conditions is not yet clear, because the scale of the performed field trials was too small to reliably exemplify significant effects. Nevertheless, the data suggest that increasing Suc uptake potential into grains by HvSUT1 overexpression could be a promising approach and worth pursuing toward increasing grain yield and/or grain protein yield.

HvSUT1 Overexpression in Grains Stimulates Prolamin Accumulation

Fractionation of HOSUT10 grain proteins into albumins/globulins and the prolamin classes gliadins and glutenins clearly shows that only prolamins are significantly increased (Table I), indicating a specific effect of increased Suc uptake capacity on prolamin biosynthesis. Many data reveal stimulatory effects from nitrogen supply and fertilization on grain protein content (Barneix, 2007). This led to the general conclusion that grain protein content is strictly responsive to nitrogen. However, in HOSUT10 grains, a specific effect from Suc or Suc fluxes has to be assumed. Physiological evidence shows different effects of assimilate supply on starch and protein accumulation. Whereas starch is not very sensitive to variations of assimilate supply within normally observed limits, protein content responds more directly (Perez et al., 1989; Jenner et al., 1991). Such a relationship can explain the positive effect only on protein but not on starch. Moreover, in maize kernels, Suc has been reported to increase storage product gene expression (Giroux et al., 1994), and in Arabidopsis, it can induce storage-related genes such as oleosins, 2S and 12S globulins, as well as *Lec*- and *Fus*-like transcription factors (Tsukagoshi et al., 2007). In grain legumes, Suc induces and sustains storage product formation, shown by in vitro culture (Weber et al., 1996), mutant analysis (Perez et al., 1993), and transgenic approaches where sugar levels were increased (Weigelt et al., 2009). In all these cases, seed protein content responds positively to sugar supply and/or concentration. Moreover, Suc transporter overexpression in pea cotyledons leads to earlier onset of protein accumulation (Rosche et al., 2002, 2005).

Notably, transcript profiling of HOSUT10 in comparison with wild-type grains shows predominant changes within the cluster of prolamin genes, with strong up-regulation at the transition from prestorage to storage phase, DAF 8 to 12 (Fig. 4A). This is in accordance with higher levels of prolamin-type pro-

teins (Table I). We conclude that, especially at the onset of the storage phase, improved Suc supply stimulates prolamin gene expression and protein accumulation.

Increased Suc Uptake into HOSUT10 Grains Exerts Metabolic Effects

Significant changes in gene expression and metabolite levels related to central carbon metabolism and amino acid biosynthesis are summarized in Figure 7. Plastidial Gln synthetase and Asp kinase were strongly up-regulated, especially at later stages, suggesting increased synthesis of Gln and of amino acids of the Asp branch in HOSUT grains (Fig. 6). Such up-regulation is accompanied by higher levels of certain amino acids between 22 and 26 DAF and may indicate that prolonged seed filling is due to improved availability of amino acids. There is no indication for altered gene expression of amino acid transporters in the endosperm. However, it cannot be excluded that such stimulation occurs in leaf phloem. Together, the alterations argue for certain deregulation of the carbon-nitrogen balance in HOSUT grains, which ultimately indicates carbon sufficiency and relative depletion of nitrogen. First, adenosine 5′-phosphosulfate reductase, a key enzyme of sulfate reduction, is up-regulated at 8, 22, 30, and 34 DAF. In Arabidopsis, adenosine 5′-phosphosulfate reductase transcripts and activity respond positively to sugar supply (Hesse et al., 2003). This indicates that increased Suc uptake capacity in HOSUT10 activates sulfate assimilation. Second, GDH is strikingly down-regulated, especially at 30 and 34 DAF. Its major role is deamination of Glu and feeding of carbon into the tricarboxylic acid cycle to adjust high nitrogen-carbon ratios (Miyashita and Good, 2008). Accordingly, Suc can suppress GDH gene expression in tobacco (*Nicotiana tabacum*; Masclaux-Daubresse et al., 2005). In contrast, under conditions of excess amino acid availability such as remobilization, GDH is up-regulated (Thiel et al., 2009). Thus, GDH

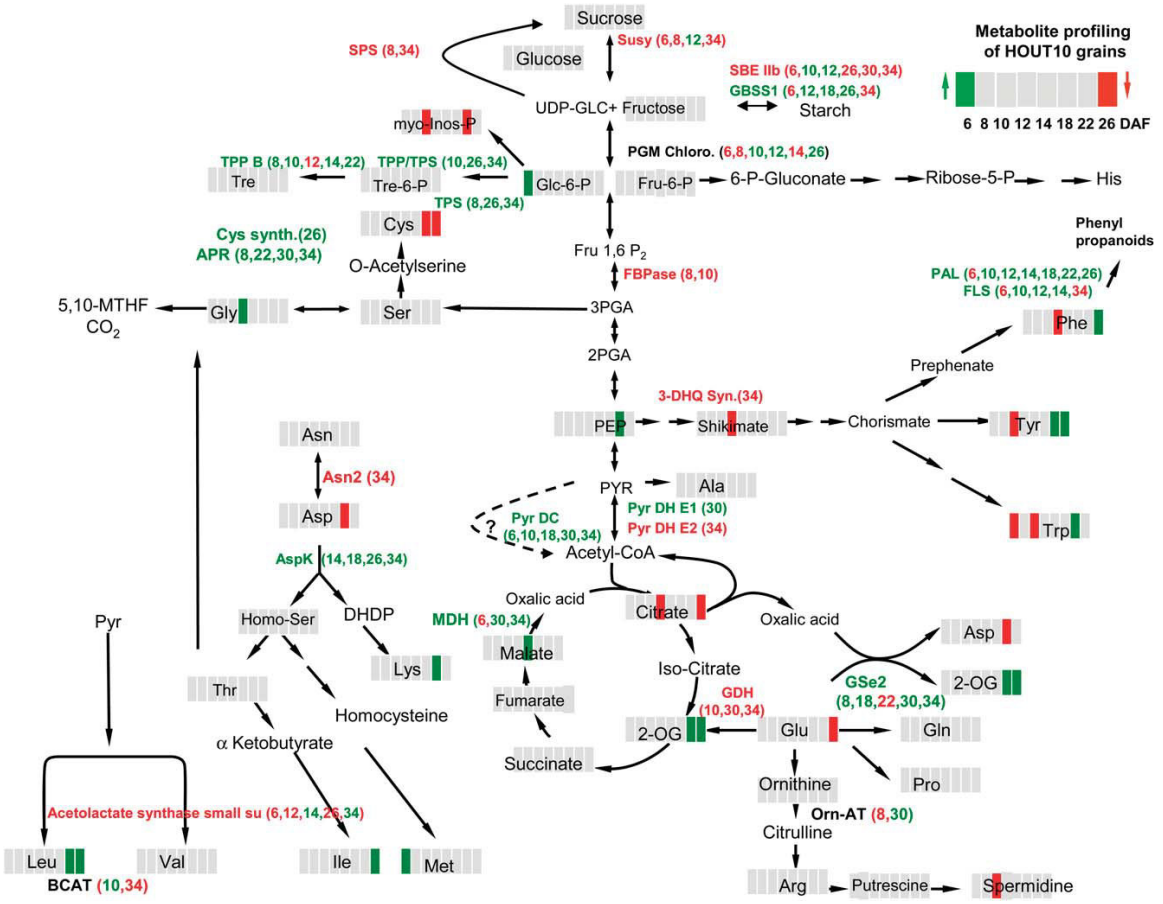

Figure 7. Summary of changed transcript and metabolite levels in HOSUT10 caryopses. Data are derived from Supplemental Tables S2 (transcripts) and S3 (metabolites). Color code is as follows: red, down-regulated; green, up-regulated in HOSUT10 caryopses with respect to the wild type.

down-regulation in HOSUT grains indicates adequate carbon availability and relative depletion of nitrogen. Third, preferential up-regulation of gene expression related to mitochondrial carbohydrate metabolism and respiration (Supplemental Table S2) indicates increased usage and respiration of carbohydrates, which can be expected under conditions of increased carbon flux. Striking up-regulation of PDC throughout HOSUT10 grain development is surprising at first view. However, PDC may bypass pyruvate dehydogenase and therefore could support carbon flux into the tricarboxylic acid cycle. Such a role for PDC has been described, especially under conditions of high sugars and glycolytic fluxes (Gass et al., 2005). Fourth, higher 2-oxoglutarate and malate levels at mid/late stages indicate ample availability of carbon acceptors for amino acid biosynthesis, indicating that HvSUT1 overexpression stimulates both amino acid metabolism and the synthesis of organic acids as carbon skeletons for amino acid biosynthesis. Such stimulation was observed after overexpression of a phospho*enol*pyruvate carboxylase and repression of ADP-Glc pyrophosphorylase (Radchuk et al., 2007; Weigelt et al., 2009).

Most amino acid levels show relative depression in HOSUT10 grains between 8 and 14 DAF, which coincides with the period when prolamin gene expression is strongly stimulated (Fig. 6). Thus, amino acids in HOSUT grains become transiently limited (Fig. 6) at the stage of the pronounced burst of prolamin gene expression (Fig. 4A). Decreased levels of Asp and Glu as precursors of a range of other amino acids indicate stimulated amino acid biosynthesis at later stages in HOSUT10 grains. It can be concluded that endosperm-specific SUT1 expression leads to stimulation of prolamin gene expression at earlier stages and activates and maintains amino acid biosynthesis during late maturation. Both effects can be related to signaling and metabolic effects from improved sugar supply. Probably an enhanced Suc flux potential will only become effective at later stages, when Suc uptake normally becomes limited. Bypassing such limitation may lead to prolonged fresh weight accumulation.

HvSUT1 Overexpression Stimulates a Network of Sugars and Hormonal Signals

Assuming that Suc or its increased flux capacity in HOSUT grains stimulates prolamin gene expression, it can be hypothesized that genes that show a similar pattern of up-regulation are coregulated and therefore might be also under metabolic control and potentially involved in sugar signaling. Such a cluster, similar to that of the prolamin genes, includes genes involved in sugar-starch metabolism, some of which were up-regulated in Arabidopsis seedlings and pea seeds with increased sugar levels (Osuna et al., 2007; Weigelt et al., 2009). Up-regulated gene expression related to cytokinin and brassinosteroid functions as well as cell proliferation reveals positive regulation of growth and cell proliferation due to assimilate supply (Rosche et al., 2002, 2005; Hartig and Beck, 2006; Li et al., 2007; Weigelt et al., 2009). Other members include *Early flowering4* and *flavonol synthase*, which are inducible by Suc and nitrogen depletion (Lillo et al., 2008). The transcription factor *ABI5* is potentially involved in ABA signaling and transcriptionally activated in response to sugars (Arroyo et al., 2003). Notably, coregulation of *ABI5* together with storage protein genes, as observed in HOSUT10 grains, suggests a positive response to sugars and points to a key role of ABI5 in metabolic signaling of prolamin gene expression in wheat grains.

Another cluster of deregulated genes with striking oscillations (Fig. 4, C and D) reveals a pattern that is inverse to that observed in the clusters shown in Figure 4, A and B. Such members include 9-cis-epoxycarotenoid dehydrogenase, a key enzyme of ABA synthesis found to be down-regulated in pea embryos accumulating excess sugars (Weigelt et al., 2009), and cytokinin-*O*-glycosyltransferase, which inactivates cytokinins and causes growth retardation when overexpressed in maize (Pineda Rodo et al., 2008). Three other members encode Myb- and bZIP-like transcription factors, whereas four are related to trehalose and SnRK1 pathways, with potential involvement in the regulation of carbohydrate metabolism (Lunn et al., 2006; Radchuk et al., 2006). In Arabidopsis, trehalose-6-phosphate synthase and a SnRK1 subunit rapidly decreased upon Suc feeding (Osuna et al., 2007). It could be that in wheat grain development, such gene products (Fig. 4, C and D) modulate and/or counterbalance the effect from increased carbon flux or sugar and as such function as negative regulators of Suc signaling.

In summary, the analysis of specific clusters (Fig. 4) leads to the conclusion that overexpression of HvSUT1 on the one hand stimulates grain protein accumulation but partially deregulates the metabolic status of wheat grains. This is accompanied by an inverse oscillatory behavior of gene expression of positive and negative regulators related to assimilate supply and sugar signaling. As such, metabolic alterations can be effectively balanced by different signaling components (Fig. 4, C and D), which together have the capacity to adjust grain storage metabolism throughout development in response to metabolic alterations. Alternating stimulation of positive and negative regulation due to HvSUT1 expression may cause such an oscillatory pattern of gene expression and show the high flexibility of wheat grain storage metabolism.

MATERIALS AND METHODS

Generation of Transgenic Wheat Plants

The HvSUT1 cDNA (1,894 bp; accession no. AJ272309) was fused to the HorB1 promoter (550 bp; accession no. X87232) and the HorB1 terminator (1,663 bp; accession no. FN643080). The HorB1P::HvSUT1:HorT construct was cloned into binary vector pPZP200 (Hajdukiewicz et al., 1994). Plant trans-

formation was carried out either by particle bombardment of immature wheat (*Triticum aestivum*) embryos (HOSUT10) coated with the plasmids pJFBar and HorB1::HvSUT1/pPZP200 in equimolar ratios as described by Varshney and Altpeter (2001) or by *Agrobacterium tumefaciens*-mediated gene transfer using plasmid HorB1::HvSUT1/pPZP200 (HOSUT20 and -11) largely following the protocol of Hensel et al. (2009).

Plant Growth Conditions

Seeds of winter wheat (cv Certo) were germinated in greenhouses (20°C) in trays with substrate mix (www.klasmann-deilmann.de/) for 2 weeks, followed by 8 weeks of incubation in vernalization chambers (4°C/4°C, 8-h/16-h day/night regime). Plantlets were stepwise adapted to an 18°C/14°C, 16-h/8-h day/night regime (SON-T-Agro 400 high-pressure sodium bulbs with 25,000 lux) in 2.5-L pots containing cultivation substrate (substrate 2; www.klasmann-deilmann.de/). Fertilization of greenhouse plants was conducted as described by Hensel et al. (2009). To create field-related conditions, plants were grown in soil beds under glass without supplemental light or temperature regulation from October to July. Soil bed plants were fertilized with 0.3% Hakaphos blau (www.compo.de/) once a week. Field trials were performed on a 106-m^2 area at IPK Gatersleben, designed as a 4×4 Latin square, with 200 plants per line and single planting with 0.2-m distance. Nitrogen fertilization was performed as recommended by Agrolab (www.agrolab.de).

For mRNA expression studies and metabolite measurements, immature seeds were collected 6 to 34 DAF from the first four emerged spikes per plant, separated into maternal and filial fractions, and frozen at −80°C.

Nucleic Acid Isolation and Hybridization

High-quality genomic DNA was prepared from 150 mg of leaf material as described by Palotta et al. (2000). Fifteen micrograms of total DNA was digested with *Hin*dIII or *Eco*RI. DNA gel-blot analysis was performed as described by Hensel et al. (2009). PCR primers to prove transgenic HvSUT1 integration and copy number were 5′-GCCGGGCGGTCGCAGCTCGC-GTCTA-3′ and 5′-GCTGCTGAAATTTCACCATCCATTC-3′ (accession no. AM055812).

Gene Expression Analysis by Quantitative Real-Time PCR

Total RNA was isolated using phenol-chloroform extraction as described by Heim et al. (1993) and treated with Turbo DNase I (Invitrogen). First-strand cDNA was synthesized with oligo(dT) primer and SuperScript III reverse transcriptase (Invitrogen). Real-time PCR from three biological replicates was performed using 2× SybrGreen PCR Mastermix on an ABI Prism 7900HT Sequence Detection System (Applied Biosystems). A total of 109 genes from the Affymetrix GeneChip Wheat Genome hybridization results (Supplemental Table S1) that obviously showed altered gene expression were selected. Primer design and reaction parameters were as described by Czechowski et al. (2005). Amplification efficiency was assessed with the LinRegPCR program (Ramakers et al., 2003). Determined ΔΔct-values from "transgenics" were related to that of "wild-type" plants at respective stages. Wheat *actin* (accession no. AB181991) was used as housekeeping gene for normalization. Primer sequences are given in Supplemental Table S4.

Determination of Suc, Starch, Proteins, Total Carbon and Nitrogen, and Suc Uptake Studies

Starch and Suc were determined as described by Weigelt et al. (2009). Total carbon and nitrogen in dried wheat flour were determined with the Vario EL Elementar analyzer (www.elementar.de), and protein content was calculated from percentages of total nitrogen by multiplication by conversion factor 5.7 for wheat grains (Sosulski and Imafidon, 1990). Protein fractions albumin/globulin and gliadin were sequentially extracted as described by Wieser (1997). Extracted wheat protein fractions were quantified using the colorimetric Pierce BCA Protein Assay (Thermo Scientific). Bovine serum albumin and gliadin from wheat (G3375; Sigma-Aldrich) were used as standards. Glutenin fractions were determined from the difference of total protein and albumin/globulin/gliadin fractions. In vitro Suc uptake was determined as described by Wardlaw et al. (1995).

Statistical analyses were performed with Student's *t* test or, alternatively, with the Wilcoxon rank-sum test with Sigma-Stat software (www.systat.com/).

Determination of ABA

ABA was extracted from plant material and analyzed according to Miersch et al. (2008) with the following modifications. Fresh material (10–500 mg) was homogenized with 10 mL of methanol and appropriate amounts (1 ng of standard per 5 mg of plant material) of [$^2H_6$]cis,trans-ABA as internal standard. Homogenates were filtered, placed on columns filled with 3 mL of DEAE-Sephadex A25 (Amersham Pharmacia Biotech; Ac^- form; methanol), followed by washing with 3 mL of methanol and 3 mL of 0.1 M acetic acid in methanol. Fractions were eluted with 3 mL of 1 M acetic acid in methanol and 3 mL of 1.5 M acetic acid in methanol, combined, evaporated, and separated by preparative HPLC (Eurospher 100-C18, 5 μm, 250 × 4 mm; www.knauer.net/) using a gradient of 40% to 100% methanol in 0.2% (v/v) aqueous acetic acid in 25 min. The fraction at retention time 10 to 12 min was collected, evaporated, derivatized into pentafluorobenzyl esters, and analyzed by GC-negative chemical ionization-MS. Retention times of pentafluorobenzyl esters were as follows: [$^2H_6$]cis,trans-ABA, 17.70 min; cis,trans-ABA, 17.78 min. Fragments with mass-to-charge ratio 269 (standard ABA) and mass-to-charge ratio 263 (ABA) were used for quantification.

Transcript Profiling by 55k Microarray Analysis

Total RNA was isolated as described by Radchuk et al. (2007), and integrity and concentration were examined on the Agilent 2100 Bioanalyzer using the RNA 6.000 LabChip Kit (www.agilent.com). Five micrograms of total RNA was used to prepare double-stranded cDNA (SuperScript II; www.invitrogen.com) primed with oligo(dT) containing a T7 RNA polymerase promoter site. cDNA was purified by phenol-chloroform extraction before in vitro transcription using the in vitro transcription labeling kit (www.affymetrix.com) to synthesize copy RNA. Unincorporated nucleotides were removed using the RNeasy kit (Qiagen). Copy RNA was fragmented and hybridized to the Affymetrix GeneChip Wheat Genome array according to the manufacturer's instructions. The array was scanned with a third generation Affymetrix GeneChipScanner 3000. Affymetrix GeneChip data representing approximately 55,000 transcripts with complete Wheat Genome coverage were extracted from fluorescence intensities and scaled in order to normalize data for interarray comparison using the MicroArray Suite software package MAS 5.0 (Affymetrix). Data quality control, normalization of raw data, estimation of signal intensity, average expression values, and *P* values was as described by Sreenivasulu et al. (2008).

Metabolite Profiling by GC-MS

Frozen filial preparations from developing grain tissue were extracted using conventional methanol/chloroform extraction. A conventional polar fraction was prepared by liquid partitioning into water-methanol, and a 0.5-mL fraction was dried and derivatized for GC-MS profiling (Lisec et al., 2006; Erban et al., 2007). GC coupled to electron impact ionization/time-of-flight MS was performed using an Agilent 6890N24 gas chromatograph with splitless injection connected to a Pegasus III time-of-flight mass spectrometer (www.leco.de/). Metabolites were quantified using at least three specific mass fragments. GC data preprocessing and compound identification were performed using TagFinder software (Luedemann et al., 2008) and mass spectral and retention time index collection of the Golm metabolome database (Kopka et al., 2005). Six biological replicates of each sample were analyzed by GC coupled to electron impact ionization/time-of-flight MS, and numerical processing was performed as described previously (Van Dongen et al., 2009).

Supplemental Data

The following materials are available in the online version of this article.

Supplemental Figure S1. Hierarchical clustering using Euclidian distance and complete linkage.

Supplemental Table S1. Subset of sequences with altered gene expression between HOSUT10 and wild-type grains.

Supplemental Table S2. Quantitative real-time PCR analysis of a subset of 109 sequences with clear annotations.

Supplemental Table S3. Metabolite profiling based on GC-MS.

Supplemental Table S4. List of primers used for quantitative real-time PCR; results are given in Supplemental Table S3.

ACKNOWLEDGMENTS

We thank Gabriele Einert, Elsa Fessel, Uta Siebert, Ines Fehrle, Birgit Ortel, and Angela Stegmann for excellent technical assistance.

Received November 12, 2009; accepted December 9, 2009; published December 14, 2009.

LITERATURE CITED

Ambrose MJ, Wang TL, Cook SK, Hedley CL (1987) An analysis of seed development in *Pisum sativum* L. IV. Cotyledon cell population in vitro and in vivo. J Exp Bot **38:** 1909–1920

Aoki N, Whitfield P, Hoeren F, Scofield G, Newell K, Patrick J, Offler C, Clarke B, Rahman S, Furbank RT (2002) Three sucrose transporter genes are expressed in the developing grain of hexaploid wheat. Plant Mol Biol **50:** 453–462

Arroyo A, Bossi F, Finkelstein RR, León P (2003) Three genes that affect sugar sensing (*abscisic acid insensitive 4*, *abscisic acid insensitive 5*, and *constitutive triple response 1*) are differentially regulated by glucose in Arabidopsis. Plant Physiol **133:** 231–242

Bagnall N, Wang XD, Scofield GN, Furbank RT, Offler CE, Patrick JW (2000) Sucrose transport-related genes are expressed in both maternal and filial tissues of developing wheat grains. J Plant Physiol **27:** 1009–1020

Balconi CE, Rizzi E, Manzocchi L, Soave C, Motto M (1991) Analysis of *in vivo* and *in vitro* grown endosperms of high and low protein strains of maize. Plant Sci **73:** 9–18

Barneix AJ (2007) Physiology and biochemistry of source-regulated protein accumulation in the wheat grain. J Plant Physiol **164:** 581–590

Ben-Tzvi Tzchori I, Perl A, Galili G (1996) Lysine and threonine metabolism are subject to complex patterns of regulation in *Arabidopsis*. Plant Mol Biol **32:** 727–734

Borrás L, Slafer GA, Otegui ME (2003) Seed dry weight response to source-sink manipulations in wheat, maize and soybean: a quantitative reappraisal. Field Crops Res **86:** 131–146

Bush DR (1989) Proton-coupled sucrose transport in plasmalemma vesicles isolated from sugar beet (*Beta vulgaris* L. cv Great Western) leaves. Plant Physiol **89:** 1318–1323

Choi Y, Lee Y, Jeon BW, Staiger CJ, Lee Y (2008) Phosphatidylinositol 3- and 4-phosphate modulate actin filament reorganization in guard cells of day flower. Plant Cell Environ **31:** 366–377

Corke FMK, Hedley CL, Wang TL (1990) An analysis of seed development in *Pisum sativum*. XI. Cellular development and the position of storage protein in immature embryos grown in vivo and in vitro. Protoplasma **155:** 127–135

Czechowski T, Stitt M, Altmann T, Udvardi MK, Scheible WR (2005) Genome wide identification and testing of superior reference genes for transcript normalization in Arabidopsis. Plant Physiol **139:** 5–17

Erban A, Schauer N, Fernie AR, Kopka J (2007) Non-supervised construction and application of mass spectral and retention time index libraries from time-of-flight gas chromatography-mass spectrometry metabolite profiles. Methods Mol Biol **358:** 19–38

Finkelstein RR, Gampala SS, Rock CD (2002) Abscisic acid signalling in seeds and seedlings. Plant Cell (Suppl) **14:** S15–S45

Gass N, Glagotskaia T, Mellema S, Stuurman J, Barone M, Mandel T, Roessner-Tunali U, Kuhlemeier C (2005) Pyruvate decarboxylase provides growing pollen tubes with a competitive advantage in petunia. Plant Cell **17:** 2355–2368

Giroux MJ, Boyer C, Feix G, Hannah LC (1994) Coordinated transcriptional regulation of storage product genes in the maize endosperm. Plant Physiol **106:** 713–722

Hajdukiewicz P, Svab Z, Maliga P (1994) The small, versatile pPZP family of *Agrobacterium* binary vectors for plant transformation. Plant Mol Biol **25:** 989–994

Hartig K, Beck E (2006) Crosstalk between auxin, cytokinins, and sugars in the plant cell cycle. Plant Biol **8:** 389–396

Heim U, Manteuffel R, Bäumlein H, Stenbiss HH, Wobus U (1995) Transient expression of a lysine-rich vicilin gene of *Vicia faba* in barley endosperm detected by immunological tissue printing after particle bombardment. Plant Cell Rep **15:** 125–128

Heim U, Weber H, Bäumlein H, Wobus U (1993) A sucrose-synthase gene of *Vicia faba* L.: expression pattern in developing seeds in relation to starch synthesis and metabolic regulation. Planta **191:** 394–401

Hensel G, Kastner C, Oleszczuk S, Riechen J, Kumlehn J (2009) Agrobacterium-mediated gene transfer to cereal crop plants: current protocols for barley, wheat, triticale, and maize. Int J Plant Genomics. **2009:** 835608

Hernández-Sebastià C, Marsolais F, Saravitz C, Israel D, Dewey RE, Huber SC (2005) Free amino acid profiles suggest a possible role for asparagine in the control of storage-product accumulation in developing seeds of low- and high-protein soybean lines. J Exp Bot **56:** 1951–1963

Hesse H, Trachsel N, Suter M, Kopriva S, von Ballmoos P, Rennenberg H, Brunold C (2003) Effect of glucose on assimilatory sulphate reduction in *Arabidopsis thaliana* roots. J Exp Bot **54:** 1701–1709

Jenner CF, Ugalde TD, Aspinall D (1991) The physiology of starch and protein deposition in the endosperm of wheat. Aust J Plant Physiol **18:** 211–226

Koch K (2004) Sucrose metabolism: regulatory mechanisms and pivotal roles in sugar sensing and plant development. Curr Opin Plant Biol **7:** 235–246

Kopka J, Schauer N, Krueger S, Birkemeyer C, Usadel B, Bergmuller E, Dörmann P, Weckwerth W, Gibon Y, Stitt M, et al (2005) GMD@CSB. DB: the Golm Metabolome Database. Bioinformatics **21:** 1635–1638

Li F, Asami T, Wu X, Tsang EW, Cutler AJ (2007) A putative hydroxysteroid dehydrogenase involved in regulating plant growth and development. Plant Physiol **145:** 87–97

Lillo C, Lea US, Ruoff P (2008) Nutrient depletion as a key factor for manipulating gene expression and product formation in different branches of the flavonoid pathway. Plant Cell Environ **31:** 587–601

Lisec J, Schauer N, Kopka J, Willmitzer L, Fernie AR (2006) Gas chromatography mass spectrometry-based metabolite profiling in plants. Nat Protoc **1:** 387–396

Luedemann A, Strassburg K, Erban A Kopka J (2008) TagFinder for the quantitative analysis of gas chromatography-mass spectrometry (GC-MS) based metabolite profiling experiments. Bioinformatics **24:** 732–737

Lunn JE, Feil R, Hendriks JH, Gibon Y, Morcuende R, Osuna D, Scheible WR, Carillo P, Hajirezaei MR, Stitt M (2006) Sugar-induced increases in trehalose 6-phosphate are correlated with redox activation of ADPglucose pyrophosphorylase and higher rates of starch synthesis in *Arabidopsis thaliana*. Biochem J **397:** 139–148

Ma QH, Tian B (2005) Characterization of a wheat histidine-containing phosphotransfer protein (HP) that is regulated by cytokinin-mediated inhibition of leaf senescence. Plant Sci **168:** 1507–1514

Masclaux-Daubresse C, Carrayol E, Valadier MH (2005) The two nitrogen mobilisation- and senescence-associated GS1 and GDH genes are controlled by C and N metabolites. Planta **221:** 580–588

McWatters HG, Kolmos E, Hall A, Doyle MR, Amasino RM, Gyula P, Nagy F, Millar AJ, Davis SJ (2007) ELF4 is required for oscillatory properties of the circadian clock. Plant Physiol **144:** 391–401

Miersch O, Neumerkel J, Dippe M, Stenzel I, Wasternack C (2008) Hydroxylated jasmonates are commonly occurring metabolites of jasmonate and contribute to a partial switch-off in jasmonate signaling. New Phytol **177:** 114–127

Miflin BJ, Lea PJ (1977) Amino acid metabolism. Annu Rev Plant Physiol **28:** 299–329

Miyashita Y, Good AG (2008) NAD(H)-dependent glutamate dehydrogenase is essential for the survival of *Arabidopsis thaliana* during dark-induced carbon starvation. J Exp Bot **59:** 667–680

Müller M, Knudsen S (1993) The nitrogen response of a barley C-hordein promoter is controlled by positive and negative regulation of the GCN4 and endosperm box. Plant J **4:** 343–355

Osuna D, Usadel B, Morcuende R, Gibon Y, Bläsing OE, Höhne M, Günter M, Kamlage B, Trethewey R, Scheible WR, et al (2007) Temporal responses of transcripts, enzyme activities and metabolites after adding sucrose to carbon-deprived *Arabidopsis* seedlings. Plant J **49:** 463–491

Palotta MA, Graham RD, Langridge P, Sparrow DHB, Barker SJ (2000) RFLP mapping of manganese efficiency in barley. Theor Appl Genet **101:** 1100–1108

Park S, Rancour DM, Bednarek SY (2008) In planta analysis of the cell cycle-dependent localization of AtCDC48A and its critical roles in cell division, expansion, and differentiation. Plant Physiol **148:** 246–258

Perez MD, Chambers SJ, Bacon JR, Lambert N, Hedley CL, Wang TL (1993) Seed protein content and composition of near-isogenic and induced mutant pea lines. Seed Sci Res **3:** 187–194

Perez P, Martinez-Carrasco R, Martín Del Molino IM, Rojo B, Ulloa M (1989) Nitrogen uptake and accumulation in grains of three winter wheat varieties with altered source-sink ratios. J Exp Bot **40:** 707–710

Pineda Rodo A, Brugière N, Vankova R, Malbeck J, Olson JM, Haines SC, Martin RC, Habben JE, Mok DW, Mok MC (2008) Over-expression of a zeatin O-glucosylation gene in maize leads to growth retardation and tasselseed formation. J Exp Bot **59:** 2673–2686

Radchuk R, Radchuk V, Götz KP, Weichert H, Richter A, Emery RJN, Weschke W, Weber H (2007) Ectopic expression of PEP carboxylase in *Vicia narbonensis* seeds: effects of improved nutrient status on seed maturation and transcriptional regulatory networks. Plant J **51:** 819–839

Radchuk R, Radchuk V, Weschke W, Borisjuk L, Weber H (2006) Repressing the expression of the SUCROSE NONFERMENTING-1-RELATED PROTEIN KINASE gene in pea embryo causes pleiotropic defects of maturation similar to an abscisic acid-insensitive phenotype. Plant Physiol **140:** 263–278

Ramakers C, Ruijter JM, Lekanne Deprez RH, Moorman AFM (2003) Assumption-free analysis of quantitative real-time polymerase chain reaction (PCR) data. Neurosci Lett **339:** 62–66

Reynolds M, Foulkes MJ, Slafer GA, Berry P, Parry MA, Snape JW, Angus WJ (2009) Raising yield potential in wheat. J Exp Bot **60:** 1899–1918

Rosche E, Blackmore D, Tegeder M, Richardson T, Schroeder H, Higgins TJ, Frommer WB, Offler CE, Patrick JW (2002) Seed-specific over-expression of a potato sucrose transporter increases sucrose uptake and growth rates of developing pea cotyledons. Plant J **30:** 165–175

Rosche EG, Blackmore D, Offler CE, Patrick JW (2005) Increased capacity for sucrose uptake leads to earlier onset of protein accumulation in developing seeds. Funct Plant Biol **32:** 997–1007

Salon C, Munier-Jolain NG, Duc G, Voisin AS, Grandgirard D, Larmure A, Emery RJN, Ney B (2001) Grain legume seed filling in relation to nitrogen acquisition: a review and prospects with particular reference to pea. Agronomie **21:** 539–552

Scofield GN, Hirose T, Gaudron JA, Upadhyaya NM, Ohsugi R, Furbank RT (2002) Antisense suppression of the rice sucrose transporter gene, OsSUT1, leads to impaired grain filling and germination but does not affect photosynthesis. Funct Plant Biol **29:** 815–826

Simmonds NW (1995) The relation between yield and protein in cereal grain. J Food Agric **67:** 309–315

Sinclair TR (1998) Historical changes in harvest index and crop nitrogen accumulation. Crop Sci **38:** 638–643

Smeekens S (2000) Sugar-induced signal transduction in plants. Annu Rev Plant Physiol Plant Mol Biol **51:** 49–81

Sosulski FW, Imafidon GI (1990) Amino acid composition and nitrogen-to-protein conversion factors for animal and plant foods. J Agric Food Chem **38:** 1351–1356

Sreenivasulu N, Usadel B, Winter A, Radchuk V, Scholz U, Stein N, Weschke W, Strickert M, Close TJ, Stitt M, et al (2008) Barley grain maturation and germination: metabolic pathway and regulatory network commonalities and differences highlighted by new MapMan/PageMan profiling tools. Plant Physiol **146:** 1738–1758

Tegeder M, Wang XD, Frommer WB, Offler EO, Patrick JW (1999) Sucrose transport into developing seeds of *Pisum sativum*. Plant J **18:** 151–161

Thiel J, Müller M, Weschke W, Weber H (2009) Amino acid metabolism at the maternal-filial boundary of young barley seeds: a microdissection-based study. Planta **230:** 205–213

Tsukagoshi H, Morikami A, Nakamura K (2007) Two B3 domain transcriptional repressors prevent sugar-inducible expression of seed maturation genes in *Arabidopsis* seedlings. Proc Natl Acad Sci USA **104:** 2543–2547

Van Dongen JT, Fröhlich A, Ramírez-Aguilar SJ, Schauer N, Fernie AR, Erban A, Kopka J, Clark J, Langer A, Geigenberger P (2009) Transcript and metabolite profiling of the adaptive response to mild decreases in oxygen concentration in the roots of *Arabidopsis* plants. Ann Bot (Lond) **103:** 269–280

Vannini C, Locatelli F, Bracale M, Magnani E, Marsoni M, Osnato M, Mattana M, Baldoni E, Coraggio I (2004) Overexpression of the rice *Osmyb4* gene increases chilling and freezing tolerance of *Arabidopsis thaliana* plants. Plant J **37:** 115–127

Varshney A, Altpeter F (2001) Stable transformation and tissue culture response in current European winter wheats (*Triticum aestivum*, L.). Mol Breed **8:** 295–309

Vertregt N, de Vries P (1987) A rapid method for determining the efficiency of biosynthesis of plant biomass. J Theor Biol **128:** 109–119

Wardlaw IF, Moncur L, Patrick JW (1995) The response of wheat to high temperature following anthesis. II. Sucrose accumulation and metabolism by isolated kernels. Aust J Plant Physiol **22:** 399–407

Weber H, Borisjuk L, Heim U, Sauer N, Wobus U (1997a) A role for sugar transporters during seed development: molecular characterization of a hexose and a sucrose carrier in faba bean seeds. Plant Cell **9:** 895–908

Weber H, Borisjuk L, Wobus U (1996) Controlling seed development and seed size in *Vicia faba*: a role for seed coat-associated invertases and carbohydrate state. Plant J **10:** 823–834

Weber H, Borisjuk L, Wobus U (1997b) Sugar import and metabolism during seed development. Trends Plant Sci **22:** 169–174

Weber H, Borisjuk L, Wobus U (2005) Molecular physiology of legume seed development. Annu Rev Plant Biol **56:** 253–279

Weber H, Heim U, Golombek S, Borisjuk L, Wobus U (1998) Assimilate uptake and the regulation of seed development. Seed Sci Res **8:** 331–345

Weigelt K, Küster H, Radchuk R, Müller M, Weichert H, Fait A, Fernie AR, Saalbach I, Weber H (2008) Increasing amino acid supply in pea embryos reveals specific interactions of N and C metabolism and highlights the importance of mitochondrial metabolism. Plant J **55:** 909–926

Weigelt K, Küster H, Rutten T, Fait A, Fernie AR, Miersch O, Wasternack C, Emery RJN, Desel C, Hosein F, et al (2009) ADP-glucose pyrophosphorylase deficient pea embryos reveal specific transcriptional and metabolic changes of carbon-nitrogen metabolism and stress responses. Plant Physiol **149:** 395–411

Weschke W, Panitz R, Sauer N, Wang Q, Neubohn B, Weber H, Wobus U (2000) Sucrose transport into barley seeds: molecular characterisation of two transporters and implications for seed development and starch accumulation. Plant J **21:** 455–467

Wieser H (1997) Turbidimetrische Bestimmung einzelner Kleberprotein-typen in Weizenmehl. Getreide Mehl und Brot **51:** 333–334